THE ROLE OF SYNTENIN-1 IN MODULATING EPHRIN-B2 PATHWAYS IN BREAST EPITHELIAL CELLS

By

Michael Parks

A thesis submitted to the Division of Cancer Studies at the University of Birmingham for the degree of DOCTOR OF PHILOSOPHY

Cancer Research UK Institute for Cancer Studies

University of Birmingham

November 2013

ABSTRACT

Eph receptor tyrosine kinases and their ligands ephrins are involved in many physiological processes, including tissue homeostasis, vascularisation and development. They are also involved in promoting angiogenesis and metastasis in many cancers, including breast, colon and lung. Upon interaction with EphB receptors, ephrinB ligands signal through SH2- and PDZ-interacting cytoplasmic adaptors. To date, little is known on PDZ-mediated ephrinB signalling. The aim of our study was to determine the role of PDZ domain-containing proteins in modulating ephrinB2 signalling and trafficking pathways in the context of epithelial breast cancer cells, with a specific focus on the scaffolding protein syntenin-1. We also endeavoured to determine whether the ephrinB2 – syntenin-1 axis affects breast cancer tumourigenesis. Our findings demonstrate that syntenin-1 modulates ephrinB2 internalization upon receptor-induced stimulation and that this affects ephrinB signalling. Furthermore, we found that phospho-Tyr330 on ephrinB2 increases binding to the PDZ domain-containing proteins syntenin-1 and PAR3. Finally, we report that ephrinB2 drives MCF7 colony growth in 3D cultures and that syntenin-1 is involved in boundary formation between ephrinB2 and EphB4 expressing cells. These findings describe, for the first time, the role of syntenin-1 in ephrinB2 signalling and the functional relevance of the ephrinB2 – syntenin-1 axis in epithelial breast cancer pathways.

FOR MY WIFE

AKNOWLEDGEMENTS

As the source of constant and unfaltering support which has seen me stand tall and persevere throughout these last four years, I would like to thank with all my heart my darling wife, Zineb. Next, an enormous and heartfelt thank you to my caring parents for always supporting me in all my decisions and enabling me to pursue my career.

I am also very grateful to my supervisors Dr Fedor Berditchevski and Dr Elena Odintsova for giving me the opportunity of working in their lab and guiding me throughout my PhD. A special thank you to Dr Rajesh Sundaresan for helping me with Biacore experiments, providing the NMR data and helping me develop my project from a protein structure perspective. I would also like to thank Dr Vera Novitskaia and Dr Hanna Romanska for teaching me how to set up and analyse 3D cultures; Dr Douglass Ward for all his help in producing and analysing mass spectrometry data; and Dr Mahboob Salim for teaching me how to conduct Biacore analysis. During my project, I had the pleasure of working with and learning from outstanding researchers which shared their wisdom and supported me every step of the way. To Dr Eva McGrowder, Dr Gouri Baldwin, Dr Dale Powner, Dr Rafal Sadej, Dr Sven Peterson, Dr Ruzica Bago, Dr Simon Chanas and Izabela Bombik I would like to express my utmost gratitude for all the constant help and support. I would not be the researcher I am today without having met all of you. Finally I would like to thank my friends Laura Hindle, Laura Quinn, Luke Williams, Piraveen Gopalasingam, Rachel Cartlidge, Richard Amoroso and Beckie Port for the great times spent together and for always being there when I needed them.

I would like to conclude by thanking CRUK for funding my project and the University of Birmingham for providing all of the needed facilities.

Table of content

LIST OF FIGURES

LIST OF TABLES

Abbreviations

aa = amino acid
Abi-1 = Abl interactor 1
Abl = Abelson murine leukemia viral oncogene homolog 1
ADAM10 = a disintegrin and metalloproteinase domain-containing protein 10
AGM = axon guidance molecule
AMPA = α-amino-3-hydroxy-5-methyl-4-isoxazolepropionic acid
AP = adaptor protein
aPKC = atypical protein kinase C
Arf = ADP-ribosylation factor
Arg = Abelson murine leukemia viral oncogene homolog 2
Arp = actin-related proteins
CAP = catabolite activator protein
Cas = Crk-associated substrate
CASK = calcium/calmodulin-dependent serine protein kinase
Cbl = Casitas B-lineage lymphoma protein
Cdc42 = cell division control protein 42 homolog
CEACAM = carcinoembryonic antigen-related cell adhesion molecule
CFNS = craniofrontonasal syndrome
CRD = cysteine rich domain
Crk = CT10 Regulator of kinase
Csk = c-Src kinase
CTD = C-terminal domain
CTF1,2 = cytoplasmic terminal fragments 1 and 2
CXCR4 = C-X-C chemokine receptor type-4
Dab2 = disabled-2
DEP = dishevelled, Egl-10 and pleckstrin domain
DIX = dishevelled-axin domain
DLL4 = delta-like protein 4
DOCK180 = dedicator of cytokinesis protein 180 kDa
EBP = ERM (ezrin/radixin/moesin) binding phosphoprotein
ECM = extra-cellular matrix
EEA1 = early endosome antigen 1
EGF = epidermal growth factor
EIF4A = eukaryotic translation initiation factor 4A
EMT or EndoMT = endothelial-to-mesenchymal transition
ER = oestrogen receptor
ERK = extracellular signal-regulated kinase
FAK = focal adhesion kinase
FAP1 = Fas-associated phosphatase 1

FGF = fibroblast growth factor
FGFR = fibroblast growth factor receptor
GAP = GTPase-activating protein
GEF = guanidine nucleotide exchange factor
GIT = G protein-coupled receptor kinase-interacting protein
GluR = glutamate receptor
GPI = glycosyl-phospho-inositol
Grb4 = growth factor receptor-bound protein 4
GMP = guanosine monophosphate
GRIP1,2 = glutamate receptor interacting protein 1 and 2
GTP = guanosine triphosphate
GST = glutathion s-trasnferase
HCC = hepatocellular carcinoma
Her-2 = human epidermal growth factor receptor 2
HIF = hypoxia-inducible factor
HIV-TAT = human immunodeficiency virus – trans activator of transcription
hnRNPK = heterogeneous nuclear ribonucleoprotein K
HNSCC = head and neck squamous cell carcinoma
HUVEC = human umbilical vein endothelial cells
HSV = herpes simplex virus
IFN = interferon
IGFBP-2 = insulin growth factor-binding protein-2
IKEPP = intestinal and kidney enriched PDZ protein
IL-5 = interleukin-5
JAK = janus kinase
JNK = c-Jun N-terminal kinase
kDa = kilo dalton
LBD = ligand binding domain
Lck = lymphocyte-specific protein tyrosine kinase
LTP = long term potentiation
MET = mesenchymal-to-epithelial transition
MAPK = mitogen-activated protein kinase
MHC = major histocompatibility complex
MMP = matrix metallo-proteinases
mRNA = messenger RNA
MRP = multidrug resistance protein
MSC = mesenchymal stem cells
NCBI = National Centre for Biotechnology Information
Nck = non-catalytic region of tyrosine kinase adaptor protein 1
NF-ķB = nuclear factor kappa-light-chain-enhancer of activated B cells
NHERF = Na(+)/H(+) exchanger regulatory factor
NMDA = N-methyl-D-aspartate

NMR = nuclear magnetic resonance
NOS = nitric oxide synthase
Notch = neurogenic locus notch homolog protein
NTD = N-terminal domain
OD = optical density
PAG/Cbp = phosphoprotein associated with GEMs / Csk-binding protein
Pak1 = p21-activated kinase 1
PAR3 = partitioning defective 3 homolog
PAR6 = partitioning defective 6 homolog
PBM = PDZ binding motif
PDGF = platelet-derived growth factor
PDZ = postsynaptic density protein, disc large, zona occludens
PI3K = phosphatidyl-inositol 3-kinase
PI3K = phosphatidyl-inositol 4-kinase
PKC = protein kinase C
PICK1 = protein interacting with PRKCA 1
PINCH = particularly interesting new Cys-His protein
PIP2 = phosphatidyl-inositol 4,5-bisphosphate
PKG = cGMP-dependent protein kinase
PR = progesterone receptor
PS1 = presenilin-1
PTPL1 = protein tyrosine phosphatase L1
PTP-BL = protein tyrosine phosphatase – basophil-like
PTPη = r-protein tyrosine phosphatase η
RGS3 = regulator of G-protein signalling 3
RHBDL2 = human rhomboid intramembrane serine protease
RKIP = Raf kinase inhibitor protein
ROCK = Rho-associated protein kinase
SAM = sterile alpha motif
SDF-1 = stromal cell-derived factor-1
SH2 = Src homology 2 domain
SH3 = Src homology 3 domain
shRNA = small hairpin RNA
siRNA = short interference RNA
Sox4 = SRY (sex determining region Y)-box 4 protein
STAT = signal transducers and activators of transcription protein
SynCAM = synaptic cell adhesion molecule
Tcf = T-cell factor
TERM = tetraspanin enriched microdomain
TGF = transforming growth factor
TNFα = tumour necrosis factor-α
Tspan = tetraspanin

Ulk1 = Unc-51-like kinase 1
VEGF = vascular endothelial growth factor
VEGFR = vascular endothelial growth factor receptor
VP16 = etoposide
WASp = Wiskott-Aldrich syndrome protein
WAVE = WASp-family verprolin-homologous protein
ZAP-70 = zeta-chain-associated protein 70
Zhx2 = zinc fingers and homeoboxes 2

INTRODUCTION

1.1 Eph receptors and ephrin ligands

1.1.1 The Eph superfamily of tyrosine kinase receptors and their ligands ephrins

Eph receptors are the largest known superfamily of receptor tyrosine kinases in humans and their cognate ligands are called ephrins. Both receptors and ligands are involved in various physiological and pathological processes in many cell types and different organs (Pasquale 2008). In cancer, different Eph and ephrin expression patterns have been found to play important roles in tumour development and progression (Pasquale 2010). There are 14 members of the Eph receptors superfamily which are subdivided into A and B sub-families, depending on the type of ephrin ligands they bind to. EphrinA ligands are anchored to the plasma membrane via a glycosyl-phosphatidyl-inositol tail (GPI-linked), while ephrinB ligands possess a single transmembrane region. Nine EphA receptors bind to five ephrinA ligands and five EphB receptors bind to three ephrinB ligands, although some promiscuity between the two classes of receptors and ligands has also been observed (Kullander and Klein 2002; Gauthier and Robbins 2003; Pasquale 2008). The high diversity of these proteins is due to recent gene duplication events, as Eph receptor genes can be found in gene clusters on chromosomes 1, 3 and 7 (Kullander and Klein 2002).

1.1.1.1 Structural characteristics of Eph receptors and ephrin ligands

The structural domains which characterize all Eph receptors include: 1) an extracellular moiety consisting of an immunoglobulin-like globular domain with ligand-interacting functions (LBD) followed by a cysteine-rich region (CRD), containing a Sushi domain tightly packed to an EGF like module, and two fibronectin type III repeats; 2) a single transmembrane region containing two conserved tyrosine residues; 3) an intracellular kinase domain followed by a sterile alpha motif (SAM), which participates in the formation of heterodimers, and a "postsynaptic density protein, disc large, zona occludens" (PDZ) binding motif (PBM) (figure 1.1) (Kullander and Klein 2002; Janes, Nievergall et al. 2012). The extracellular domain is also characterized by a high affinity binding site for ephrin ligands and two low affinity binding sites which facilitate clustering of multiple-Eph-ephrin complexes (Pasquale 2008).

Both ephrinA and ephrinB ligands have an extracellular domain consisting of a high affinity receptor binding loop. EphrinB ligands possess a transmembrane region and an intracellular moiety containing 5-6 tyrosine residues and a C-terminal PDZ binding motif, while ephrinA ligands are anchored to the plasma membrane via a GPI-link (Andres and Ziemiecki 2003). The C-terminal tail of ephrinB ligands adopts a well-packed β-hairpin structure between amino acids 301 and 322 in a non phosphorylated state. Upon protein phosphorylation

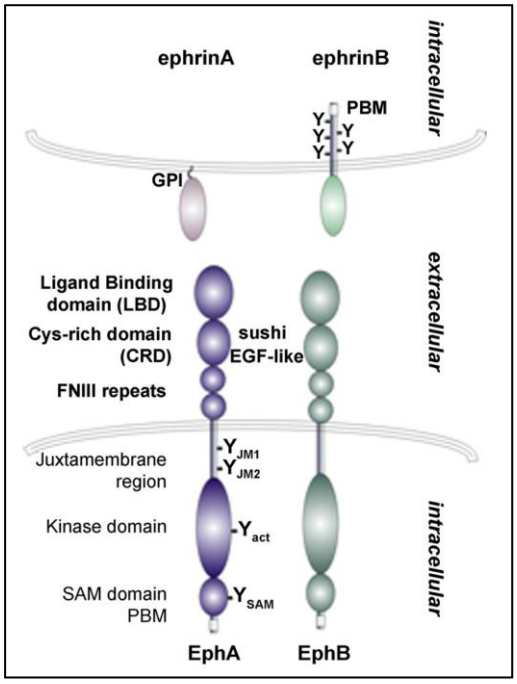

Figure 1.1: structure of Eph receptors and ephrin ligands (Janes, Nievergall et al. 2012).

on tyrosines 304, 311 or 316, the β-hairpin structure is lost (Song 2003).

1.1.1.2 Eph – ephrin interaction mechanisms

Prior to cell contact, ephrin ligands are present on the cell surface as homodimers, while Eph receptors remain mostly separate and display minimal kinase activity when not stimulated (Himanen, Saha et al. 2007). During cell-cell contact, Eph receptors interact with ephrin ligand homodimers present on neighbouring cells (figure 1.2). The initial recognition and binding of ephrin ligands to Eph receptors involve a hydrophobic cavity of the Eph LBD where a long ephrin loop penetrates and drives the formation of the complex (Nikolov, Xu et al. 2013). This interaction subsequently induces the formation of circular tetrameric structures held together by lower affinity binding events in which each ephrin is bound to two Eph receptors and vice-versa (Himanen, Yermekbayeva et al. 2010; Seiradake, Harlos et al. 2010). From a structural perspective, the binding domain of ephrinB ligands has a β-barrel conformation and can form *cis*-homodimers. Moreover, the surface exposed G-H loop and the G β-strand of the extracellular domain are necessary for the initial *trans*-heterodimerization with EphB receptors, while the C-D loop participates in the formation of *trans*-heterotetramers between two receptors and two ligands (Blits-Huizinga, Nelersa et al. 2004). Eph receptors are also able to bind together

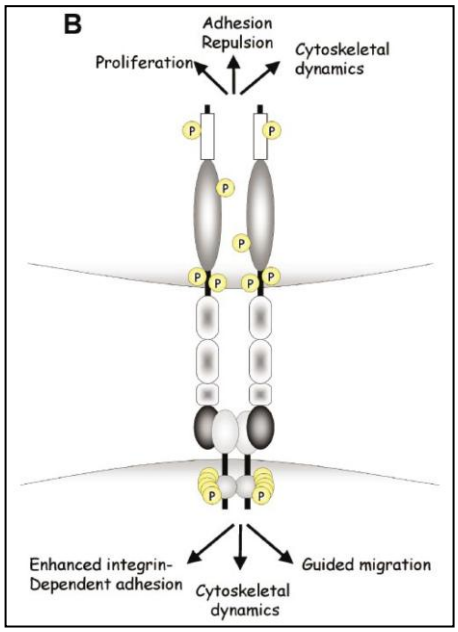

Figure 1.2: interaction mechanism between Eph receptors and ephrin ligands (Andres and Ziemiecki 2003)

upon ephrin-induced clustering via their extracellular domains in order to form higher order multimers (Nikolov, Xu et al. 2013). Only membrane-bound or artificially clustered ligands/receptors can activate the cognate receptor/ligand signalling, whilst non-clustered soluble ligands/receptors act as antagonists (Janes, Nievergall et al. 2012). The clustering of two Eph molecules is sufficient to activate the receptors. Similarly, clustering of two ephrin ligands is also required to trigger reverse signalling (Poliakov, Cotrina et al. 2004). It has also been hypothesized that interactions with PDZ domain-containing proteins might help oligomerization events of Eph receptors and ephrinB ligands (Bruckner, Pablo Labrador et al. 1999; Lin, Gish et al. 1999). Although dimerization of Eph receptors and ephrin ligands is necessary to trigger a biological response, multimerization strongly increases and sometimes even alters the signalling pathways involved (figure 1.3) (Blits-Huizinga, Nelersa et al. 2004). In fact, recent reports suggest that the switch between Eph/ephrin induced cell adhesion or cell repulsion is determined by the degree of Eph/ephrin clustering (Lackmann and Boyd 2008).

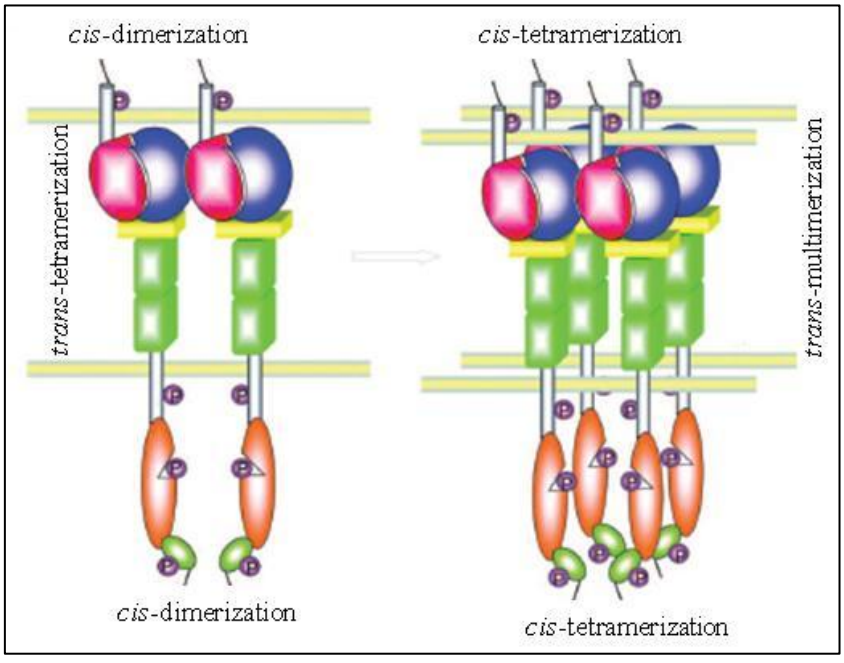

Figure 1.3: formation of Eph-ephrin multimeric complexes upon receptor – ligand interaction (Blits-Huizinga, Nelersa et al. 2004).

Eph receptors and ephrin ligands are capable of interacting *in trans* and/or *in cis* (figure 1.4). Various studies have suggested that Eph-ephrin *trans* interactions generate an activating biological response, whilst *cis* interactions inhibit this

response (Arvanitis and Davy 2008). While co-expression of Eph receptors and ephrin ligands is likely to result in formation of *cis* complexes, it is also possible that they segregate in different membrane microdomains, thereby decreasing *cis* interactions (Noren and Pasquale 2007).

Lastly, Eph receptors and ephrin ligands have also been shown to interact *in cis* with other cell surface receptors, such as FGF, PDGF, VEGF and ErbB receptors (Arvanitis and Davy 2008; Pasquale 2008; Pitulescu and Adams 2010; Vermeer, Bell et al. 2012; Vermeer, Colbert et al. 2013). Intriguingly, Eph receptors are also able to form heterodimers with other Eph receptors which share the same ephrin ligand, as recently reviewed by (Janes, Nievergall et al. 2012). For example, EphB1 and EphB4 form complexes with kinase-dead EphB6, resulting in its *trans*-phosphorylation (Truitt, Freywald et al. 2010), whilst EphA3 and EphA4 co-localize in COS-7 cells upon stimulation with ephrinA5 (Marquardt, Shirasaki et al. 2005).

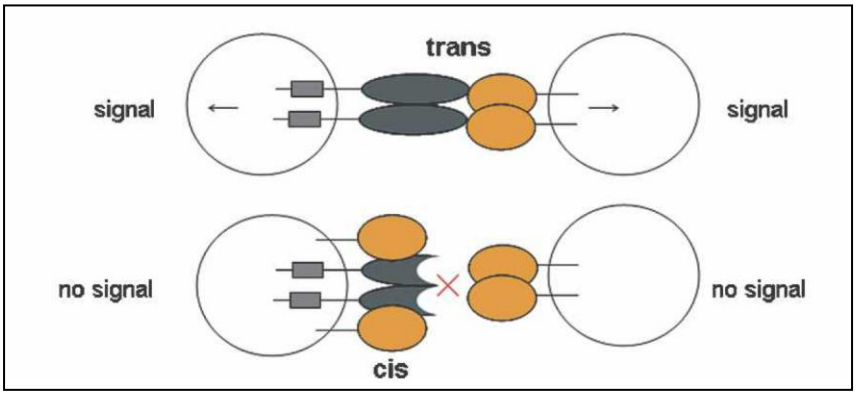

Figure 1.4: Eph-ephrin interaction can occur *in cis* or *in trans* (Arvanitis and Davy 2008).

1.1.2 Physiological Functions

The Eph superfamily of tyrosine kinase receptors and their ephrin ligands are widely expressed in the majority of organs and tissues. Expression gradients of Eph receptors and ephrin ligands in different cell types determine tissue assembly and control cell movement through cell repulsion and adhesion (Poliakov, Cotrina et al. 2004). Importantly, coordinated spatial and temporal expression of Eph receptors and ephrin ligands control development, tissue homeostasis, formation of tissue boundaries and tissue patterning, assembly of neuronal circuits and the remodelling of blood vessels and organ size. At the cellular level, Eph receptor signalling has been shown to control cell morphology, adhesion, migration and invasion by modifying the actin cytoskeleton and the activity of various types of adhesion molecules, such as integrins, claudins and cadherins (Pasquale 2010; Nievergall, Lackmann et al. 2012).

1.1.2.1 Eph – ephrin interaction can mediate cell adhesion or repulsion

Eph receptors and ephrin ligands tightly control the formation of boundaries between neighbouring cells of different tissues. The equilibrium between expression levels of Eph receptors on one side and ephrin ligands on the other determines whether Eph expressing cells will adhere or retract from ephrin expressing cells (Daar 2012). For example, when cell adhesion is triggered, activation of ephrinA ligands induces β1-integrin interaction with laminin (Huai and Drescher 2001) and caveola-mediated cell adhesion to fibronectin (Davy, Gale et al. 1999). EphrinB ligands can regulate cell repulsion by impairing tight junctions

assembly (Daar 2012). A study conducted in *Xenopus* embryos found that ephrinB1 competes with the small GTPase Cdc42 for association with PAR6, thus disrupting the PAR6/aPKC/Cdc42 complex which is responsible for the formation of cell-cell junctions (Lee, Nishanian et al. 2008). However, the same group also found that phosphorylation of ephrinB1 upon interaction with EphB receptors causes dissociation of PAR6 from the ligand and, consequentially, promotes tight junction assembly and cell-cell adhesion (Lee, Nishanian et al. 2008). In the case of cell repulsion, when Eph receptors and ephrin ligands interact, both proteins trigger independent signalling cascades. Eph receptor phosphorylation induced by ephrin interaction activates ROCK and Cdc42, which regulate cell morphology and trigger rounding and repulsion of Eph expressing cells from ephrin expressing cells (Groeger and Nobes 2007; Lee and Daar 2009; Daar 2012). When ephrinB ligands are phosphorylated they interact with the scaffolding protein Dishevelled which activates ROCK-mediated cell retraction (Tanaka, Kamo et al. 2003). Also, ephrinA and EphA interaction can activate the metalloproteinase ADAM10 which is responsible for shedding the ligand's extracellular region and allowing cell detachment (Janes, Wimmer-Kleikamp et al. 2009). Finally, EphB4 can inhibit integrin-mediated cell adhesion independently of ephrinB2 interaction (Pitulescu and Adams 2010). A diagram of ephrinA and ephrinB reverse signalling pathways which affect cell adhesion and movement is illustrated in figure 1.5.

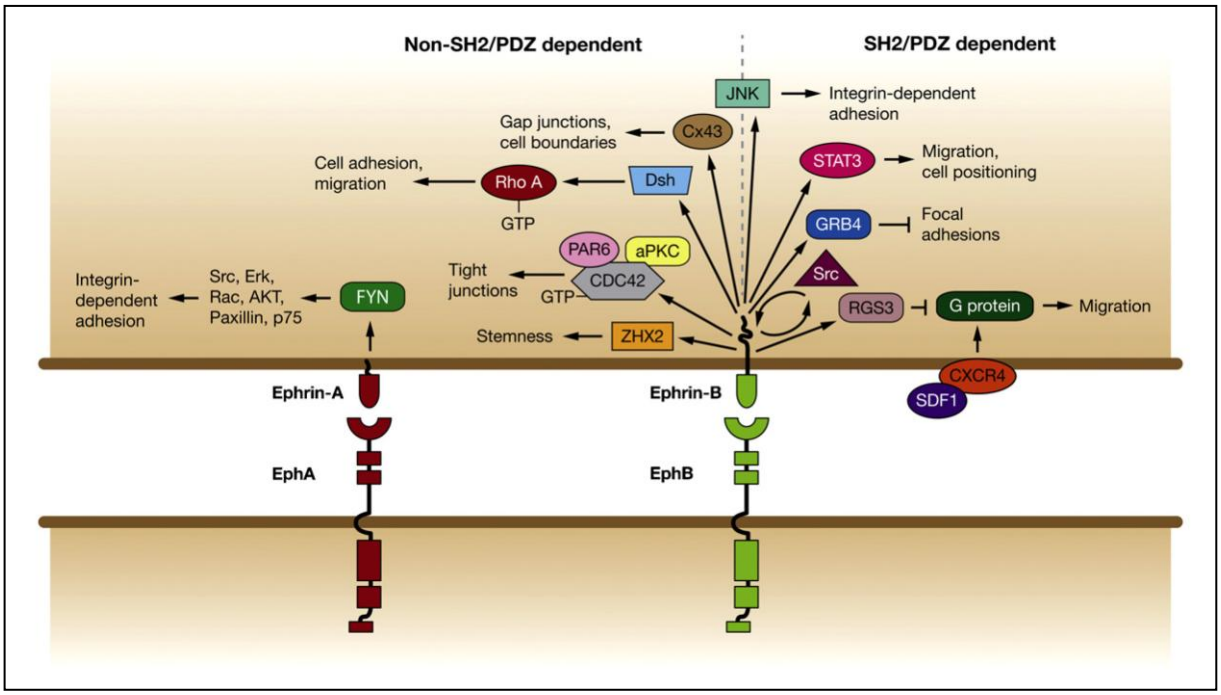

Figure 1.5: reverse signalling pathways induced by ephrinA and ephrinB ligands in cell adhesion and movement. EphrinB-mediated signalling is divided into non-SH2/PDZ dependent and SH2/PDZ dependent pathways (Daar 2012).

1.1.2.2 The role of Eph/ephrin signalling in vascularisation

Various studies have shown that during embryogenesis the ephrinB2 ligand becomes exclusively expressed in embryonic arteries, while the EphB4 receptor in embryonic veins (Andres and Ziemiecki 2003; Gauthier and Robbins 2003). Later studies have determined that while the EphB4 receptor is sufficient to determine venous and arterial differentiation, ephrinB2 ligand expression in the surrounding tissue might serve to direct vessel sprouting (Poliakov, Cotrina et al. 2004). In fact, both receptor and ligand expression are fundamental for embryonic survival past day 11 in mice, as the absence of either one of these proteins disrupts angiogenesis and leads to an incomplete vascular system (Blits-Huizinga, Nelersa et

al. 2004). Knock out of the ephrinB2 or EphB4 gene in mice produces a phenotype which displays arteriovenous malformations (Krebs, Starling et al. 2010). Interestingly, during embryogenesis only the extracellular portion of the ephrinB2 ligand is necessary, by acting as an activator for EphB4 signalling. EphrinB2 reverse signalling becomes vital only after birth during neonatal survival (Cowan, Yokoyama et al. 2004). In the retina, higher phosphorylation of ephrinB ligands in the developing retinal vasculature of newborn mice was observed when compared to adult retinas. Moreover, phosphorylation of ephrinB ligands in vascular cells is involved in wound healing, probably serving as a marker for angiogenic vessels (Salvucci, Maric et al. 2009).

Eph receptors and ephrin ligands also regulate vascular remodelling and vessel sprouting in adulthood. As reviewed by (Salvucci and Tosato 2012), various studies have reported EphB/ephrinB signalling as a major modulator of angiogenesis during the menstrual cycle, pregnancy, skeletal bone growth and wound repair. During adulthood, the ephrinB2 ligand is still expressed in arteries, subsets of microvessels at sites of neovascularisation and within tumour vasculature, while the EphB4 receptor is still expressed in veins (Merlos-Suarez and Batlle 2008). Both receptor and ligand mediate communication signals between the arterial and venous endothelia: the expression of the EphB4 receptor attenuates endothelial cell growth and inhibits vascular network formation, while ephrinB2 ligand expression stimulates these processes (Andres and Ziemiecki 2003).

1.1.2.3 Other roles of Eph/ephrin signalling in development

The complementary and mutually exclusive expression patterns of Eph receptors and ephrin ligands during embryogenesis is fundamental in the formation of spatial boundaries and tissue morphogenesis (Gauthier and Robbins 2003). During the early stages of development Eph receptors and ephrin ligands are involved in cell segregation and positioning; cell migration, axon guidance and topographic mapping; and skeletal morphogenesis (Klein 2012). For instance, EphB/ephrinB interactions control cell positioning and segregation along the crypt-villus axis of the small intestine (Batlle and Wilkinson 2012). In the developing neural system, Eph/ephrin signalling controls axonal pathfinding of lateral and medial motor column neurons and the formation of topographic maps (Klein 2012). During somitogenesis and heart development, mesenchymal-to-epithelial transition (MET) and endothelial-to-mesenchymal transition (EndoMT) are essential for cell-cell communication in establishing boundaries between endothelial/epithelial and mesenchymal tissues and cell identity. Eph/ephrin signalling is involved in this process and is able to control both MET and EndoMT (Nievergall, Lackmann et al. 2012).

1.1.2.4 Eph – ephrin interaction is fundamental in mammary gland development

Eph receptors and ephrin ligands also play a fundamental role during mammary gland development and the oestrus cycle in women. The mammary gland is composed of the ectodermal parenchyma, formed by the secretory epithelium and the contractile

myoepithelium, and the mesodermal adipose stroma within which the parenchyma develops. During puberty, the epithelium elongates forming a ductal network within the surrounding stroma. This process is induced by oestrogen and depends on hormones and epithelial – stroma interactions. The expression of the EphB4 receptor and the ephrinB2 ligand is tightly controlled by oestrogen during the mammary development and especially the oestrus cycle. EphrinB2 expression is confined to the epithelial cells, while EphB4 is present in both myoepithelial and epithelial cells, although it is only expressed in the latter during the proliferative phase of mammary gland development (Munarini, Jager et al. 2002). In the mature mammary gland, the EphB4 receptor is specifically localized to myoepithelial cells of alveolar and ductal structures. Receptor and ligand levels are then up-regulated in their respective cell types during the oestrogen driven part of the oestrus cycle, concomitant with cell proliferation, and then their expression is decreased in the progesterone driven part. Studies in ovariectomized mice have shown that expression of the EphB4 receptor and the ephrinB2 ligand could be restored to normal levels after oestrogen injections (Nikolova, Djonov et al. 1998). Although the responsive element of the transcription factor activated by oestrogen is present in the EphB4 receptor and ephrinB2 ligand genes, the levels of mRNA remain unaffected in the presence or absence of the hormone. Thus, the effect of oestrogen on receptor and ligand levels is likely to be indirect (Nikolova, Djonov et al. 1998; Andres and Ziemiecki 2003; Merlos-Suarez and Batlle 2008). The equilibrium between expressed ephrinB2 and EphB4 is vital for the correct development of the mammary gland. In mice, over-expression of EphB4 causes disrupted proliferation of the ductal epithelium and diminished branching of the ducts during pregnancy-related mammary development, while after pregnancy it caused delayed post-lactation apoptosis (Munarini, Jager et al. 2002). EphrinB2 signalling is also necessary for a correct development of the mammary gland. A

study by (Kaenel, Antonijevic et al. 2012) showed that epithelial mammary cells expressing a mutant form of the ephrinB2 ligand, where the cytoplasmic tail had been truncated, formed overgrown ducts which seemed to have an impaired contact inhibition phenotype. These ducts displayed multilayered organization and lacked an internal lumen. Cells expressing this ephrinB2 mutant were also less differentiated, retained some proliferation capability and lower apoptosis activity and they exhibited aberrant polarization.

1.1.2.5 Eph/ephrin signalling drives cellular segregation during cell differentiation in the intestine's villi

In the intestine, Eph receptors and ephrin ligands control the segregation of differentiating cells moving from the stem cell compartment towards the epithelium of the villi (Batlle and Wilkinson 2012). This process is driven by a gradual change in Eph and ephrin expression pattern. In the crypts, undifferentiated cells gradually lose EphB receptors expression whilst acquiring ephrinB ligands expression, which causes cells to differentiate and migrate towards the epithelium surface in the villi (Poliakov, Cotrina et al. 2004). The Wnt signalling pathway is responsible for the induction of EphB2 and EphB3 receptors and the repression of ephrinB1 and ephrinB2 ligands in the proliferative stem cell compartment in the crypts (Merlos-Suarez and Batlle 2008; Genander and Frisen 2010; Pitulescu and Adams 2010). The balance between receptor and ligand expression regulated by the β-catenin/Tcf pathway demarcates the undifferentiated cell population from the differentiating one (Andres and Ziemiecki 2003). Disruption of the EphB/ephrinB signalling pathway in embryonic and

adult intestine disturbs cell positioning and inhibits cell proliferation (Batlle, Henderson et al. 2002).

1.1.2.6 Involvement of Eph receptors and ephrin ligands in other tissue homeostasis processes

Given their important functions in cell morphology, adhesion and invasion, it is not surprising that Eph receptors and ephrin ligands are also involved in many other physiological processes. For example, Eph/ephrin signalling axes regulate synaptic formation and plasticity and the development of the nervous system by controlling axon guidance and patterning of neuronal connections. In this case, ephrin ligands control axonal pathfinding by acting as repulsive cues to Eph receptor bearing axons (Gauthier and Robbins 2003). Also, in neuronal stem/progenitor cells, Eph/ephrin signalling is important during development and adulthood for the maintenance and self-renewal of the stem cell niche (Genander and Frisen 2010).

Eph/ephrin signalling also controls cell segregation during differentiation in the hair follicle and epidermis. In this context, ephrinA and ephrinB ligands are able to negatively regulate proliferation of progenitor cells in the hair follicle of adult mice, although it is still unclear whether this is mediated by ephrin-induced reverse signalling or Eph-driven forward signalling (Genander, Holmberg et al. 2010; Lin, Wang et al. 2012).

Recent studies have reported the expression of Eph and ephrin proteins in bone cells. Although little is known about the role of these proteins in skeletal development, Eph/ephrin signalling is thought to mediate communication between osteocytes and osteoclasts or osteoblasts in response to various stimuli. Moreover, the EphB4 – ephrinB2 axis might be

responsible for the formation of new capillaries in the bone. Skeletal malformations have also been attributed to the disruption of Eph/ephrin signalling, as mutations in the *EFNB1* gene are associated with craniofrontonasal syndrome (CFNS) (Matsuo and Otaki 2012).

1.1.3 Eph/ephrin signalling

Eph receptors and ephrin ligands trigger two different signalling cascades. On receptor – ligand contact and subsequent clustering, Eph receptors are activated and phosphorylate specific tyrosines on their cytoplasmic tail via their kinase domain. This creates phospho-docking sites for Src Homology type-2 (SH2) domain-containing proteins and triggers so called "forward" signalling. Activated Eph receptors also mediate other types of signalling through protein-protein interactions via the SAM and PDZ-binding motifs (Kullander and Klein 2002; Noren, Lu et al. 2004). Key components of Eph forward signalling are the Rho family of GTPases (RhoA, CDC42, Rac), which are involved in the regulation of the actin cytoskeleton, cell movement and adhesion (Klein 2009). Phosphorylated Eph receptors associate and activate a number of Rho GEFs, including Vav2, Tiam, Kalirin and Intersectin (Cowan, Shao et al. 2005; Klein 2009; Salvucci and Tosato 2012). Although Eph receptors are also involved in other signalling pathways, details of these will be omitted unless directly affecting ephrin-triggered signalling, given that the focus of this study is on ephrinB-induced reverse signalling.

Ephrin ligands can also trigger signalling pathways, called "reverse" signalling, when interacting with Eph receptors or, as in the case of ephrinB ligands, through lateral interactions with other tyrosine kinase receptors (Gauthier and Robbins 2003; Pasquale 2008).

Given the many physiological functions in which Eph receptors and ephrin ligands are involved in, it is not surprising that Eph/ephrin signalling produces various downstream effects. One of the main targets for Eph/ephrin signalling axes is the actin cytoskeleton. (Marston, Dickinson et al. 2003) observed that lamellipodia and filopodia only assemble in EphB4 receptor expressing cells and that the phosphorylated receptor co-localizes with

lamella and the tips of filopodia, suggesting that EphB4 receptor activation stimulates their formation. Also, Eph receptors can activate RhoA and inhibit Cdc42 and Rac kinases, shifting cytoskeleton dynamics towards increased contraction and reduced extension (Salvucci and Tosato 2012). Moreover, the Abelson family of non-cytoplasmic tyrosine kinases Abl and Arg (Abl related gene) can bind both phosphorylated and non-phosphorylated EphB2 and these interactions seem to play a critical role in actin cytoskeleton regulation during Eph-mediated axon pathfinding (Kullander and Klein 2002). Similarly, ephrinB ligands regulate the Rho family of GTPases and the phosphorylated tyrosines on their cytoplasmic tail act as docking sites for the Grb4 adaptor protein. Importantly, Grb4 can activate various proteins able to modulate cytoskeleton dynamics, such as Axin, CAP, Dynamin, FAK and paxillin (Cowan and Henkemeyer 2001).

E-cadherin plays an important role in the regulation of cell adhesion through Eph/ephrin signalling. More specifically, ectopic expression of E-cadherin in breast cancer cells, which lack endogenous E-cadherin, increased EphA2 phosphorylation and caused decreased cell adhesion to the extracellular matrix (Zantek, Azimi et al. 1999). Conversely, in colorectal cancer cells, stimulation of EphB3 expressing cells caused cell clustering and redistribution of E-cadherin to the cell membrane. Furthermore, down-regulation of E-cadherin impaired Eph-induced cell clustering and sorting (Cortina, Palomo-Ponce et al. 2007). Interestingly, this mechanism does not apply to heterotypic contacts between EphB3 expressing cells and ephrinB1 expressing cells. A subsequent study from the same group reported that EphB3/ephrinB1 signalling induces cell segregation between EphB3 and ephrinB1 expressing MDCK cells by inhibiting E-cadherin-mediated cell adhesion at heterotypic contacts. In this process, ephrinB1-induced activation of EphB3 stimulates ADAM10 activity, which, in turn, targets E-cadherin at sites of EphB3-ephrinB1 interaction (Solanas, Cortina et al. 2011). Thus,

through the modulation of E-cadherin activity, EphB receptors seem to possess the ability to increase adhesion between homotypic cell populations and form cell boundaries at sites of heterotypic contacts. However, the molecular mechanism underlying this process seems to differ depending on the type of EphB receptors and ephrinB ligands involved. A recent study by (Fagotto, Rohani et al. 2013) conducted on *Xenopus laevis* described a different mechanism of Eph/ephrin-induced formation of spatial boundaries between the notochord and the presomitic mesoderm tissues. The authors observed high expression levels of EphB4 in the presomitic mesoderm and high levels of ephrinB2 in the notochord. Disruption of EphB4/ephrinB2 signalling prevented the formation of spatial boundaries between these tissues. As E-cadherin clustering is enhanced upon inhibition of EphB4/ephrinB2 signalling and causes adhesion between heterotypic contacting cells, the authors concluded that EphB4/ephrinB2 signalling is responsible for the inhibition of E-cadherin clustering and for tissue separation by controlling myosin activity.

Studies have shown that Eph receptors and ephrin ligands can directly interact with claudins *in cis* and increase paracellular permeability by reducing claudin-4 integration in tight junctions. Interestingly, claudin-4 interaction with ephrinB1 on the extracellular domain caused ligand phosphorylation, which in turn affected intercellular adhesion (Tanaka, Kamata et al. 2005).

In neuronal cells of the central nervous system, EphB – ephrinB interactions are responsible for growth-cone collapse and axon pathfinding. Ephrin ligands also have a role in positionally selective synaptogenesis between motor neurons and muscle fibres (Klein 2001), while ephrinB2 PDZ-mediated reverse signalling upon EphB interaction is responsible for the recruitment of presynaptic machinery during the development of presynaptic and postsynaptic compartments (McClelland, Sheffler-Collins et al. 2009). Interestingly, the role of ephrinB

ligands in modulating physiological functions in the nervous system is mainly linked to phosphorylation-dependent reverse signalling (Bush and Soriano 2012). For example, mutation of all five tyrosines in mouse ephrinB2 resulted in defects in hippocampal long term potentiation (LTP) (Bouzioukh, Wilkinson et al. 2007), and postnatal pruning of mossy fibre axons was attributed to the phosphorylation-dependent reverse signalling initiated by ephrinB3 (Xu and Henkemeyer 2009).

Apart from affecting cell adhesion and repulsion, Eph/ephrin signalling can also modulate gene expression by cross-activating other receptors or via the JAK-STAT and the MAPK pathways (Poliakov, Cotrina et al. 2004). In fact, studies have shown that Eph activation reduces ERK activity thus inhibiting mitogenic signals and enhancing cytoskeleton modifications. Eph receptors are also able to induce or suppress integrin activity depending on the cellular context (Kullander and Klein 2002). For example, EphB2-dependent inhibition of cell adhesion involves phosphorylation and inactivation of R-Ras, which in turn suppress integrin-ECM interaction (Zou, Wang et al. 1999). By contrast, EphB1 signalling was found to enhance αVβ1 integrin-mediated cell adhesion in transfected human kidney cells (Huynh-Do, Stein et al. 1999).

1.1.4 EphrinB ligands

The three types of ephrinB ligands (ephrinB1, ephrinB2 and ephrinB3) are highly homologous, contain 333 to 346 amino acids in humans and their 33 aa C-terminal cytoplasmic tails are 95% identical. They are the main players in the Eph/ephrin reverse signalling pathway. The C-terminal region of these three proteins contains 5-6 conserved tyrosine residues, a polyproline stretch and a PDZ binding motif at the C-terminus (Gauthier and Robbins 2003). Referring to the human ephrinB2 ligand, the tyrosine residues are located at positions 304, 311, 316, 330 and 331. Interestingly, the ephrinB1 ligand has an additional tyrosine residue at position 313 (see table 1.1 for ephrinB cytoplasmic tail sequences and positions of tyrosine residues). EphrinB2 residues 311, 316 and 330 are phosphorylated during EphB receptor binding and serve as docking sites for SH2 domain-containing proteins, while the PDZ-binding motif acts as an independent binding site for PDZ domain-containing proteins. A study by (Kalo, Yu et al. 2001) on chicken ephrinB1, found that EphB receptor binding causes ligand phosphorylation on tyrosines at sites 312, 317 and 331 (corresponding to tyrosine residues 311, 316 and 330 in human ephrinB2, see table 1.1). In particular, they observed that tyrosine 331 in chicken ephrinB1 is highly phosphorylated upon receptor interaction, while tyrosines 312 and 317 are phosphorylated to a lesser degree. In human ephrinB2, tyrosines 330 and 331 are located within the last four amino acids of the C-terminal region, which corresponds to the PDZ binding motif. Using carboxyl-terminal peptides of ephrinB ligands, (Lin, Gish et al. 1999) reported that tyrosine phosphorylation at the -3 position impairs PDZ mediated binding of an adaptor protein syntenin-1, but not FAP1 (PTPL1), a PDZ domain-containing tyrosine phosphatase. Indeed, phosphorylation of tyrosines within the PDZ binding motif sequence is known to regulate PDZ mediated binding

in certain cases, as reviewed by (Ivarsson 2012). However, SH2 mediated signalling and PDZ mediated signalling are generally thought to be independent from each other, as the structural conformation of the last 33 amino acids of the C-terminal region of ephrinB ligands allows for both SH2 and PDZ interactions to occur simultaneously (Su, Xu et al. 2004). As the topic of SH2 versus PDZ binding is pivotal to the aims of this study, we will expand on it in greater detail later on in the introduction.

Protein	Species	Sequence of C-terminal 36 aa (Tyr highlighted)	aa positions
ephrinB1	*Homo sapiens*	NNYCPHYEKVSGDYGHPVYIVQEMPPQSPANIYYKV 313 317 324 329 343-344	311-346
ephrinB2	*Homo sapiens*	SVFCPHYEKVSGDYGHPVYIVQEMPPQSPANIYYKV 304 311 316 330-331	298-333
ephrinB3	*Homo sapiens*	PPFCPHYEKVSGDYGHPVYIVQDGPPQSPPNIYYKV 311 318 323 337-338	305-340
ephrinB1	*Gallus gallus*	NNYCPHYEKVSGDYGHPVYIVQEMPPQSPANIYYKV 301 305 312 317 331-332	299-334
ephrinB1	*Xenopus laevis*	NNYCPHYEKVSGDYGHPVYIVQEMPPQSPANIYYKV 296 300 307 312 326-327	294-329

Table 1.1: protein sequences of the C-terminal region of human ephrinB1, ephrinB2 and ephrinB3 (*Homo sapiens*); chicken ephrinB1 (*Gallus gallus*); and *Xenopus* ephrinB1 (*Xenopus laevis*). Tyrosine residues are highlighted and their positions within the wild type sequence are included. Information source: NCBI protein library.

1.1.4.1 EphrinB ligands' activation through phosphorylation

Upon EphB receptor interaction, ephrinB ligands are phosphorylated by Src family kinases (Palmer, Zimmer et al. 2002). This, however, is not necessary for ephrinB ligand phosphorylation by other tyrosine kinase receptors, such as FGF, PDGF, VEGF and ErbB receptors (Arvanitis and Davy 2008; Pasquale 2008; Pitulescu and Adams 2010; Vermeer, Colbert et al. 2013). Both ephrinB ligands and Src kinases are recruited to lipid rafts upon EphB receptor binding and clustering (Palmer, Zimmer et al. 2002). It has been reported that EphB/ephrinB binding causes cleavage of the ligand's extracellular domain by Matrix Metallo-Proteinases (MMP) and association with presenilin-1 (PS1). PS1 subsequently recruits γ-secretase which cleaves the C-terminal region of ephrinB to generate two cytoplasmic terminal fragments (CTF1 and CTF2). CTF2 is able to bind to PAG/Cbp, which is part of a tripartite complex with C-src kinase (Csk) inhibitor and Src (figure 1.6). This allows the detachment of Csk inhibitor from Src, thus allowing Src to auto-phosphorylate and become active. CTF2 is also able to bind directly to activated Src and further enhance its activity. As a result of PS1 – γ-secretase cleavage, the cytoplasmic domain of ephrinB1 can also translocate to the nucleus and enhance Zhx2 transcriptional activity to maintain neural progenitor state (Georgakopoulos, Litterst et al. 2006; Tomita, Tanaka et al. 2006; Wu, Qiu et al. 2009). Once Src is activated, it phosphorylates tyrosine residues on the C-terminal tail of ephrinB ligands which have not yet made contact with EphB receptors. This prevents γ-secretase from cleaving the ligand and creates SH2 docking sites for SH2 domain-containing proteins, such as Grb4 and STAT3 (Georgakopoulos, Litterst et al. 2006; Georgakopoulos, Xu et al. 2011). Studies have shown that after 2-5 minutes from EphB – ephrinB interaction, ephrinB ligands co-localize with Src family kinases, which reach their peak of

phosphorylation/activation within 10 minutes, together with ephrinB ligand phosphorylation. 30 minutes after the removal of EphB, PTP-BL (PTPL1), a PDZ domain-containing phosphatase, interacts with ephrinB ligands and reduces its level of phosphorylation thus terminating reverse signalling (Palmer, Zimmer et al. 2002). Another mechanism of signal termination involves ligand endocytosis and degradation: as (Foo, Turner et al. 2006) reported that prolonged ephrinB2 stimulation with EphB4/Fc caused complete depletion and degradation of the ligand.

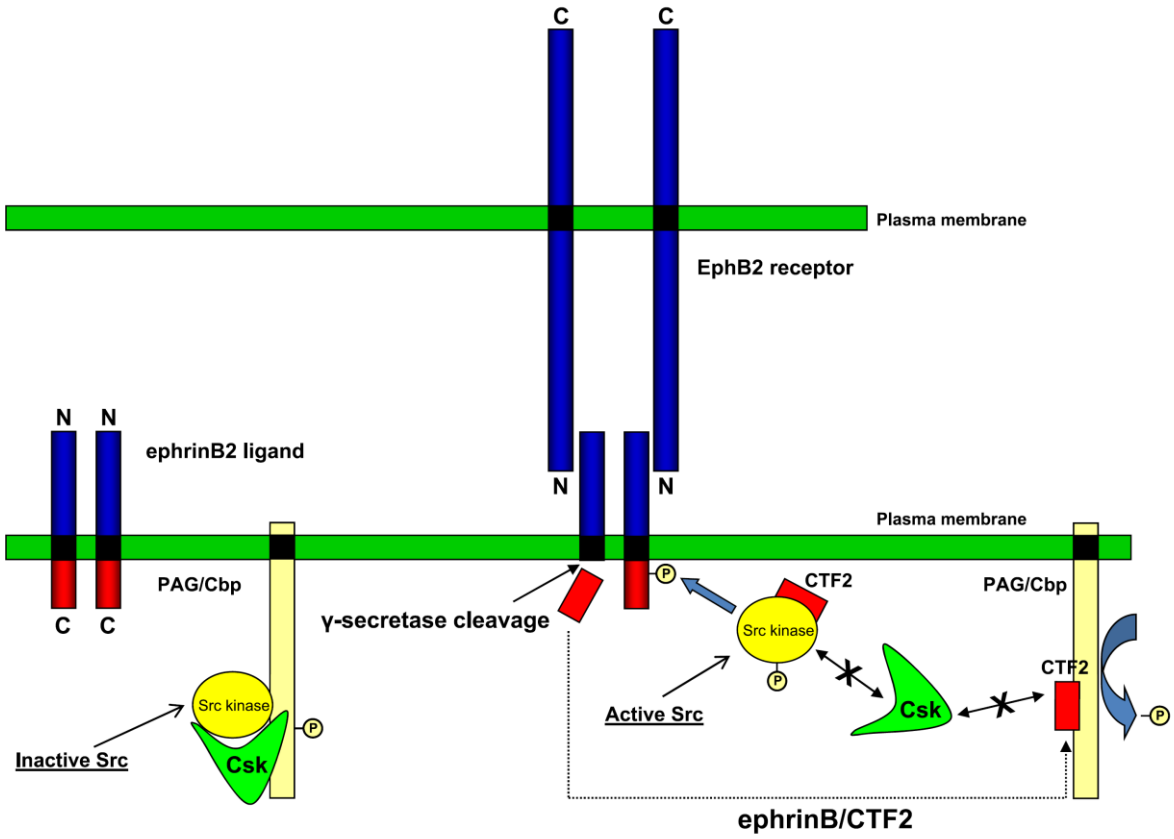

Figure 1.6: Src-mediated ephrinB2 phosphorylation mechanism as described by (Georgakopoulos, Xu et al. 2011).

1.1.4.2 EphrinB ligand signalling via Grb4 adaptor protein

Grb4 is an adaptor protein containing a single SH2 domain and three SH3 domains. When ephrinB ligands are phosphorylated, Grb4 binds to specific phospho-tyrosines via its SH2 domain and serves as a docking protein for SH3-binding domain-containing proteins (figure 1.7) (Andres and Ziemiecki 2003; Gauthier and Robbins 2003). In human ephrinB2, the 22 amino acids sequence in position 301-322, which contains 3 of the 5 conserved tyrosine residues, is fundamental for Grb4 binding (Cowan and Henkemeyer 2001; Su, Xu et al. 2004). In fact, phosphorylation of tyrosine residues at sites 311 and 316 increase protein structure flexibility. This facilitates phosphorylation of tyrosine site 304, generating the SH2-binding motif to which Grb4 binds (Song 2003; Su, Xu et al. 2004). A similar study by (Bong, Park et al. 2004) on *Xenopus* ephrinB1, reached the same conclusion and added that phosphorylation on Tyr300 (which the authors refer to as Tyr298 and which corresponds to Tyr304 in human ephrinB2) is induced by FGFR1 activation. Once bound to the cytoplasmic tail of ephrinB ligands, Grb4 acts as a scaffolding platform via its three SH3 domains, which are bound by various cytoskeletal regulating proteins, such as Abi-1,Axin, CAP, Dynamin, hnRNPK, Pak1, PINCH, DOCK180, Cbl and Abl tyrosine

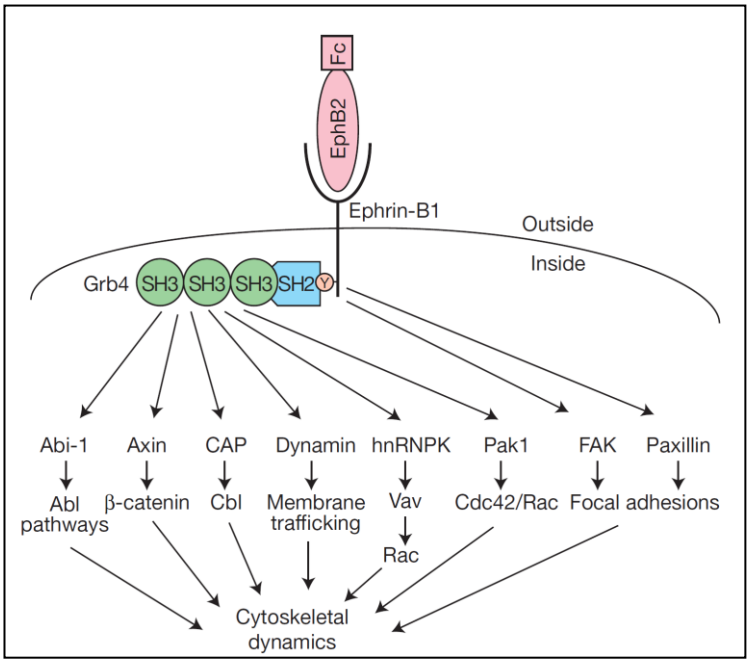

Figure 1.7: summary of proposed ephrinB pathways triggered through Grb4 binding (Cowan and Henkemeyer 2001).

kinase (figure 1.7). These proteins can then modulate cell adhesion and actin dynamics (inducing the loss of polymerized F-actin structures) and cause disassembly of focal adhesions (Cowan and Henkemeyer 2002; Kullander and Klein 2002). Also, Grb4 binding to phosphorylated ephrinB ligands has been shown to activate focal adhesion kinase (FAK), which induces cell rounding (Cowan and Henkemeyer 2001), through activation of the G protein-coupled receptor kinase-interacting protein (GIT) 1 (Segura, Essmann et al. 2007).

1.1.4.3 EphrinB ligands promote gene expression through STAT3

Another protein that binds to the phosphorylated C-terminal tail of ephrinB ligands via its SH2-binding motif is the transcription factor STAT3. In *Xenopus* ephrinB1, the tyrosine residue which serves as a docking site for this protein is located at position 312 (which the authors refer to as Tyr310 and which corresponds to Tyr316 in human ephrinB2). Although STAT3 is able to bind to any of the three phosphorylated ephrinB ligands, phosphorylation of tyrosine in position 296 (referred to as 294 by the authors and exclusive only to ephrinB1) of *Xenopus* ephrinB1 strongly enhances its binding to phospho-Tyr312 (referred to as 310 by the authors) (Bong, Lee et al. 2007). When the ligand is phosphorylated either through EphB interaction or by FGF receptor-mediated activation, STAT3 binds to phospho-Tyr312 (referred to as 310 by the authors) via its SH2 domain and is phosphorylated/activated by Jak2, which was found to interact with the C-terminal tail of non-phosphorylated *Xenopus* ephrinB1 (Bong, Lee et al. 2007). The transcription factor then separates from the ephrinB ligand, forms homodimers with other phosphorylated STAT3 proteins and translocates to the nucleus, where it induces gene expression of proteins involved in migration, survival,

apoptosis and modulation of inflammation (Bong, Lee et al. 2007). A study by (Salvucci, Maric et al. 2009) using human umbilical vein endothelial cells (HUVEC) and mesenchymal stem cells (MSC) (both expressing the ephrinB2 ligand and the EphB4 receptor on the cell surface) cultured in Matrigel-based 3D cultures, underlined the importance of Src and Jak2 kinases in the ephrinB reverse signalling pathway. In fact, silencing of the ephrinB2 ligand in this model prevented the formation of cord-like structures and this event could be mimicked by using Src and Jak2 inhibitors, thus highlighting the importance of these proteins during ephrinB reverse signalling events.

1.1.4.4 EphrinB ligands signal via Dishevelled

Activation of ephrinB ligands through phosphorylation of their tyrosine residues induces RhoA activation via Dishevelled and c-Jun N-terminal kinase (JNK) activation, which leads to cell rounding and detachment (Kullander and Klein 2002).

Dishevelled is a cytoplasmic protein containing a DIX, a PDZ and a DEP domain. It binds to SH3 domains of Grb4-bound proteins and by doing so is involved in ephrinB ligand signalling. Upon ephrinB phosphorylation, Grb4 binds to the SH2 docking sites of the ligand, allowing Dishevelled to bind to its SH3 domains and to recruit RhoA and ROCK, which mediate cell retraction. Interestingly, Dishevelled is also able to bind ephrinB ligands in non-phosphorylated conditions. This interaction, however, is not PDZ domain-dependent, but relies on the protein's DEP domain (Lee, Bong et al. 2006). Moreover, when ephrinB ligands are phosphorylated, Dishevelled is phosphorylated as well, although the functional meaning of this event is still unclear (Tanaka, Kamo et al. 2003). It could either be induced by ephrinB

ligand phosphorylation together with SH2 domain-containing proteins or by phosphorylation independent activation of JNK (Xu, Lai et al. 2003). In the retina, knock down of Dishevelled prevented ephrinB1 expressing retinal progenitor cells from dispersing to the eye field. The same phenotype was observed upon knock down of ephrinB1, which could be rescued by over-expression of Dishevelled (Lee, Bong et al. 2006). A later study from the same group reported that FGFR-induced phosphorylation of *Xenopus* ephrinB1 on Tyr326 and 327 (which correspond to Tyr330 and 331 in human ephrinB2; referred to as Tyr324 and 325 by the authors) disrupted ephrinB1 – Dishevelled interaction, thus modulating progenitor cell movement (Lee, Mood et al. 2009).

1.1.4.5 PDZ-mediated signalling in ephrinB ligands

EphrinB ligands contain a PDZ binding motif at the C-terminus of their cytoplasmic tail, which is formed by the last four C-terminal amino acids. This motif is fundamental to the physiological role of ephrinB ligands. Moreover, PDZ-derived signalling through interacting PDZ domain-containing proteins is often independent of Eph – ephrin interaction and SH2/phospho-tyrosine mediated signalling (Pasquale 2008). Many PDZ domain-containing proteins have been found to interact with the PDZ binding motif of ephrinB ligands, such as PTPL1 (FAP1), GRIP1, GRIP2, PDZ-RGS3, PICK1, PAR3 and syntenin-1 (figure 1.8). It has been hypothesized that some of these proteins might be able to facilitate assembly of ephrinB ligands in supramolecular signalling complexes and modulate their activation by cluster formation (Lin, Gish et al. 1999; Cowan and Henkemeyer 2002; Kullander and Klein 2002; Gauthier and Robbins 2003). An early study by (Lin, Gish et al. 1999) reported that ephrinB1

tyrosine phosphorylation at position -2, which is located within the PDZ binding motif of ephrinB ligands, impairs PDZ mediated-binding of syntenin-1. However, phosphorylation of tyrosine at position -3 does not influence PDZ binding. The same study also reported that FAP1 binding to ephrinB ligands remains unaffected by phosphorylation of either tyrosine at position -2 or -3. Another study has shown that PDZ binding of PDZ-RGS3 is not affected by any phosphorylation events of tyrosine residues present within the last C-terminal 33 amino acids of ephrinB ligands (Su, Xu et al. 2004). In a similar way, GRIP1 and GRIP2 binding to ephrinB2 is not affected by tyrosine phosphorylation on the cytoplasmic tail, but is enhanced upon phosphorylation of serine at position -8 (Essmann, Martinez et al. 2008). These reports suggest that ephrinB ligand phosphorylation modulates PDZ mediated-binding of specific PDZ domain-containing proteins. Indeed, modulation of PDZ binding via phosphorylation of tyrosine, serine and threonine residues located within the PDZ binding motif sequence, or in close proximity to it, has been reported in many other protein-protein interactions (Ivarsson 2012).

The importance of the PDZ binding motif in ephrinB ligands under physiological conditions was highlighted by *in vivo* experiments (Bush and Soriano 2012). In a study by (Makinen, Adams et al. 2005), the authors reported that mice expressing a truncated form of the ephrinB2 ligand, lacking the C-terminus region, showed lymphatic vascular malformation and died in embryonic stage, while mice expressing a version of the ligand which was mutated at tyrosine phospho-sites survived. This suggests that the PDZ binding motif of the ephrinB2 ligand is fundamental for lymphatic vascular formation, but probably not for blood vascular remodelling.

Another study also highlighted the importance of PDZ-mediated reverse signalling of ephrinB1 in normal axon guidance during formation of the corpus callosum. Phosphorylation-

mediated reverse signalling does not play a role in this process or impairs PDZ-mediated signalling (Bush and Soriano 2009).

At the cellular level, the PDZ binding motif is critical for modulating cell contraction and membrane blebbing in ephrinB2 ligand expressing cells even in the absence of EphB4 receptor interaction. This is necessary to promote increased cell mobility and migration, which are Grb4 and Rac dependent. This observation proves that PDZ-mediated signalling can happen independently of ephrinB stimulation by EphB receptors and is able to regulate different aspects of ephrinB ligands functions (Bochenek, Dickinson et al. 2010).

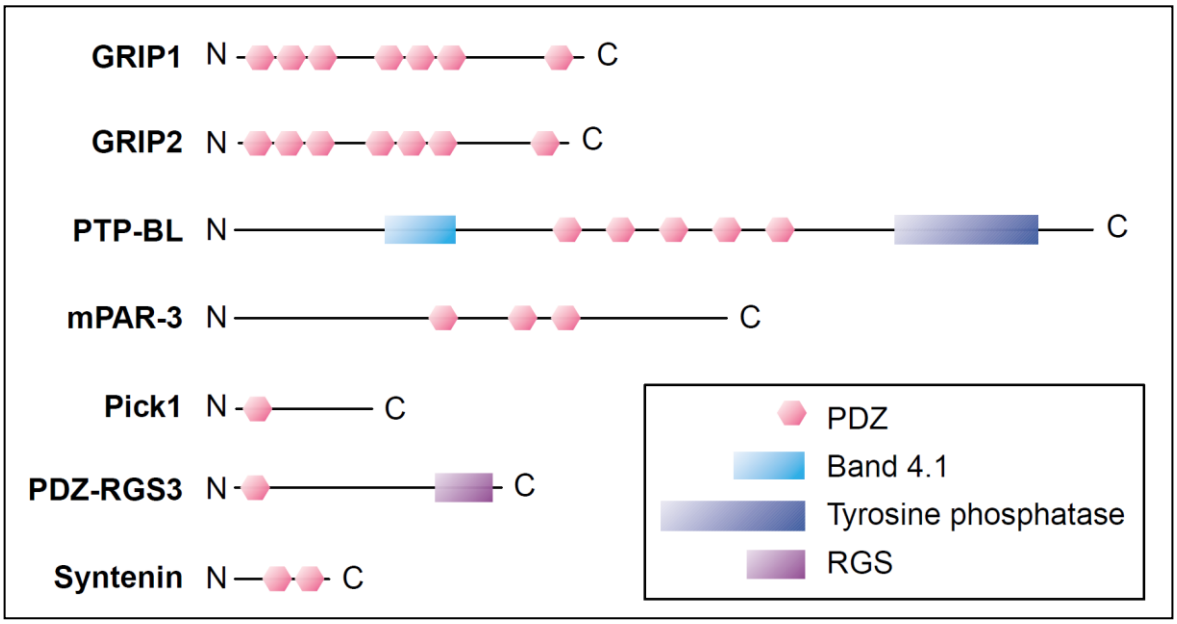

Figure 1.8: PDZ domain-containing proteins which interact with ephrinB ligands (Cowan and Henkemeyer 2002).

1.1.4.6 EphrinB ligands signal through various PDZ domain-containing proteins

FAP1 (PTPL1) is a PDZ domain-containing tyrosine phosphatase and binds to ephrinB ligands via its fifth PDZ domain (Lin, Gish et al. 1999). Currently, it is the only phosphatase known to de-phosphorylate ephrinB ligands (Gauthier and Robbins 2003). Recently it has been described as a tumour suppressor, as its decreased expression in breast cancer correlates with poor overall patient survival rate (Vermeer, Bell et al. 2012). Studies have shown that PTPL1 co-localizes with ephrinB ligands and Src family kinases in lipid rafts and when it binds to the PDZ domain of ephrinB ligands it can de-phosphorylate both the ligand and Src kinases (Palmer, Zimmer et al. 2002).

In neuronal cells, syntenin-1 acts as a homodimerized scaffolding protein and binds to the PDZ binding motif of ephrinB ligands, possibly forming complexes necessary during maturation of presynaptic specializations (Cowan and Henkemeyer 2002). Recent data has emphasized the importance of syntenin-1 in EphB-dependent development of presynaptic and postsynaptic compartments via ephrinB1 and ephrinB2 ligands (McClelland, Sheffler-Collins et al. 2009). Moreover, syntenin-1 binding to ephrinB3 is required during ephrinB3-driven dendrite pruning and synapses formation upon EphB receptor stimulation (Xu, Sun et al. 2011).

PDZ-RGS3 is a regulatory protein which acts as a GTPase-activating protein (GAP) for the α-subunits of trimeric G proteins. When it binds to ephrinB ligands via its PDZ domain it can neutralize C-X-C chemokine receptor type-4 (CXCR4) attraction to stromal cell-derived factor-1 (SDF-1), thus allowing inward migration of cerebellular granule cells (Cowan and Henkemeyer 2002). Interestingly, a study by (Makinen, Adams et al. 2005) found that PDZ-

RGS3 localization in lymphatic vessel endothelium was disturbed in ephrinB2$^{\Delta V/\Delta V}$ mutant mice and suggested that the ephrinB2 – PDZ-RGS3 axis might be involved in cell migration during remodelling of the lymphatic vasculature. A more recent study in HUVEC cells also found that ephrinB2-induced cell motility, independently of stimulation by EphB receptors, requires the PDZ-mediated interaction between the ligand and PDZ-RGS3 (Bochenek, Dickinson et al. 2010). Finally, an *in vivo* study on the role of PDZ-RGS3 in maintaining self-renewal processes in neuronal progenitor cells, found that loss of PDZ-RGS3 mimicked the loss of ephrinB1 and caused progenitor cells to differentiate (Qiu, Wang et al. 2010). Therefore, the authors concluded that the ephrinB1 – PDZ-RGS3 axis might be essential in the maintenance of neuronal progenitor cells.

GRIP proteins are multi PDZ domain-containing scaffolding proteins which have the postulated role of clustering other proteins containing PDZ binding motifs together. GRIP is able to bind EphB2 and EphA7 receptors and ephrinB ligands through its PDZ domains 6 and 7. It is also able to bind AMPA receptors via its 4th and 5th PDZ domain, thus allowing GRIP to act as a bridge between ephrinB ligands and AMPA receptors (Torres, Firestein et al. 1998). Early studies reported that ephrinB ligands are able to recruit GRIP proteins to lipid rafts via PDZ-mediated interaction (Bruckner, Pablo Labrador et al. 1999). More recently, EphB2-driven ephrinB2 phosphorylation on Ser325 has been identified as a positive switch for PDZ-mediated GRIP binding, which in turn regulates AMPA receptors turnover at post-synaptic sites (Essmann, Martinez et al. 2008).

PICK1 contains a single PDZ domain and mediates clustering of ephrinB ligands, albeit not when EphB2 is co-expressed in the same cell. Given its ability to interact with PKC, it has been postulated that this protein might functionally couple ephrinB ligands with other signalling cascades (Torres, Firestein et al. 1998). In neurons, ephrinB3 has been shown to

regulate dendrite pruning and synapses formation upon EphB receptor stimulation via PDZ-mediated binding to PICK1 (Xu, Sun et al. 2011).

Through the PDZ binding motif, ephrinB ligands also play a role in organizing cytoskeletal complexes that are involved in establishing or maintaining cell polarity via PAR3 activity. This protein binds to ephrinB ligands via its second or third PDZ domain and forms ternary complexes with atypical protein kinase C (aPKC) and PAR6. These complexes, after binding and activating Cdc42 and Rac1, regulate asymmetrical cell division and establish and maintain cell polarity (Cowan and Henkemeyer 2002). Association of ephrinB1 with PAR6 can also modulate cell-cell adhesion and paracellular permeability through the formation of tight junctions. EphrinB1 competes with Cdc42 for association with PAR6, which constitutively binds aPKC. Upon ephrinB1 phosphorylation caused by EphB receptors *in trans* or FGF receptors and claudins *in cis*, PAR6 dissociates from ephrinB1 and associates with Cdc42. This causes activation of aPKC, which induces the formation of tight junctions (Lee, Nishanian et al. 2008).

1.1.4.7 EphB/ephrinB endocytosis pathway

The endocytic process triggered by receptor/ligand interaction involves the whole EphB/ephrinB complex, which can be internalized either in the EphB receptor or the ephrinB ligand expressing cell. This particular type of endocytosis is called *trans*-endocytosis (illustrated in figure 1.9). However, while in EphB receptor expressing cells the kinase domain is required for complex endocytosis, internalization of the complex into ephrinB-expressing cells may not be dependent on ligand phosphorylation or PDZ-mediated reverse signalling (Pitulescu and Adams 2010). The internalization of the EphB/ephrinB complex starts 10 minutes after cell contact. During the initial stages of *trans*-endocytosis, the receptor/ligand complex is mostly internalized in ephrinB ligand expressing cells. After 60 minutes from cell contact, this process is reversed, and most of the internalized complex can be observed within EphB receptor expressing cells (Zimmer, Palmer et al. 2003). Interestingly, stimulation of ephrinB2 expressing cells with an EphB4/Fc chimeric protein for time periods longer than 2 hours caused a total depletion of ephrinB2 from the cell surface for up to 24 hours, while stimulation for 1 hour did not. This suggests that ephrinB expressing cells might be able to terminate reverse signalling through ligand internalization and degradation (Foo, Turner et

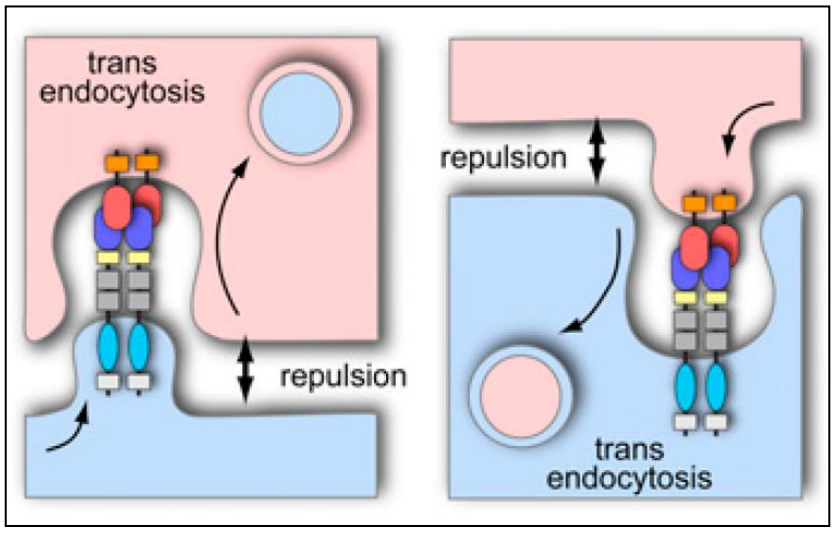

Figure 1.9: *trans*-endocytosis of the EphB/ephrinB complex can occur in either the EphB or ephrinB expressing cell (Pitulescu and Adams 2010).

al. 2006). Truncation of the cytoplasmic tail of EphB receptors causes *trans*-endocytosis to be directed only towards ephrinB ligand expressing cells, while truncation of the cytoplasmic tail of the ligand inverts this process and allows internalization to occur only into the receptor expressing cell. Interestingly, truncation of the cytoplasmic tail of both receptor and ligand simultaneously completely abolishes the *trans*-endocytosis process and results in strong cell adhesion (Zimmer, Palmer et al. 2003). Various studies have revealed that *trans*-endocytosis does not follow a canonical endocytic pathway, as the vesicles containing the receptor/ligand complex do not co-localize with any known endocytic markers, including clathrin and caveolin. Instead, it is thought that the mechanism driving this process resembles phagocytosis or macro-pinocytosis. In fact, activation of Rho GTPases and actin polymerization are needed during *trans*-endocytosis. In this respect, Cdc42 has been shown to promote the formation of filopodia and dendritic spines, and Rho-A to regulate actin dynamics, cell contractility and phagocytosis (Marston, Dickinson et al. 2003; Zimmer, Palmer et al. 2003; Groeger and Nobes 2007; Pitulescu and Adams 2010). In spite of this, it has been suggested that trans-endocytosis of the EphB/ephrinB complexes into ephrinB-expressing cells may, in fact, involve clathrin. In this regard, ephrinB ligands do have three conserved YXXϕ sequences (with X representing any aminoacid and ϕ a hydrophobic aminoacid) within the terminal 33 amino acids of their cytoplasmic tails, which might serve as target sequences for clathrin-dependent endocytosis adaptor proteins (AP) (Traub 2003; Edeling, Smith et al. 2006). In one study, internalized vesicles containing the EphB/ephrinB complex co-localized with the endocytic marker for early endosomes EEA1 and blocking dynamin or lowering potassium concentration inhibited ephrinB1 internalization upon EphB1 stimulation (Parker, Roberts et al. 2004). Eph receptors were also found to concentrate in caveolae enriched regions on the cell membrane and EphB1 was reported to associate with

caveolin-1. This suggests that Eph signalling might be able to control both the early and late phases of clathrin-mediated endocytosis (Vihanto, Vindis et al. 2006). In this regard, EphB receptors have also been reported to inhibit the late phases of clathrin-mediated endocytosis by inducing phosphorylation of synaptojanin-1, thus inhibiting its association with endophilin and impairing clathrin un-coating (Irie, Okuno et al. 2005).

After internalization of the EphB/ephrinB complex, EphB receptors maintain their phosphorylation status and possibly their signalling activity until they are processed for degradation (Zimmer, Palmer et al. 2003; Pitulescu and Adams 2010). *Trans*-endocytosis of the receptor/ligand complex allows the contacting cells to retract from one another. At this point EphB receptor expressing cells round up and then re-spread. Interestingly, receptor/ligand internalization within EphB receptor expressing cells is not necessary for cell retraction, but is fundamental for cell re-spreading. This process takes place even in the constant presence of ephrinB2/Fc chimeric protein, suggesting that active ephrinB/EphB complex is critical for re-spreading in EphB receptor expressing cells (Groeger and Nobes 2007).

1.1.4.8 EphB/ephrinB processing by proteolytic cleavage

Proteolytic cleavage can also be triggered by Eph/ephrin interaction. This process involves both EphB receptors and ephrinB ligands. After binding to ephrinB2, the EphB2 receptor is cleaved by MMP-2 and MMP-9 at two sites of the protein, producing two soluble fragments: an extracellular long fragment and an intracellular fragment. Interestingly, only one of the two cleavage sites of EphB2 is conserved in EphB3 and EphB1, suggesting that

Eph receptors can be processed differently. Moreover, MMP mediated EphB2 receptor cleavage induced by ephrinB2 ligand interaction is necessary for cell repulsion events and EphB2 receptor phosphorylation and activation. In fact, in the absence of MMP cleavage, the EphB2 receptor is rapidly de-phosphorylated, which suggests that MMP mediated cleavage can regulate duration of EphB2-dependent signalling (Lin, Sloniowski et al. 2008).

Proteolytic cleavage also affects ephrinB ligands. Binding of the EphB2 receptor to ephrinB1 stimulates secretion of MMP-8 through PDZ-mediated reverse signalling and activation of Arf1. MMP-8 then cleaves the extracellular domain of the ephrinB1 ligand, producing a 35 kDa soluble fragment which retains the ability to inhibit motility of EphB2 receptor expressing cells. Moreover, ephrinB1 ligand extracellular cleavage acts as a negative feedback event for future EphB2 – ephrinB1 interactions (Tanaka, Sasaki et al. 2007). Other reported proteolytic cleavage events include ephrinB ligands cleavage by PS1 and γ-secretase (described in section 1.1.4.1), ADAM10 and γ-secretase cleavage of EphB receptors upon ephrinB ligand interaction (Arvanitis and Davy 2008) and also human rhomboid intramembrane serine protease (RHBDL2) cleavage of ephrinB3 ligands at the transmembrane domain when bound to EphB receptors (Tanaka, Sasaki et al. 2007).

1.1.4.9 Cross-talk between ephrinB ligands and tyrosine kinase receptors

EphrinB ligands were shown to interact with other tyrosine kinase receptors, such as PDGF, FGF, VEGF and ErbB receptors (Kullander and Klein 2002; Poliakov, Cotrina et al. 2004; Arvanitis and Davy 2008; Pasquale 2008; Pitulescu and Adams 2010; Vermeer, Colbert et al. 2013). EphrinB1 is able to physically interact with FGF receptors and is phosphorylated

on tyrosine as a consequence. Specifically, the aminoacid sequence between position 302 and 308 as well as tyrosine phosphorylation on residues 305 and 310 in *Xenopus* ephrinB1 are required for its association with FGF receptors. Moreover, ligand-induced stimulation of FGF receptors leads to endogenous tyrosine phosphorylation of ephrinB1. This phosphorylation event depends on the FGF receptor kinase domain and is independent from Src kinase activation (Chong, Park et al. 2000). A later study from the same group also reported that FGF-dependent phosphorylation of *Xenopus* ephrinB1 triggers Grb4-mediated reverse signalling (see section 1.1.4.2) (Bong, Park et al. 2004). Conversely, ephrinB ligands can be involved in regulation of cellular responses to FGFs. Specifically, ephrinB2 was linked to FGF receptor signalling through syndecans. Stimulation of ephrinB2 causes expression and shedding of syndecan-1 from the membrane, which then forms complexes with FGF receptors and inhibits its activity (Yuan, Hong et al. 2004).

EphrinB ligands are functionally linked with VEGF receptor signalling and this has a fundamental role in the formation of new vessels and angiogenesis. EphrinB2 is expressed in endothelial cells together with VEGFR-2 and VEGFR-3. Upon VEGF stimulation, ephrinB2 is activated and co-localizes with VEGF receptors. In turn, ephrinB2 reverse signalling activates VEGF receptors and mediates their internalization, which triggers activation of ERK1/2 and Akt signalling pathways (Germain and Eichmann 2010; Sawamiphak, Seidel et al. 2010). In ephrinB2 knock-out mice, VEGFR-3 activation by VEGF-C is impaired, causing down-regulation of Rac1, Akt and ERK1/2 activation (Wang, Nakayama et al. 2010). The PDZ binding motif of ephrinB2 is essential for its association with VEGF receptors. Moreover, activation and internalization of these receptors are driven by PDZ-mediated reverse signalling (figure 1.10). On the other hand, tyrosine phosphorylation of the cytoplasmic tail of ephrinB2 is not required (Germain and Eichmann 2010; Pitulescu and

Adams 2010; Sawamiphak, Seidel et al. 2010; Wang, Nakayama et al. 2010). In a more recent study, (Nakayama, Nakayama et al. 2013) reported that ephrinB2-induced internalization of VEGFR-2 and VEGFR-3 is mediated by PAR3 and the clathrin-associated sorting protein disabled-2 (Dab2) in a clathrin-dependent manner. More specifically, PAR3 recruits Dab2 to VEGFR-2, VEGFR-3 / ephrinB2 complexes via PDZ interactions with the PDZ binding motif of ephrinB2, thus mediating internalization of the protein complex. Interestingly, VEGF stimulation of VEGF receptor positive endothelial cells also induced aPKC phosphorylation, which in turn prevented VEGF receptor internalization in a seemingly negative feedback loop.

Other tyrosine kinase receptors, such as PDGF receptors and tie-2 receptor, can also associate and phosphorylate ephrinB ligands *in cis* upon activation (Palmer, Zimmer et al. 2002; Bong, Park et al. 2004). For example, in hepatic stellate cells PDGF signalling through ephrinB2 regulates cell motility and vascular coverage in the liver (Das, Shergill et al. 2010).

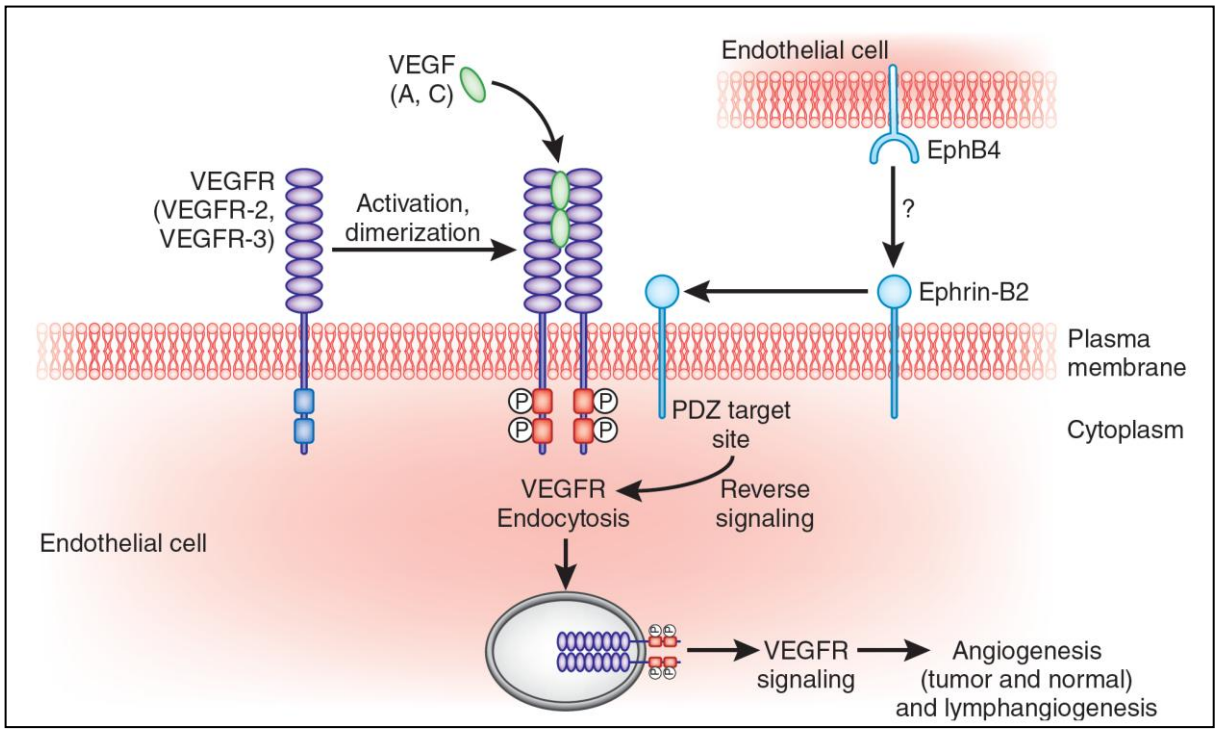

Figure 1.10: VEGF receptor internalization is mediated by PDZ-mediated ephrinB2 reverse signalling (Germain and Eichmann 2010).

Finally, ephrinB1 associates with ErbB2 and ErbB1 by directly interacting through their transmembrane domains. Moreover, ephrinB1 – ErbB1,2 complexes co-localize at cell-to-cell junctions (Vermeer, Colbert et al. 2013). High levels of ErbB2 are concomitant with high levels of ephrinB1 phosphorylation and consequent increase in ERK1/2 activation (Vermeer, Bell et al. 2012; Vermeer, Colbert et al. 2013).

1.1.5 EphB receptors and ephrinB ligands are involved in cancer progression

Within the vast field of cancer research, significant attention has been focused on angiogenesis and metastasis, the former being fundamental for tumour growth and the latter for malignant disease progression. Given their role in modulating cell migration, adhesion and repulsion, it is not surprising that Eph tyrosine kinase receptors and their cognate ephrin ligands are considered to be pivotal proteins in cancer angiogenesis and metastasis. Indeed, Eph receptors and/or ephrin ligands are de-regulated in most types of cancer cells (Pasquale 2008; Genander and Frisen 2010; Nievergall, Lackmann et al. 2012). Moreover, de-regulation of Eph/ephrin signalling promotes the development of aggressive metastatic tumours (Lee and Daar 2009). In support of this, recent studies have reported that gene inactivation by CpG hyper-methylation in the promoter region of various Eph receptors and ephrin ligands is linked with increased aggressiveness of several types of tumours, including colorectal, prostate and breast cancer (Arvanitis and Davy 2012). Various studies have also found a strong correlation between higher expression levels of many Eph/ephrin family members and increased invasiveness of a number of aggressive tumours (Liu, Jung et al. 2004; Campbell and Robbins 2008).

Data collected from many studies has proven that only in exceptional cases does Eph/ephrin protein up-regulation increase the cell proliferation rate. Rather, the involvement of Eph/ephrin signalling axes in tumourigenesis is likely to be linked with regulation of cell-ECM and cell-cell adhesion or repulsion, both of which increase cell motility and metastasis. Usually, high expression levels of Eph receptors and low levels of ephrin ligands facilitate tumour growth and metastasis, as seen in breast, colon, liver and prostate carcinomas (Mosch,

Reissenweber et al. 2010). In other cases, such as uterine cancer, high co-expression of the EphB4 receptor and ephrinB2 ligand was found to enhance proliferation, migration and invasion of tumour cells, and this correlated with grade and stage of the tumour and poor prognosis for patients (Alam, Fujimoto et al. 2007). In malignant glioblastomas, ephrinB2 and ephrinB1 ligands are over-expressed and highly phosphorylated, which also correlates with poor prognosis and overall survival of patients (Nakada, Anderson et al. 2010). Although many members of the Eph/ephrin superfamily are up-regulated in cancer, some advanced forms of tumour show down-regulated levels of these proteins. It has been hypothesized that initial Eph receptor up-regulation could subsequently be switched off through hyper-methylation of its gene promoter region (Brantley-Sieders 2012). Table 1.2 lists all reported cases of abnormal expression of EphB and ephrinB proteins in various different types of cancer.

Other reports have shown that tumour associated cytokines and growth factors, such as tumour necrosis factor-α (TNFα) and vascular endothelial growth factor A (VEGFA), as well as stress conditions such as cyclic stretch and hypoxia, up-regulate various Eph receptors and ephrin ligands. Mutations within the tyrosine kinase and the ephrin binding domains of Eph receptor genes have also been identified in human gastric, prostate and colorectal tumours and melanoma. Other cancer associated genetic changes involve loss of heterozygosity (Pasquale 2010). Because phosphorylated Eph receptors suppress tumour cell growth by inhibiting oncogenic pathways, such as h-Ras-ERK, PI3K-Akt and Abl-Crk pathways, it is feasible that these mutations might indirectly promote tumour growth. In fact, up-regulation of Eph receptors leads to their reduced activation. This suggests that the pro-oncogenic effect of Eph receptors over-expression depends on their role as activators of ephrinB reverse signalling (Pasquale 2010).

Within the B subclass of the Eph receptor and ephrin ligand superfamily, EphB4 and EphB2 receptors and ephrinB2 and ephrinB1 ligands are the most studied in cancer progression. These proteins are over-expressed in highly invasive and metastatic tumours and their expression levels correlate with clinical stage and histological grade of many cancers (Campbell and Robbins 2008). EphB2 receptor expression, for example, was found to negatively associate with overall survival of breast cancer patients, while EphB4 receptor protein levels increased with clinical stage and histological grade of the tumour (Wu, Suo et al. 2004). EphB4 receptor and ephrinB2 ligand expression levels are modulated by different signalling pathways. In more than half of known breast cancers and tumour cell lines, the

Eph B class family member	Cancer type	↑/↓ Relative to normal tissue
EphB1	Colon	↓ (Transition to invasive cancer)
	Gastric	↓ (Transition to invasive cancer)
EphB2	Breast	↑
	Colon	↑/↓ (Transition from adenoma to carcinoma)
	Gastric	↓
	Glioblastoma	↑ Tyrosine phosphorylation
	Neuroblastoma	↑ (Higher levels in low stage)
	Hepatocellular	↑
EphB3	Colon	↑/↓ (Transition from adenoma to carcinoma)
	Lung (NSCLC)	↑
EphB4	Breast	↓/↑
	Ovarian	↑
	Cervix	↑ (Correlates with MVD)
	Endometrium	↑
	Colon	↑/↓ (Transition from adenoma to carcinoma)
	Prostate	↑
EphB6	Breast	↓/↑
	Glioma	↑ Variant protein
	Neuroblastoma	↑ (Higher levels in low stage)
	Melanoma	↓
Ephrin-B1	Ovarian	↑
	Glioblastoma	↑ Total and tyrosine phosphorylated
	Hepatocellular	↑ Associated with tumor angiogenesis
Ephrin-B2	Ovarian	↑
	Cervix	↑ (Correlates with MVD)
	Endometrium	↑
	Colon	↑
	Esophageal	↑
	Glioblastoma	↑ Total and tyrosine phosphorylated
	Melanoma	↑
Ephrin-B3	Ovarian	↑
	Glioblastoma	↑/increased tyrosine phosphorylation
	Neuroblastoma	↑ (Higher levels in low stage)

Table 1.2: expression profile of EphB receptors and ephrinB ligands in human epithelial malignancies (Brantley-Sieders 2012).

EphB4 receptor is up-regulated by JNK, Akt and Wnt pathways and also by oestrogen-controlled gene expression and gene amplification. Interestingly, the Wnt pathway can down-regulate the ephrinB2 ligand in the same cancers and cell lines (Noren and Pasquale 2007).

Only in a few cases has EphB/ephrinB signalling been linked with an increase in cell proliferation. In a study by (Steinle, Meininger et al. 2002), stimulation of EphB4 receptor with ephrinB2/Fc soluble ligand caused a 38% increase in endothelial cell proliferation. The same stimulation also caused a 63% increase in migration and both of these effects could be inhibited by using ERK1/2 or Akt inhibitors, which suggests that cell proliferation and migration might be linked in this particular case. A recent study by (Vermeer, Colbert et al. 2013) has also revealed that ephrinB1 association with ErbB1 or ErbB2 induces ERK1/2 phosphorylation, thus promoting cell proliferation and survival.

1.1.5.1 EphB receptors and ephrinB ligands induce cancer angiogenesis

Hypoxia is a common stress condition in cancer tissues and it can influence many aspects of cell survival and gene expression. For example, it can up-regulate HIF-1α, a protein which plays a pivotal role in cancer angiogenesis. Interestingly, it has also been shown to reduce EphB4 receptor levels and promote ephrinB2 ligand expression indirectly through VEGFR up-regulation in the tumour-associated endothelium (Bochenek, Dickinson et al. 2010; Mosch, Reissenweber et al. 2010). Indeed, ephrinB2 is up-regulated in both physiological and pathological angiogenesis (Wang, Nakayama et al. 2010). Increase in ephrinB ligand expression has widely been associated with increased tumour angiogenesis (Kandouz 2012). For instance, high levels of ephrinB1 in hepatocellular carcinoma (HCC)

tissues increase tumour vessel number in vivo (Sawai, Tamura et al. 2003). In malignant melanoma, increased expression of ephrinB2 correlates with higher tumour vascularisation (Vogt, Stolz et al. 1998). Furthermore, ephrinB2 mRNA levels were found to be higher in metastatic melanoma cell lines rather than in the primary isogenic counterpart (Liu, Jung et al. 2004). EphrinB2 is also involved in the modulation of mammary gland vascularisation (Haldimann, Custer et al. 2009), which will be described in more detail further on in this chapter.

At the molecular level, VEGF-triggered changes in expression of EphB4 and ephrinB2 involve the Delta-Notch signalling pathway. The ultimate effect of this process is to turn venous endothelial cells into arterial cells, thus enhancing angiogenesis (Hainaud, Contreres et al. 2006). Conversely, activation of ephrinB2 induces VEGFR-2 internalization and activation, thereby controlling tip cell filopodial extension and vascular sprouting, which initiate angiogenesis (Sawamiphak, Seidel et al. 2010). Also, ephrinB2 activates JNK and PI3K pathways, which both stimulate protease release into the extracellular matrix and cause its degradation. This facilitates endothelial invasion of cells to the surrounding tissue and forms new vessels within the growing tumour (Noren, Lu et al. 2004). The EphB4 receptor, which is expressed in the majority of the tumour tissue, also plays an important role in the angiogenic process by acting as a positive cue for endothelial ephrinB2 ligand expressing cells (Merlos-Suarez and Batlle 2008). In fact, deletion of either the EphB4 receptor or the ephrinB2 ligand in these interacting cells produces an identical phenotype and ultimately inhibits tumour growth (Hainaud, Contreres et al. 2006).

1.1.5.2 The role of EphB receptors and ephrinB ligands in cancer metastasis

EphrinB ligands also play an important role in regulating tumour metastasis (Kandouz 2012). For example, elevated ephrinB2 expression in oesophageal squamous carcinomas induces metastatic progression (Tachibana, Tonomoto et al. 2007). In migrating and invading glioma cells, ephrinB2 and ephrinB3 were over-expressed and highly phosphorylated (Nakada, Drake et al. 2006; Nakada, Anderson et al. 2010).

Various studies have reported that the ephrinB2 – EphB4 axis is responsible for inducing or suppressing cancer metastasis depending on the tumour type. In melanoma cells, ephrinB2-mediated activation of EphB4 increases cell migration via RhoA activation (Yang, Pasquale et al. 2006). By contrast, ephrinB2-stimulated EphB4 inhibits motility and invasion of breast cancer cells via a pathway which involves Abl family tyrosine kinases and Crk (Noren, Foos et al. 2006). EphrinB2 reverse signalling is also involved in regulating cancer metastasis. Over-expression of a mutant form of ephrinB2 with a truncated cytoplasmic tail promotes metastasis of mammary tumours and results in a tumour phenotype presenting a majority of cells with stem/progenitor characteristic (Kaenel, Antonijevic et al. 2012). The ability of ephrinB2 to reverse signal is fundamental to keep EphB4 activated and regulate its expression by causing its internalization and degradation after receptor/ligand interaction. If reverse signalling is defective, EphB4 expression on neighbouring cells increases and this event ultimately may promote metastasis (Harburg and Hinck 2011). In other cases, ephrinB ligand reverse signalling can also cause cancer cell migration and invasion by promoting Src and Rac1 activation (Pasquale 2010). In human brain glioblastoma tumours, ephrinB2 phosphorylation induced cellular migration and invasion in the glioblastoma cell line U251

(Nakada, Anderson et al. 2010). Additionally, ephrinB2 up-regulation has been shown to enhance integrin-mediated attachment, while ephrinB1 up-regulation induces MMP-8 secretion, which promotes invasion, and STAT3 activation, which is involved in cancer progression (Tanaka, Sasaki et al. 2007; Pasquale 2010).

1.1.5.3 Breast cancer and the EphB4/ephrinB2 model in mammary gland carcinoma

Breast cancer is the most common cancer in women. In 2008-2010 in the UK, the rate of breast cancer incidence in women was 126 per 100,000, more than three times higher than the second most common cancer in women, which is lung cancer (40 per 100,000 women). With an estimated survival rate of ~80%, breast cancer maintained a mortality rate of 26 per 100,000 women in 2008-2010, making it the second most deadly type of cancer in women after lung cancer (Office of National Statistics) (http://www.ons.gov.uk/ons/rel/cancer-unit/cancer-incidence-and-mortality/2008-2010/stb-cancer-incidence-and-mortality-in-the-united-kindom--2008-2010.html).

From a pathological perspective, breast cancer can be subdivided in several entities with distinct clinical behaviour. Based on gene expression profiling, breast cancer is commonly classified in the following five classes: luminal A, luminal B, normal breast-like, HER2-positive and basal-like (Geyer, Marchio et al. 2009). However, recent genome-wide expression profiling was able to identify two new subtypes, namely luminal C and claudin-low classes (Kittaneh and Gluck 2011). The luminal A subtype represent 40% of all breast cancers and are characterized by over-expression of oestrogen receptor (ER) and under-

expression of HER2 and proliferation-related genes. It is usually associated with favourable prognosis (Kittaneh and Gluck 2011). Luminal B breast tumours have a lower expression of ER-related genes, variable HER2 expression and higher expression of proliferation-related genes. They represent 20% of breast cancers and are associated with higher risk of relapse (Kittaneh, Montero et al. 2013). The luminal C intrinsic subtype is distinguished by luminal A and B subtypes by the high expression of a cluster of genes of presently unknown function which is also present in basal-like and HER2-enriched subtypes (Sorlie, Perou et al. 2001). The HER2-positive subtype represents 20-30% of all breast cancers and is characterized by over-expression of HER2 and, usually, under-expression of ER and PR. The prognosis for this subtype of breast cancer is often poorer compared to the luminal A subtype (Sorlie, Tibshirani et al. 2003). The basal-like subtype represents 15% of breast cancers and its name is derived from shared gene expression patterns with normal basal epithelial cells. Basal-like tumours are often ER-negative, PR-negative and HER2-negative and thus are commonly referred to as "triple-negative" breast cancers. They frequently contain *BRCA1* mutations and are particularly resistant to chemotherapy (Bayraktar and Gluck 2013). The recently recognized claudin-low subtype is characterized by over-expression of genes associated with epithelial-to-mesenchymal (EMT) transition. The majority of these tumours have no expression of luminal differentiation markers and are ER, PR and HER2 negative (Prat, Parker et al. 2010). Finally, the normal breast-like subtype resembles normal breast tissue with relatively high expression of adipose and other non-epithelial cell type genes and low expression levels of luminal epithelial cell genes (Rakha, Reis-Filho et al. 2008).

EphA2 and EphB4 receptors are often over-expressed in breast cancer and correlate with cancer progression, while over-expression of EphA4, EphA7 and EphB6 also correlates with reduced overall patient survival. Specifically, it was found that EphA2, EphA4, EphA7,

EphB4 and EphB6 are highly expressed in human invasive ductal carcinoma (Brantley-Sieders, Jiang et al. 2011). Clinical data on breast cancer progression has shown that ephrinB2 expression is lost in 75% of breast cancers sampled, while EphB4 is over-expressed in 65% of breast cancers. In most cases, the EphB4 receptor was found in up to 58% of the tumour tissue, while ephrinB2 ligand expression is confined to endothelial vascular cells (Kumar, Singh et al. 2006). Interestingly, although EphB/ephrinB signalling has been linked to ER, HER2 and claudin pathways, no functional correlation between expression levels of these proteins has been observed, or indeed investigated, in the context of breast cancer. Based on the many studies which have investigated the role of Eph and ephrin proteins in breast cancer, it appears that Eph/ephrin expression does not directly correlate with the presence/absence of a specific marker (ie ER, PR, HER2, claudin) (Brantley-Sieders, Jiang et al. 2011; Brantley-Sieders 2012). However, the co-expression of Eph/ephrin proteins with one or more of these markers produces an effect on the malignancy of the tumour and patient prognosis (Brantley-Sieders, Jiang et al. 2011). To the best of our knowledge, a study directly addressing the correlation between Eph/ephrin expression and known breast cancer markers has not yet been conducted.

During mammary gland carcinogenesis, ephrinB2 expression diminishes in epithelial cells at early stages, while EphB4 expression gradually shifts from myoepithelial cells to epithelial cells, following tumour progression. However, once the carcinogenesis process reaches its final stages, EphB4 expression is lost or can only be found in anaplastic cells interspersed in the tumour mass. This observation suggests that EphB4 functions as a tumour suppressor (Nikolova, Djonov et al. 1998). Thus it has been suggested that, during the early stages of tumour cell proliferation, EphB4 acts as a tumour suppressor by limiting tumour expansion. However, further during tumour development, ephrinB2 expression is lost and

EphB4 activity interrupted, allowing the tumour to expand and invade the surrounding tissue (Garber 2010).

Specifically, EphB4 over-expression in epithelial breast cancer cells promotes tumour progression and metastasis by acting as a cue for ephrinB2 expressing cells and thus enhancing tumour vascularisation. However, ligand-induced EphB4 activity is associated with tumour suppression, as it inhibits cell proliferation, motility and invasion (Noren, Foos et al. 2006). At a molecular level, EphB4 phosphorylation creates SH2 phospho-sites on the cytoplasmic tail of the receptor which are bound by Abl and Crk contemporarily. Abl then phosphorylates Crk, thus inactivating it and impeding its binding to Cas. This event inhibits cell migration, by blocking MMP-2 production, and survival, while promoting apoptosis (Noren, Foos et al. 2006). However, by interacting with ephrinB ligands, EphB receptors stimulate their oncogenic activity (Pasquale 2010). Therefore, the equilibrium between EphB4 and ephrinB2 protein levels is crucial to determine the receptor's function as a tumour promoter or suppressor. In the case of low levels of ephrinB2 and high levels of EphB4, the latter's activation will be relatively low. At the same time, EphB4 will strongly activate the ephrinB2 reverse signalling pathway, thus promoting angiogenesis by acting as a cue for endothelial invading cells. In the opposite case of high levels of ephrinB2 and low levels of EphB4, the latter will be strongly activated and function as a tumour suppressor by inhibiting cell growth (Noren and Pasquale 2007). Interestingly, ephrinB ligands might also be involved in stimulating cell proliferation and survival in breast cancer cell lines by associating with ErbB receptors (Vermeer, Bell et al. 2012). In this pathway, ephrinB1 interaction with ErbB1 or ErbB2 was found to induce high levels of ERK1/2 phosphorylation in HNSCC cells (Vermeer, Colbert et al. 2013).

In support of these findings, studies have shown that EphB4 kinase activity inhibits cell proliferation of human breast cancer cells MDA-MB-435 in tumour xenografts. Instead, over-expression of an EphB4 kinase deficient mutant in the same model produced faster growing and highly metastatic tumours *in vivo* by activating the ephrinB2 reverse signalling pathway in endothelial cells and thus enhancing angiogenesis (Noren, Lu et al. 2004). However, both over-expression of the EphB4 receptor in the mammary epithelium of xenograft models (Brantley-Sieders, Jiang et al. 2011) and over-expression of ephrinB2 in a NeuT transgenic animal model (Haldimann, Custer et al. 2009) accelerated tumour onset and lung metastasis, suggesting that strong imbalances towards higher EphB4 or ephrinB2 expression are both capable of promoting tumour progression.

1.1.5.4 EphB receptors and ephrinB ligands targeted therapies

The importance of Eph/ephrin superfamily members in cancer angiogenesis and metastasis has spurred the research for new cancer therapies which target these proteins. Antibodies and antagonistic peptides targeting Eph receptors, as well as function-blocking soluble Eph receptors, have been widely tested to inhibit ephrin ligand stimulation. Recently, anti-Eph/ephrin therapies using EphB4 receptor and ephrinB2 ligand monomers, monoclonal antibodies and RNA interference oligonucleotides have been developed (Mosch, Reissenweber et al. 2010). In a study by (Krasnoperov, Kumar et al. 2010), anti-EphB4 monoclonal antibodies were found to inhibit tumour angiogenesis, tumour growth and metastasis in mouse xenografts.

Given the strong evidence brought forward by many studies regarding the inhibition of cancer growth, angiogenesis and metastasis by disrupting Eph/ephrin signalling, many research groups have focused their attention on developing small peptides able to bind the extracellular domain of Eph receptors in order to disrupt interaction with the cognate ephrin ligands. Other similar approaches include the generation of peptides able to disrupt clustering of Eph receptors and interaction with other cell membrane receptor tyrosine kinases. As reviewed by (Noberini, Lamberto et al. 2012), in the last decade many inhibitory peptides have been generated for EphB receptors, including EphB1, EphB2 and EphB4. Recently, newly generated molecules which act as peptidomimetics to selectively inhibit the protein-protein interface between EphB4 and ephrinB2 have also been developed (Duggineni, Mitra et al. 2013). EphrinB2 reverse signalling has also been targeted by using a chimeric protein consisting of the soluble extracellular domain of EphB4 fused to human serum albumin. By impairing ephrinB2 clustering and activation, this molecule is able to inhibit growth factors-induced migration and invasion of Kaposi sarcoma cells *in vitro*, while *in vivo* it increased hypoxia and reduced pericyte recruitment and vessel density and perfusion (Scehnet, Ley et al. 2009). Similarly, tumour growth and intra-tumoural microvessel density are reduced in melanoma cells expressing a soluble monomeric form of the EphB4 receptor (Martiny-Baron, Korff et al. 2004). EphrinB1 reverse signalling has been targeted in scirrhous gastric cancer: by using a synthetic peptide consisting of the 15 C-terminal amino acids of ephrinB1 fused to HIV-TAT, ephrinB1 interaction with Dishevelled was disrupted, thus blocking RhoA activation and MMP secretion. Ultimately, this diminished tumour cell migration and cancer metastasis (Tanaka, Kamata et al. 2010). In the near future, these short synthetic peptides and peptidomimetics bode well for the development of new targeted anti-cancer therapies.

The kinase domain of Eph receptors has also been targeted using various small molecule inhibitors. For instance, NVP-BHG712, which inhibits EphB4 kinase activity, suppressed VEGF-driven vessel formation and angiogenesis (Martiny-Baron, Holzer et al. 2010). In pilot studies, the use of siRNA against EphB4 resulted in inhibition of malignant cell behaviour. Moreover, recombinant Eph receptors and ephrin ligands are also considered as cancer targeting agents for specific drug delivery or to activate the T-cell immune response (Pasquale 2010).

1.2 Syntenin-1

1.2.1 The PDZ domain-containing protein syntenin-1

Syntenin-1 is a PDZ domain-containing protein initially identified as a binding partner of syndecan-1 with hypothesized scaffolding function (Grootjans, Zimmermann et al. 1997). In a separate study, syntenin-1 was also identified as melanoma differentiation-associated gene 9 (*mda9*) in SV-40 immortalized human melanocytes and human melanoma cells treated with recombinant IFN-γ (Lin, Jiang et al. 1998). It contains 298 amino acids and is composed of the N-terminal domain (NTD), two PDZ domains and the C-terminal domain (CTD). The NTD is 113 amino acids long and contains three LYPXL sequences (where X is any aminoacid) centred at position 5, 47 and 51. The first of these sequences has been identified as a ubiquitin binding motif (Rajesh, Bago et al. 2011). The PDZ1 and PDZ2 domains are 80 to 100 amino acids long each and comprise of

Binding partner	Function
Syndecan	Syndecan recycling
Ephrin/EphR	Scaffold; function unknown
proTGFα	Targetting proTGFα to cell surface
β-neurexin	Function unknown
Neurofascin	Function unknown
PTPη	Function unknown
IL5Rα	Activation of SOX4-mediated transcription
Schwannomin	Subcellular trafficking to plasma membrane
GluR	Function unknown
SynCAM	Function unknown
PICK	Function unknown
Unc51.1	Scaffold for linking Unc51.1 to Rab5
Rab5	Scaffold for linking Unc51.1 to Rab5
GlyT2	Scaffold mediating interaction with syntaxin 1A
Syntaxin1A	Scaffold mediating interaction with GlyT2
eIF5A	Regulation of p53 activity
CD6	Scaffold; function unknown
ERC2	Scaffold; function unknown
CD63	CD63 internalization
Delta1	Delta1 internalization
Traf6	Inhibition of IL1- and TLR4-induced NF-κB activation
Frizzled 3,7,8	Non-canonical Wnt signalling during *Xenopus* gastrulation
NG2	Oligodendrocyte precurser migration
Kalirin-7	Function unknown
Neuroglian	Function unknown
SynGAPα1	Function unknown
Rab7	Function unknown
Phospho-inositol lipids	Plasma membrane localization, subcellular trafficking of syndecans

Table 1.3: interacting partners of syntenin-1 (Beekman and Coffer 2008).

six β-sheets and two α-helices. The short CTD is only 24 amino acids long. The PDZ domains, which carry out most of the protein's functions, bind multiple PDZ binding motif sequences (Beekman and Coffer 2008). A list of reported proteins which interact with syntenin-1 can be found in table 1.3. The name "syntenin" was coined after preliminary evidence showed that this protein could interact with the COOH-terminal domain of all four syndecans (Sarkar, Boukerche et al. 2008). Syntenin-1 is widely expressed in all adult tissues (Grootjans, Zimmermann et al. 1997; Lin, Jiang et al. 1998; Zimmermann, Tomatis et al. 2001) and is particularly abundant in the skin, spinal cord, heart and lung during foetal development of mouse embryos (Jeon, Das et al. 2013). Based on database entries, a homologous protein of syntenin-1 was identified and named syntenin-2. This protein shares 70% identity of the PDZ domains of syntenin-1 and is expressed as isoform α or isoform β. Syntenin-2β lacks 85 amino acids at the N-terminus compared to isoform α. Syntenin-2 is also capable of PDZ-mediated binding, but does not share all the same partners with syntenin-1. Interestingly, the two proteins were found to form heterodimers as well as homodimers (Koroll, Rathjen et al. 2001).

1.2.1.1 Syntenin-1's localization

PDZ domain-containing proteins are often localized on the cytoplasmic side of the plasma membrane and are restricted to specific subcellular compartments. In epithelial cells, syntenin-1 is located at areas of cell-cell contacts where it co-localizes with F-actin, syndecans, E-cadherin, β-catenin and α-catenin. In fibroblasts, syntenin-1 localizes at focal adhesions and stress fibres (Zimmermann, Tomatis et al. 2001). Phosphatidyl-Inositol 4,5-

bisphosphate (PIP_2) and phospholipase Cδ assist its anchorage to the plasma membrane (Zimmermann, Meerschaert et al. 2002). Syntenin-1 is also localized in the endoplasmic reticulum, intermediate compartment, *cis*-Golgi and apical endosomes (Fernandez-Larrea, Merlos-Suarez et al. 1999).

1.2.1.2 Characteristics of syntenin-1's PDZ domains

Syntenin-1 contains two PDZ domains very similar in sequence, which vary in binding affinity to different PDZ binding motifs on different target proteins. However, in most cases both PDZ domains cooperate in binding to PDZ binding sequences (Grootjans, Reekmans et al. 2000). For example, the PDZ-mediated interaction of syntenin-1 with syndecans and neurexins is strengthened upon binding of both PDZ domains to the same PDZ binding sequence, although individually the PDZ2 domain has a higher affinity than the PDZ1 domain. When the PDZ2 domain of syntenin-1 interacts with the PDZ binding motif sequence, PDZ1 is able to bind to the same sequence in a non-conventional manner (Grembecka, Cierpicki et al. 2006). This study confirms previous reports that the cytoplasmic sequence of ephrinB ligands does not detectably associate with syntenin-1's PDZ1 domain and only weakly with PDZ2 when tested separately (Lin, Gish et al. 1999) and that strong interaction was only detected when both PDZ domains were present (Song, Vranken et al. 2002). The selectivity of the PDZ interaction is mediated by the side chains of amino acids P_0 and P_{-2} of the target protein. There are three known types of PDZ binding sequences which have been reported and to which syntenin-1 can bind: class I sequences contain a X[S/T]Xϕ motif at amino acids $P_{-3}P_{-2}P_{-1}P_0$ of the PDZ-binding motif (where ϕ represents a hydrophobic

side chain and X any side chain); class II sequences contain a XϕXϕ motif at amino acids $P_{-3}P_{-2}P_{-1}P_0$; class III sequences contain a X[D/E]Xϕ motif at amino acids $P_{-3}P_{-2}P_{-1}P_0$ (Ivarsson 2012). Additionally, syntenin-1 is capable of low-to-medium affinity degenerative binding to unconventional PDZ-binding motifs (Kang, Cooper et al. 2003; Grembecka, Cierpicki et al. 2006). At the structural level, Val209, Gly210 and Phe211 in the PDZ2 domain form the binding pocket for the C-terminal P_0 aminoacid of the target protein, while Phe213 interacts with aminoacid P_{-2}. Interestingly, a glutamic acid in position P_{-3} of the target protein contacts Arg128 of the PDZ1 domain of the neighbouring syntenin-1 protein, which is part of the head-to-tail homodimer, and stabilizes the PDZ interaction (Grembecka, Cierpicki et al. 2006).

It has been suggested that the PDZ1 domain can have a chaperone-like function by stabilising folding of the PDZ2 domain. (Boukerche, Aissaoui et al. 2010). This mode of regulation seems to be important for interaction of syntenin-1 PDZ2 domain with c-Src (Boukerche, Su et al. 2008).

Phosphorylation of Ser/Thr/Tyr residues located in close proximity or within the PDZ-binding motif is known to modulate PDZ-mediated binding (Ivarsson 2012). For example, tyrosine phosphorylation at position -1 of syndecan-1 disrupts its association with syntenin-1 (Sulka, Lortat-Jacob et al. 2009), while phosphorylation of serine at position -9 of ephrinB ligands increases binding to GRIP proteins (Essmann, Martinez et al. 2008). Interestingly, interaction of ephrinB ligands with other PDZ domain-containing proteins remains unaffected by phosphorylation events. For example, tyrosine phosphorylation at position -2 and/or -3 of ephrinB ligands does not alter association with the PDZ domain-containing phosphatase FAP1 (PTPL1) (Lin, Gish et al. 1999). In the case of syntenin-1 interaction with ephrinB

ligands, phosphorylation of tyrosine at position -2, but not -3, was found to impair PDZ-mediated binding of syntenin-1 (Lin, Gish et al. 1999).

1.2.1.3 Syntenin-1's CTD and NTD functions

Apart from PDZ domains, the NTD and CTD also play an important role in syntenin-1 functions. The NTD, for example, controls localization of the protein to the plasma membrane; it is necessary for homo- and hetero-dimerization; and can interact with transcription factors Sox4 and Eukaryotic translation Initiation Factor 4A (EIF4A). Also, the NTD contains various tyrosine residues which can be phosphorylated by Src kinases and act as docking sites for zeta-chain-associated protein 70 (ZAP-70) and Src kinases (Beekman and Coffer 2008). Recently, a study on syntenin-1 interaction with ubiquitylated proteins has uncovered the importance of the NTD for syntenin-1 binding to ubiquitin molecules. More specifically, the $L^{4}YPXL^{8}$ domain proved to be indispensable in this context (Rajesh, Bago et al. 2011). Also, the three LYPXL domains present in the NTD and centred at positions 5, 47 and 51, were found to be necessary for the interaction with ALIX during syndecan-lead cargo recruitment to exosomal compartments (Baietti, Zhang et al. 2012).

A role for the NTD and CTD in modulating syntenin-1 targeting to the plasma membrane was proposed by (Wawrzyniak, Vermeiren et al. 2012). In this study, the authors reported that phosphorylation of Tyr56, which is located in the NTD, decreased syntenin-1 localization at the plasma membrane, while the negative charges of residues K280/R281 at the CTD increased cell membrane localization. The shorter CTD is also required for CD63 high

affinity interaction with syntenin-1 while the NTD is involved in shifting CD63 clathrin-dependent to clathrin-independent endocytosis (Latysheva, Muratov et al. 2006).

1.2.1.4 Syntenin-1 mediates protein trafficking and recycling

Syntenin-1 interacts with many different proteins located at the cell surface and by doing so is able to modulate both trafficking and recycling processes of its targets (Beekman and Coffer 2008). An extensive study by (Zimmermann, Zhang et al. 2005) reported that syntenin-1 modulates syndecan recycling dynamics via interaction with $PI(4,5)P_2$ through Rab11 and Arf6 positive endosomal compartments. Furthermore, cell membrane receptors associated with syndecans (e.g. FGF receptors) might be recycled together with the syntenin-1 – syndecan complex. Interestingly, syndecan-4 phosphorylation at Ser183 disrupts association with syntenin-1, thus suggesting that phosphorylation could play a critical role in modulating syndecan recycling via syntenin-1 (Koo, Jung et al. 2006). A recent study by (Baietti, Zhang et al. 2012) has also reported the formation of a syndecans – syntenin-1 – ALIX tripartite complex in connection with cargo recruitment to exosomal compartments. The authors demonstrated that clustering of syndecan cargo, such as FGF receptors, induces recruitment of syntenin-1 – ALIX. The syndecan – syntenin-1 – ALIX complex is then able to recruit syndecan cargo to specific CD63 positive budding exosomes and actively supports budding processes and the production of exosomes.

Alternatively, syntenin-1 can also inhibit protein internalization by retaining the target on the plasma membrane. Deletion of the C-terminal valine of Notch-associated Delta1 ligand as well as syntenin-1 depletion via siRNA caused decreased presence of Delta1 on the cell

surface (Estrach, Legg et al. 2007). Similarly, syntenin-1 interaction with tetraspanin CD63 impairs its internalization (Latysheva, Muratov et al. 2006), possibly by competing with the clathrin-dependent endocytosis-associated protein AP2 and shifting CD63 internalization to a clathrin-independent endocytosis pathway (Janvier and Bonifacino 2005).

Syntenin-1 is also involved in protein trafficking to the cell surface, as mutation of the C-terminal valine of proTGFα was shown to disrupt association with syntenin-1 and cause proTGFα's retention in the endoplasmic reticulum (Fernandez-Larrea, Merlos-Suarez et al. 1999).

1.2.1.5 Syntenin-1 plays various roles as a scaffolding protein

Given its ability to bind many different target proteins, syntenin-1 is known to have a crucial role as a scaffolding protein, taking part in many different pathways and processes. In neurons, syntenin-1 localizes at sites of synapse formation and growth cones. Interactions between syntenin-1 and adhesion molecules, such as SynCAM, neurexin and neurofascin, as well as cytoplasmic proteins, such as Sch-1 and PICK1, may contribute to synaptic structure formation. Association of syntenin-1 with glutamate receptors GluR5 and GluR6 might be important to induce membrane protrusions during brain development (Beekman and Coffer 2008). A detailed study by (McClelland, Sheffler-Collins et al. 2009) reported that syntenin-1 interaction with ephrinB ligands is necessary for the recruitment of pre-synaptic machinery during the EphB/ephrinB driven development of presynaptic and postsynaptic compartments in neurons.

Syntenin-1 was initially found to interact with ephrinB ligands by (Lin, Gish et al. 1999). Since then, there has been much speculation on the possible significance of this interaction. It has been widely hypothesized that syntenin-1 might facilitate ephrinB clustering, given its role as a scaffolding protein (Cowan and Henkemeyer 2002). However, a study by (Grembecka, Cierpicki et al. 2006) reported that from a structural perspective it is more probable that preferential binding occurs after ephrinB multimerization.

Other syntenin-1 functions involve Interleukin-5 (IL-5) mediated activation of Sox4, by acting as a bridge between the transcription factor and the IL-5 receptor α (Sarkar, Boukerche et al. 2004). A recent study by (Beekman, Vervoort et al. 2012) has also reported that syntenin-1 interaction with the C-terminus of Sox4 causes syntenin-1 relocation to the nucleus, where it stabilizes Sox4 expression by inhibiting proteasomal-driven degradation of the transcription factor. Syntenin-1 is also a component of cell adhesion sites, microfilaments and apical early endosomes and may directly or indirectly affect Rho family GTPases activity (Koo, Lee et al. 2002).

Recently, a study by (Rajesh, Bago et al. 2011) has reported that syntenin-1 may play a pivotal role in ubiquitin-dependent sorting of its transmembrane cargo. Syntenin-1 is able to bind mono-ubiquitin through a non conventional pocket which includes amino acids 71-74 on the ubiquitin molecule with residues 8-12 providing a stabilizing interaction. The L^4YPXL^8 sequence in syntenin-1 is fundamental for ubiquitin binding. Furthermore, syntenin-1's ability to bind ubiquitin is controlled by Ulk1 kinase, which can phosphorylate syntenin-1 at Ser6, thus inhibiting ubiquitin binding. The authors speculate that syntenin-1 plays a role in sorting of ubiquitylated proteins in endocytic vesicles with Ulk1 kinase regulating this trafficking pathway.

1.2.1.6 Syntenin-1's role as a modulator of FAK/Src signalling

One of the well described roles of syntenin-1 as a scaffolding protein is linked to FAK and c-Src pathway activation upon cell adhesion to fibronectin. This event induces syntenin-1 expression and PKCα phosphorylation and subsequent activation of c-Src and FAK. At the molecular level, cell adhesion to fibronectin leads to PIP_2-bound syntenin-1 association with syndecan-4 and PKCα. The latter then binds PIP_2, thus inducing PKCα auto-phosphorylation and activation, which is accompanied by FAK phosphorylation and syntenin-1 expression through a positive feedback loop. FAK is recruited to phospho-PKCα sites where it becomes activated and associates with c-Src, causing its phosphorylation and activation. The outcome of phosphorylation of these two kinases is the activation of p38, JNK, ERK and nuclear factor NF-ķB pathways. In this process syntenin-1 acts as a scaffolding protein by recruiting and holding into complex PKCα, FAK and c-Src, allowing these kinases to interact and activate each other. A simplified diagram of this pathway is illustrated in figure 1.11. Down-regulation of either syntenin-1 or PKCα causes the other to decrease in expression levels, which suggests that these two proteins are interdependent of each other and necessary for fibronectin-dependent activation of FAK and c-Src (Hwangbo, Kim et al. 2010).

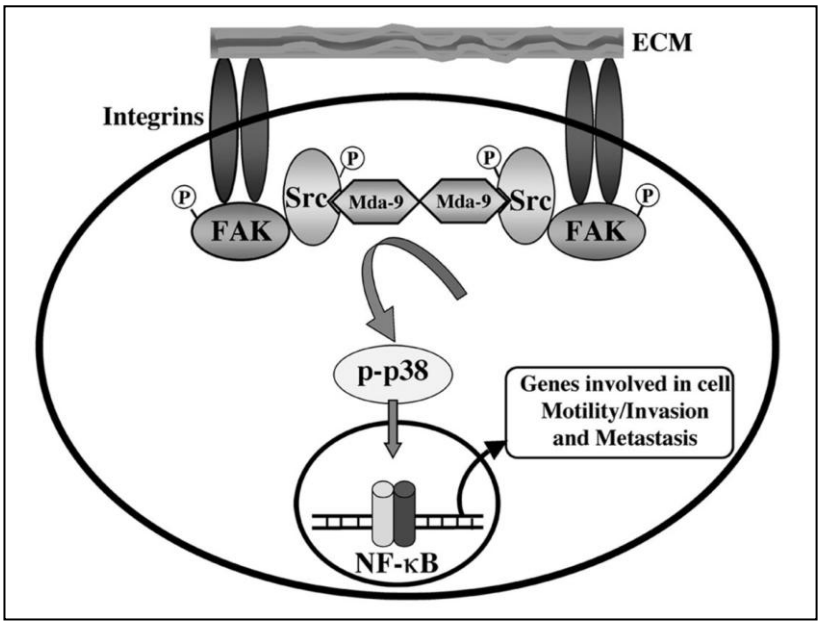

Figure 1.11: model of signalling pathway regulated by syntenin-1 through its interaction with c-Src (Boukerche, Su et al. 2008).

The same group also found that syntenin-1 modulates collagen-1-induced stimuli by recruiting the integrin-linked kinase (ILK)-PINCH1-α-parvin (IPP) complex to integrin β1-associated signalling platform, leading to Akt, Rac1 and ERK1/2 activation (Hwangbo, Park et al. 2011).

1.2.2 Syntenin-1 promotes cancer metastasis and angiogenesis

Syntenin-1 is over-expressed in many highly metastatic tumours. It was initially identified as a melanoma differentiation-associated gene (*mda9*) by (Lin, Jiang et al. 1998). In human melanoma cells, syntenin-1 contributes to the activation of FAK and c-Src kinases upon cell interaction with fibronectin, which in turn cause activation of JNK, p38 and NF-ķB pathways, thus promoting anchorage-independent growth and metastasis (Beekman and Coffer 2008; Boukerche, Su et al. 2008). This pathway can be inhibited by the metastasis suppressor Raf kinase inhibitor protein (RKIP), which physically interacts with syntenin-1 and prevents its association with FAK and c-Src kinases (Das, Bhutia et al. 2012). Syntenin-1-mediated activation of c-Src kinases also induces EGF receptor activation in uroepithelial cells, thus increasing their proliferation and invasion properties (Dasgupta, Menezes et al. 2013). Also, syntenin-1 activation of NF-ķB through FAK phosphorylation induces activation of pro-MMP-2, which is then secreted and induces migration and invasion by increasing degradation of ECM proteins (Boukerche, Su et al. 2008; Sarkar, Boukerche et al. 2008; Boukerche, Aissaoui et

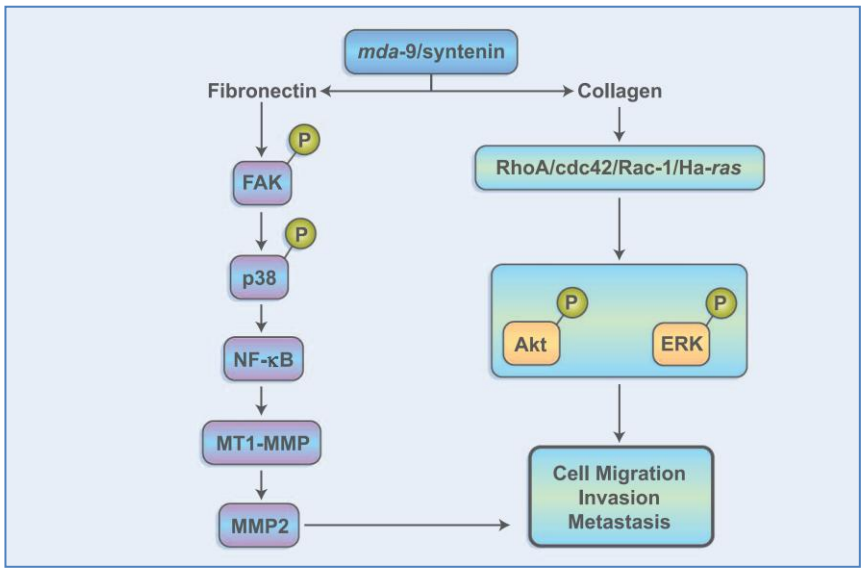

Figure 1.12: signalling pathways activated by syntenin-1 to increase migration, invasion and metastasis (Sarkar, Boukerche et al. 2008).

al. 2010). The PDZ2 domain of syntenin-1 plays a fundamental role in this process by binding to c-Src and thus recruiting it in FAK/Src complexes. In fact, mutations within the PDZ2 domain completely abolish syntenin-1's effect on migration and metastasis in general (Boukerche, Aissaoui et al. 2010). Syntenin-1 can also indirectly activate the PI3K-Akt and the ERK1/2 pathways, which are involved in invasion processes, as illustrated in figure 1.12 (Sarkar, Boukerche et al. 2008).

Syntenin-1-dependent activation of the PI3K-Akt pathway in human melanoma cells has recently been linked to increased angiogenesis. As previously described, fibronectin-induced activation of FAK and c-Src kinases is modulated by syntenin-1 and triggers the PI3K-Akt pathway. Activated Akt causes HIF-1α translocation to the nucleus, which induces insulin growth factor-binding protein-2 (IGFBP-2) expression. After secretion, IGFBP-2 interacts with αVβ3 integrin on endothelial cells, causing activation of the PI3K-Akt pathway and subsequent generation of the pro-angiogenic factor VEGF-A (see figure 1.13). Thus, syntenin-1 plays an important role in inducing angiogenesis in human melanoma (Das, Bhutia et al. 2013).

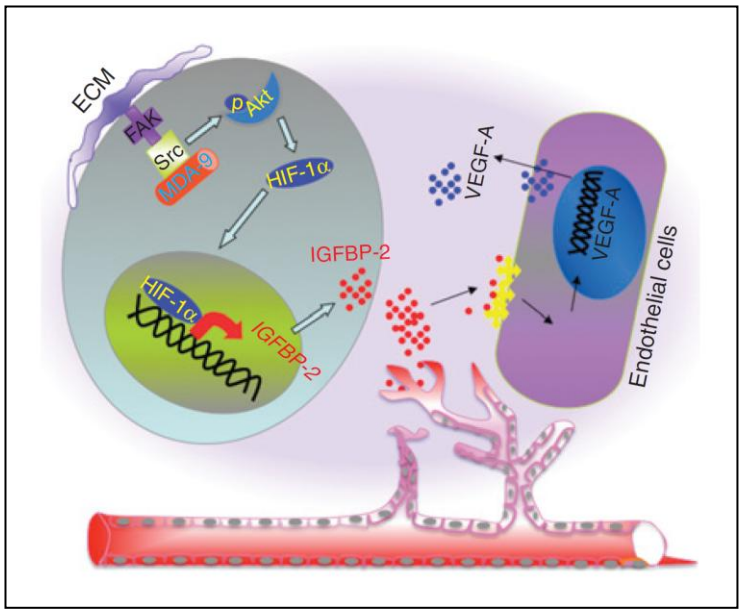

Figure 1.13: hypothetical model of syntenin-1 induction of angiogenesis (Das, Bhutia et al. 2013).

1.2.2.1 Syntenin-1's role in breast cancer

Studies on MCF7 breast carcinoma cells have observed that syntenin-1 over-expression increased their migration and invasion properties (Koo, Lee et al. 2002; Sarkar, Boukerche et al. 2008). Recently, high syntenin-1 expression levels have been linked with tumour size, lymph node status and recurrence in breast cancer. Syntenin-1 was found to correlate with patient overall survival and disease free survival, acting as an independent prognostic factor for these values. The same study reported that over-expression of syntenin-1 increased cell migration of MDA-MB-231 breast cancer cells *in vitro* and proliferation *in vivo*. The authors linked these processes to syntenin-1-induced over-expression of integrin β1 and subsequent increase in ERK1/2 activity, which lead to cell migration and angiogenesis. These findings were supported by the observation of increased metastasis to lungs and tumour growth in orthotopic xenograft tumour models in nude mice. However, syntenin-1 over-expression did not increase MMP expression, suggesting that only cell migration and not invasion is induced in this model (Yang, Hong et al. 2013). Although this study could not find any correlation between the expression levels of syntenin-1 and oestrogen receptors (ER), progesterone receptors (PR) or human epidermal growth factor receptor 2 (Her-2), a report by (Qian, Li et al. 2013) identified a negative correlation between syntenin-1 expression and ER positivity in a large panel of breast cancer cell lines. Moreover, stimulation of ER positive MCF7 cells with 17-β estradiol down-regulated syntenin-1 expression. In this study, syntenin-1 was also found to increase cell proliferation by promoting cyclin E expression in ER negative breast cancer cell lines, thus providing ER negative tumours with an alternative means to promote tumour growth.

1.3 Hypothesis and research objectives

Eph tyrosine kinase receptors and ephrin ligands are involved in various stages of embryogenesis, organ development and tissue homeostasis. Furthermore, increasing evidence has shown that these proteins play an important role in cancer progression. Although Eph forward signalling has been widely studied, less is known on ephrin reverse signalling and, particularly, PDZ-dependent signalling.

One of the best characterized PDZ domain-containing partners of ephrinB ligands is syntenin-1, a scaffolding protein known for its ability to modulate trafficking of membrane proteins and facilitate the formation of signalling complexes. Whilst the significance of the ephrinB – syntenin-1 interaction is still largely unknown, there is a certain degree of overlap between ephrinB and syntenin-1 pathways. Endocytosis of ephrinB ligands is fundamental for EphB/ephrinB-induced repulsion between contacting cells and can also be triggered to terminate ephrinB reverse signalling upon prolonged stimulation with EphB receptors. The molecular mechanisms underlying this process are still not completely understood and widely debated. Previous work from our group has reported that syntenin-1 binds to CD63 via PDZ-mediated interaction and modulates its internalization. Therefore, syntenin-1 might also be capable of modulating ephrinB internalization. Finally, both ephrinB ligands and syntenin-1 have been shown to affect progression in breast, colon, pancreatic and ovarian cancers.

The overall aim of this study was to understand how the ephrinB – syntenin-1 complex may function in the context of breast cancer. Specific aims of our study were as follows:

1. to examine the contribution of syntenin-1 to ephrinB2 signalling pathways;
2. to establish the role of syntenin-1 in trafficking of ephrinB2;

3. to analyse the functional consequences of disrupting the ephrinB2 – syntenin-1 axis in the context of breast cancer epithelial cells.

MATERIALS AND METHODS

2.1 Cell culture and cell lines

2.1.1 Cell lines

Origin and characteristics of all cell lines used in this study are listed in table 2.1 below. MCF7, T47D and HEK293T cells were from Cancer Research UK, while MCF7 TetOn tetracycline inducible cells were purchased from Clontech. Information on growth culture medium and supplements used for each cell line is listed in Appendix 1. Appendix 3 contains recipes of all solutions used in this study.

Cell line	Tissue	Type	ER	Tumour
MCF7	Breast	Epithelial	Positive	Adenocarcinoma
T47D	Breast	Epithelial	Positive	Ductal carcinoma
MCF7 TetOn	Breast	Epithelial	Positive	Adenocarcinoma
HEK293T	Embryonic Kidney	Epithelial	Negative	NA

Table 2.1: list of cell lines used in this study.

2.1.2 Cell maintenance

MCF7 and HEK293T cells were routinely grown in T25 and T75 flasks (Corning) in Dulbecco's Modified Eagle's Medium (DMEM) supplemented with 10% Fetal Calf Serum (FCS) and penicillin/streptomycin antibiotics. Stably transfected MCF7 cells were grown in supplemented DMEM medium containing 1 µg/ml Puromycin. T47D cells were grown in Roswell Park Memorial Institute (RPMI) medium with 10% FCS supplemented with

penicillin/streptomycin. MCF7 tetracycline inducible cell lines (MCF7 TetOn) were maintained in DMEM medium supplemented with 10% tetracycline-free FCS, penicillin/streptomycin and 100 µg/ml Geneticin. Stably transfected MCF7 TetOn cells were grown in the above medium supplemented with 100 µg/ml Zeocin. Stably transfected MCF7 TetOn cells transduced with lentiviruses were grown in the presence of 100 µg/ml Zeocin and 1 µg/ml puromycin. All cell lines were maintained in a 37°C, 5% CO_2 incubator (Galaxy R CO_2 Incubators, RS Biotech) to ensure optimal growth. When passaging cells, growth medium was discarded and cells were washed with warm 1x Phosphate Buffer Saline (PBS). Cells were subsequently detached from plastic by incubating with 0.05% Trypsin-EDTA solution at 37°C for 3-5 minutes. Floating cells were re-suspended in 5 ml of complete growth medium and centrifuged at 400 g for 3 minutes. The cell pellet was suspended in complete growth medium and cells were seeded at required density.

2.1.3 Freezing and Thawing Procedures

After reaching 80% confluency, cells were washed, detached and centrifuged as described in section 2.1.2. The cell pellet was then suspended in 1 ml of freezing medium and transferred into a 1 ml CryoTube™ vial (Nunc). Vials were wrapped in paper towels and placed at -80°C for 24 hours before being transferred to liquid nitrogen for long-term storage.

When thawing cells from liquid nitrogen, frozen vials were briefly incubated at 37°C in a water bath until completely thawed and then transferred to 4 ml of warm complete medium. Cells were subsequently centrifuged at 400 g for 3 minutes and cell pellet was gently

suspended in complete growth medium. Cells were seeded in T25 flasks and growth medium was changed on the next day to remove floating cell debris.

2.1.4 Transfection of eukaryotic cells using FuGene® 6 reagent

Following manufacturer's recommendations, cells were split 16-24 hours before planned transfection and plated in 35 mm or 60 mm Petri dishes (Corning) in order to achieve 50-80% confluency on the day of transfection. Ratio of FuGene® 6 transfection reagent (Roche) to plasmid DNA quantity was maintained at 3:1 (3 µl of reagent to 1 µg of plasmid) for all transfections. Quantities used for different plating conditions can be found in table 2.2. Before use, FuGene® 6 transfection reagent was incubated at room temperature for 5 minutes and then added to serum-free medium and incubated at room temperature for additional 5 minutes. Plasmid DNA was thawed, vortexed for a few seconds and spun down in a mini centrifuge before being added to FuGene® 6 reagent-containing medium. The transfection mixture was then delicately mixed by tapping and incubated for 25 minutes at room temperature to allow lipid-DNA complexes to form. The FuGene® 6 reagent-DNA solution was added directly to the growth medium and gently mixed to allow even distribution of lipid-DNA complexes. Cells were subsequently placed in the incubator (37°C, 5% CO_2) for 24-48 hours before being used. Co-transfections were conducted maintaining a 1:1 ratio of plasmid DNA. A ratio of 3:1 was used when wanting to achieve antibiotic resistance: 3 parts of gene-containing plasmid to 1 part of antibiotic resistance-containing plasmid. A list of plasmids used in this study is shown in table 2.3 at the end of section 2.1.9.

Container	Surface Area (cm^2)	FuGene® 6 (µl)	DNA (µg)	Serum Free Medium (µl)	Total Volume of Medium (ml)
35 mm	8	3.0 – 9.0	1.0 – 2.0	100	2.0
60 mm	21	6.0 – 20.0	2.0 – 4.5	200	4.0 – 6.0
100 mm	55	17.0 – 51.0	5.6 – 11.0	600	10.0

Table 2.2: quantities and volumes of DNA, FuGene® 6 transfection reagent and growth medium used for each culture dish in this study following manufacturer's guidelines.

2.1.5 Transfection of eukaryotic cells using FuGene® 6 reagent for lentivirus production

Following the same procedure as described in paragraph 2.1.4, HEK293T cells were plated on 6 or 10 cm dish (Corning) the day before in order to obtain 70-80% confluency on day of transfection. Cells were co-transfected with three plasmids including the lentiviral-based plasmid of interest, psPAX2 and pMD2.G at a ratio of 2:2:1, respectively. The lentiviral-based plasmid contained the gene of interest, while the psPAX2 and pMD2.G plasmids encoded the proteins necessary for the production of lentivirus particles. After 24 hours the antibiotics-free medium was replaced with complete growth medium. Lentiviral supernatant was harvested at 48 and 72 hours after transfection and cells were supplemented with fresh complete growth medium. The culture supernatant was centrifuged at 400 g for 5 minutes to remove cell debris, filtered using 0.22 µm filters (Millipore) and kept at 4°C for short term storage if not used immediately. For long term storage, lentiviral supernatant was frozen at -80°C. Cells for lentiviral infection were plated on T25 or T75 flasks 16-24 hours before planned infection in order to reach 30-50% confluency on the day of infection. Growth medium was replaced with lentiviral supernatant supplemented with sterile Polybrene (8

µg/ml) and placed in the incubator (37°C, 5% CO_2) for 24 hours. Cells were re-infected on the following day with fresh lentiviral supernatant (supplemented with Polybrene) and incubated for further 24 hours. The supernatant was subsequently replaced with fresh complete growth medium and cells were used for further analysis as required.

2.1.6 Generation of stable ephrinB2 expressing MCF7 cells

As described in section 2.1.4, MCF7 cells were co-transfected with pCDNA3.1(-)-ephrinB2-Flag and pCDNA3.1(-)-puro plasmids at a ratio of 3:1 respectively. The former endoced N-terminus Flag tagged human ephrinB2 wild type cDNA, while the latter encoded for puromycin resistance. Growth medium was changed 24 hours after transfection and at 48 hours cells were lifted and seeded on a T75 flask. Puromycin was subsequently added to the growth medium at a final concentration of 1 µg/ml in order to select cells for antibiotic resistance. After selection (2-3 weeks time), cells were stained with anti-Flag mAb and sorted for positive expression using Fluorescent Activated Cell Sorting (FACS) as described in section 2.3.2. The resulting cell line was called MCF7-ephrinB2.

2.1.7 Generation of tetracycline inducible MCF7 cells expressing ephrinB2, ephrinB2/G and ephrinB2/ΔV

As described in section 2.1.4, MCF7 TetOn cells were co-transfected with pBI-ephrinB2-Flag constructs (pBI-ephrinB2-Flag, pBI-ephrinB2/G-Flag, pBI-ephrinB2/ΔV-Flag) and pZeoSV at a ratio of 3:1, respectively. Growth medium was changed 24 hours after transfection and at 48 hours cells were lifted and seeded on a T75 flask. Zeocin was then added to the medium at the initial concentration of 400 µg/ml for 3-4 days. Growth medium was subsequently changed and Zeocin concentration was reduced to 100 µg/ml. After further selection (3-4 weeks), cells were stained with anti-Flag mAb and sorted for positive expression using FACS as described in section 2.3.2. The resulting cell lines were called MCF7 Tet-ephrinB2, MCF7 Tet-ephrinB2/G and MCF7 Tet-ephrinB2/ΔV.

Tetracycline inducible cell lines were routinely stimulated with 1 µg/ml doxycycline, according to manufacturer's guidelines (Clontech), for 48 hours to ensure maximum protein expression. Unless otherwise specified, all MCF7 tetracycline inducible cell lines were stimulated in this manner 24 hours after plating for any experiment.

2.1.8 Generation of syntenin-1 knock down tetracycline inducible ephrinB2 expressing MCF7 cells

MCF7 Tet-ephrinB2 cells were infected with lentiviral particles derived after transfection with pLKO.1-puro plasmid encoding shRNA which targets syntenin-1 (purchased

from Sigma). A list of tested shRNA sequences targeted against styntenin-1 is shown in Appendix 2. pLKO.1-puro plasmid encoding shRNA (5) was used to infect cells, which were then selected in growth medium containing 1 µg/ml puromycin. After selection (2-3 weeks), syntenin-1 expression was analyzed by Western blotting (WB) to assess the level of syntenin-1 knock down.

2.1.9 Generation of RFP expressing MCF7 tetracycline inducible cell lines and GFP expressing T47D cells

MCF7 TetOn cell lines were transfected with the pBabe-RFP plasmid, using FuGene6® transfection reagent (protocol described in section 2.1.4). RFP-expressing cells were selected using 1 µg/ml puromycin. T47D cells were infected with lentiviral particles encoding GFP (pVLTHM vector), as described in section 2.1.5. FACS analysis was then performed to select the T47D cell population expressing GFP (section 2.3.2). All plasmids used in this study are listed in table 2.3.

Plasmid	Gene encoded	Resistance	Source
pCDNA3.1(-)	empty	puromycin	provided by F. Berditchevski
pCDNA3.1(-)-ephrinB2-Flag	human ephrinB2-Flag	NA	provided by F. Berditchevski
pZeoSV	empty	Zeocin	Invitrogen
pBI	empty	NA	provided by F. Berditchevski
pBI-ephrinB2-Flag	human ephrinB2-Flag	NA	made in-house
pBI-ephrinB2/G-Flag	human ephrinB2/G-Flag	NA	made in-house
pBI-ephrinB2/ΔV-Flag	human ephrinB2/ΔV-Flag	NA	made in-house
pLKO.1-shSyntenin-1	shRNA against syntenin-1	puromycin	Sigma
psPAX2	lentivirus packaging	NA	Addgene
pMD2.G	lentivirus envelop	NA	Addgene
pCMV2-PTPL1-Flag	human PTPL1-Flag	NA	provided by F. Berditchevski
p-EGFP-PICK1-myc	human PICK1-myc	NA	provided by F. Berditchevski
GRIP1-myc	human GRIP1-myc	NA	provided by F. Berditchevski
GRIP2-myc	human GRIP2-myc	NA	provided by F. Berditchevski
PAR3-Flag	human PAR3-Flag	NA	provided by F. Berditchevski
pCDNA3.1(-)-RGS3-myc	human PDZ-RGS3-myc	NA	provided by G. Willars
pVLTHM	Green Fluorescent Protein	NA	Addgene
pBabe-RFP	Red Fluorescent Protein	puromycin	provided by F. Berditchevski

Table 2.3: list of plasmids used in this study.

2.1.10 3D cultures in collagen

The day before embedding cells in 3D collagen, cells were detached from tissue culture dish and re-plated as described in section 2.1.2. Collagen Type I was reconstituted from powder solution by leaving O/N on a rotating platform in 0.1 M acetic acid at a concentration of 1.6 mg/ml and was always kept on ice when used. On the day of experiment, cells were detached and counted using a Burker chamber (Marienfeld). 100 µl of collagen were diluted with 110 µl of complete growth medium and neutralized with 10 µl of 1M NaOH. 10^4 cells in 100 µl of growth medium were then added to the collagen mixture (ratio of 1:2 (v/v)) and mixed thoroughly. Collagen mixture containing cells (40-50 µl containing ~$1.5*10^3$ cells) was then plated in an 8-well chamber glass slide (Labtek) and incubated at 37°C, 5% CO_2 for 20-30 minutes to allow collagen to solidify. Subsequently, 400 µl of complete growth medium was carefully added to each well and the slide was returned to an incubator for long-term culture. Growing medium was changed every 4-5 days by replacing 200 µl of growth medium. During culturing, cells in selected wells were stimulated with the EphB4/Fc chimera molecule (R&D) every two days. Prior to use, EphB4/Fc (100 µg/ml) was pre-clustered with anti-human Fc IgG antibody (2.5 mg/ml) at a ratio of 10:1 (v/v) for 1 hour at 4ºC, as described in the study by (Palmer, Zimmer et al. 2002). EphB4/Fc was added directly to the growth medium at a final concentration of 5 µg/ ml.

2.1.11 3D cultures in 2% Matrigel

The day before embedding in 3D Matrigel, cells were detached from the tissue culture dish and re-plated as described in section 2.1.2. Frozen Matrigel aliquots were left to thaw on ice in a cold room until ready to use and were kept on ice during the preparation of cells. On the day of the experiment, the wells of the 8-well chamber glass slide (Labtek) was coated with a mixture composed of 50% MG (v/v) in complete growth medium (40 µl/well) and placed in incubator at 37°C for 20-30 minutes to allow MG to solidify. In the meantime, cells were detached and counted using a Burker chamber (Marienfeld). In order to obtain a concentration of 10^4 cells/ml. Cell suspension was added to 4% MG in complete growth medium at a ratio of 1:1 (v/v) and mixed thoroughly. Cell suspension containing ~10^3 cells 2% MG (v/v) was then added to wells (400 µl/well) and the slide was placed in the incubator for long-term culture. Growing medium was changed every 4-5 days by replacing 200 µl of growth medium. As described in section 2.1.10, EphB4/Fc was added to the growth medium every two days to selected wells at a final concentration of 5 µg/ ml.

2.2 Molecular biology techniques

2.2.1 Sub-cloning of ephrinB2 from pCDNA3.1(-) to pBI plasmid

The pCDNA3.1(-)-ephrinB2-Flag plasmid was provided by Dr Fedor Berditchevski. This plasmid was generated by inserting the ephrinB2 cDNA, obtained by reverse transcription PCR of ephrinB2 RNA extracted from mammary epithelial cells (HB2), in a pCDNA3.1(-) empty vector. A Flag sequence (DYKDDDDK) was added at the N-terminus of the protein, after the leader peptide sequence.

The ephrinB2-Flag was PCR amplified using the pCDNA3.1(-)-ephrinB2-Flag plasmid as a template and primers which included sites for recognition by PstI endonuclease (forward primer) and SalI endonuclease (reverse primer). A full list of primer sequences used in this study is shown in Appendix 2. PCR was conducted using High Fidelity TAQ Polymerase (Roche) following manufacturer's guidelines. The 50 µl PCR mix was prepared in a Dome Cap 200 µl PCR tube (Appleton Woods) and contained 1x polymerase buffer, 1 nmole of each primer, 50 ng of template DNA, 0.4 mM of dNTP mix (0.1 mM of each NTP) and 2.5 units of DNA polymerase, all in d H_2O. The tubes were placed in a GeneAmp PCR system 2700 thermal cycler (Applied Biosystems) which was programmed with the following settings: initial DNA denaturation of 5 minutes at 95ºC; then 35 cycles of 95ºC for 30 seconds (denaturation), 56ºC for 30 seconds (annealing), 72ºC for 1 minute (elongation); and a final elongation interval of 7 minutes at 72ºC.

These two restriction sites were present on the MCS of the pBI plasmid and allowed us to insert the ephrinB2-Flac cDNA fragment into it. After sub-cloning, large copy numbers of the pBI-ephrinB2-Flag plasmid were produced via transformation of 5-alpha I^q competent E. coli cells (NEB) and maxi-prep plasmid DNA purification. Finally, the concentration and purity of the plasmid were measured and the plasmid was diluted to a 1 mg/ml concentration in dH_2O.

2.2.1.1 Agarose gel electrophoresis and DNA gel extraction

Amplified PCR fragments were separated and purified from backbone vector using agarose gel electrophoresis. Agarose gels were prepared by mixing 1% agarose (w/v) and 5 µl of Syber Safe DNA dye in 100 ml of TAE buffer; heating the mixture at 100ºC until the slurry had completely dissolved; and then pouring it in a gel casting chamber and allowing it to set. The gel was subsequently placed in a horizontal mini DNA tank (Geneflow) and completely immersed in 1x TAE buffer. 5 µl of PCR products supplemented with 1 µl of 5x DNA gel loading dye (Qiagen) were then loaded in each well of the gel, with one well used to load a 1 Kb DNA size marker (Fermentas). The samples were separated by electrophoresis at 100 Volts for 1 hour.

DNA fragments were visualized under UV light and the ephrinB2-Flag fragment was excised from the gel using a scalpel and was placed in a 1.5 ml tube. The Qiagen DNA gel extraction kit was used to extract the ephrinB2-Flag fragment from the gel according to manufacturer's protocol. Efficiency of purification was assessed by loading 1/10 of the purified ephrinB2-Flag on 1% agarose gel as described above.

2.2.1.2 DNA digestion using restriction enzymes

The ephrinB2-Flag PCR fragment and the pBI vector DNA were digested with SalI and PstI endonucleases (Roche) over night at 37ºC according to manufacturer's protocol. The digestion was set up in 50 µl of d H_2O containing 1x buffer H (Roche) and 10 units of each endonuclease. The digested ephrinB2-Flag fragment and pBI empty vector were resolved in 1% agarose gel at 100 Volts for 1 hour as previously described. Both the digested pBI plasmid and ephrinB2-Flag fragment were purified from the gel as previously described.

2.2.1.3 DNA ligation and bacterial transformation

The ligation mix was 25 µl in volume and contained 1x T4 ligation buffer (NEB), 200 units of T4 ligase (NEB), 3 µl of digested pBI plasmid (~1.5 µg) and 19 µl of digested ephrinB2-Flag fragment. The ligation was carried out over-night at room temperature.

Half of the ligation reaction was used for transformation and transferred to a 1.5 ml tube containing 18 µl of 5-alpha I^q competent E. coli cells (NEB). Transformation procedure was conducted according to manufacturer's protocol. Transformation mix was kept on ice for 30 minutes; heated at 42ºC in a water bath for 45 seconds; and then placed back on ice for 5 minutes. The mix was subsequently supplemented with 250 µl of 2% Lysogeny Broth (LB) and placed on an orbital shaker for 1 hour at 37ºC. 50 µl of the transformation mix were then aseptically streaked on a 10cm LB agar plate containing 100 µg/ml ampicillin. The plate was incubated over-night at 37ºC.

2.2.1.4 Mini-prep DNA purification and DNA sequencing

5 clones were picked from the agar plate and transferred to 5 ml of LB supplemented with 100 µg/ml ampicillin. The tubes were then incubated over-night on a shaker at 37ºC. Bacterial cells were pelleted at 5000 g for 5 minutes and DNA was purified using a Qiagen mini-prep kit, following manufacturer's protocol. An aliquot of purified plasmid was digested with PstI and SalI for 2 hours (as described in section 2.2.1.2) and resolved in a 1% agarose gel at 100 Volts for 1 hour (as described in section 2.2.1.1).

Plasmids containing an insert of the expected size were sequenced using a capillary sequencer ABI 3730 (Functional Genomics facility, Biosciences building, University of Birmingham). The following mixture was prepared for sequencing in a final volume of 20 µl: 3.2 pmoles of pBI MCS2 forward primer, 3.2 pmoles of ephrinB2 internal forward primer, 300 ng of pBI-ephrinB2 plasmid DNA and 1x BigDye Reaction Mixture (BDRM). The sequences were matched against the ephrinB2-Flag cDNA sequence used as a template for PCR.

2.2.1.5 Maxi-scale DNA purification

A small volume (200 µl) of bacterial used for DNA mini-scale purification suspension was added to 400 ml of LB supplemented with 100 µg/ml ampicillin and incubated on a heated shaker at 37ºC over-night. The next day, bacterial cells were pelleted at 5000 g for 5 minutes and the plasmid DNA was purified using a Qiagen maxi-prep kit following

manufacturer's protocol. The plasmid DNA was finally diluted in dH_2O at a final concentration of 1 mg/ml.

2.2.2 Generation of ephrinB2/G and ephrinB2/ΔV mutants

Quick Change Mutagenesis approach was used to generate the ephrinB2/G and ephrinB2/ΔV mutants. The following PCR mix was prepared in a final volume of 50 µl: 1x Pfu polymerase buffer (Fermentas), 50 ng of plasmid DNA, 1 nmole of each primer, 1 mM of dNTP mix (0.25 mM of each dNTP) and 2.5 units of Pfu polymerase enzyme (Fermentas). The PCR was carried out in the thermal cycler which was programmed with the following settings: initial DNA denaturation of 5 minutes at 95ºC; then 18 cycles of 95ºC for 30 seconds (denaturation), 56ºC for 60 seconds (annealing),72ºC for 12 minutes (elongation); and a final elongation interval of 7 minutes at 72ºC. 10 units of DPN1 (Roche) were then added to the PCR mix and incubated at 37ºC for 1 hour to digest the template pBI-ephrinB2-Flag plasmid DNA. The PCR mix was subsequently transferred in a 1.5 ml tube and supplemented with 2 volumes of 100% ethanol and 4 µl of 5 M NaCl (final NaCl concentration of 0.13 M). The tube was placed at -80ºC for 3 hours to allow plasmid DNA precipitation. DNA was then pelleted via centrifugation at 12,000 g for 30 minutes in a mini-centrifuge and the supernatant was discarded. The DNA was washed with 500 µl of 70% ethanol and pelleted at 12,000 g for 15 minutes. Supernatant was removed and the DNA pellet was left to dry at room temperature and successively diluted in 7 µl of dH_2O.

Following the same procedures described in the previous sections, the newly generated pBI-ephrinB2/G-Flag and pBI-ephrinB2/ΔV-Flag plasmids were transformed in bacterial

competent cells and plated on agar plates containing ampicillin. 5 clones for each plasmid were then picked, amplified in 5 ml of LB, digested with SalI and PstI endonucleases and resolved in a 1% agarose gel in order to verify that no recombination events had occurred during PCR. The plasmids were then sequenced as described in section 2.2.1.4 and purified on large scale as described in section 2.2.1.5.

2.3 Cell biology techniques

2.3.1 Flow cytometry analysis

Cells were detached using enzyme-free cell dissociation buffer (Invitrogen) and counted using a Burker chamber. Cells were then centrifuged at 400 g for 3 minutes and re-suspended in ice-cold PBS at 3-5x10^5/50 µl. All the following steps were conducted on ice. 50 µl of 1% BSA/PBS per well were aliquoted to a 96-well U-bottom plate (Iwaki, Japan) and left on ice for 20 minutes to block unspecific binding of antibodies to plastic. Blocking buffer was then replaced with primary antibody diluted in 1% BSA/PBS (150 µl/well). Cells were added to the antibodies and incubated for 1 hour on ice. After centrifugation (400 g for 3 minutes), cells were washed twice in ice-cold PBS (175 µl/well). Cells were then re-suspended in appropriate fluorochrome-labeled secondary antibody diluted in 1% BSA/PBS (150 µl/well). Cells were incubated for 1 hour on ice in the dark and then washed with ice-cold PBS twice, as above. Cells were re-suspended in 250 µl of ice-cold PBS per sample and transferred into flow cytometry tubes (BD Falcon) containing 250 µl of ice-cold 2% paraformaldehyde. Samples were kept in the dark at 4°C prior to analyses on a Beckman Coulter Epics XL or BD Accuri C6 flow cytometer. Primary and secondary antibodies used in this study are listed in table 2.4 at the end of section 2.4.5.4.

2.3.2 Fluorescence Activated Cell Sorting (FACS)

The day before the planned cell sorting experiment, cells were split using trypsin in order to avoid the formation of cell clamps on the day of sorting. All the following procedures were conducted under sterile conditions. Cells were detached using enzyme-free dissociation buffer and pelleted by centrifugation at 400 g for 3 minutes at 4°C. Cells were then re-suspended in 1.5 ml of sterile filtered ice-cold complete growth medium containing primary antibody and incubated on ice for 1 hour. Cells were then centrifuged at 400 g for 3 minutes at 4°C and washed twice with 2 ml of ice-cold complete growth medium. Cells were subsequently re-suspended in 1.5 ml of sterile filtered ice-cold complete growth medium containing appropriate fluorochrome-labeled secondary antibody and incubated on ice in the dark for 1 hour. Cells were washed twice with ice-cold complete growth medium as described above. After final centrifugation at 400 g for 3 minutes at 4°C, cells were re-suspended in 2 ml of ice-cold complete growth medium. Cell suspension was passed through Cell Trics filters (Partec) to remove cell clamps and transferred in sterile FACS tubes (BD Falcon). Two collecting tubes containing 2 ml of ice-cold complete growth medium were prepared in order to separate negative and positive cell populations. Cells were sorted using a Beckman Coulter MoFlo Legacy FACS machine. After sorting, cells were centrifuged at 400 g for 3 minutes, re-suspended in complete growth medium containing double quantity of penicillin/streptomycin antibiotics and plated on Petri dish. Cells were kept in incubator (37°C, 5% CO_2) for 24-48 hours before growth medium was replaced with normal complete growth medium.

2.3.3 Immunofluorescence staining

Cells were plated on ethanol-sterilized 16 mm round glass cover-slips (VWR) placed in a 12-well plate (Corning). When cells reached required density, growth medium was discarded and cells were washed twice in PBS. Subsequently, cells were fixed for 20 minutes with 2% paraformaldehyde/PBS at room temperature. Fixed cells were then washed three times in PBS and permeabilized with 0.1% TritonX-100/PBS for 3 minutes at room temperature. After three more washes in PBS, cells were incubated for 1 hour with blocking solution containing 20% heat inactivated goat serum in PBS. Cover-slips were subsequently placed face-down on a 30 µl drop of primary antibody diluted in blocking solution aliquoted on nescofilm (Bando Chemical) which had been previously arranged in a humid chamber. Incubation with primary antibody lasted 1 hour. Cover-slips were then placed back in the 12-well plate and washed three times for 10 minutes with PBS on an orbital shaker at room temperature. Incubation with fluorescent secondary antibody diluted 1:200 and subsequent washes (under aluminium foil) was performed using the procedure described above. Stained coverslips were air-dried and mounted on glass slides using 10 µl of anti-fade fluorescence mounting medium containing 0.1 µg/ml Hoechst 33342. Cover-slips were sealed on the edges by transparent nail varnish and stored at -20ºC. Immunofluorescence staining was analyzed at a ZEISS LSM510 META confocal microscope.

2.3.4 Hoechst staining of 3D colonies grown in 2% MG

Colonies grown in 2% Matrigel were carefully washed with 400 µl of PBS and subsequently fixed with 400 µl of 3% paraformaldehyde/PBS for 40 minutes at room temperature. Colonies were then washed once with PBS as described above and incubated with 200 µl of 0.1% TritonX-100/PBS at room temperature for 3-5 minutes. Permeabilizing solution was removed and 200 µl of 0.05% TritonX-100/PBS containing 0.1 µg/ml Hoechst 33342 was added to wells to stain nuclei. Colonies were incubated for 40 minutes at room temperature in the dark. The excess of staining solution was removed and colonies were washed twice (10 minutes for each wash) with 400 µl of PBS at room temperature. Finally, washing solution was replaced with 200 µl of PBS containing 0.02% Sodium Azide (NaN_3). Cells were left in the dark at 4ºC over night before pictures were taken at a ZEISS LSM510 META confocal microscope using a 20x objective.

2.3.5 Gap-closure assay

Cells were detached and counted in a Burker chamber. Cells were resuspended in 1 ml of complete growth medium in a 15 ml tube (Corning) at a concentration of $3*10^5$ cells/ml and 70 µl were aliquoted and plated in the chambers of a 35mm µ-Dish culture insert (Ibidi), as described in step 2 of figure 2.1. The dish was placed in the incubator at 37ºC, 5% CO_2 for 24 hours and, the next day, cells were stimulated with 1µg/ml doxycycline for further 24 hours in the incubator. The chamber insert was removed (step 3), leaving a 500 µm wide gap between the two cell populations. 2 ml of fresh growth medium containing 1 µg/ml

doxycycline was added to the dish (step 4). Cells were returned to the incubator and gap-closure was observed using a Nikon Eclipse TS100 inverted fluorescence microscope every 24 hours for 8 days. When RFP and GFP expressing cells were used, the 8 day time-point was photographed using red and green filters at the same microscope.

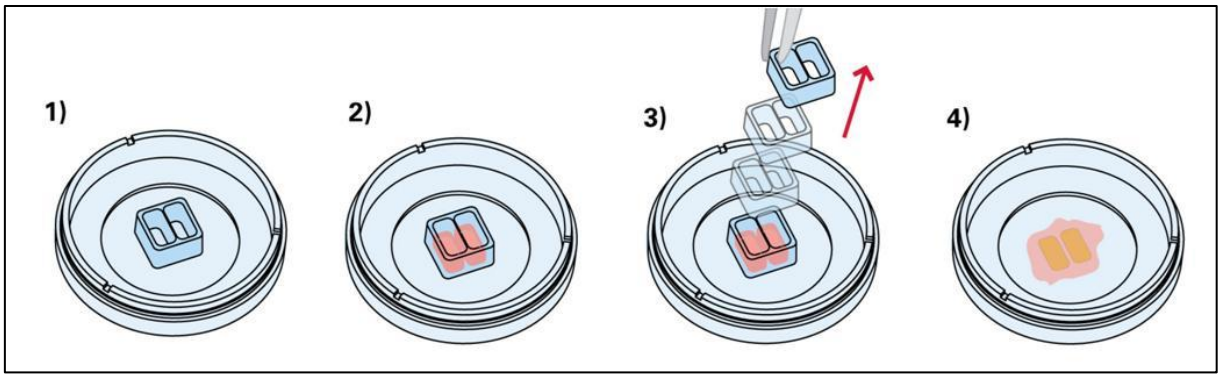

Figure 2.1: diagram illustrating a gap-closure assay. 1) Silicon insert formed of two chambers glued to the glass bottom of a 35mm dish (Ibidi); 2) 70 µl of cell suspension are added to each chamber of the insert; 3) after cells have reached confluency within the chambers, the silicon insert is removed using forceps; 4) cells are covered with 2 ml of fresh growth medium and placed in incubator. The 500 µm gap between the two cell populations is closed as cells proliferate and migrate outward.

2.4 Biochemical methods

2.4.1 Protein extraction for Western blot analysis

Cells were grown in 35 mm or 60 mm Petri dishes until they reach 90% confluency. Growth medium was removed from dishes and cells were washed twice with PBS. Depending on cell confluency and dish size, 50-200 µl of freshly made Laemmli lysis buffer (without bromophenol blue) was added to the dishes and cells were scraped from the surface using disposable plastic cell scrapers (Sarsted). Cell lysates were then transferred to 1.5 ml plastic tubes (Starlabs), heated at 95°C for 15 minutes and spun down. At this point, samples were either frozen at -80°C for long term storage or directly assayed for protein concentration and prepared for separation on SDS-PAGE.

When preparing samples for signalling experiments (section 3.1.2.2), cells were starved in serum-free medium for 4 hours and stimulated with the chimeric molecule EphB4/Fc for various time intervals prior to lysis. EphB4/Fc was pre-clustered with anti-human Fc IgG antibody as described in section 2.1.10 and subsequently added to the growth medium at a final concentration of 5 µg/ml.

When inhibiting Src family kinases in signalling experiments (section 3.1.2.2), the Src inhibitor SU6656 (Calbiochem) was added to serum-free medium at a final concentration of 10 µM, 1 hour prior to stimulation with the EphB4/Fc chimera molecule. The inhibitor was left in growth medium throughout the time-course of EphB4/Fc stimulation as described in the study by (Palmer, Zimmer et al. 2002).

2.4.2 Protein Assay

Frozen cell lysates were left to thaw at room temperature, heated at 95°C for 5 minutes and spun down. Samples were assayed in a 96-well flat-bottom plate (BD Falcon) using BioRad D_C protein assay kit, according to the manufacturer's protocol (Bio-Rad Laboratories). Protein concentration for each sample was determined using Excel Datasheet (Windows Office 2007). Protein lysates were diluted with Laemmli buffer to equalize protein concentration and supplemented with ¼ volume of 4x Laemmli buffer. If necessary, samples were supplemented with 2-β-mercaptoethanol at a final concentration of 5% to keep proteins reduced. Once samples were prepared for loading and mixed homogenously, samples were heated at 95°C for 5 minutes and loaded on a SDS-PAGE gel or frozen at -80°C for long term storage.

2.4.3 SDS – PAGE and Immunoblotting

Protein samples were resolved using SDS-polyacrylamide gel electrophoresis (PAGE). Proteins were separated using 8 or 10% SDS-PAGE (Appendix 3). If used, frozen samples were thawed at room temperature and heated at 95°C for 5 minutes before loading. Proteins were resolved at 12 mA using BioRad electrophoretic equipment (power pack, gel tank and gel glasses). Pre-stained protein markers (NEB) were used to monitor sample separation. Resolved proteins were subsequently transferred to nitrocellulose membrane (VWR) via electroblotting at 40 V over-night using BioRad electroblotting equipment (power pack, gel tank, blotting sandwich holders and sponges). The membranes were rinsed in PBS-Tween

0.1% and then incubated in 5% dry skimmed milk (Marvel) diluted in PBS-Tween to block unspecific binding of antibodies. Membranes were incubated with primary antibody over night at 4°C on a rotating platform and then washed three times for 10 minutes each with PBS-Tween. When blots were developed on film, membranes were incubated with the appropriate horseradish peroxidase (HRP)-conjugated secondary antibody for 1 hour at room temperature on an orbital shaker and then washed three times for 10 minutes with PBS-Tween. Proteins were detected using Enhanced Chemiluminescence Plus reagents (ECL Plus) (Biological Industries) followed by autoradiography: films were developed using a Kodak X-OMAT 1000 developer. All primary antibodies used for immunoblotting are listed in table 2.4 at the end of section 2.4.5.4. When detecting phospho-proteins, membranes were washed and incubated in TBS-Tween 0.1%.

When developing membranes using the Odyssey CLx infrared imaging system (Licor), IRDye 800CW or 680CW secondary antibodies were used. Incubation with these antibodies and subsequent washes were performed in the dark. Membranes were then placed on the glass panel of the imaging system and infrared fluorescence was recorded.

2.4.4 Densitometric analysis on the Odyssey CLx

Densitometric analysis was carried out on the images of Western blots obtained with the Odyssey CLx infrared imaging system (Licor). Equal square boxes were drawn around each band and the infrared fluorescence absorbance within the boxes was measured. The background level for each individual blot was calculated on an area free of bands and subtracted from the absorbance readings of the measured bands. These raw absorbance values

represented the denistometric value which we used to quantify the levels of protein expression in Western blots throughout this study.

2.4.5 Pull down and co-immunoprecipitation assays

2.4.5.1 Protein extraction

Cells grown on 35 or 60 mm Petri dishes were washed twice with PBS and 300 or 600 µl of ice cold 1% TritonX-100 lysis buffer was added (see Appendix 3 for buffer composition). All solutions, Petri dishes and samples were kept on ice during procedures. Cells were scraped using disposable plastic cell scrapers and cell lysates were transferred to a 1.5 ml tube and placed at 4ºC on a rotary wheel for 30 minutes to ensure total lysis. Samples were then centrifuged at 12,000 g for 10 minutes in a mini-centrifuge (Eppendorf) to remove insoluble material.

When preparing samples for signalling experiments (section 3.2.1.1 and 3.2.1.2), cells were starved in serum-free medium for 4 hours and stimulated with the chimeric molecule EphB4/Fc for multiple time-points prior to lysis, as described in section 2.4.1.

2.4.5.2 Pull down assay

NeutrAvidin™-conjugated agarose beads (50% slurry solution) were transferred to 1.5 ml tubes (30 µl/tube) and washed twice with 500 µl of ice cold PBS. Two tubes containing NeutrAvidin agarose beads were prepared for each sample. In one tube, NeutrAvidin agarose beads were incubated with custom made biotin-conjugated peptides in 400 µl of ice cold PBS at 4ºC on a rotary wheel for 1 hour and subsequently washed twice with 500 µl of PBS. The second tube was kept for pre-clearance of cell lysates.

Prior to pre-clearance, 45 µl of cell lysate where aliquoted from each sample and prepared for WB loading to serve as whole lysate control. Cell lysates were then incubated with the NeutrAvidin agarose beads prepared for pre-clearance for 45 minutes at 4ºC on a rotary wheel. Subsequently, pre-clearance NeutrAvidin agarose beads were discarded and cell lysates were incubated with peptide-conjugated NeutrAvidin beads over-night at 4ºC on a rotary wheel.

The next day, peptide-conjugated NeutrAvidin beads were spun down in a mini-centrifuge and the supernatant was discarded. The beads where then washed three times with ice cold TBS-Tween 0.1%.

2.4.5.3 Co-immunoprecipitation assay

Anti-Flag mAb (M2) conjugated to agarose beads was prepared for immunoprecipitation as described above (30 µl/sample). Cell lysates were incubated with anti-Flag conjugated agarose beads over-night on a rotary wheel at 4ºC. Anti-Flag conjugated agarose beads were then washed three times as described above.

2.4.5.4 Sample preparation for WB analysis

Each sample was prepared for WB by adding 15 µl of 2x Laemmli buffer containing 10% 2-β-mercaptoethanol. Samples were then shortly vortexed, spun down in a mini-centrifuge and boiled at 95ºC for 5 minutes. Whole lysate control samples were prepared for WB loading by adding 15 µl of 4x Laemmli buffer and 1.5 µl of 2-β-mercaptoethanol to each sample. Samples were either loaded immediately on SDS-PAGE gels or frozen at -80ºC for long term storage. When loading samples on SDS-PAGE gels, beads were discarded.

Primary antibodies	Target antigen	Target MW (kDa)	Source	Supplier	Catalogue number
anti-Flag pAb	Flag sequence	-	Rabbit	Sigma	F7425
anti-Flag M2 mAb	Flag sequence	-	Mouse	Sigma	F1804
ephrinB1/2/3 (C-18) pAb	C-terminus of human ephrinB1/2/3	45-55	Rabbit	Santa Cruz	sc-910
phospho-ephrinB pAb	human pEphrinB (Tyr324/329)	45-55	Rabbit	Cell Signaling	3481
Src (36D10) mAb	C-terminus of human Src	60	Rabbit	Cell Signaling	2109
phospho-Src Family pAb	human pSrc (Tyr416)	60	Rabbit	Cell Signaling	2101
EphB4	mouse EphB4 extracellular domain	120	Goat	R&D	AF446
CASK mAb	CASK aa353-486	120	Mouse	BD Transduction Laboratories	610782
β-actin mAb	N-terminus of β-actin	42	Mouse	Sigma	A5441
SDCBP (M01) mAb (syntenin-1)	human SDCBP aa 1-101	33	Mouse	Abnova	H0000638 6-M01
Dvl-2 mAb (30D2)	Human Dishevelled-2	90-95	Rabbit	Cell Signaling	3224
anti-myc (A-14)	C-terminus of human c-myc	-	Rabbit	Santa Cruz	sc-789
anti-GST (B-14)	GST protein	26	Mouse	Santa Cruz	sc-138
4C5G	mouse PI4K	-	Mouse	LGC Standards	CRL-2538
CD81 (M38)	human CD81	22-24	Mouse	hybridoma provided by	-

Table 2.4: list of primary antibodies used in this study.

Secondary antibodies	Target antigen	Source	Supplier	Catalogue number
anti-human Fc IgG	human IgG, Fc specific	Goat	Sigma	I2136
anti-mouse Igs/HRP	Mouse IgG, IgA, IgM	Goat	DakoCytomation	P0447
anti-rabbit Igs/HRP	All rabbit Igs	Goat	DakoCytomation	P0448
anti-goat Igs/HRP	All goat Igs	Rabbit	DakoCytomation	P0449
anti-rabbit IgG/IRDye 800CW	Rabbit IgG	Goat	Licor	926-32211
anti-mouse IgG/IRDye 680RD	Mouse IgG	Goat	Licor	926-68078
anti-mouse FITC	Mouse IgG	Goat	Sigma	F2012
Alexa Fluor® 488 F(ab')2 anti-mouse	Mouse IgG	Goat	Life Techonologies	A11017

Table 2.5: list of secondary antibodies used in this study.

2.4.6 Biotinylation assay

2.4.6.1 Biotin labelling and internalization

Cells were grown in 60 mm Petri dishes and were 80-90% confluent on the day of the experiment. Duplicate plates were prepared for each condition, as each sample required a control. All procedures were performed on ice and, when necessary, in a cold room with all solutions chilled prior to use. Cells were washed twice in PBS* (PBS supplemented with 1 mM $MgCl_2$ and 0.5 mM $CaCl_2$). 3 ml of PBS* containing EZ link NHS-SS-Biotin (Thermo Scientific) were then added to cells and the dishes were incubated on a rotating platform at 4ºC for 1 hour. After incubation, biotin solution was removed and remaining free biotin was quenched by washing cells three times for 5 minutes with PBS* containing 50 mM glycine and 0.5% BSA at 4ºC. Cells were washed twice with PBS* and subsequently incubated at 37ºC, 5% CO_2 for 15 or 60 minutes in pre-warmed complete growth medium containing either anti-Fc IgG antibody at a final concentration of 2.5 µg/ml or EphB4/Fc at a final concentration of 5 µg/ml, as described in section 2.4.1.

2.4.6.2 MESNA treatment and pull down assay

After the incubation period which allowed cell surface proteins to be internalized, cells were washed twice with PBS*. Cells on one of the plates were lysed in 1% TritonX-100 lysis buffer as described in section 2.4.5.1. Cells on the other plate were successively incubated four times with MESNA at 4ºC for 15 minutes on a rotating platform. Cells were

subsequently washed twice with PBS** (PBS supplemented with 0.33 mM $MgCl_2$ and 0.9 mM $CaCl_2$) and incubated with PBS** containing 5 mg/ml iodoacetamide at 4ºC for 15 minutes to quench residual MESNA. After the incubation, cells were washed three times with PBS** and lysed as above. Biotinylated proteins from protein lysates were collected on NeutrAvidin-conjugated agarose beads after over-night incubation at 4ºC on a rotary wheel (15 µl of agarose beads were used per reaction). Samples were washed three times with TBS-Tween 0.1% and resolved by SDS-PAGE as described in section 2.4.5.4. Resolved proteins were transferred to nitrocellulose membrane and blots were developed using the Odyssey CLx infrared imaging system (Licor) as described in section 2.4.3. Densitometric analysis was performed using the Odyssey CLx imaging software (Licor).

2.4.7 Label-free interaction analysis (Biacore)

Label-free interaction analysis was conducted on a Biacore 3000. Biacore sensor CM5 chips (GE Healthcare) were coated with streptavidin (GE Healthcare) using EDC/NHS, ethanolamine and glycine 0.1 M solutions. Response Units (RU) were then normalized and biotin-conjugated peptides were added to the streptavidin-coated chips by means of applying a constant flow of HBS-EP solution containing 100 µg/ml of peptide and 1% DMSO. A list of peptides used can be found in Appendix 2. Once peptide binding to streptavidin reached saturation, the flow was interrupted, the RU were normalized and recombinant full length syntenin-1 protein was injected to the flow of HBS-EP solution. As syntenin-1 binding reached a saturation plateau, the injection of protein-containing solution was substituted with HBS-EP buffer and the constant flow was maintained until syntenin-1 was completely removed from peptides. The binding curves, or "sensorgrams", for each peptide (including the negative control peptide NET5) were normalized and presented in a unified graph for comparison.

RESULTS AND DISCUSSION

3.1 Establishing an epithelial breast cancer model system to study ephrinB2 biology

Normal breast epithelial cells naturally express low levels of the ephrinB2 ligand, while myoepithelial cells express the cognate EphB4 receptor. However, during the proliferative phase of the mammary gland development epithelial cells temporarily express the EphB4 receptor as well (Munarini, Jager et al. 2002). The difficulty in finding a suitable cell line in which to study ephrinB2 biology derives from the fact that many breast epithelial cancer cells acquire the ability to express the EphB4 receptor. In fact, during mammary gland carcinogenesis EphB4 receptor expression is shifted from myoepithelial to epithelial cells (Nikolova, Djonov et al. 1998). Moreover, in most breast cancers the EphB4 receptor is found in 58% of the tumour tissue (Kumar, Singh et al. 2006).

3.1.1 Identifying a suitable epithelial breast cancer cell model

As a first step, it was necessary to screen a wide range of epithelial breast cancer cell lines to identify cells that don't express (or express low relative levels of) ephrinB ligands. This was fundamental, as our intention was to create a model system in which we could establish a stable expression of the ephrinB2 protein or ephrinB2 mutants in an epithelial breast cancer cell line.

We performed Western Blotting (WB) analysis on a panel of 21 breast cancer cell lines to assess the endogenous expression levels of ephrinB ligands. Myoepithelial and HB2 cells (a non-tumorigenic mammary epithelial cell line which displays luminal phenotype) were also included in the screening. WB data shown in figure 3.1 demonstrates that ephrinB ligands are heterogeneously expressed within the panel of cell lines tested. Furthermore, the expression levels vary considerably, with some cell lines expressing high levels of ephrinB ligands (such as MDA-MB-330, CAMA-1, ZR75.1 and SUM149), whilst others expressing smaller amounts (such as HB2, MDA-MB-134, MRSV, BT549, DCIS, GI101 and MDA-MB-231). We have also found that expression of ephrinB ligands was below the level of detection in several cell lines (such as MDA-MB-175, MDA-MB-435, MCF7, T47D, BT474, SKBR3, MYO, BT20, CAL51 and MDA-MB-468). As ephrinB ligands are all relatively similar in size (ephrinB1 = 346 aa; ephrinB2 = 333 aa; ephrinB3 = 340 aa) and are subject to N-glycosylation (data not shown), it was difficult to distinguish between them on the blot when using pan anti-ephrinB pAb. The lower molecular weight band (between 25 and 30 kDa) is probably associated with EphB-induced ligand degradation.

As the preferential receptor for ephrinB2 is the EphB4 receptor (Pasquale 2008), we also analysed endogenous EphB4 levels in these cell lines (figure 3.1). Interestingly, we observed that EphB4 was expressed at different levels in nearly all these cell lines, with only MDA-MB-134, MCF7 and MDA-MB-157 cells expressing minimal amounts or no protein. Within EphB4 expressing cell lines, we noticed that MDA-MB-330, T47D, ZR75.1, BT474, SKBR3, ZR75.30, DCIS, GI101 and MDA-MB-468 expressed higher levels of the EphB4 receptor compared to the remaining cell lines.

One of the main aims of our study was to understand the significance of the ephrinB2 – syntenin-1 axis in the context of epithelial breast cancer. Although syntenin-1 is widely

expressed in different cell types and usually abundant in epithelial cells (Beekman and Coffer 2008), we analysed endogenous syntenin-1 expression levels in the same panel of cell lines using WB (figure 3.1). As expected, all cell lines expressed medium to high levels of endogenous syntenin-1, apart from MDA-MB-157 cells in which syntenin-1 was barely detectable.

Table 3.1 summarizes the data on expression levels of ephrinB ligands, EphB4 and syntenin-1. Based on these data, the MCF7 cell line (lane 7, figure 3.1) stood out as the best candidate to use as a model system. Although it expresses lower levels of syntenin-1 compared to some of the other cell lines, it presents minimal levels of endogenous EphB4 and no ephrinB ligands.

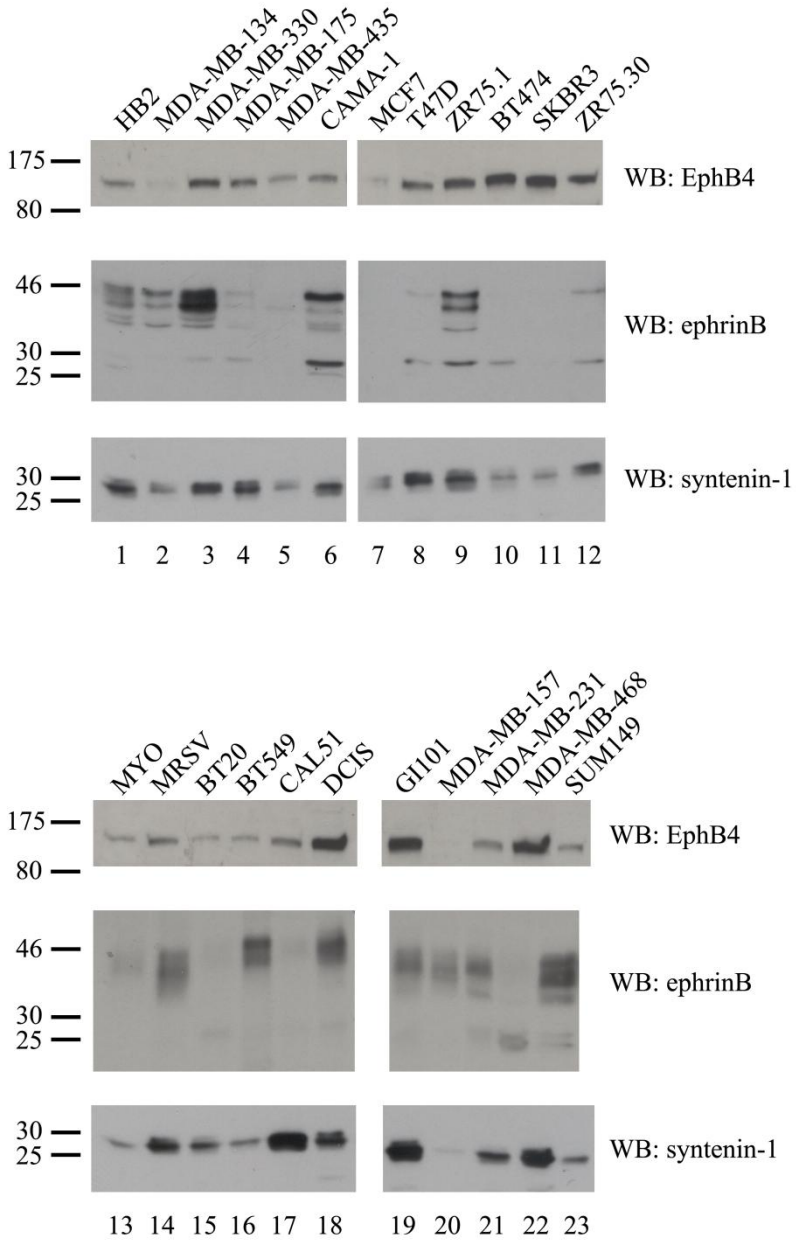

Figure 3.1: ephrinB, EphB4 and syntenin-1 expression in a panel of breast cell lines.
A panel of breast cancer cell lines together with myoepithelial and non-tumourigenic HB2 mammary cells was tested for EphB4 receptor, ephrinB ligands and syntenin-1 expression using WB. Cell lysates were provided by Dr Fedor Berditchevski and protein concentrations were measured and standardized to ensure equal loading on SDS-PAGE. Endogenous EphB4 was detected with anti-EphB4 pAb; endogenous ephrinB ligands were detected with anti-ephrinB pAb which recognizes the C-terminal tail of all three ephrinB ligands; endogenous syntenin-1 was detected with anti-syntenin-1 mAb.

Cell line	EphB4 expression	ephrinB expression	syntenin-1 expression	WB lane
HB2	LOW	MEDIUM	MEDIUM	1
MDA-MB-134	MINIMAL	MEDIUM	LOW	2
MDA-MB-330	MEDIUM	HIGH	MEDIUM	3
MDA-MB-175	MEDIUM	LOW	MEDIUM	4
MDA-MB-435	LOW	MINIMAL	LOW	5
CAMA-1	LOW	HIGH	MEDIUM	6
MCF7	LOW	NONE	LOW	7
T47D	MEDIUM	MINIMAL	MEDIUM	8
ZR75.1	HIGH	HIGH	MEDIUM	9
BT474	HIGH	NONE	LOW	10
SKBR3	HIGH	NONE	LOW	11
ZR75.30	MEDIUM	LOW	MEDIUM	12
MYO	LOW	LOW	LOW	13
MRSV	MEDIUM	MEDIUM	MEDIUM	14
BT20	LOW	MINIMAL	MEDIUM	15
BT549	LOW	MEDIUM	LOW	16
CAL51	MEDIUM	MINIMAL	HIGH	17
DCIS	HIGH	MEDIUM	MEDIUM	18
GI101	HIGH	MEDIUM	HIGH	19
MDA-MB-157	NONE	MEDIUM	MINIMAL	20
MDA-MB-231	LOW	MEDIUM	MEDIUM	21
MDA-MB-468	HIGH	MINIMAL	HIGH	22
SUM149	LOW	HIGH	LOW	23

Table 3.1: general indications on the level of overall expression of EphB4, ephrinB ligands and syntenin-1 proteins in 23 epithelial mammary cell lines analyzed via WB analysis. Indications refer to the signal strength detected by WB: none = no signal detected; minimal = signal barely visible; low-high: relative signal strength, with high being the highest signal detected for a specific protein.

3.1.2 Generation and characterization of MCF7 cells expressing wild type ephrinB2

In generating our model system, we decided to establish an MCF7 cell line which expressed the wild type ephrinB2 protein containing a Flag sequence at the N-terminus. This modification should not alter protein functionality or binding ability to the EphB4 receptor and allowed us to use anti-Flag antibodies throughout our study to monitor expression levels of transfected ephrinB2 for some of the planned experiments. In order to achieve stable protein expression, we stably transfected MCF7 cells with ephrinB2-Flag as described in section 2.1.4 of Materials and Methods. Fluorescence-activated Cell Sorting (FACS) using anti-Flag antibody was subsequently performed in order to select and separate ephrinB2-Flag expressing cells from non-expressing cells, as described in section 2.3.2 of Materials and Methods. FACS was performed twice to obtain a homogenous population of MCF7 cells expressing high levels of ephrinB2 on the cell surface. From this moment onward, we will refer to ephrinB2-Flag expressing MCF7 cells as MCF7-ephrinB2.

3.1.2.1 Assessing cell surface expression, overall expression and cell localization of ephrinB2

After having established the MCF7-ephrinB2 cell line, we verified cell surface expression levels using flow cytometry; overall expression levels by WB analysis; and protein localization within cells using immunofluorescence. The histogram in figure 3.2A illustrates mean fluorescence values obtained with flow cytometry performed on MCF7-ephrinB2 and MCF7 parental cells using anti-Flag antibody. Figure 3.2B illustrates results of WB with both anti-Flag and anti-ephrinB antibodies to detect ephrinB2 overall expression. EphrinB2 appears as a doublet due to different glycosylation status. We also assessed phosphorylation of ephrinB2 using a phospho-specific ephrinB antibody and observed that the basal level of phosphorylation was low in MCF7-ephrinB2 cells. In order to determine localization of ephrinB2 in MCF7 cells, we carried out immunofluorescence analysis on MCF7-ephrinB2 cells using anti-Flag antibody. Hoechst 33342 was used to stain the nuclei. Figure 3.2C shows that ephrinB2 is mostly detected at the plasma membrane. Taken together, the flow cytometry, WB analysis and immunofluorescence prove that ephrinB2 is expressed in MCF7-ephrinB2 cells and that it is mainly localized on the cell surface.

A)

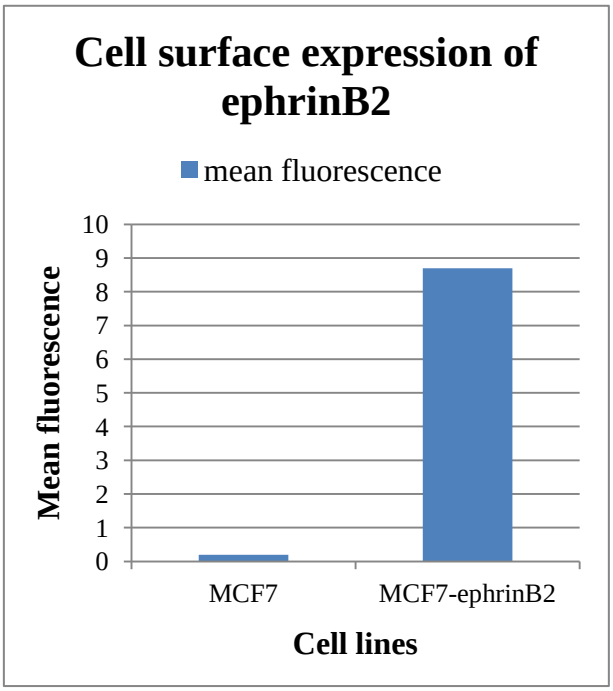

B)

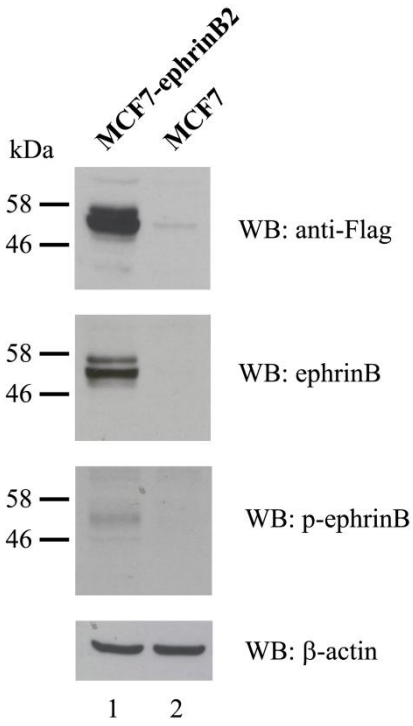

C)

Immunofluorescence on MCF7-ephrinB2 cells

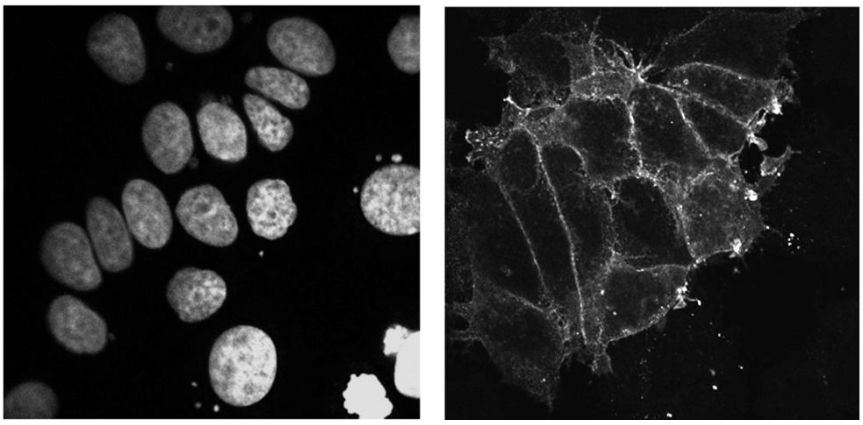

Hoechst 33342 anti-Flag

Figure 3.2: the stably transfected MCF7-ephrinB2 cell line shows robust expression and clear localization of ephrinB2 on the cell surface.
MCF7 cells were stably transfected with a plasmid encoding Flag-tagged ephrinB2 wild type and sorted for ephrinB2 expression on the cell surface via FACS. **A**) flow cytometry analysis using anti-flag mAb to detect ephrinB2 cell surface expression in parental MCF7 cells and stably transfected MCF7-ephrinB2 cells after sorting. The histogram shows the mean fluorescence values measured. **B**) MCF7-ephrinB2 and MCF7 parental cells were lysed in 1x Laemmli buffer and protein samples resolved on SDS-PAGE. EphrinB2 total expression was detected with anti-Flag mAb and anti-ephrinB pAb. Phosphorylated ephrinB2 was detected with phospho-specific anti-ephrinB pAb. β-actin was detected with anti-β-actin mAb as loading control. **C**) immunofluorescence images taken at the confocal microscope of MCF7-ephrinB2 cells fixed with 2% PFA and probed with anti-Flag mAb. Hoechst33342 staining was used for nuclear detection.

3.1.2.2 Assessing the functionality of ephrinB2

To confirm the functionality of ephrinB2-Flag in MCF7 cells, we stimulated MCF7-ephrinB2 cells with a soluble EphB4/Fc molecule and examined ephrinB2 and Src phosphorylation using WB analysis. In a parallel experiment, we added the Src family kinase inhibitor SU6656 to cells 1 hour prior to EphB4/Fc stimulation. This allowed us to determine whether ephrinB2 phosphorylation upon EphB4/Fc stimulation is Src dependent. We stimulated MCF7-ephrinB2 cells with the EphB4/Fc soluble protein after 4 hours of serum deprivation to minimize possible basal phosphorylation of the protein. Taking into consideration previous studies on ephrinB2 phosphorylation induced by soluble EphB4 ligand (Georgakopoulos, Litterst et al. 2006; Georgakopoulos, Xu et al. 2011), we stimulated cells with 5 µg/ml EphB4/Fc chimera pre-clustered with anti-human Fc IgG antibody in order to maximize ephrinB2 phosphorylation. In fact, multimerization of ephrinB ligands strongly increases signal activation (Blits-Huizinga, Nelersa et al. 2004).

Figure 3.3A shows the WB analysis of MCF7-ephrinB2 cells stimulated with EphB4/Fc. Phosphorylation of Src family kinases is induced at the earliest time-point of 5 minutes (lane 2) and remains stable up to the final time-point of 240 minutes, where it decreases (lane 7). EphrinB2 phosphorylation appears at the 15 minute time-point (lane 3) and increases over time, reaching its peak between 60 and 120 minutes (lanes 5 and 6 respectively). At the 240 minute time-point (lane 7) ephrinB2 phosphorylation diminishes, which is consistent with signal termination and protein degradation described previously (Pasquale 2008). Indeed, ephrinB2 overall expression levels also decreased at the longer time-points (120 and 240 minutes, lanes 6 and 7, respectively). As expected, Src overall expression levels remained unchanged.

Figure 3.3B illustrates the effect of Src inhibitor on EphB4-induced phosphorylation of ephrinB2 and Src. In accordance to previous studies, we used SU6656 at a concentration of 10 μM (Palmer, Zimmer et al. 2002; Georgakopoulos, Litterst et al. 2006). As a consequence of the treatment, Src phosphorylation remained essentially unchanged with only slight increase at the later time-points (lanes 5-7). Importantly, EphB4/Fc-induced ephrinB2 phosphorylation levels were also decreased and only started appearing after 30 minutes from stimulation (lane 4). Total ephrinB2 expression levels only slightly decreased at the later time-points of 120 and 240 minutes (lanes 6 and 7 respectively).

Taken together, these results proved that ephrinB2 was functional and that EphB4/Fc stimulation triggered ligand phosphorylation via Src activation. We concluded that our MCF7-ephrinB2 cell line was a good model to use in our study. Additionally, we observed that the basal level of ephrinB2 phosphorylation was low in non-stimulated conditions, while the basal level of Src phosphorylation was relatively high (probably due to basal integrin-dependent signalling). Furthermore, we noticed that the decrease in ephrinB2 total levels at the later time-points was less pronounced in the presence of the SU6656 inhibitor, suggesting that Src and/or ephrinB2 phosphorylation might increase ligand degradation.

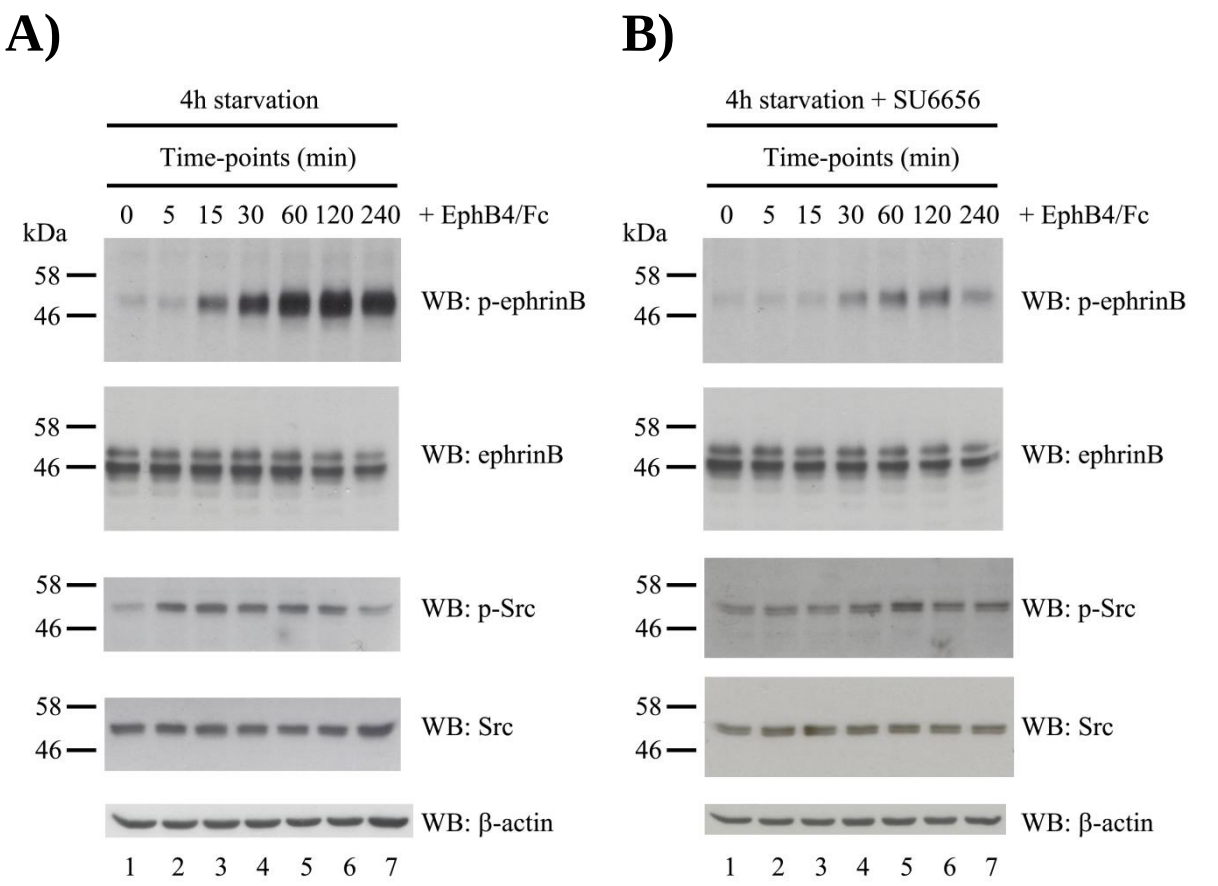

Figure 3.3: ephrinB2 phosphorylation is induced by soluble EphB4/Fc and is dependent on Src activation. EphrinB2 functionality was tested by stimulating cells with EphB4/Fc in the presence or absence of the Src family inhibitor SU6656 and detecting phospho and total levels of ephrinB2 and Src proteins by WB. MCF7-ephrinB2 cells were starved in serum-free medium for 4 hours and then stimulated with 5 µg/ml of EphB4/Fc, pre-clustered with anti-Fc IgG, for 5, 15, 30, 60, 120 and 240 minutes (panel **A**). In panel **B**, the Src inhibitor SU6656 was added to the medium 1 hour prior to stimulation at a concentration of 10 µM and was left in medium throughout the stimulation time-course. Cells were lysed in Laemmli buffer and protein samples resolved on SDS-PAGE. Phospho and total levels of ephrinB2 and Src were detected using phospho-specific anti-ephrinB pAb (Tyr324/329), anti-ephrinB pAb, phospho-specific anti-Src family pAb (Tyr416) and anti-Src family pAb. β-actin was detected using anti- β-actin mAb as loading control. Note, in the presence of Src inhibitor SU6656 (panel **B**), both ephrinB2 and Src phosphorylation is strongly impaired.

3.1.2.3 Impact of ephrinB2 expression on 3D colony growth of MCF7 cells

Culturing of cells in extracellular matrix (3D-ECM) provides valuable knowledge on how basic biological processes can impact higher-order tissue architecture. Some of the mammary epithelial cell lines grown in 3D-ECM are able to form spherical structures with a central lumen resembling breast acini. Thus, 3D-based systems are often used to identify proteins and signalling pathways that regulate mammary morphogenesis and cancer development. This type of cell culturing represents a more physiological-like setting, thus revealing protein functions which would not be necessarily detectable when cells are grown as a monolayer on plastic (Hebner, Weaver et al. 2008). MCF7 cells can be cultured in 3D collagen and Matrigel (MG), where they form round colonies (Kirshner, Chen et al. 2003). EphrinB2 reverse signalling plays an important role in cell segregation and cell polarity during mammary gland morphogenesis (Nikolova, Djonov et al. 1998; Munarini, Jager et al. 2002); and induces angiogenesis and metastasis during breast tumour progression (Pasquale 2010). Thus, growing MCF7-ephrinB2 cells in 3D cultures and stimulating them with EphB4/Fc should allow us to uncover physiologically and pathologically relevant functions of ephrinB2 reverse signalling which might have remained undetected under *in vitro* standard settings.

For these reasons, we carried out a preliminary experiment whereby we cultured MCF7 parental cells and MCF7-ephrinB2 cells in either 3D collagen I or Matrigel in the presence or absence of the EphB4/Fc chimera. Cells were embedded in 3D-ECM and allowed to grow for 12 days, during which EphB4/Fc pre-clustered with anti-Fc IgG was added to the growing medium every two days.

When we cultured cells in collagen, colonies formed by MCF7-ephrinB2 and MCF7 parental cells grew as uniform compact spheres with no clearly detectable cell-to-cell boundaries (figure 3.4A). After 12 days of culturing, we were unable to observe any differences in morphology and only limited differences in size of the colonies formed by the control MCF7 and MCF7-ephrinB2 cells (Figure 3.4A, upper panels). Moreover, EphB4/Fc stimulation did not appear to affect either morphology or size of the colonies formed by control MCF7 and MCF7-ephrinB2 cells (Figure 3.4A, lower panels). In order to carry out a statistical analysis of colony size, we used Nikon software to calculate the surface area (in pixels) of the colony's circumference, which was manually drawn around the widest point of the colony. 30 colonies per condition were analysed. The histogram and the table outlining the distribution of colony size highlighted a decrease in the quantity of MCF7-ephrinB2 colonies in the 20-25 size class compared to MCF7 colonies (figure 3.4B). Furthermore, there were no EphB4/Fc-stimulated MCF7 colonies in the <15 size class. However, as we detected MCF7-ephrinB2 colonies in the 25-30 and >30 size classes and as the size distribution pattern of MCF7 colonies stimulated with EphB4/Fc was not particularly different to the pattern of MCF7 colonies in the other size classes, we concluded that these differences were probably due to variability within the experimental settings. Subsequent experiments conducted in the same conditions proved that this was indeed the case (data not shown).

When cells were cultured in Matrigel, we observed considerable differences both in morphology and size between colonies formed by MCF7-ephrinB2 and MCF7 control cells. After 12 days of growth, colonies formed by control MCF7 cells appeared sphere-like and cell -cell boundaries were partially detectable at the periphery of the colonies (figure 3.4C). In comparison, the colonies formed by MCF7-ephrinB2 cells were considerably larger with less defined shape. The colony margins were not clearly defined, as the more peripheral cells

seemed to spread and/or migrate away from the main body of the colony. The size distribution analysis confirmed that MCF7-ephrinB2 colonies tended to be larger and more varied in size (figure 3.4D). More specifically, most MCF7 colonies fell in the 20-40 size class (56%) and the 40-60 class size (28%), while very few colonies were present in the higher size classes (8% in the 60-80 size class and 4% in the >80 size class). MCF7-ephrinB2 colonies were notably larger, with 20% measured in the 20-40 size class, 48% in the 40-60 size class, 28% in the 60-80 size class and 4% in the >80 size class. Surprisingly, EphB4/Fc stimulation only marginally increased colony size of MCF7-ephrinB2 colonies, while it did not affect the colony size of control MCF7 cells. Most of the MCF7 colonies stimulated with EphB4/Fc still fell in the 20-40 size class (68%) and the 40-60 size class (20%) with very few colonies in the 60-80 size class (8%). EphB4/Fc stimulation only slightly increased MCF7-ephrinB2 colony size, with 4% of colonies in the 20-40 size class, 32% in the 40-60 size class, 44% in the 60-80 size class and 20% in the >80 size class. As 3D culture experiments are subject to a certain degree of variability depending on the matrix used, we repeated the experiment twice and confirmed that the size distribution patterns for both cell lines and conditions were consistent (data not shown). Colony morphology remained unaffected by EphB4/Fc stimulation in both control MCF7 and MCF7-ephrinB2 colonies.

These results suggest that only the Matrigel environment allows ephrinB2 to alter the morphology and size of MCF7 colonies. As the stimulation of ephrinB2 with the EphB4/Fc chimeric molecule only marginally increased MCF7 colony size, it is possible that the mere presence of ephrinB2 on the cell surface might be sufficient to induce the changes in colony size and morphology that we observed. Therefore, this effect might have been caused by ephrinB2-driven activation of the EphB4 receptor, rather than through ephrinB2 reverse signalling. Also, from these results it is unclear whether the increase in size of the MCF7-

ephrinB2 colonies is caused by a different cell organization within the colony architecture or by increased cell growth. In order to address this issue, the colonies were fixed and Hoechst staining performed. We then analyzed the colonies by taking images of optical slices running through the middle of the structure. The images presented in figure 3.4E show a wide internal lumen within MCF7-ephrinB2 colonies. This suggests that the increase in MCF7-ephrinB2 colony size might be aided by the formation of a lumen and might not be entirely caused by increased cell proliferation. This finding is intriguing, as reports in literature suggest that MCF7 colonies do not form a lumen in Matrigel 3D cultures (Kirshner, Chen et al. 2003). However, further analyses are needed to determine the contribution of lumen formation and cell proliferation to colony size.

A)

3D colony growth in collagen I at day 12 from plating

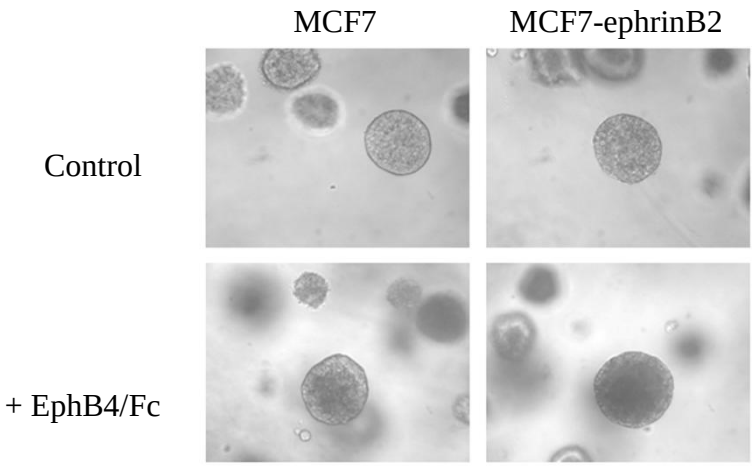

B)

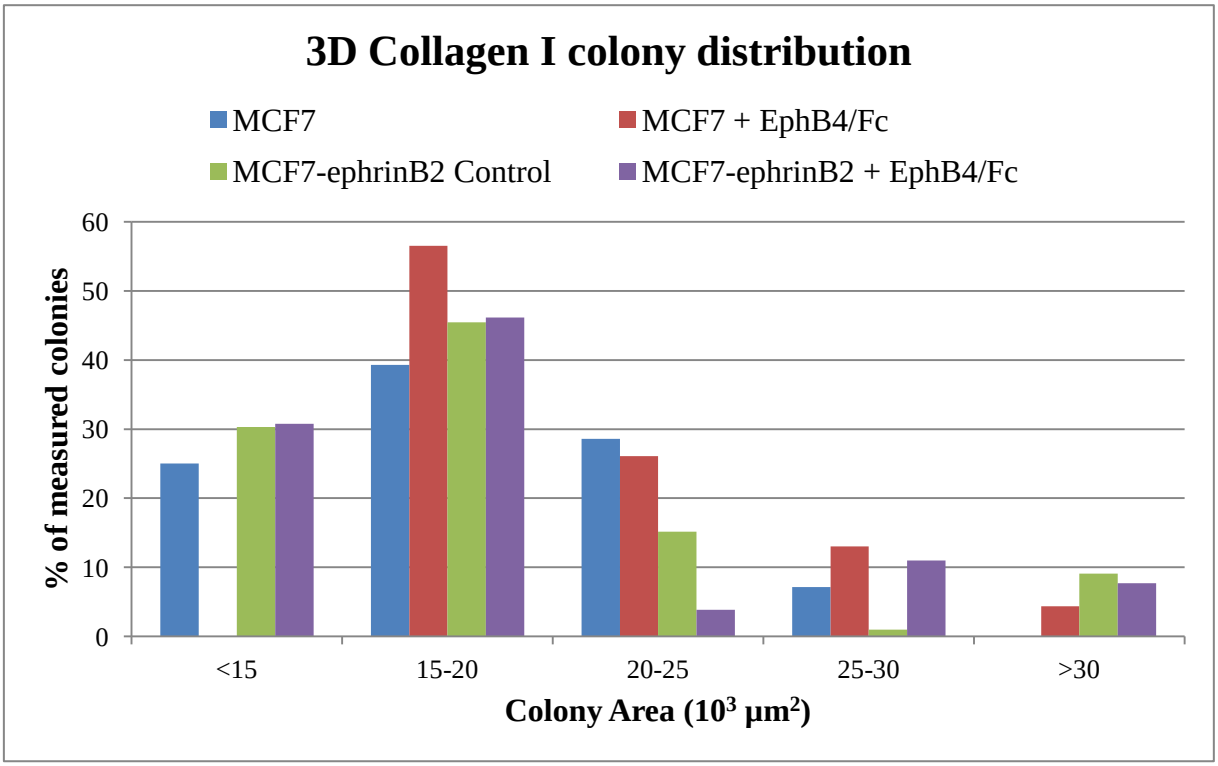

Cell lines:	<15	15-20	20-25	25-30	>30
MCF7	25%	39%	29%	7%	0%
MCF7 + EphB4/Fc	0%	57%	26%	13%	4%
MCF7-ephrinB2	30%	45%	15%	1%	9%
MCF7-ephrinB2 + EphB4/Fc	31%	46%	4%	11%	8%

C)

3D colony growth in 2% Matrigel at day 12 from plating

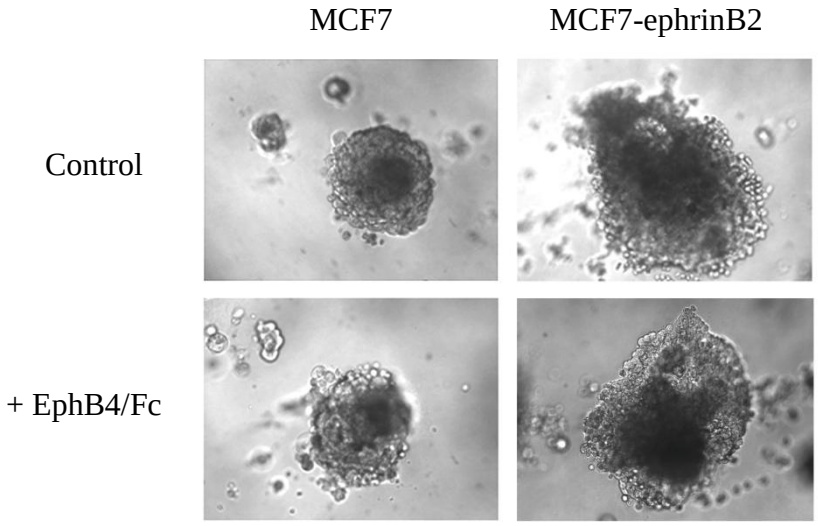

D)

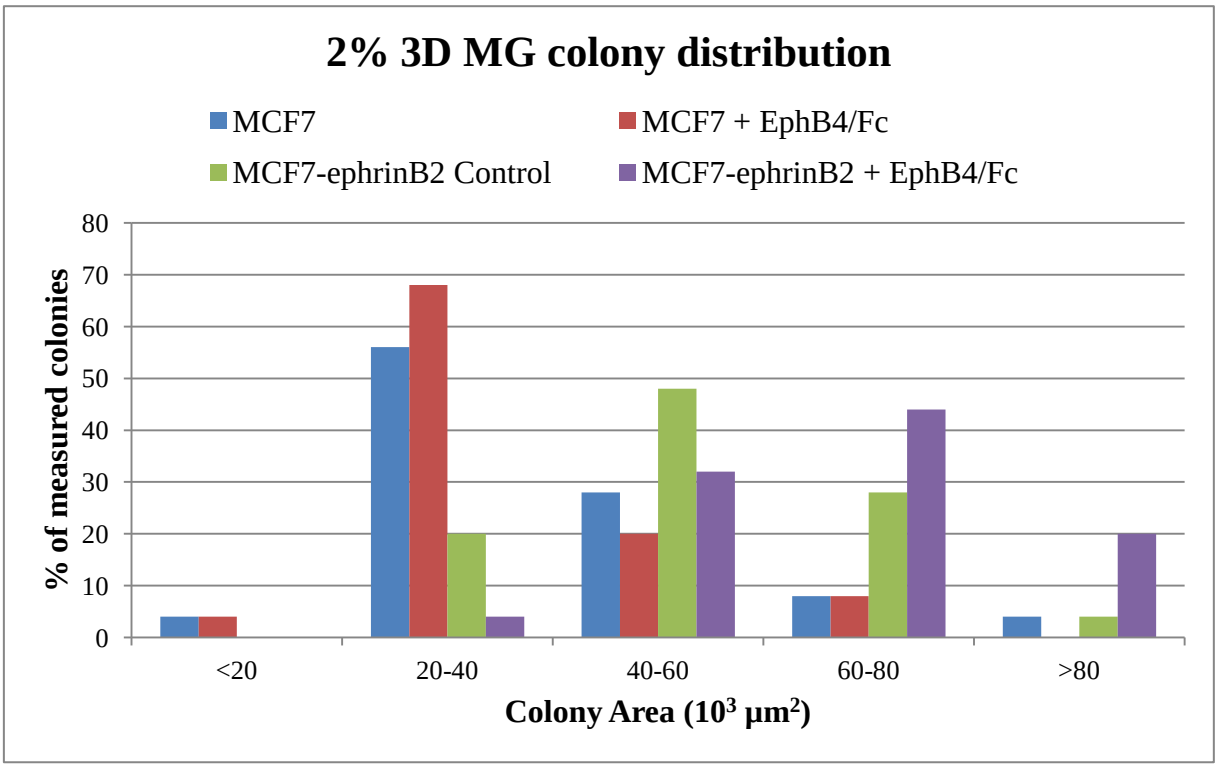

Cell lines:	<20	20-40	40-60	60-80	>80
MCF7	4%	56%	28%	8%	4%
MCF7 + EphB4/Fc	4%	68%	20%	8%	0%
MCF7-ephrinB2	0%	20%	48%	28%	4%
MCF7-ephrinB2 + EphB4/Fc	0%	4%	32%	44%	20%

E)

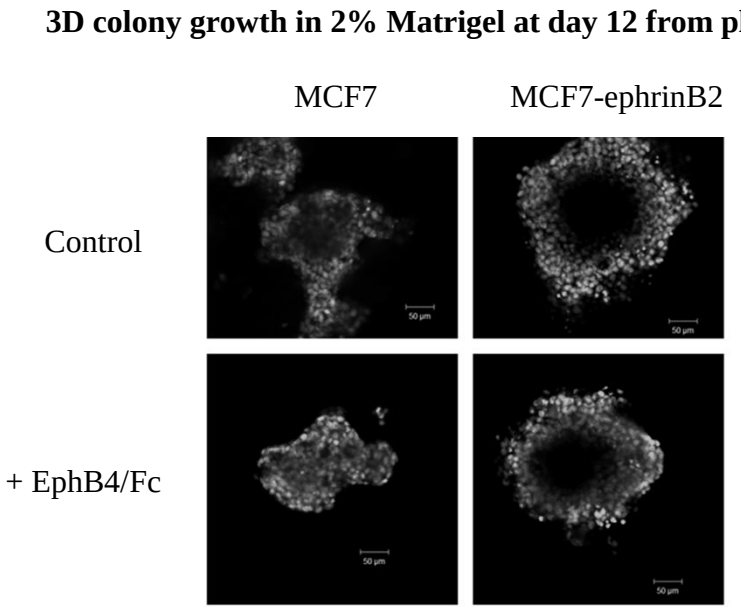

Figure 3.4: ephrinB2 expression drives MCF7 colony growth in 3D Matrigel, but not 3D collagen I.
MCF7 parental cells and MCF7-ephrinB2 cells were plated in 3D collagen I (panels **A** and **B**) or Matrigel (MG) (panels **C** and **D**) in the presence or absence of 5 µg/ml EphB4/Fc pre-clustered with anti-Fc IgG added every 2 days for 12 days. **A**) Representative photographs of 30 colonies per condition grown in collagen. **B**) The surface area of the circumference drawn around each colony at its widest point was calculated using Nikon software and plotted on a histogram showing the percentage of analysed colonies categorized under a certain size class. 30 colonies were analysed for each condition. The data is also presented as a table. **C**) Representative photographs of MG grown colonies. **D**) Quantification of MG colony size presented as histogram and table. **E**) Images of colonies grown in MG in the same conditions described in panel C, fixed to the glass bottom of the chamber slide and stained with Hoechst 33342. Images of optical slices positioned in the middle of the colony were taken using the confocal microscope.

3.1.3 Generation and characterization of tetracycline inducible MCF7 cell lines expressing the wild type and mutants of ephrinB2

One of the main aims of our study was to characterize contribution of PDZ domain-containing proteins to ephrinB2 signalling in breast cancer cells. Specifically, we were interested in proteins interacting with the PDZ binding motif of ephrinB2. Towards this goal we generated the ephrinB2/ΔV mutant with deletion of the C-terminal valine (Val333), which, according to previously published reports, does not bind to PDZ domain containing partners of ephrinB2 (Makinen, Adams et al. 2005). In another mutant, Val333 was substituted with Gly (ephrinB2/G) (figure 3.5). Based on the studies carried out in our laboratory (unpublished), the substitution of the last hydrophobic aminoacid in PDZ binding type I motifs had a less dramatic effect on the interaction with PDZ domain containing proteins. Hence, we expected ephrinB2/G to retain some of the interactions with PDZ-domain containing partners, thus allowing us to discriminate their contribution to ephrinB2 function. In particular, syntenin-1's unique ability to bind all three types of PDZ binding motifs as well as degenerated PDZ binding sequences (Ivarsson 2012), lead us to believe that it might retain binding to the ephrinB2/G mutant. If this were the case and syntenin-1 was the only PDZ domain-containing protein to retain binding to ephrinB2/G, then we would be able to understand and pinpoint the specific role of syntenin-1 in ephrinB2 pathways using ephrinB2 and ephrinB2/ΔV as positive and negative controls respectively.

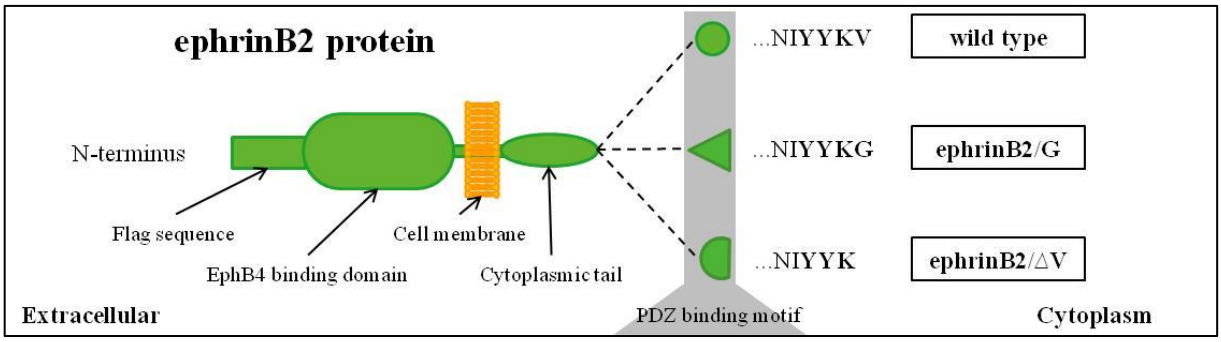

Figure 3.5: diagram of the ephrinB2-Flag proteins used in our study.

3.1.3.1 Mutations of the ephrinB2 PDZ binding motif affect binding of PDZ domain-containing proteins

Before generating cell lines expressing the ephrinB2/G or ephrinB2/ΔV mutants, we tested their ability to bind all the PDZ domain-containing proteins known to interact with the PDZ binding motif of ephrinB2. These include syntenin-1, PICK1, PTPL1, PAR3, GRIP1 and GRIP2. In order to do so, we conducted pull down assays using biotin-conjugated peptides representing the C-terminal 14 amino acids of wild type and ephrinB2 mutants. Given that Dishevelled-2 is known to bind ephrinB2 in the same region through its DEP domain (section 1.1.4.4 of the introduction), we decided to verify whether it too was able to bind the ephrinB2 C-terminal peptides. This would give us additional information on whether non-PDZ domain-containing proteins are able to compete with PDZ domain-containing proteins for the PDZ binding motif of ephrinB2. Apart from syntenin-1 and Dishevelled-2, the interaction with PDZ domain-containing proteins was examined using transiently transfected MCF7 cells.

The blot in figure 3.6A clearly shows that syntenin-1 partially retained its ability to bind the ephrinB2/G peptide (lane 4), albeit to a lower extent than the ephrinB2 wild type peptide (lane 3). As expected, the interaction of syntenin-1 with the ephrinB2/ΔV peptide was completely abolished (lane 5). We used an unrelated PDZ domain-containing protein CASK, which is endogenously expressed in MCF7 cells, as a negative control in order to ascertain that syntenin-1 binding to the peptides was specific. Dishevelled-2 and PICK1 were not able to bind the ephrinB2 wild type peptide and thus were not tested for ephrinB2/G and ephrinB2/ΔV (figures 3.6B and 3.6C respectively). PTPL1, PAR3, GRIP1 and GRIP2 were all able to bind the ephrinB2 wild type peptide, but not the ephrinB2/G or the ephrinB2/ΔV mutant peptides (figure 3.6, panels D, E, F and G respectively).

Taken together, these results revealed that the Val to Gly mutation at the C-terminus of ephrinB2/G abolished PDZ-mediated binding to all known PDZ domain-containing partners of ephrinB2, except syntenin-1. Thus, by using this mutant we would be able to discriminate the effects of the interaction between syntenin-1 and ephrinB2 from the effects of the other known interacting PDZ domain-containing partners. However, these results do not exclude the possibility that other yet unidentified proteins might be able to retain binding to the ephrinB2/G mutant in a PDZ-dependent or independent manner.

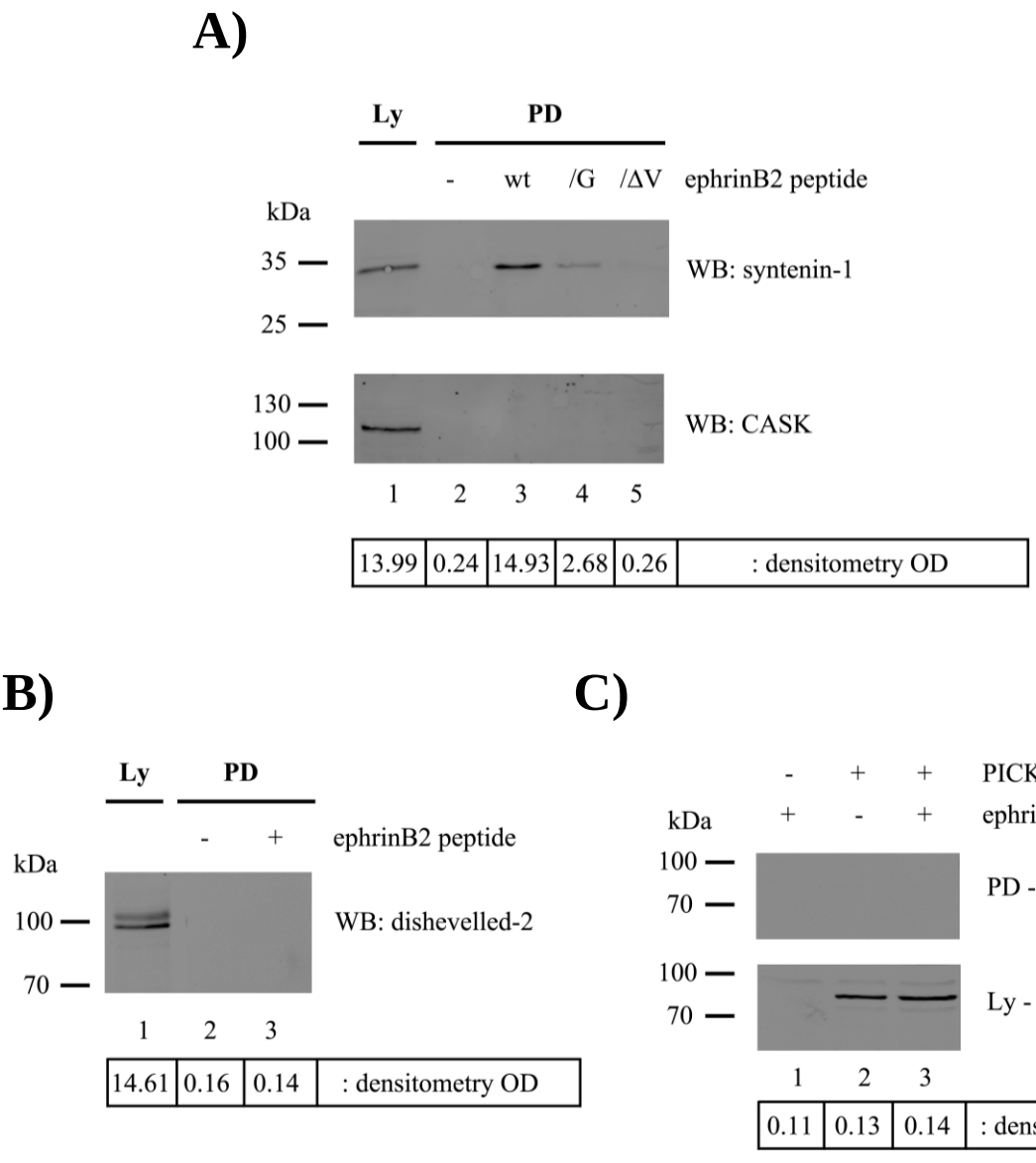

D)

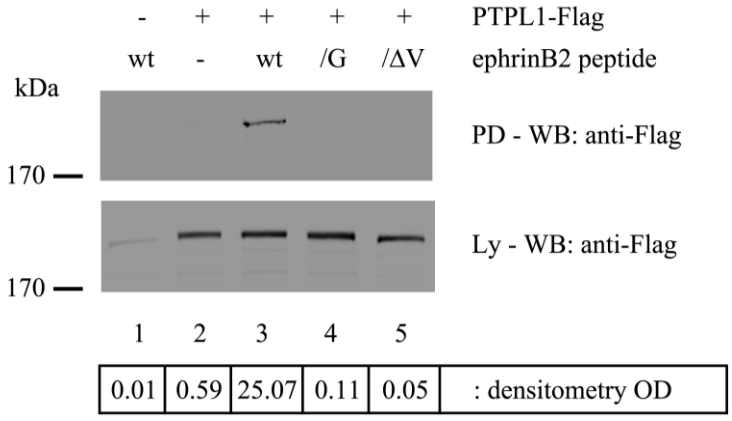
- + + + + PTPL1-Flag
wt - wt /G /ΔV ephrinB2 peptide
kDa
170
PD - WB: anti-Flag
170
Ly - WB: anti-Flag
1 2 3 4 5
0.01 0.59 25.07 0.11 0.05 : densitometry OD

E)

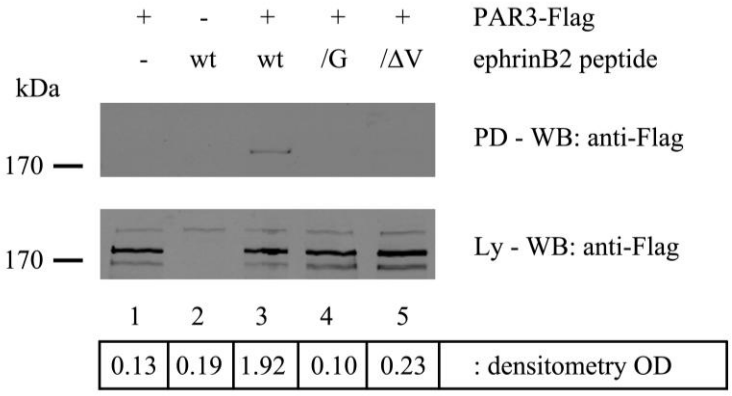
+ - + + + PAR3-Flag
- wt wt /G /ΔV ephrinB2 peptide
kDa
170
PD - WB: anti-Flag
170
Ly - WB: anti-Flag
1 2 3 4 5
0.13 0.19 1.92 0.10 0.23 : densitometry OD

F)

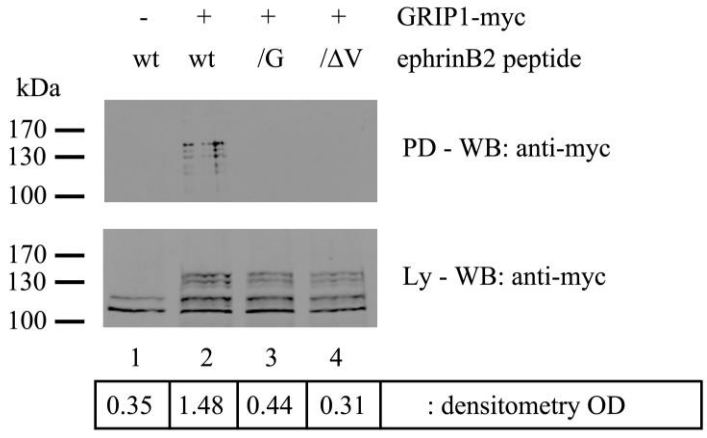
- + + + GRIP1-myc
wt wt /G /ΔV ephrinB2 peptide
kDa
170
130
100
PD - WB: anti-myc
170
130
100
Ly - WB: anti-myc
1 2 3 4
0.35 1.48 0.44 0.31 : densitometry OD

G)

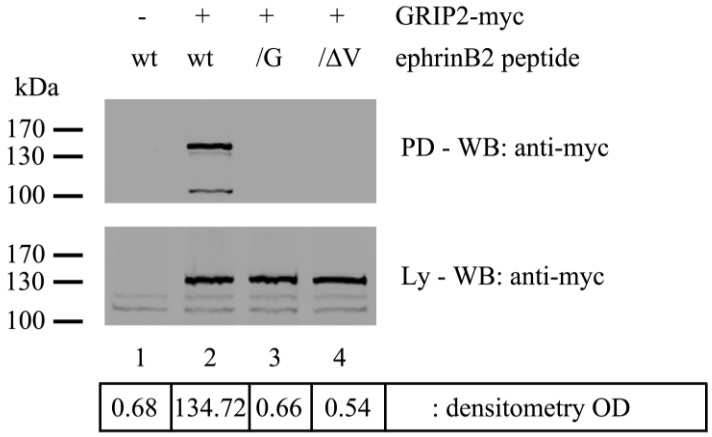

Figure 3.6: the C-terminal ephrinB2 peptide interacts with all known PDZ partners of ephrinB2 in MCF7 cells, except PICK1. The /ΔV mutation completely impairs PDZ binding, while the /G mutation retains a discrete level of binding only to syntenin-1.

Interaction of ephrinB2 PDZ domain-containing partners with ephrinB2 wild type, ephrinB2/G and ephrinB2/ΔV C-terminal peptides assessed by pull down assay. The interaction with Dishevelled-2 and syntenin-1 was analysed using antibodies recognising endogenous proteins. The interaction with PICK1, PTPL1, PAR3, GRIP1 and GRIP2 was analysed using MCF7 cells which were transiently transfected to express epitope-tagged proteins. Cells were lysed using 1% TritonX-100 buffer and pulled-down proteins (PD) were collected on peptides-conjugated NeutrAvidin-agarose beads and separated on SDS-PAGE. Whole lysates (Ly) samples were also resolved on SDS-PAGE as internal control. Proteins of interest which did not show any interaction with ephrinB2 wild type peptide were not tested for mutant peptides. Densitometry analysis was performed on pull down blots and optical densities (OD) shown for each lane. **A**) Endogenous syntenin-1 was detected using anti-syntenin-1 mAb. The unrelated endogenous PDZ domain-containing protein CASK was also detected as internal negative control using anti-CASK mAb. Note, syntenin-1 was able to retain partial binding to the ephrinB2/G peptide. Densitometry analysis was performed only on syntenin-1 blot. **B**) Endogenous Dishevelled-2 was detected using anti-deshevelled-2 mAb. **C**) PICK1, **F**) GRIP1 and **G**) GRIP2 transfected proteins contained a c-myc tag and were detected using anti-c-myc pAb. **D**) PTPL1 and **E**) PAR3 transfected proteins contained a flag tag and were detected using anti-flag pAb. Note, dishevelled-2 and PICK1 did not interact with the ephrinB2 wild type peptide, while PTPL1, PAR3, GRIP1 and GRIP2 interacted with the wild type, but not mutant ephrinB2 peptides.

3.1.3.2 Generating and characterizing tetracycline inducible MCF7 cell lines expressing ephrinB2, ephrinB2/G and ephrinB2/ΔV

In order to assess the biological activities of ephrinB2, ephrinB2/G or ephrinB2/ΔV, we needed the expression levels of the mutants to be comparable with that of the wild type protein. Therefore, we decided to generate tetracycline inducible MCF7 cell lines which expressed ephrinB2 wild type or the mutants only in the presence of the antibiotic tetracycline (or doxycycline). This system presented us with the opportunity of growing the newly generated MCF7 cell lines under standard conditions and actively regulating the expression of the proteins at our discretion. We decided to use the MCF7 TetOn cells (purchased from Clontech). According to the supplier's manual, these cells are stably transfected with the pTet-On Advanced vector which encodes the Tet-On Advanced transcriptional activator. This engineered transcription factor consists of a mutant *E. coli* TetR protein (rTetR) fused to three minimal "F"-type activation domains derived from the herpes simplex virus (HSV) VP16 protein. In the presence of doxycycline, Tet-On Advanced binds to the *tetO* sequences in the P_{Tight} inducible promoter on a different expression vector (in our case, the pBI vector) containing the gene of interest and induces gene expression. As P_{Tight} lacks binding sites for endogenous mammalian transcription factors, it is virtually silent in the absence of induction by doxycycline. Before generating our cell lines of interest, we established that the levels of endogenous EphB4 and syntenin-1 were comparable to those seen in our MCF7 cells. We also found that like MCF7 cells, MCF7 TetOn cells did not express ephrinB ligands (data not shown). We then stably transfected MCF7 TetOn cells with the tetracycline inducible pBI plasmid encoding either the wild type or the ephrinB2 mutants. Tetracycline-dependent expression was initially tested by flow cytometry (data not shown). Cells were subsequently

sorted by FACS using anti-Flag mAb for high expression of wild type or ephrinB2 mutants on the cell surface 48 hours after stimulation with doxycycline. We conducted FACS sorting twice in order to obtain a homogenous cell population expressing high levels of ephrinB2 upon doxycycline stimulation. Newly generated cell lines were called MCF7 Tet-ephrinB2, MCF7 Tet-ephrinB2/G and MCF7 Tet-ephrinB2/ΔV. We also generated a MCF7 Tet-ephrinB2 cell line in which we depleted endogenous syntenin-1 using a lentiviral-based approach. After testing five different commercial shRNA lentiviral constructs targeting syntenin-1 in MCF7 TetOn cells (data not shown), we selected the most effective and used it to generate the MCF7 Tet-ephrinB2/shSyntenin-1 cell line. As shown in figure 3.7C, we managed to achieve ~75% knock down of endogenous syntenin-1 in these cells.

In order to characterize the newly established tetracycline inducible cell lines, we performed flow cytometry analysis and immunofluorescence staining using anti-Flag mAb. We also verified expression levels of ephrinB2 and syntenin-1 by Western blotting. For all experiments, we analyzed cells before and after stimulation with doxycycline. In figure 3.7A, the histogram shows cell surface expression levels of ephrinB2 and mutants. These results are presented as percentages of ephrinB2 mean fluorescence intensity upon doxycycline stimulation (considered as 100%). These data are also presented in table format in figure 3.7B with negative and positive control values. Unstimulated cells expressed low levels of ephrinB protein on the cell surface (blue columns), which was expected, as inducible expression systems are subject to gene expression leakiness. Expression levels of ephrinB2/G and ephrinB2/ΔV after doxycycline stimulation (red columns), were ~20% lower than ephrinB2. However, in syntenin-1-depleted MCF7 Tet-ephrinB2 cells, ephrinB2 expression was ~30% higher. Interestingly, we noticed that cell surface expression of tetraspanin CD81 (ie the positive control) was also notably higher in syntenin-1-depleted cells.

The overall protein expression levels of ephrinB2/G and ephrinB2/ΔV (lanes 4 and 6 respectively) where slightly lower than ephrinB2 (lane 2) when measured by Western blotting (figure 3.7C). As expected, syntenin-1 levels were considerably lower in syntenin-1-depleted cells (lanes 7 and 8). β-actin levels were also measured and served as internal loading control. In order to obtain accurate values of overall expression levels, which we would be able to compare to flow cytometry values, we performed densitometric analysis of Western blots and presented the results as percentages of the expression level of ephrinB2 wild type upon stimulation with doxycycline (taken as 100%) (figure 3.7D). Our results show that the difference in cell surface expression observed for ephrinB2/G and ephrinB2/ΔV were probably caused by differences in overall expression, as the two mutants are expressed at ~20% lower levels than ephrinB2. Interestingly, the total ephrinB2 expression level in the presence of syntenin-1 knock down was ~10% lower than that in non-depleted cells.

Immunofluorescence staining of ephrinB2, ephrinB2/G and ephrinB2/ΔV proteins using anti-Flag antibody confirmed that PDZ binding motif mutations and syntenin-1 depletion did not alter cell surface localization (figure 3.7E). As in the stable MCF7-ephrinB2 cell line, stronger staining was observed on the plasma membrane. However, in MCF7 Tet-ephrinB2/shSyntenin-1 cells ephrinB2 staining appeared to be more diffuse.

In summary, these experiments confirmed that the tetracycline-inducible system worked and that stimulation with 1 μg/ml doxycycline for 48 hours was sufficient to ensure high levels of protein expression in all four cell lines. More importantly, all cell lines expressed comparable levels of ephrinB2 proteins, albeit with minor differences.

A)

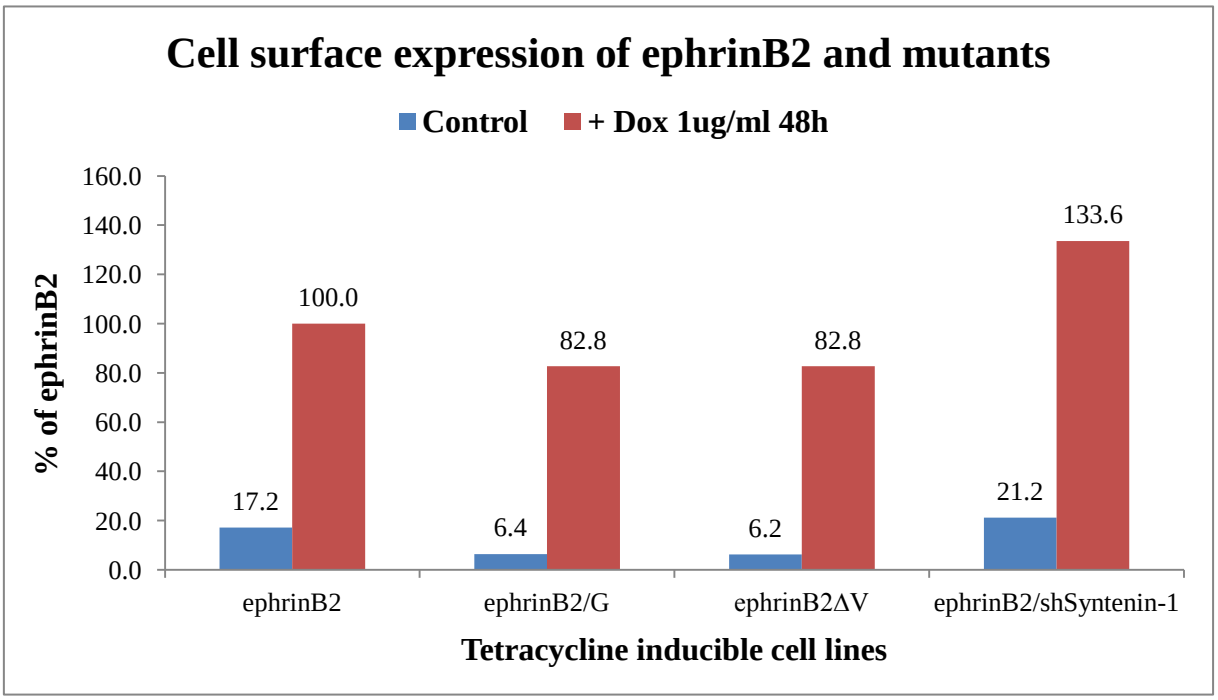

B)

Cell lines: MCF7 Tet-	anti-Flag Control	anti-Flag + dox 48h	Negative control (PI4K)	Positive control (CD81)
ephrinB2	17.2%	100%	3.3%	371.6%
ephrinB2/G	6.4%	82.8%	3.2%	431.0%
ephrinB2/ΔV	6.2%	82.8%	3.4%	407.3%
ephrinB2/shSyntenin-1	21.2%	133.6%	3.5%	481.6%

C)

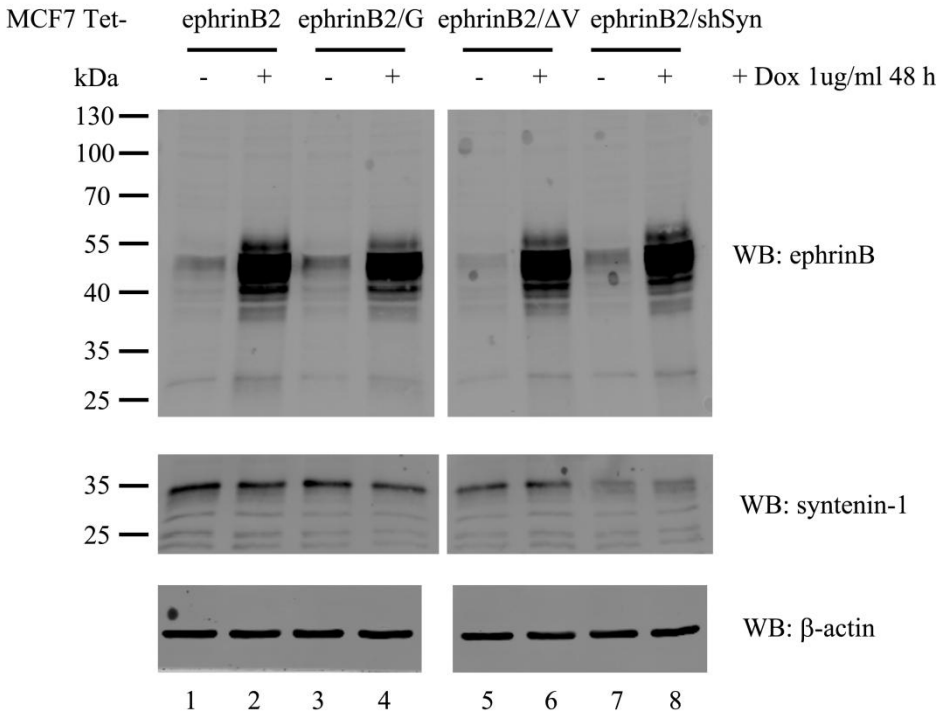
MCF7 Tet-
ephrinB2
ephrinB2/G
ephrinB2/ΔV
ephrinB2/shSyn
kDa
- + - + - + - +
+ Dox 1ug/ml 48 h
130
100
70
55
40
35
25
WB: ephrinB
35
25
WB: syntenin-1
WB: β-actin
1 2 3 4 5 6 7 8

D)

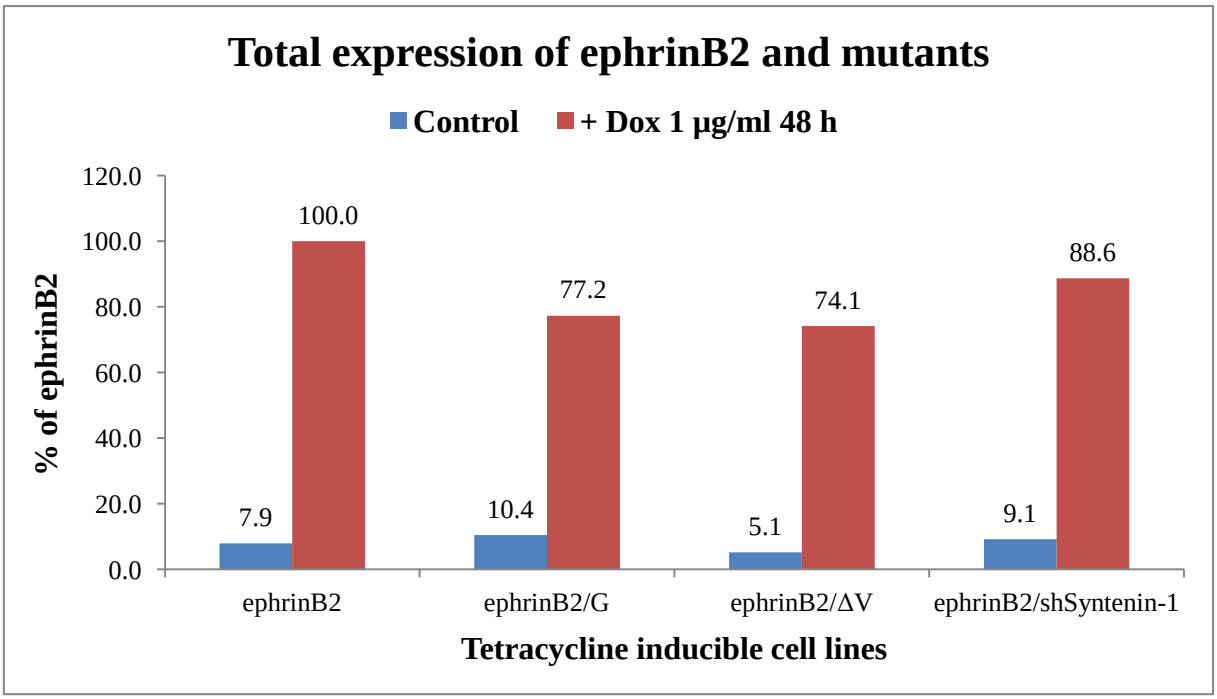
Total expression of ephrinB2 and mutants
Control
+ Dox 1 µg/ml 48 h
% of ephrinB2
120.0
100.0
80.0
60.0
40.0
20.0
0.0
7.9
100.0
10.4
77.2
5.1
74.1
9.1
88.6
ephrinB2
ephrinB2/G
ephrinB2/ΔV
ephrinB2/shSyntenin-1
Tetracycline inducible cell lines

E) Immunofluorescence on MCF7 tetracycline inducible cell lines

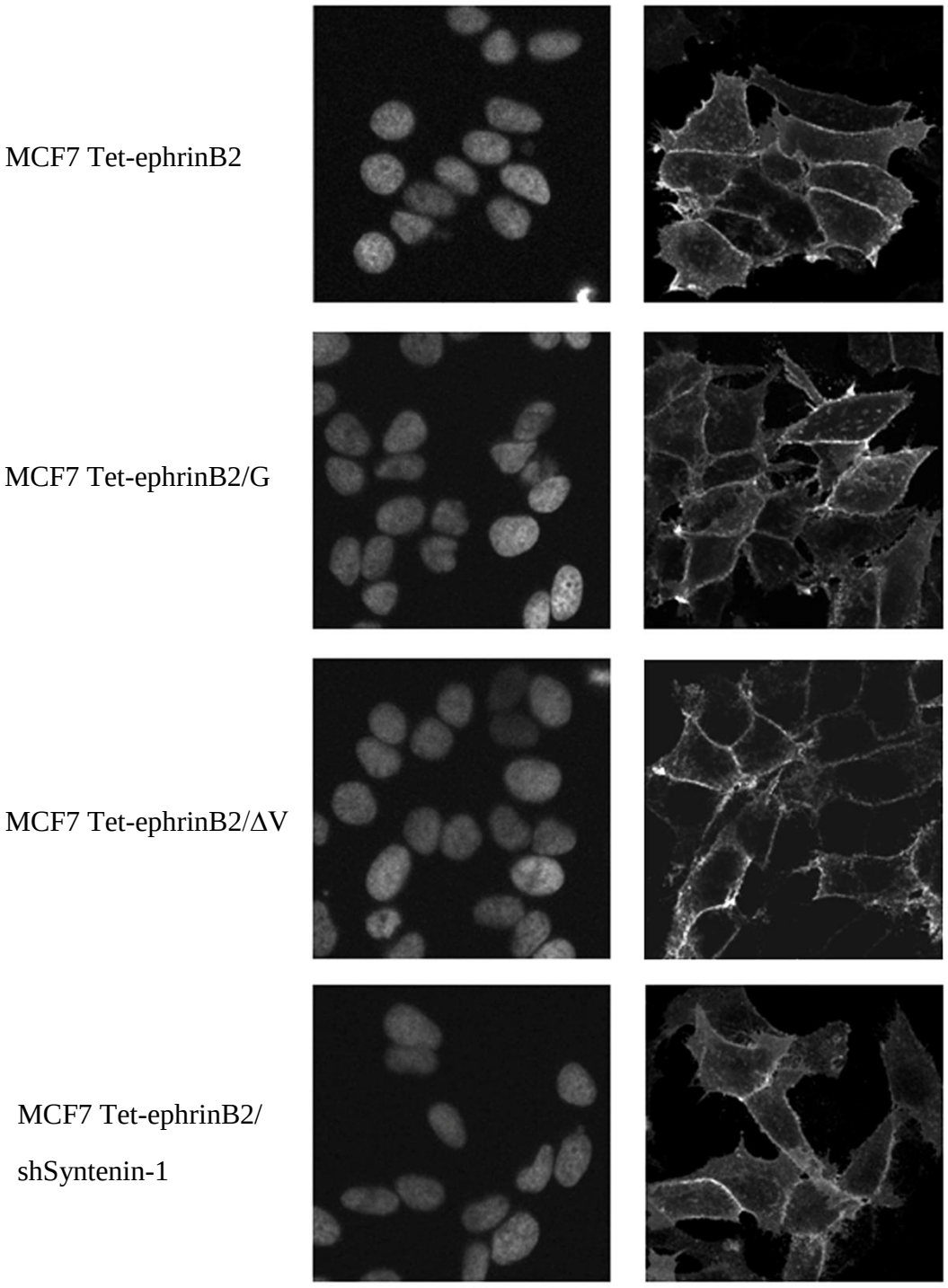

Figure 3.7: doxycycline stimulation of tetracycline inducible MCF7 cell lines leads to strong and comparable ephrinB2, ephrinB2/G and ephrinB2/ΔV expression on the cell surface, although low levels of leaky expression are present in non-stimulated conditions.
Characterization of MCF7 Tet-ephrinB2, MCF7 Tet-ephrinB2/G, MCF7 Tet-ephrinB2/ΔV and MCF7 Tet-ephrinB2/shSyntenin-1 cell lines. **A**) The histogram illustrates the mean fluorescence intensities obtained by flow cytometry analysis of all four cell lines in normal conditions (control) or after 48 hours stimulation with 1 µg/ml doxycycline using anti-Flag mAb. The results are presented as percentage values related to the mean fluorescence of ephrinB2 expressing cells upon doxycycline stimulation (considered as 100%). **B**) The table lists the percentage values shown in the histogram (A) alongside the negative and positive controls of the flow cytometry analysis for each cell line. Anti-PI4K mAb as negative control; anti-CD81 mAb was used to detect the endogenous membrane protein CD81 as positive control. **C**) The same samples presented in panel A were analyzed via WB. Cells were lysed in 1x Laemmli buffer and proteins were resolved on SDS-PAGE. EphrinB2 total protein levels were detected with anti-ephrinB pAb. Syntenin-1 total levels were detected with anti-syntenin-1 mAb and β-actin was detected with anti-β-actin mAb as internal loading control. **D**) The histogram shows densitometric values obtained with Odyssey software (Licor) from WB (C) and presented as percentages of ephrinB2 expression after doxycycline stimulation (considered as 100%). **E**) Immunofluorescence images of MCF7 tetracycline inducible cells 48 hours after stimulation with 1 µg/ml doxycycline. Cells were fixed with 2% PFA and probed with anti-flag mAb.

3.1.3.3 EphrinB2 expression affects colony growth of MCF7 TetOn cells in Matrigel based 3D cultures

As already mentioned, 3D culture systems are commonly used to analyze protein functions in higher-order tissue architecture during mammary morphogenesis and cancer development (Hebner, Weaver et al. 2008). Having discovered that ephrinB2 expression in stably transfected MCF7 cells alters colony size and morphology in Matrigel based 3D cultures, we decided to evaluate the effect of ephrinB2, ephrinB2/G and ephrinB2/ΔV expression in the MCF7 tetracycline inducible model. We first conducted a pilot experiment whereby MCF7 TetOn parental cells and MCF7 Tet-ephrinB2 cells were plated in 2% Matrigel and colonies allowed to grow for 12 days in the presence or absence of doxycycline. The cells which formed the colonies were then lysed and the protein extracts were analyzed by WB in order to detect ephrinB2 expression levels. By doing so, we were able to confirm that doxycycline stimulation induced ephrinB2 expression in 3D Matrigel (figure 3.8C).

Figure 3.8A shows representative images of MCF7 TetOn (parental) and MCF7 Tet-ephrinB2 colonies. In contrast to the MCF7 cells we used to generate the stable MCF7-ephrinB2 cell line, MCF7 TetOn cells formed smaller colonies with well defined borders. MCF7 Tet-ephrinB2 cells formed relatively large and round colonies in the presence or absence of doxycycline stimulation. The morphology of these colonies differed from the one we observed in MCF7-ephrinB2 cells: the colonies were compact, had clear and defined borders and were not characterized by single cells escaping from the main body. We concluded that the MCF7 TetOn cell line behaved differently when grown in 2% Matrigel, as both the size of MCF7 TetOn colonies and the morphology of MCF7 Tet-ephrinB2 colonies was notably different from MCF7 and MCF7-ephrinB2 colonies. Moreover, doxycycline

stimulation did not seem to affect the size or shape of MCF7 Tet-ephrinB2 colonies. Quantification of these experiments (conducted as explained in section 3.1.2.3) is presented in figure 3.8B. All the MCF7 TetOn colonies fell in the lower <10 size class in the presence or absence of doxycycline stimulation. MCF7 Tet-ephrinB2 colonies were considerably larger, with 3% falling in the 10-20 size class, 53% in the 20-30 size class, 27% in the 30-40 size class and 17% in the >40 size class. As already mentioned, doxycycline did not alter colony distribution size of MCF7 Tet-ephrinB2 colonies, as 20% of measured colonies fell in the 10-20 size class, 37% in the 20-30 size class, 17% in the 30-40 size class and 27% in the >40 size class.

Taken together, these results suggest that even low levels of ephrinB2 expression are sufficient to drive colony growth in MCF7 TetOn cells when grown in 2% Matrigel. However, the morphology of the colonies seemed to remain unchanged. The small colonies formed by MCF7 TetOn cells suggest that colony growth is strongly impaired in this cell line when grown in Matrigel 3D cultures. Moreover, the fact that the size and shape of MCF7 Tet-ephrinB2 colonies remained unaffected by doxycycline stimulation probably indicates that colony growth was not driven by ephrinB2 reverse signalling. More likely, it seems that small amounts of ephrinB2 were sufficient to activate endogenous EphB receptors or other cell surface communication systems on neighbouring cells which in turn increased colony growth. Data from previous experiments using EphB4/Fc stimulation in MCF7-ephrinB2 3D cultures, described in section 3.1.2.3, also seems to suggest that ephrinB2 reverse signaling did not play a role in 3D colony growth. If indeed activation of the reverse signalling pathway did not contribute to growth of MCF7 colonies in 3D cultures, then one would not expect the experiments using ephrinB2/G and ephrinB2/ΔV expressing cells to yield any useful information. Moreover, the use of MCF7 Tet-ephrinB2 cells depleted of syntenin-1 via

shRNA knock down did not prove useful, as syntenin-1 depletion strongly inhibits MCF7 colony growth in 2% Matrigel as ascertained in previously conducted pilot experiments (data not shown).

To summarize, by culturing MCF7 Tet-ephrinB2 cells in Matrigel-based 3D cultures, we determined that small amounts of ephrinB2 expression were sufficient to drive colony growth of MCF7 TetOn cells. Thus, ephrinB2 reverse signalling does not seem to play a role in this process and for this reason we decided not to pursue this assay any further.

A)

3D colony growth in 2% MG at day 12 from plating

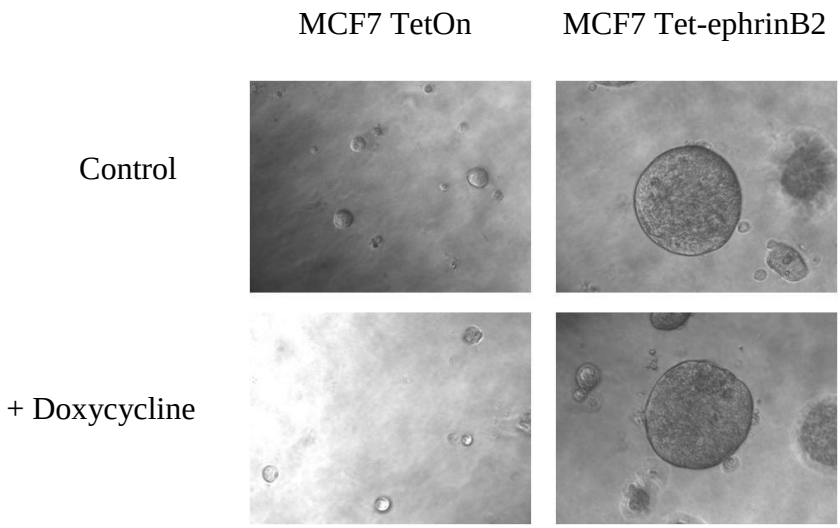

B)

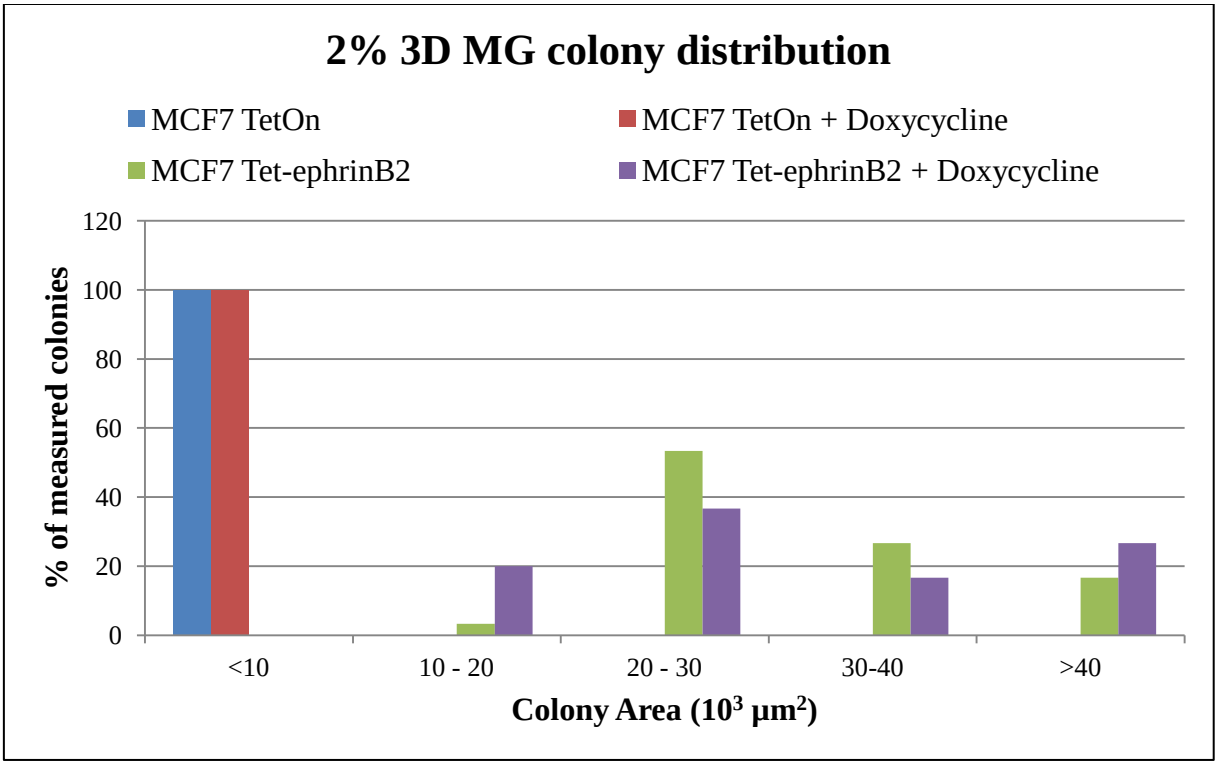

Cell lines:	<10	10-20	20-30	30-40	>40
MCF7 TetOn	100%	0%	0%	0%	0%
MCF7 TetOn + doxycycline	100%	0%	0%	0%	0%
MCF7 Tet-ephrinB2	0%	3%	53%	27%	17%
MCF7 Tet-ephrinB2 + doxycycline	0%	20%	37%	17%	27%

C)

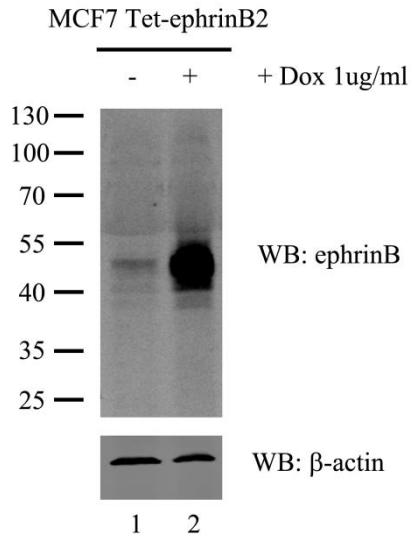

Figure 3.8: low levels of ephrinB2 expression are sufficient to drive colony growth of tetracycline inducible MCF7 cells in 3D Matrigel, while doxycycline-induced over-expression of ephrinB2 does not show an added effect.

A) representative photographs of MCF7 Tet-ephrinB2 and MCF7 TetOn parental cells grown in 2% Matrigel (MG) for 12 days in the presence or absence of 1 µg/ml doxycycline (added to the growth medium every 48 hours). Photographs were taken at an inverted light microscope at 20x magnification. **B**) Statistical analysis of colony size was conducted as described in figure 3.4 and presented in the histogram and the table as percentage of measured colonies which fell under a pre-determined size class. **C**) After 30 colonies were photographed for each condition, MCF7 Tet-ephrinB2 cells were lysed in 1x Laemmli buffer and cell lysates were loaded on SDS-PAGE. EphrinB2 was detected using anti-ephrinB pAb. β-actin was detected as internal loading control.

3.1.3.4 Assessing syntenin-1 binding to ephrinB2 and mutants in tetracycline inducible MCF7 cells

When analyzing interactions between two proteins, pull down assays using short peptides are not always representative of the binding dynamics observed in cells. One of the reasons is that binding between full-length proteins can be affected by their tertiary structure. Another reason is that proteins in cells are compartmentalized differently. Therefore, it was important to verify the binding of syntenin-1 to wild type and ephrinB2 mutants expressed in tetracycline inducible MCF7 cells. After stimulating cells with doxycycline, we performed a co-immunoprecipitation (co-IP) assay using anti-Flag antibody conjugated to agarose beads followed by WB with anti-ephrinB pAb and anti-syntenin-1 pAb.

Figure 3.8A shows the WB analysis of both co-IP and whole lysate samples. Similarly to the pull down assay, syntenin-1 binding to ephrinB2/G was strongly impaired but not abolished (lane 3). By contrast, binding of syntenin-1 to ephrinB2/ΔV was hardly detectable (lane 4). As expected, in MCF7 Tet-ephrinB2/shSyntenin-1 cells the residual level of binding of syntenin-1 to ephrinB2 reflected the incomplete level of syntenin-1 knock down (lanes 5). Because the amount of precipitated protein can slightly differ between samples in co-immunoprecipitation experiments, we performed densitometric analysis on both ephrinB and syntenin-1 levels and calculated the ratio between them. The histogram in figure 3.8B illustrates the percentage of syntenin-1 binding in all cell lines with MCF7 Tet-ephrinB2 considered to be 100%. By doing so, we observed that syntenin-1 binding to ephrinB2/G was 20 fold lower when compared to the wild type ephrinB2. The binding ability of syntenin-1 to ephrinB2/ΔV was more than 70 fold lower. This experiment confirmed that ephrinB2/G still retains the ability to bind syntenin-1, albeit at a much lower level than ephrinB2.

To summarize, we proved that the tetracycline inducible cell lines that we generated worked according to expectations and that endogenous syntenin-1 binding to ephrinB2 and mutants yielded comparable results to the ones observed in pull down assays.

A)

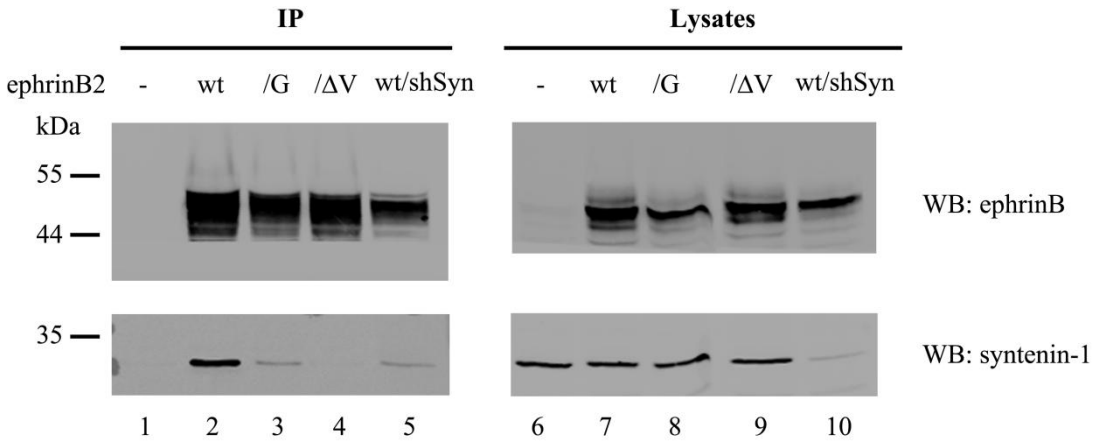

B)

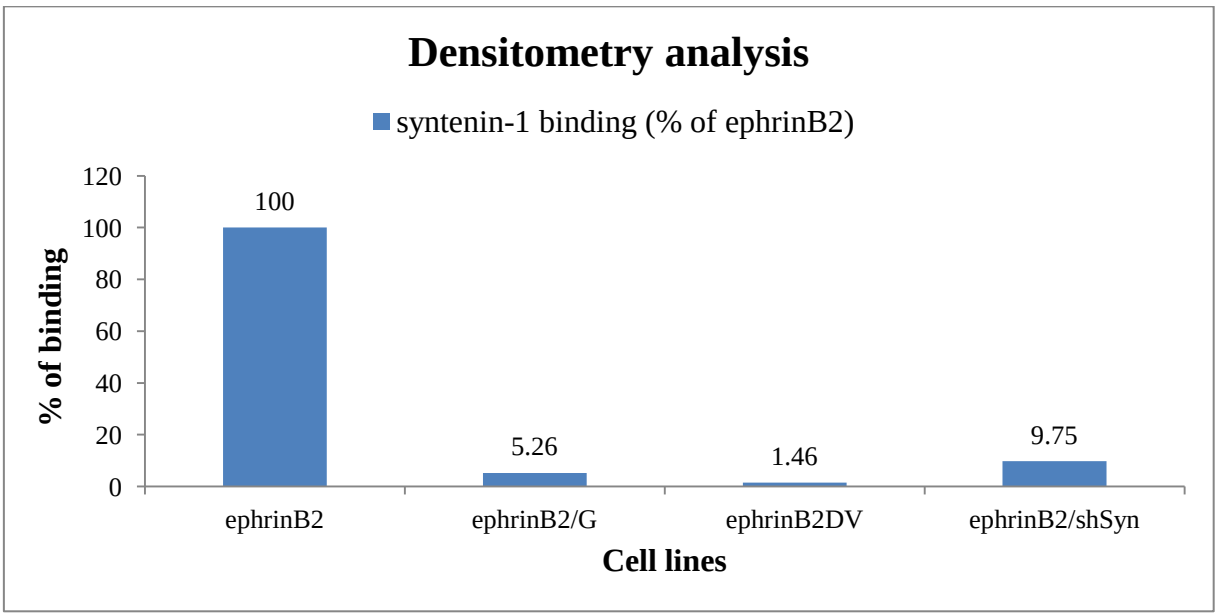

Figure 3.9: ephrinB2/G retains a discrete level of binding to syntenin-1, while ephrinB2/ΔV does not.
EphrinB2, ephrinB2/G and ephrinB2/ΔV interaction with syntenin-1 was assessed using co-immunoprecipitation (co-IP) assay. MCF7 TetOn and MCF7 Tet-ephrinB2/shSyntenin-1 cell lines were also tested. Cells were lysed in 1% TritonX-100 buffer and protein complexes were collected on anti-Flag antibody-conjugated agarose beads. Co-immunoprecipitated proteins (IP) were eluted from agarose beads and resolved on SDS-PAGE. Whole lysate samples (Ly) were also analysed as internal control. **A**) EphrinB2 was detected with anti-ephrinB pAb, while syntenin-1 was detected with anti-syntenin-1 pAb. Note, syntenin-1 retained partial binding to ephrinB2/G, but was unable to bind ephrinB2/ΔV. **B**) Densitometry analysis was conducted on WB (A). Ratios between densitometry values of immunoprecipitated ephrinB2 proteins and co-immunoprecipitated syntenin-1 was calculated for each sample and presented as percentage of the wild type ephrinB2/syntenin-1 ratio (considered as 100%) in the histogram.

3.1.4 Discussion

In normal physiological conditions, ephrinB2 is expressed in luminal epithelial cells in the mammary gland, while EphB4 is expressed in the surrounding myoepithelial cells (Munarini, Jager et al. 2002). During mammary gland tumourigenesis, luminal epithelial cells gradually suppress ephrinB2 expression and induce EphB4 expression. At later stages of tumour development, EphB4 expression is also suppressed (Nikolova, Djonov et al. 1998). Therefore, ephrinB2 and EphB4 expression levels differ greatly between epithelial breast cancer cell lines (Berclaz, Flutsch et al. 2002; Andres and Ziemiecki 2003; Kumar, Singh et al. 2006; Noren, Foos et al. 2006).

For these reasons, we analyzed endogenous expression levels of EphB4, ephrinB ligands and syntenin-1 in 21 breast cancer epithelial cell lines and 2 non-tumourigenic mammary epithelial cell lines in order to select an adequate cell line to use as a model system (figure 3.1). To our knowledge, this screening was the largest conducted to date and proved that EphB4 and ephrinB ligands expression varies considerably between these cell lines. Previous studies have either analysed mRNA levels of the EphB4 receptor alone (Berclaz, Andres et al. 1996) or have included fewer breast cancer cell lines in their screening (Wu, Suo et al. 2004; Kumar, Singh et al. 2006; Noren, Foos et al. 2006). Only one study conducted a methodical examination of mRNA levels of all Eph and ephrin proteins in representative cell lines of normal breast epithelium (MCF10A), non-invasive breast carcinoma (MCF7) and invasive breast carcinoma (MDA-MB-231) (Fox and Kandpal 2004). In our screening, most cell lines expressed medium to high levels of EphB4, but only 12 expressed appreciable levels of ephrinB ligands. For the purpose of our study, we selected the breast adenocarcinoma MCF7 cell line, as it did not express any ephrinB ligands and expressed minimal levels of

EphB4. Interestingly, a previous study has observed high levels of EphB4 and low levels of ephrinB2 expression in MCF7 cells (Kumar, Singh et al. 2006). Additionally, ephrinB2 mRNA levels were found to be higher than EphB4 levels in the study by (Fox and Kandpal 2004). Whilst the correlation between mRNA levels and protein levels is not direct and thus may account for some of these discrepancies, other factors may come into play, such as the expression levels of other proteins which induce protein expression (high ErbB2 levels induce EphB4 expression in MCF7 cells (Kumar, Singh et al. 2006)) or simply the source of cell lines used and slight variations in culturing conditions. By contrast, the ZR75.30, T47D and SKBR3 cell lines analysed in the study previously mentioned (Kumar, Singh et al. 2006) showed comparatively similar levels of EphB4 and ephrinB2 expression as detected in our study.

We generated a MCF7 cell line stably expressing an ephrinB2 wild type protein tagged with a flag sequence on the extracellular portion at the N-terminus. As expected, Flag-ephrinB2 was detected on the cell surface (figure 3.2A). Interestingly, we could detect low basal level of ligand phosphorylation (figure 3.2B). This phenomenon was also observed in previous studies focused on ephrinB ligands phosphorylation dynamics (Bruckner, Pasquale et al. 1997; Palmer, Zimmer et al. 2002). Various pathways could be involved in basal ephrinB2 phosphorylation. Firstly, endogenous EphB4 might induce ephrinB2 phosphorylation via *trans* interaction. However, various reports have suggested that ephrinB ligands over-expression in cell lines cultured *in vitro* tend to lose EphB receptor expression, possibly through continuous ligand-induced internalization and degradation (Pasquale 2008). Secondly, ephrinB2 phosphorylation might be driven by FGF receptors-induced trans-phosphorylation. Indeed, direct interaction of ephrinB1 with FGF receptors induced ligand

phosphorylation and Grb4-mediated reverse signalling in *Xenopus* embryos (Chong, Park et al. 2000; Bong, Park et al. 2004). Alternatively, *trans* activation of claudin-4 during cell-cell adhesion was shown to induce ephrinB1 phosphorylation through Src activation (Tanaka, Kamata et al. 2005). As the cytoplasmic tails of ephrinB1 and ephrinB2 are 95% identical with the C-terminal 33 amino acids sharing 100% homology, it is likely that ephrinB2 can be phosphorylated in the same manner as ephrinB1. Finally, ephrinB2 basal phosphorylation might also be caused by the presence of constitutively active Src kinases in MCF7 cells (Gonzalez, Agullo-Ortuno et al. 2006). In fact, our data suggests that Src kinases are directly responsible for ephrinB2 phosphorylation, as reported by previous studies (Palmer, Zimmer et al. 2002; Georgakopoulos, Litterst et al. 2006). Taken together, we conclude that many different pathways, related and unrelated to EphB receptors stimulation, might take part in ephrinB2 basal phosphorylation in MCF7 cells.

To determine the functionality of our MCF7-ephrinB2 cell line, we analyzed ephrinB2 phosphorylation dynamics upon EphB4/Fc stimulation by WB (figure 3.3A). In order to conduct a more comprehensive analysis of ephrinB2 phosphorylation, we included both early time-points (5, 15, 30 minutes) and late time-points (60, 120, 240 minutes) in our signalling experiments. Increase in ephrinB2 phosphorylation was first detected at 15 minutes after EphB4/Fc stimulation and peaked between 60 and 120 minutes before diminishing at 240 minutes. These results somewhat differed from a previous study on ephrinB1 phosphorylation (Bruckner, Pasquale et al. 1997). In this study, ephrinB1 phosphorylation peaked at 10 minutes after EphB2/Fc stimulation and gradually decreased at 20, 30 and 60 minutes. Notably, Bruckner and colleagues used 10 µg/ml of non-clustered EphB2/Fc to stimulate ephrinB1, which might explain the differences in phosphorylation dynamics. As ephrinB1 and

ephrinB2 share 95% homology in their cytoplasmic tail, it is possible to draw a parallel between the signalling data obtained from these two proteins. In the study by Bruckner and colleagues and in our study the decrease in ligand phosphorylation was accompanied by a decrease in total protein levels. These data are in accordance with previous reports suggesting that prolonged EphB4 stimulation eventually causes ephrinB2 internalization and degradation (Foo, Turner et al. 2006). Detection of increased Src phosphorylation after 5 minutes from EphB4/Fc stimulation, suggested that ephrinB2 phosphorylation was preceded and driven by Src activation (figure 3.3B), thus confirming literature reports on the importance of Src kinases in ephrinB2 reverse signalling (Palmer, Zimmer et al. 2002; Georgakopoulos, Litterst et al. 2006; Georgakopoulos, Xu et al. 2011). Inhibition of Src kinases with the SU6656 inhibitor prior to EphB4/Fc stimulation considerably decreased ephrinB2 phosphorylation (figure 3.3B), as previously reported in literature (Palmer, Zimmer et al. 2002). Intriguingly, we also noticed that the decrease of ephrinB2 total levels at the later time-points was less sharp upon SU6656 treatment. This observation points to the possibility that ephrinB2 phosphorylation status and/or Src activity are involved in the process of ligand degradation. This would imply, for the first time, that ephrinB degradation is not only driven by protein cleavage and EphB-induced ligand internalization, but also by ligand phosphorylation. This hypothesis is supported by the fact that prolonged stimulation with EphB receptors causes the complete degradation of ephrinB ligands (Foo, Turner et al. 2006). Therefore, we propose that ligand phosphorylation status might be responsible for a yet unreported mode of ephrinB degradation.

One of the main research objectives of this study was to analyze the functional consequences of ephrinB2 – expression in breast cancer development. In order to address this

point, we employed the use of three-dimensional (3D) culture systems (figure 3.4), which are best suited to study how proteins influence breast cancer development in a more "*in vivo*-like" setting (Hebner, Weaver et al. 2008). We tested the ability of MCF7 and MCF7-ephrinB2 cells to grow in collagen I (figure 3.4A,B) and Matrigel (figure 3.4C,D) based matrices with or without EphB4/Fc stimulation. In collagen, colonies grew as symmetrically shaped, compact spheres and were not affected by ephrinB2 expression or EphB4/Fc stimulation. In Matrigel, MCF7 cells formed compact sphere-like colonies, which grew as larger and irregularly shaped structures in the presence of ephrinB2 expression and independently of EphB4/Fc presence. Interestingly, the colonies formed by MCF7-ephrinB2 cells were characterized by a wide internal lumen (figure 3.4E), which is usually not present in typical MCF7 colonies grown in Matrigel (Kirshner, Chen et al. 2003; Krause, Maffini et al. 2010; Wang, Lacoche et al. 2013). The different colony growth patterns observed in collagen and Matrigel might be caused by the different components contained in the two matrices. For example, Matrigel contains laminin-1, collagen IV and entactin (Grant, Kleinman et al. 1985). Furthermore, collagen I and Matrigel matrices show different mechanotransduction properties, which are known to produce different effects on mammary architecture, metabolic function and differentiation in normal breast epithelium (Emerman and Pitelka 1977; Emerman, Bartley et al. 1980). Matrigel also contains various growth factors, such as FGF, EGF, TGF-β and PDGF (Benton, Kleinman et al. 2011). In this respect, various studies have reported that FGF receptor activity induces ephrinB1 phosphorylation (Chong, Park et al. 2000; Bong, Park et al. 2004), thus suggesting that the FGFR – ephrinB2 axis might be involved in the faster colony growth of MCF7-ephrinB2 cells. EphrinB2 might also be able to affect MCF7 colony growth through its association with β-integrins, which are known to increase cell proliferation and alter morphology of breast cancer cell colonies in 3D cultures

(Weaver, Petersen et al. 1997). Previous studies have shown that ephrinB2 – β1-integrin association induced cell migration in B16 melanoma cultures (Meyer, Hafner et al. 2005) and that ephrinB2 modulated αVβ1 integrin clustering at sites of cell-driven fibronectin assembly in Matrigel based 3D cultures (Julich, Mould et al. 2009). Interestingly, there are no reports on ephrinB association with β4-integrin, which interacts specifically with laminin and is responsible for cell-ECM adhesion through the formation of hemidesmosomes (Borradori and Sonnenberg 1999). β4-integrin also plays an important role in breast carcinoma progression (Mercurio, Rabinovitz et al. 2001). Specifically, α6β4-integrin is associated with ErbB2-induced mammary tumourigenesis, as reported in the study by (Guo, Pylayeva et al. 2006). Here, the authors found that ErbB2 induced phosphorylation of the signalling domain of α6β4-integrin through activation of Src kinases. Intriguingly, ephrinB1 is also phosphorylated as a result of ErbB2 activation and both proteins have been found to associate at sites of cell-cell junctions (Vermeer, Bell et al. 2012). Therefore, it is possible that ephrinB2 activation by EphB receptors, FGF receptors or ErbB2 might drive colony growth through α6β4-integrin activity upon interaction with laminin-1 in 3D Matrigel.

Although we did not conduct a detailed analysis on the effect of ephrinB2 over-expression on MCF7 cell proliferation in Matrigel 3D cultures, it appears that ephrinB2 is able to alter the cellular organization of MCF7 colonies by driving cells to spread at the periphery of the structures (figure 3.4C). This "pro-migratory" phenotype is consistent with the role of ephrinB2 in driving angiogenesis and metastasis in breast tumours described in literature (Kumar, Singh et al. 2006; Salvucci, Maric et al. 2009), although it remains unclear whether it is caused by ephrinB2 reverse signalling or EphB forward signalling. Nevertheless, ephrinB/EphB signalling-induced cell repulsion is likely to contribute to the "pro-migratory" phenotype observed in 3D Matrigel-grown colonies. Syntenin-1 might also be responsible for

this phenotype, as it promotes breast cancer cell migration by up-regulating β1-integrin expression (Yang, Hong et al. 2013). Furthermore, the role of syntenin-1 in FAK and Src activation upon integrin-mediated binding to fibronectin and collagen is important for anchorage-independent growth and migration (Boukerche, Su et al. 2008; Sarkar, Boukerche et al. 2008; Hwangbo, Kim et al. 2010), which would facilitate cell spreading to the periphery of the colony. Taking into consideration the role of Src in ephrinB2 phosphorylation and the ability of syntenin-1 to bind ephrinB ligands, it is possible that the ephrinB2 – syntenin-1 axis contributes to the "pro-migratory" phenotype of MCF7-ephrinB2 cells in 3D Matrigel-grown colonies.

Another interesting characteristic of MCF7-ephrinB2 colonies is the presence of a wide internal lumen (figure 3.3E). Matrigel-grown MCF7 colonies typically do not form a lumen, as their cells are not polarized (Kirshner, Chen et al. 2003; Krause, Maffini et al. 2010; Wang, Lacoche et al. 2013). Given the ability of ephrinB2 to interact with PAR3, it is possible that this interaction affects cell polarity and promotes lumen formation in MCF7-ephrinB2 colonies. In mammalian polarized epithelial cells, PAR3 localizes at the apical/lateral boundary of polarized cells where it recruits PAR6 and aPKC to form the PAR3 – PAR6 – aPKC PAR polarity complex, thus contributing to the formation of a correctly orientated microtubule spindle (Hebner, Weaver et al. 2008; McCaffrey and Macara 2011; Chen and Zhang 2013). Knock down of PAR3 in MCF10A cells disrupts cell polarity and lumen formation in colonies grown in 3D Matrigel (Wang, Lacoche et al. 2013). Moreover, PAR3 takes part in tight junction formation between epithelial cells (Ohno 2001; Chen and Zhang 2013) and its association with PAR6 and aPKC can be disrupted by the physical interaction of ErbB2 with PAR6 in MCF10A cells grown in 3D cultures (Aranda, Haire et al. 2006). Given the ability of ephrinB ligands to bind PAR3 via PDZ-mediated interaction (Cowan and

Henkemeyer 2002) and to cross-talk with ErbB2 signalling at sites of cell-cell junctions (Vermeer, Bell et al. 2012), it is possible that ephrinB2 modulates PAR3 and ErbB2 activity during junction formation. As ephrinB2 over-expression appeared to induce lumen formation in MCF7 colonies, it is possible that ephrinB2 is able to restore a certain level of cell polarity through interaction with PAR3 by countering the disrupting effect of ErbB2 on the PAR polarity complex. In support of this hypothesis, a study by (Kaenel, Antonijevic et al. 2012) has found that deletion of the cytoplasmic tail of ephrinB2 in luminal epithelial cells causes aberrant cell polarization *in vivo*. However, the role of ephrinB2 in this context might not be so simple, as studies have shown that ephrinB2 over-expression or knock out in mouse models is associated with aberrant lumen formation and deregulated proliferation/apoptosis ratios of normal mammary epithelial cells (Weiler, Rohrbach et al. 2009). Interestingly, this effect has been closely linked to ephrinB2 cross-talk with E-cadherin (Haldimann, Custer et al. 2009), which has been identified as a major player in the formation of MCF7 spheroid structures in 3D cultures (Ivascu and Kubbies 2007).

Therefore, ephrinB2 expression seems to play a pivotal role in driving both structure and lumen formation in epithelial mammary colonies through the possible cross-talk with integrins, E-cadherin, syntenin-1 and PAR3. Further study might reveal new connections between ephrinB ligands and other adhesion molecules involved in these processes. A possible candidate is, for example, CEACAM1, which is involved in driving lumen formation in mammary epithelial colonies (Kirshner, Hardy et al. 2004). All considered, the Matrigel based 3D cell culturing technique seemed to possess the potential for uncovering functional aspects of the ephrinB2 ligand in the context of breast cancer epithelial cells, which would have otherwise remained hidden in standard *in vitro* cultures.

After establishing the functionality of our MCF7 model system, we generated ephrinB2 mutants with a disrupted PDZ binding motif: ephrinB2/G and ephrinB2/ΔV (figure 3.5). Surprisingly, whilst assessing the interaction of wild type and ephrinB2 mutants with known PDZ domain-containing partners, we found that the ephrinB2 peptide does not bind Dishevelled-2 and PICK1 (figures 3.6B and 3.6C respectively). Dishevelled-2 was initially found to bind the cytoplasmic tail of *Xenopus* ephrinB1 in co-immunoprecipitation assays performed with recombinant GST-ephrinB1 (aa 264-346) (Tanaka, Kamo et al. 2003). The authors also stated that *Xenopus* ephrinB1 phosphorylation upon EphB2 stimulation did not affect binding affinity. Later studies reported that the DEP domain of Dishevelled-2 was essential for binding to *Xenopus* ephrinB1 and that deletion of the 6 C-terminal amino acids of ephrinB1 abolished the interaction with Dishevelled-2 (Lee, Bong et al. 2006; Lee, Mood et al. 2009). Interestingly, Lee and colleagues also reported that phosphorylation of Tyr326 and/or Tyr327 of *Xenopus* ephrinB1 (which correspond to Tyr330 and Tyr331 of human ephrinB2) strongly impairs binding to Dishevelled-2, thus contradicting the previous report by Tanaka and colleagues. As the 14 C-terminal amino acids of human, chicken and *Xenopus* ephrinB1 are 100% identical to human ephrinB2, our data suggests that this C-terminal sequence is not sufficient for ephrinB1 and ephrinB2 binding to Dishevelled-2.

PICK1 was found to interact with ephrinB1 through PDZ-mediated interaction in a yeast two-hybrid system using a 92 aminoacid long bait formed by the C-terminus sequence of ephrinB1 (Torres, Firestein et al. 1998). The interaction was also confirmed via co-immunoprecipitation in the same study. Since then, only one study has investigated the binding properties of the PICK1 – ephrinB1 interaction by using bioinformatics and biophysical docking simulations (Bolia, Gerek et al. 2012). Therefore, it is possible that the 14 C-terminal amino acids of ephrinB ligands are not sufficient to allow PICK1 binding.

In co-immunoprecipitation experiments conducted early on in our study (data not shown), we were also unable to detect PDZ-RGS3 binding to ephrinB2. PDZ-RGS3 was initially discovered as an ephrinB1 interacting protein via yeast two-hybrid screening using a bait formed by the whole cytoplasmic tail of ephrinB1 (Lu, Sun et al. 2001). The authors confirmed the existence of the interaction via pull down assays using a recombinant GST-ephrinB1 protein containing the 33 amino acids long C-terminal sequence of ephrinB1 (which is 100% identical to ephrinB2). Through the use of mutants, they also determined that the PDZ-RGS3 – ephrinB1 interaction was mediated by the PDZ domain of PDZ-RGS3 in co-immunoprecipitation assays performed in COS cells. As Lu and colleagues used our same detergent conditions for cell lysis, it is unlikely that the experimental conditions are to blame for this discrepancy. However, it is possible that ephrinB2 and PDZ-RGS3 are diversely compartmentalized in MCF7 cells, which would not allow us to detect the ephrinB2 – PDZ-RGS3 interaction by co-immunoprecipitation.

As expected, the ephrinB2/ΔV peptide was unable to pull down any of the PDZ domain-containing proteins, while the ephrinB2/G peptide retained partial binding only to syntenin-1, albeit at a considerably lower level than ephrinB2 wild type (figure 3.6). This phenomenon is probably due to the versatility of syntenin-1 PDZ-mediated binding and its ability to bind degenerated PDZ binding motif sequences (Beekman and Coffer 2008). Therefore, by generating MCF7 cell lines expressing ephrinB2, ephrinB2/G and ephrinB2/ΔV we would be able, for the first time, to distinguish the role of syntenin-1, during its interaction with ephrinB2, from all the other known PDZ partners that we have tested in this study. Nevertheless, one has to keep into account the possibility that ephrinB2/G might also retain binding to other yet unknown PDZ binding partners of ephrinB2, leading to a more cautious interpretation of the ephrinB2/G phenotype.

Although a small level of leakiness in protein expression was observed, our tetracycline inducible MCF7 cell lines worked as expected. Cell surface and total protein expression levels of ephrinB2, ephrinB2/G and ephrinB2/ΔV were comparable, with minor differences of ~20% less expression of ephrinB2/G and ephrinB2/ΔV compared to ephrinB2 (figure 3.7). These results were expected, as previous reports suggested that the PDZ binding motif is not involved in ephrinB delivery to the cell surface (Makinen, Adams et al. 2005). In MCF7 Tet-ephrinB2/shSyntenin-1 cells, ephrinB2 cell surface expression was higher than the total expression when compared to the other cell lines (figure 3.7A,B). However, this effect is probably indirect and not caused by the lack of ephrinB2 – syntenin-1 interaction, as both ephrinB2/G and ephrinB2/ΔV did not show similar discrepancies in their expression levels. Additionally, cell surface expression of tetraspanin CD81, which we used as a positive control, was also higher in syntenin-1 depleted cells. Indeed, syntenin-1 is involved in many trafficking pathways and its depletion might have widespread repercussions on cell trafficking (Beekman and Coffer 2008). For example, syntenin-1 knock down would affect syndecan recycling to the cell surface via interaction with $PI(4,5)P_2$ (Zimmermann, Zhang et al. 2005) and the formation of tripartite complexes with syndecans and Alix in connection with cargo recruitment to exosomal compartments (Baietti, Zhang et al. 2012). Furthermore, syntenin-1 is involved in CD63 endocytosis (Latysheva, Muratov et al. 2006) and is responsible for proTGFα delivery to the cell surface (Fernandez-Larrea, Merlos-Suarez et al. 1999). Therefore, the overall effect of syntenin-1 knock down on cell trafficking might have caused the slight increase in ephrinB2 cell surface expression.

Protein localization observed using immunofluorescence confirmed that ephrinB2 and mutants are expressed and localized on the cell surface of MCF7 tetracycline inducible cells

(figure 3.7E). Moreover, binding motif mutations did not seem to affect ligand localization, as has already been reported in literature (Makinen, Adams et al. 2005).

3D culture experiments on MCF7 TetOn parental cells and MCF7 Tet-ephrinB2 cells grown in Matrigel under doxycycline stimulated or non-stimulated conditions revealed that low ephrinB2 expression levels were sufficient to cause a notable increase in colony size, but no difference in colony morphology (figure 3.8). Surprisingly, MCF7 TetOn colonies were much smaller than MCF7 colonies analysed in our previous experiment (section 3.1.2.3). Although we did not investigate these differences further, it is possible that lower integrin expression levels in MCF7 TetOn cells were responsible for the colony phenotype that we observed. In fact, laminin-induced integrin activation increases colony growth in 3D Matrigel (Kirshner, Hardy et al. 2004; Cagnet, Faraldo et al. 2013). More specifically, high expression levels of β1-integrin and β4-integrin were found to increase cell proliferation and alter morphology of T4-2 breast cancer cell colonies in Matrigel based 3D cultures (Weaver, Petersen et al. 1997). The same group also reported that the role of β1-integrin in this context was tightly linked with EGFR activity. Down-regulation of either β1-integrin or EGFR resulted in impaired T4-2 colony growth in Matrigel based 3D cultures. Moreover, inhibition of EGFR signalling normalized β1-integrin expression levels in 3D cultures, but not in 2D monolayer cultures (Wang, Moorer-Hickman et al. 1998). This might explain why we detected a different phenotype between MCF7 TetOn and MCF7 cells in 3D cultures and not in 2D monolayers.

The similar morphology between control and ephrinB2 expressing cells might also be explained by the possibility that these cells express low integrin levels. Given the ability of ephrinB2 to induce cell migration in B16 melanoma cells by associating with β1-integrin (Meyer, Hafner et al. 2005) and the role of ephrinB2 in modulating αVβ1-integrin clustering

at sites of cell-driven fibronectin assembly in Matrigel based 3D cultures (Julich, Mould et al. 2009), it is possible that lower integrin levels in MCF7 TetOn cells prevented the development of the ephrinB2-induced morphological phenotype that we observed in MCF7-ephrinB2 colonies. Furthermore, low integrin levels would also impair the pro-migratory stimuli generated by syntenin-1-driven FAK-Src activation upon β1-integrin binding to fibronectin and collagen (Boukerche, Su et al. 2008). Interestingly, the increase in size of MCF7 Tet-ephrinB2 colonies appears to require low levels of ephrinB2 expression and thus is probably caused by ephrinB2-induced activation of endogenous EphB receptors and not by ligand reverse signalling.

Taken together, these results suggest that ephrinB2 expression in breast cancer epithelial cells might increase tumour progression by inducing cell proliferation via activation of EphB forward signalling and by increasing cell migration via cross-talk with integrins. However, more experimental data is needed to confirm this hypothesis. Unfortunately, these findings also inferred that the use of ephrinB2/G and ephrinB2/ΔV mutants would probably prove unhelpful in analysing the effects of disrupting the ephrinB2 – syntenin-1 axis in 3D cultures. Furthermore, the modulation of ephrinB2 expression through the tetracycline inducible system did not alter the outcome of the experiment, thus rendering this system unuseful in 3D Matrigel settings. The use of syntenin-1 depleted MCF7 Tet-ephrinB2 cells also proved unhelpful, as syntenin-1 knock down greatly impaired colony growth of MCF7 cells in Matrigel based 3D cultures (data not shown). This outcome is not surprising, as syntenin-1 is essential for cell proliferation and is involved in numerous cell signalling and trafficking pathways (Beekman and Coffer 2008). Furthermore, syntenin-1 is necessary for the correct assembly of focal adhesion complexes through activation of FAK (Hwangbo, Kim et al.

2010), which plays a pivotal role during cell-ECM interaction and consequent increase in cell proliferation (Hebner, Weaver et al. 2008).

Finally, using co-immunoprecipitation we confirmed that full length wild type and ephrinB2 mutants retained the same binding characteristics to endogenous syntenin-1, when expressed in tetracycline inducible MCF7 cells (figure 3.9), as previously observed in pull down assays on MCF7 cell lysates.

To summarize, we identified MCF7 cells to be the most suited cell line in which to study ephrinB2 pathways in the context of breast cancer and developed a flexible and functional model system based on tetracycline inducible cell lines, which enabled us to study signalling and trafficking pathways in ephrinB2, ephrinB2/G and ephrinB2/ΔV expressing cells. Importantly, we were able to generate the ephrinB2/G mutant, which has the unique ability to retain partial binding to syntenin-1 and to abolish binding to all other PDZ domain-containing partners of ephrinB2. For the first time, it was possible to selectively study the effects of the ephrinB2 – syntenin-1 interaction. Finally, we also found that ephrinB2 expression drives MCF7 colony growth in 3D Matrigel independently of EphB4/Fc stimulation.

3.2 The role of syntenin-1 in ephrinB2 signalling and trafficking pathways

Syntenin-1 interacts directly with the PDZ binding motif of ephrinB ligands, which led us to hypothesize that it could actively modulate ephrinB2 signalling and/or trafficking pathways. Therefore, we studied the phosphorylation dynamics of ephrinB2 and mutants in our newly established tetracycline inducible cell lines in order to determine whether syntenin-1 was involved in this process. We also analyzed trafficking dynamics of the wild type and ephrinB2 mutants.

3.2.1 Syntenin-1 does not play a role in EphB4-induced phosphorylation of ephrinB2

Before analyzing the phosphorylation dynamics of ephrinB2, ephrinB2/G and ephrinB2/ΔV, we tested EphB4/Fc stimulation on MCF7 Tet-ephrinB2 cells using WB analysis (described in section 3.1.2.2) (data not shown). However, ephrinB2 phosphorylation levels were barely detectable, possibly due to lower amounts of ephrinB2 protein on the cell surface compared to the stable MCF7-ephrinB2 cell line. To overcome this issue we performed immunoprecipitation (IP) using anti-Flag mAb prior to WB analysis.

3.2.1.1 EphrinB2, ephrinB2/G and ephrinB2/ΔV phosphorylation dynamics

MCF7 tetracycline inducible cell lines were stimulated with doxycycline for 48 hours in order to achieve maximum cell surface expression levels prior to EphB4/Fc stimulation for 0, 15, 30, 60, 120 and 240 minutes. Flag-tagged ephrinB2, ephrinB2/G and ephrinB2/ΔV were immunoprecipitated from cell lysates and analyzed by WB using phospho- and total-ephrinB antibodies. As illustrated in figure 3.10A, phosphorylation dynamics of ephrinB2 wild type in MCF7 tetracycline inducible cells was different compared to the MCF7-ephrinB2 stable cell line (figure 3.3A, section 3.1.2.2). Specifically, in MCF7 tetracycline inducible cells, the basal phosphorylation level of ephrinB2 under non-stimulated conditions was relatively high (lane 1) and only modestly increased upon EphB4/Fc stimulation, peaking at 30 minutes (lane 3) and sharply decreasing at 240 minutes (lane 6). Syntenin-1 depletion in ephrinB2 expressing cells did not seem to alter dynamics of phosphorylation (figure 3.10B). By contrast, ephrinB2/G and ephrinB2/ΔV mutants showed a different phosphorylation pattern (figure 3.10A and 3.10B respectively), with hardly any increase in phosphorylation detected throughout the time-course of EphB4/Fc stimulation. However, the sharp decrease in ephrinB2 phosphorylation at 240 minutes (lane 6, panel A) was also observed for ephrinB2/G (lane 12, panel A) and ephrinB2/ΔV (lane 6, panel B). The corresponding decrease in ephrinB2, ephrinB2/G and ephrinB2/ΔV total expression levels suggests that protein degradation is responsible for the decrease of phosphorylation. Furthermore, we noticed that the decrease in ephrinB2/G (lane 12, panel A) and ephrinB2/ ΔV (lane 6, panel B) total levels at 240 minutes seemed more pronounced when compared to the wild type, possibly indicating increased protein degradation. Interestingly, the highly glycosylated form of ephrinB2 (identified as the higher molecular weight band in ephrinB2 blots) showed a different pattern

of phosphorylation, which increased steadily throughout the time-course of EphB4/Fc stimulation and up to the final 240 minutes time-point. The corresponding highly glycosylated forms of ephrinB2/G and ephrinB2/ΔV showed a lower increase in phosphorylation throughout the time-course compared to the wild type. It is possible that highly glycosylated forms of ephrinB2 are more resistant to de-phosphorylation and degradation following prolonged periods of EphB4/Fc stimulation. Moreover, the effect of PDZ binding motif mutations on the phosphorylation of the glycosylated form of the ligand seemed less pronounced compared to the non-glycosylated form. Syntenin-1 depletion had no effect.

Densitometry analysis on both phospho and total ephrinB2 levels of three independent WB experiments conducted on each cell line allowed us to perform a quantitative analysis of ephrinB2, ephrinB2/G and ephrinB2/ΔV phosphorylation dynamics. Within each cell line, we calculated the ratios of phospho/total levels for each time-point and presented the data in a histogram as fold increase of phosphorylation (figure 3.10C). Thus presented, these results clearly indicate that ephrinB2 phosphorylation upon EphB4/Fc stimulation increased over time and that syntenin-1 depletion did not affect this process. On the other hand, ephrinB2/G and ephrinB2/ΔV phosphorylation remained mostly unaltered throughout the time-course of stimulation. At the 240 minute time-point, the difference between ephrinB2 and ephrinB2/G, ephrinB2/ΔV phosphorylation levels becomes statistically significant. This suggests that syntenin-1 is not directly involved in ephrinB2 phosphorylation, which is affected by mutations in the PDZ binding-motif. Yet, our results indicate that a PDZ domain-containing partner/s of ephrinB2 is/are involved in EphB4-induced ligand phosphorylation. Additionally, densitometry analysis revealed that ephrinB2 phosphorylation kept increasing over time up to the last time-point, instead of peaking at 30 minutes and then decreasing as previously

observed in WB analysis. This discrepancy is probably due to ephrinB2 internalization and degradation, which is triggered in order to terminate signalling.

A)

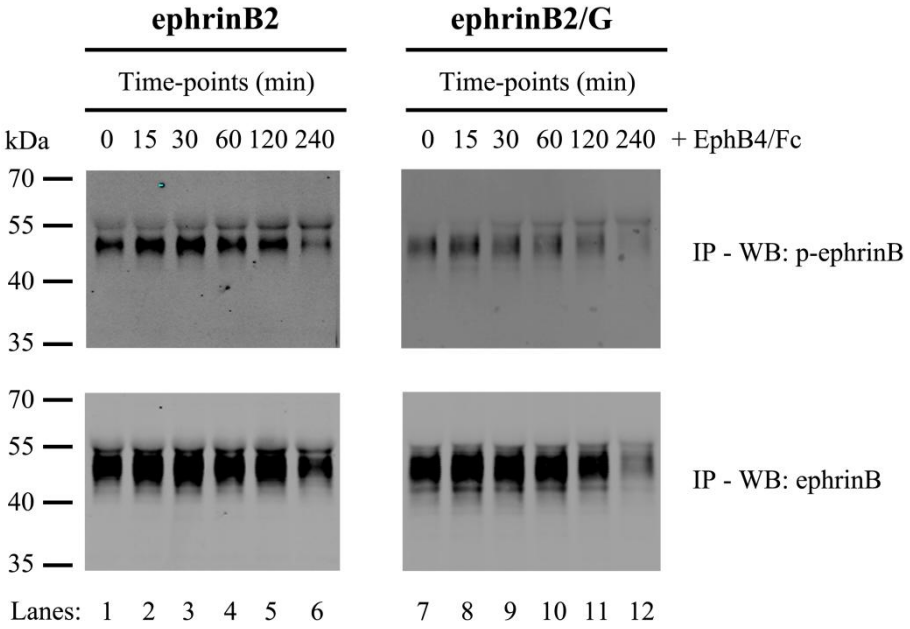

B)

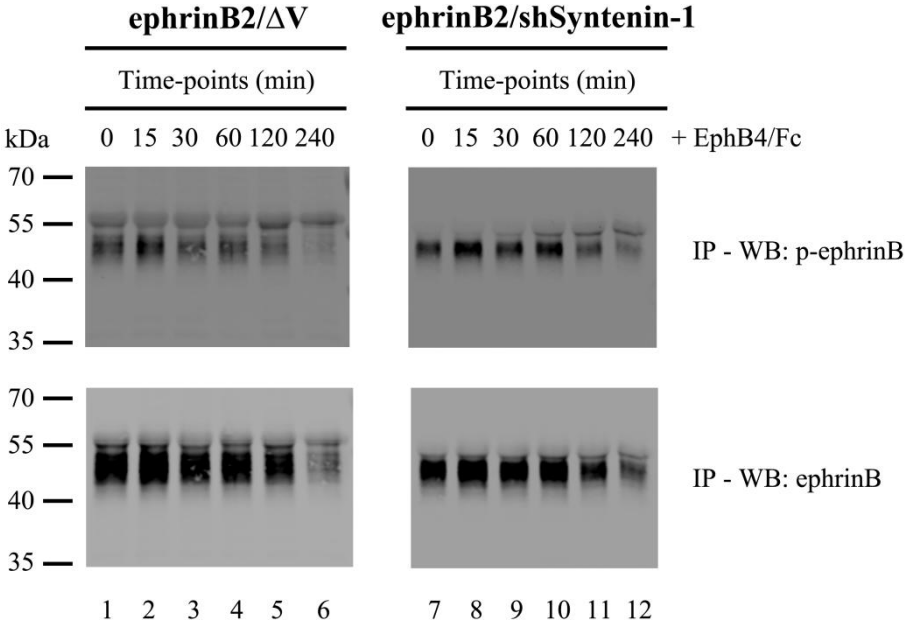

C)

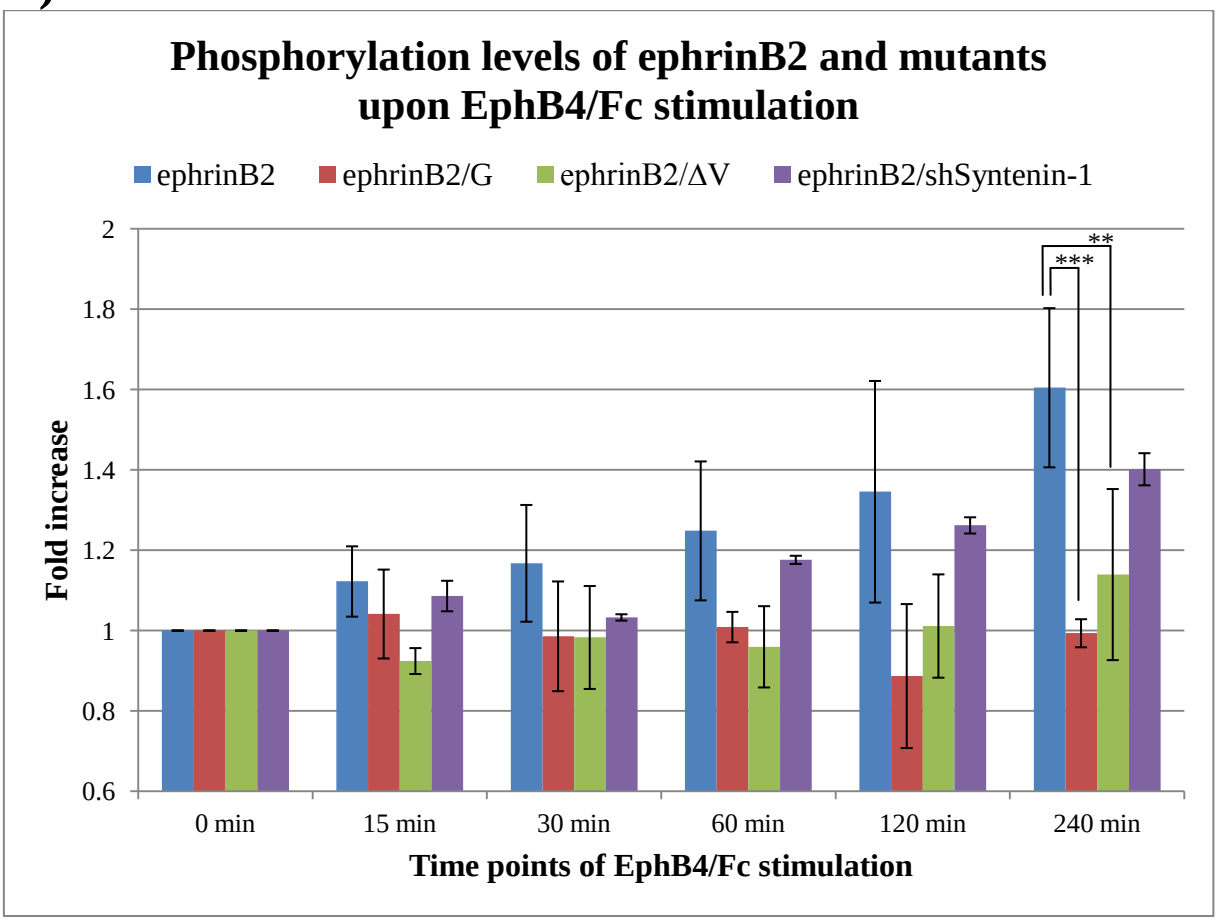

Figure 3.10: EphB4/Fc-induced phosphorylation of ephrinB2 is impaired in the presence of /G and /ΔV mutations, but not when syntenin-1 is knocked down.
Phosphorylation dynamics of ephrinB2, ephrinB2/G and ephrinB2/ΔV upon EphB4/Fc stimulation in MCF7 Tet-ephrinB2 (panel **A, left**), MCF7 Tet-ephrinB2/G (panel **A, right**), MCF7 Tet-ephrinB2/ΔV (panel **B, left**) and MCF7 Tet-ephrinB2/shSyntenin-1 (panel **B, right**) were analysed by immunoprecipitation followed by WB. Cells were stimulated with 1 µg/ml doxycycline for 48 hours prior to EphB4/Fc stimulation. Cells were then starved in serum free medium for 4 hours and subsequently stimulated with 5 µg/ml EphB4/Fc (pre-clustered for 1 hour with anti-Fc Ab) for 15, 30, 60, 120 and 240 minutes. Cells were lysed in 1% TritonX-100 buffer and lysates were incubated with anti-Flag antibody-conjugated agarose beads. Immunoprecipitated proteins (IP) were resolved on SDS-PAGE and phospho and total levels of ephrinB2 were detected with phospho-specific anti-ephrinB (Tyr325/329) pAb and anti-ephrinB pAb, respectively. **C**) The histogram shows the quantitative analysis performed on the densitometry data obtained from the blots of three independent experiments for each cell line. The ratio between densitometry values of phospho and total blots was calculated for every time-point and presented in relation to the non-stimulated control (0 minute time-point) as fold increase in ligand phosphorylation. Mean values and standard deviations of fold increase were then calculated and plotted on the histogram. Statistical significance was determined by the two-way ANOVA multiple comparison test with the Tukey-Kramer post-test, using GraphPad Prism software, whereby significance was set at 0.05 (** $P<0.01$; *** $P<0.001$). Note: densitometry measurements of phospho bands include both glycosylated and non-glycosylated forms of ephrinB2 proteins.

3.2.1.2 EphrinB2, ephrinB2/G and ephrinB2/ΔV basal levels of phosphorylation

The quantitative analysis of the fold increase in ligand phosphorylation previously described does not take into account the possibility of different basal phosphorylation levels between the wild type and ephrinB2 mutants in non-stimulated conditions (see figure 3.10). Having noticed that the basal levels of ligand phosphorylation seemed higher in MCF7 tetracycline inducible cell lines (figure 3.10A,B) compared to stable MCF-ephrinB2 cells (figure 3.3A), we wondered whether differences in basal phosphorylation were also present between wild type and ephrinB2 mutants.

We analyzed the basal phosphorylation levels of ephrinB2, ephrinB2/G and ephrinB2/ΔV in all four MCF7 tetracycline inducible cell lines in parallel under non-stimulated conditions, following the same procedure described in the previous section. The quantitative analysis conducted on densitometry values revealed that the basal phosphorylation levels of ephrinB2 and ephrinB2/G were similar, while the levels of ephrinB2/ΔV and ephrinB2 in syntenin-1-depleted cells were significantly lower by ~30% (figure 3.11). Intriguingly, these results seem to suggest that syntenin-1 plays a role in modulating the ephrinB2 basal phosphorylation status in non-stimulated conditions, although the mechanism behind this regulation remains unclear.

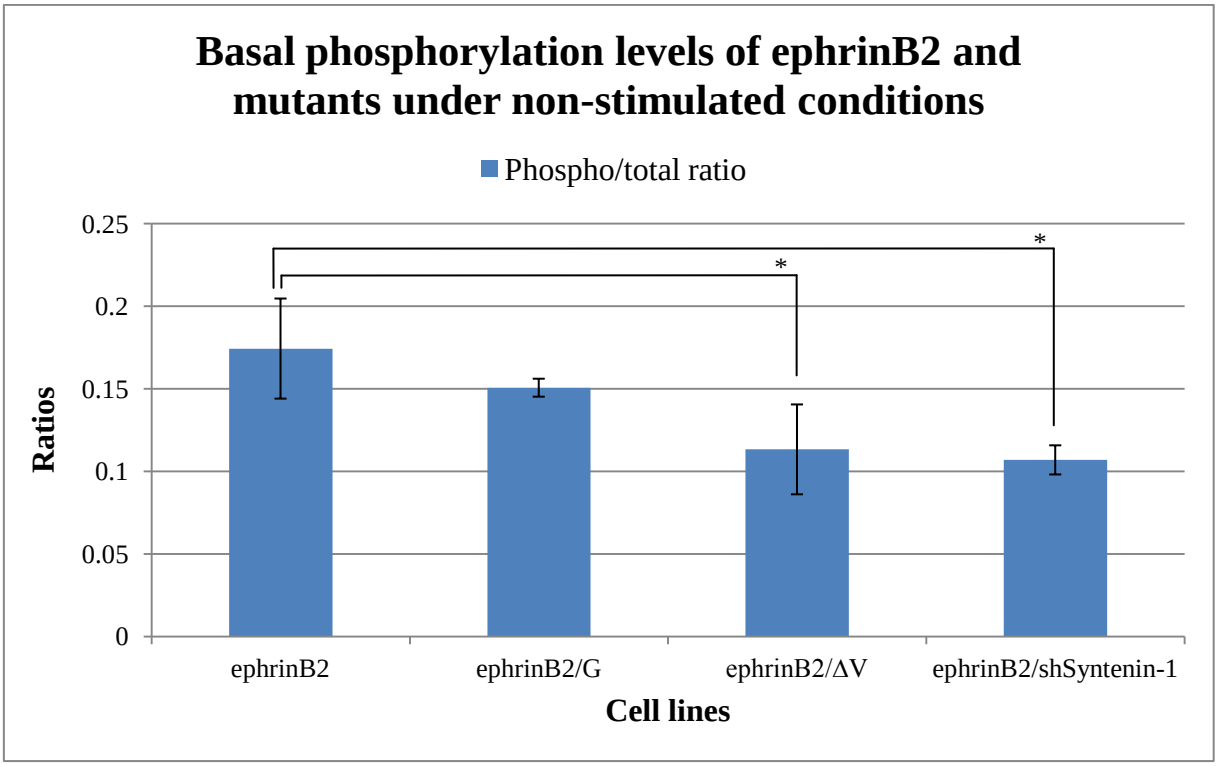

Figure 3.11: basal phosphorylation levels of ephrinB2 are lower in the presence of the /ΔV mutation and syntenin-1 knock down.

Basal phosphorylation levels of ephrinB2, ephrinB2/G and ephrinB2/ΔV in non-stimulated conditions was assessed as described in figure 3.10. Densitometric analysis was conducted on WB data and the ratio between densitometry values of phospho and total blots was calculated. Means and standard deviations were calculated and presented in the histogram. Statistical significance was determined by the one-way ANOVA multiple comparison test with the Tukey-Kramer post-test, using GraphPad Prism software, whereby significance was set at 0.05 (* $P<0.05$).

3.2.2 Syntenin-1 is involved in ephrinB2 turnover

Syntenin-1 is known to be responsible for biosynthetic trafficking, recycling and internalization of various cell surface proteins. Thus, it is possible that syntenin-1 is also involved in regulation of ephrinB2 trafficking. Therefore, we analyzed whether syntenin-1 plays a role in ephrinB2 trafficking to or from the cell surface.

3.2.2.1 Syntenin-1 is not involved in ephrinB2 trafficking to the cell surface

We used flow cytometry to analyze dynamics of cell surface levels of ephrinB2, ephrinB2/G and ephrinB2/ΔV in MCF7 tetracycline inducible cell lines after 0, 4, 8, 12 and 24 hours of doxycycline stimulation. The data are presented as fold increase in means of fluorescence intensities and compiled in a histogram and table shown in figure 3.12.

The results clearly indicate that protein delivery to the cell surface was not notably affected by the disruption of the PDZ binding sequence of ephrinB2 or depletion of syntenin-1, thus suggesting that neither syntenin-1 nor any other PDZ domain-containing proteins are involved in ephrinB2 biosynthetic trafficking. The slightly higher values of ephrinB2/G and ephrinB2/ΔV observed at the 24 hour time-point were likely due to their lower basal gene expression levels.

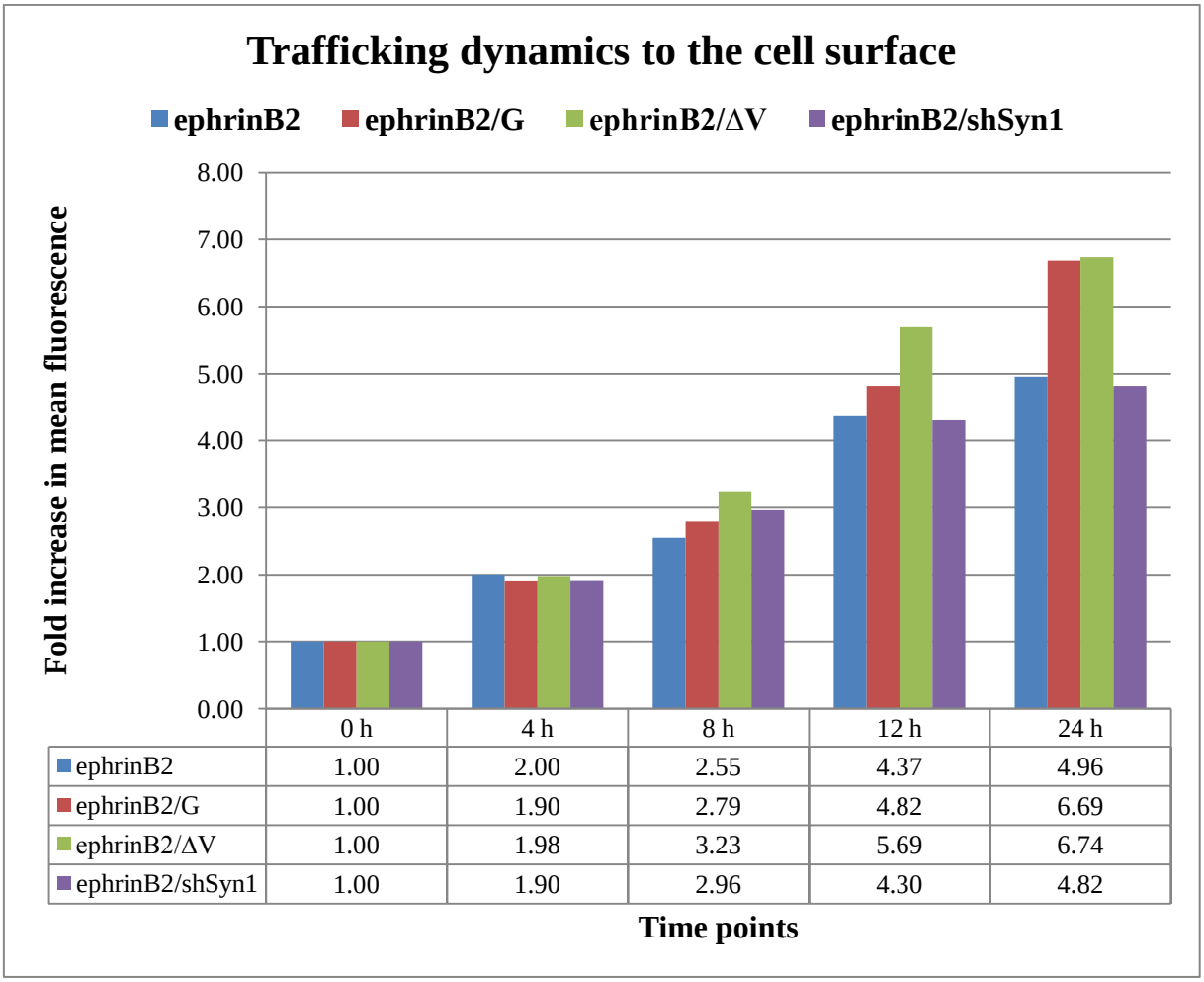

	0 h	4 h	8 h	12 h	24 h
ephrinB2	1.00	2.00	2.55	4.37	4.96
ephrinB2/G	1.00	1.90	2.79	4.82	6.69
ephrinB2/ΔV	1.00	1.98	3.23	5.69	6.74
ephrinB2/shSyn1	1.00	1.90	2.96	4.30	4.82

Figure 3.12: biosynthetic trafficking of ephrinB2 to the cell surface is unaffected by the /G and /ΔV PDZ mutations as well as syntenin-1 knock down.
Flow cytometry analysis on cell surface expression levels of ephrinB2, ephrinB2/G and ephrinB2/ΔV in MCF7 tetracycline inducible cell lines stimulated for 0, 4, 8, 12 and 24 hours with 1 µg/ml doxycycline. In the histogram, mean fluorescence values of each time-point was related to the 0 hours value within each individual cell line and presented as fold increase in cell surface expression.

3.2.2.2 Syntenin-1 modulates ephrinB2 internalization

To analyze ephrinB2 internalization, we performed biotinylation assay. We decided to perform the experiments in the presence or absence of EphB4/Fc stimulation, as the latter leads to ephrinB2 internalization and degradation (see section 1.1.4.7 of the Introduction). The biotinylation experiment is used to determine the percentage of internalized cell surface protein compared to the overall amount at any given time-point (figure 3.13A). Hence, we stimulated cells with 5 µg/ml of EphB4/Fc or anti-Fc (as a control) to maintain the same experimental settings used in the signalling experiments. However, we did not serum starve cells prior to stimulation to avoid indirect effects on ligand internalization. In these experiments we stimulated cells for 15 and 60 minutes. The earlier time-point allowed us to analyse changes in EphB4-driven ligand internalization, while the later time-point was chosen to correlate ligand phosphorylation and ephrinB2 internalization.

The WB data in figure 3.13A show the levels of total biotinylated ephrinB2 (lanes 1-4) and of internalized biotinylated ephrinB2 (lanes 5-8) after EphB4/Fc or anti-Fc stimulation. As expected, EphB4/Fc stimulation in MCF7 Tet-ephrinB2 cells increased the internalization levels of ephrinB2 (lanes 7 and8) compared to non-stimulated conditions (lanes 5 and 6). Surprisingly, ephrinB2/G internalization levels were not affected by EphB4/Fc stimulation (lanes 7 and 8) and remained unchanged when compared to non-stimulated condition (lanes 5 and 6). EphrinB2/ΔV internalization levels appeared similar to ephrinB2 under non-stimulated conditions (lanes 5 and 6), but did not notably increase after EphB4/Fc stimulation (lanes 7 and 8). Interestingly, in syntenin-1 depleted cells, ephrinB2 internalization levels appeared higher in both non-stimulated (lanes 5 and 6) and EphB4/Fc stimulated conditions (lanes 7 and 8). The histogram in figure 3.13B illustrates the WB densitometric analysis

presented as percentage of internalized relative to total protein. In control samples, we noticed that ligand internalization occurred at a slow speed. At 15 minutes, ephrinB2 internalization was 2% and barely increased to 3% after 60 minutes. Similarly, ephrinB2/G internalization was 1% at 15 minutes and less than 2% at 60 minutes. Interestingly, internalization levels of both ephrinB2/ΔV and ephrinB2 expressed in syntenin-1 depleted cells were slightly higher under non-stimulated conditions, reaching 3% after 15 minutes and over 4% after 60 minutes. Overall, these results on control samples suggest that wild type and ephrinB2 mutants remain stable on the cell surface and do not undergo rapid internalization under non-stimulated conditions. As expected, EphB4/Fc stimulation notably increased ephrinB2 internalization, which reached 4% at 15 minutes and 8% at 60 minutes. Surprisingly, ephrinB2/G internalization was not affected by EphB4/Fc stimulation, as internalization levels remained significantly lower, compared to ephrinB2, at 1% after 15 minutes and 2% after 60 minutes. In MCF7 Tet-ephrinB2/shSyntenin-1 cells, EphB4/Fc stimulation increased ephrinB2 internalization to only 4% after 15 minutes, but more than 10% after 60 minutes. EphrinB2/ΔV internalization was mostly unaffected by EphB4/Fc stimulation, as internalization levels remained at 3% after 15 minutes and barely rose over 5% after 60 minutes, thus remaining significant lower compared to ephrinB2. Summarizing, ephrinB2 internalization doubled at 15 minutes and nearly quadrupled at 60 minutes upon EphB4/Fc stimulation, while ephrinB2/G internalization remained unchanged. In MCF7 Tet-ephrinB2/shSyntenin-1 cells, ephrinB2 internalization barely rose after 15 minutes of EphB4/Fc stimulation, but increased 2.5 fold after 60 minutes. Following a similar pattern, ephrinB2/ΔV internalization remained unchanged after 15 minutes of EphB4/Fc stimulation, but rose nearly 1.5 fold after 60 minutes.

Taken together, these results suggest that syntenin-1 modulates ephrinB2 internalization, especially upon EphB4 interaction. In particular, the pattern of ephrinB2 internalization in syntenin-1 depleted cells and the absent EphB4/Fc induced internalization of ephrinB2/G seemed to suggest that syntenin-1 might be involved in stabilizing ephrinB2 on the cell surface by binding to its PDZ binding motif and preventing internalization. Moreover, this effect was significantly observed at 60 minutes after EphB4/Fc stimulation. Additionally, disruption of the PDZ binding motif impairs ephrinB2 internalization, thus suggesting that other PDZ domain-containing partners might be involved in this process. However, the mechanism behind this regulation remains unclear.

A)

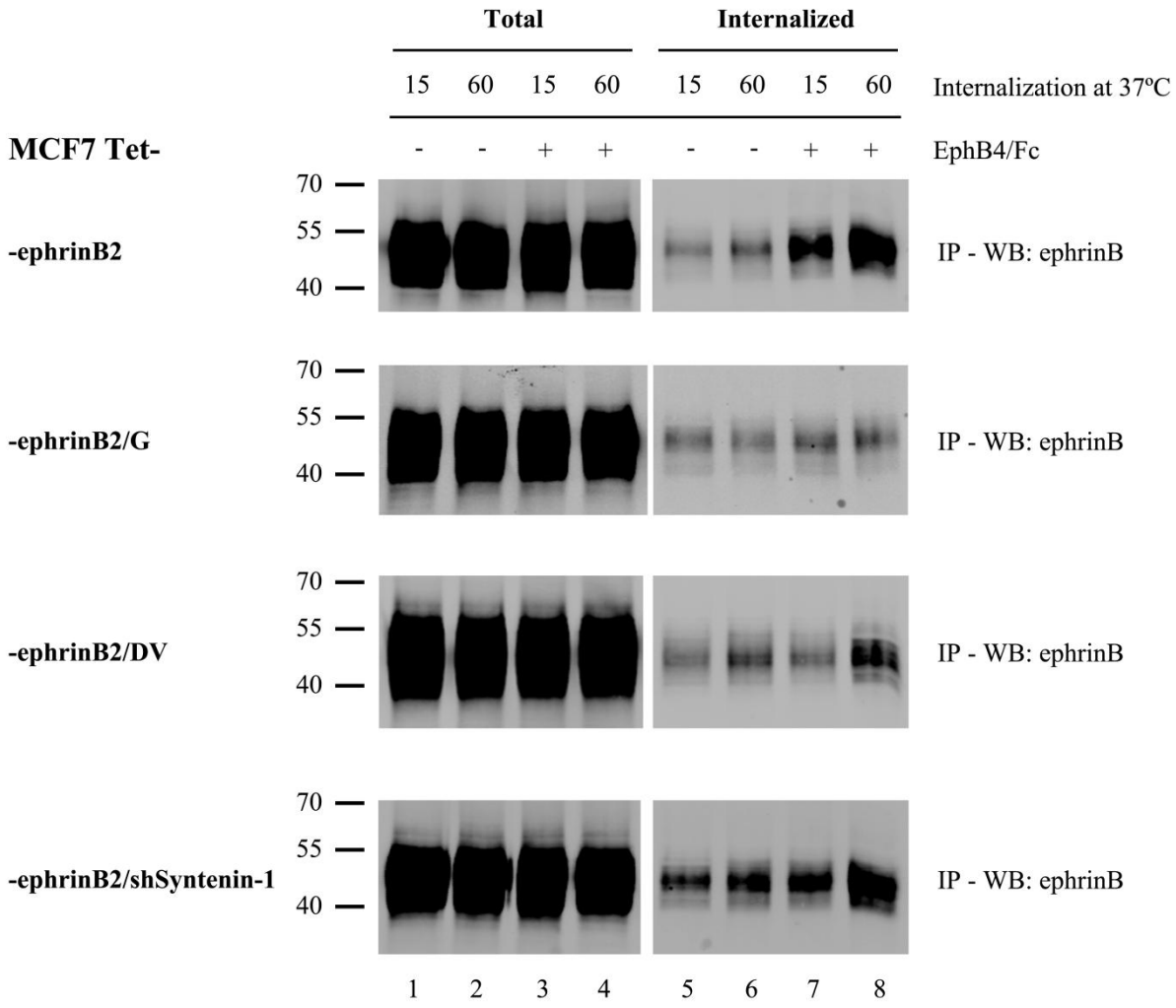
Total
Internalized
15 60 15 60 15 60 15 60
Internalization at 37ºC
MCF7 Tet- - - + + - - + +
EphB4/Fc
70
55
40
-ephrinB2
IP - WB: ephrinB
-ephrinB2/G
IP - WB: ephrinB
-ephrinB2/DV
IP - WB: ephrinB
-ephrinB2/shSyntenin-1
IP - WB: ephrinB
1 2 3 4 5 6 7 8

B)

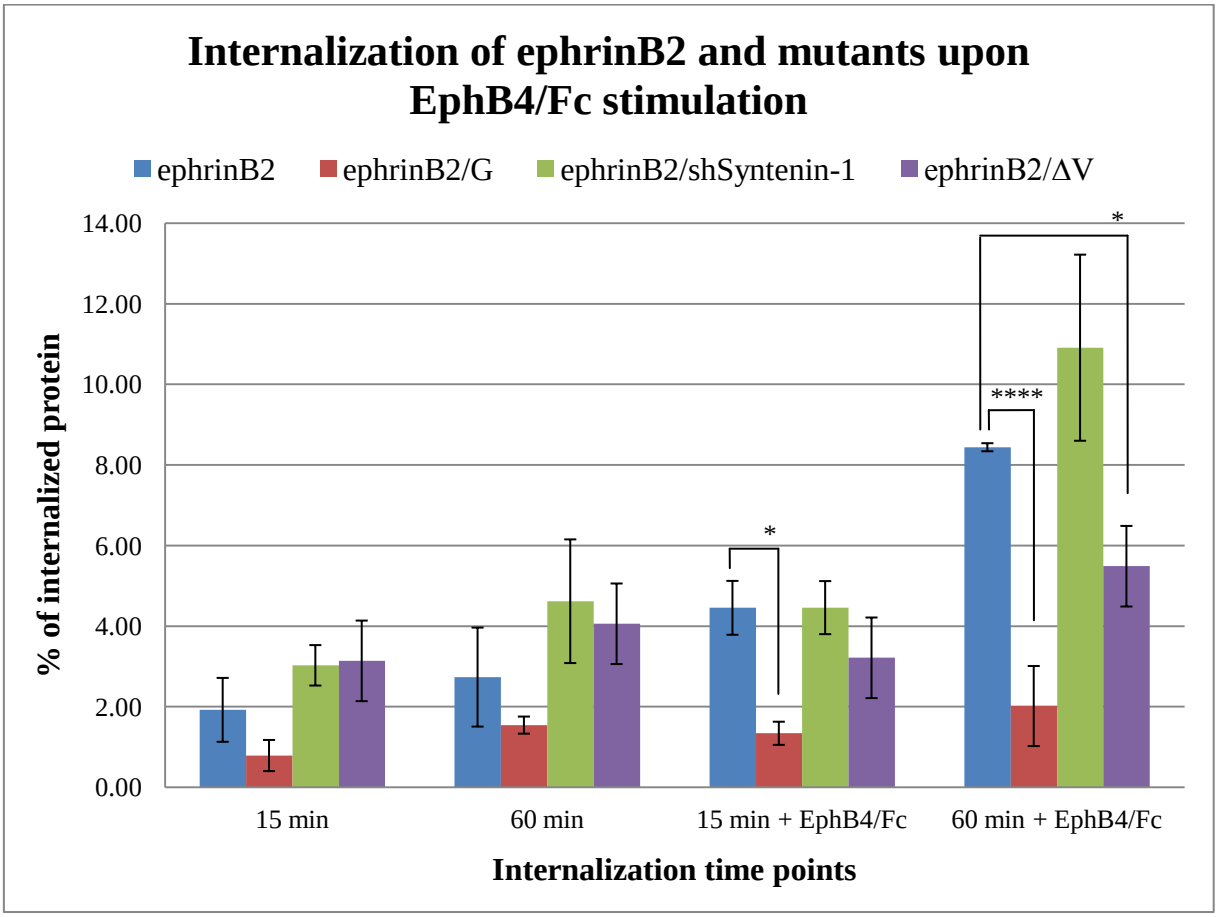

Figure 3.13: EphB4/Fc-induced internalization of ephrinB2 is strongly impaired by the /G PDZ mutation; mildly impaired by the /ΔV PDZ mutation; and slightly increased in the presence of syntenin-1 knock down.

Analysis of internalization levels of wild type and ephrinB2 mutants under basal or EphB4/Fc stimulated conditions measured using biotinylation assay. MCF7 Tet-ephrinB2, MCF7 Tet-ephrinB2/G, MCF7 Tet-ephrinB2/ΔV and MCF7 Tet-ephrinB2/shSyntenin-1 cells were stimulated with 1 µg/ml doxycycline for 48 hours and subsequently labelled with sulfo-NHS-SS-biotin for 1 hour and stimulated with EphB4/Fc or anti-Fc antibody for 15 and 60 minutes at 37ºC. The experiment was conducted in duplicate: in the control set of samples, cells were lysed after stimulation and lysates were incubated with NeutrAvidin-conjugated agarose beads to pull down all biotinylated proteins; in the other set of samples (internalized) cells were treated with MESNA to remove biotin from cell surface proteins and lysates were incubated with NeutrAvidin-conjugated agarose beads to pull down internalized biotinylated proteins. **A)** Pulled-down proteins from both set of samples were separated on SDS-PAGE and ephrinB2 was detected with anti-ephrinB pAb. **B)** Densitometric analysis was conducted on blots of three independent experiments for each cell line and the ratio between control and MESNA-treated samples was calculated. Mean values and standard deviations of ratios were calculated and presented as percentage of internalized ephrinB2 (MESNA-treated) compared to overall biotinylated ephrinB2 (control) in the histogram. Statistical significance was determined by the two-way ANOVA multiple comparison test with the Tukey-Kramer post-test, using GraphPad Prism software, whereby significance was set at 0.05 (* $P<0.05$; **** $P<0.0001$).

3.2.3 Discussion

In our signalling experiments on MCF7 tetracycline inducible cell lines, we observed that the phosphorylation pattern of ephrinB2/G and ephrinB2/ΔV differed from ephrinB2 by showing lower phosphorylation levels upon EphB4/Fc stimulation (figure 3.10). This suggests that the interaction of a PDZ domain-containing protein with the PDZ binding motif of ephrinB ligands is required for the correct phosphorylation of the latter upon EphB stimulation. However, syntenin-1, one of the well characterized PDZ domain-containing partners of ephrinB ligands, did not seem to affect ephrinB2 phosphorylation levels and dynamics upon EphB4/Fc stimulation. Nevertheless, this finding supports the hypothesis that PDZ-mediated interactions with PDZ domain-containing proteins modulate ephrinB ligands phosphorylation upon EphB stimulation and thus SH2 mediated signalling, a theory which has been often disregarded due to the ability of PDZ and SH2 mediated signalling to occur simultaneously (Su, Xu et al. 2004).

The ephrinB2 reverse signalling pathway can be triggered in multiple ways, which can lead to different biological outcomes. As described in section 1.1.4.1 of the Introduction, EphB receptor interaction with ephrinB ligands triggers Src family kinases activation which in turn is responsible for ephrinB phosphorylation (Palmer, Zimmer et al. 2002; Georgakopoulos, Litterst et al. 2006). However, ephrinB reverse signalling can also be triggered by direct interaction of the ligand with activated membrane receptor kinases such as FGF, VEGF, PDGF and ErbB receptors (Arvanitis and Davy 2008; Pitulescu and Adams 2010; Vermeer, Colbert et al. 2013). Although reports in literature suggest that ephrinB phosphorylation and PDZ-mediated signalling remain independent of each other (Su, Xu et al. 2004), there are very few studies which have analysed ephrinB phosphorylation dynamics in

detail (Holland, Gale et al. 1996; Bruckner, Pasquale et al. 1997) and none in the context of impaired PDZ interaction. Research by (Bruckner, Pasquale et al. 1997) focused on ephrinB phosphorylation at early time points while other studies analysed post-activation dynamics of PTPL1 de-phosphorylation (Palmer, Zimmer et al. 2002) and ligand degradation upon protracted EphB stimulation (Foo, Turner et al. 2006). Therefore, our data suggests, for the first time, that a functional PDZ binding motif is required for EphB-induced phosphorylation of ephrinB ligands.

Further analysis on ephrinB2, ephrinB2/G and ephrinB2/ΔV basal phosphorylation under non-stimulated conditions revealed ~30% lower phosphorylation levels in MCF7 Tet-ephrinB2/ΔV and MCF7 Tet-ephrinB2/shSyntenin-1 cells when compared to ephrinB2 and ephrinB2/G expressing cells (figure 3.11). This finding suggests that syntenin-1 interaction with ephrinB2 is able to modulate the ligand's basal phosphorylation level. Possibly, syntenin-1 might be involved in aiding ephrinB ligands phosphorylation induced by other receptor tyrosine kinases *in cis* (Pitulescu and Adams 2010). This process could involve the reported ability of syntenin-1 to form signalling complexes by acting as a scaffolding protein: at sites of integrin-mediated cell adhesion with fibronectin, syntenin-1 recruits and holds into complex FAK, Src and aPKC to allow aPKC to phosphorylate and activate FAK and Src (Hwangbo, Kim et al. 2010; Hwangbo, Park et al. 2011). Alternatively, syntenin-1 might be indirectly affecting ephrinB2 phosphorylation by modulating ligand internalization and preventing its degradation.

According to previous reports, the cytoplasmic tail of ephrinB ligands is necessary for protein trafficking to the cell surface. Deletion of the cytoplasmic tail causes ephrinB ligands to remain trapped in the Golgi network and subsequently degraded (Makinen, Adams et al.

2005). However, this effect does not seem to be related to SH2 or PDZ mediated signalling, as mutating the five tyrosines on the cytoplasmic tail and/or the PDZ binding motif of ephrinB1 does not cause ligand depletion from the cell surface (Makinen, Adams et al. 2005). We analysed the dynamics of ephrinB2, ephrinB2/G and ephrinB2/ΔV trafficking to the cell surface in order to determine whether syntenin-1 and other PDZ domain-containing proteins played a part in this process (figure 3.12). By using flow cytometry analysis on MCF7 tetracycline inducible cell lines, we determined that neither syntenin-1 nor other PDZ domain-containing proteins affected ephrinB2 trafficking to the cell surface. Our results corroborate previous reports suggesting that PDZ-mediated binding is not required for ephrinB ligands delivery to the cell surface (Makinen, Adams et al. 2005).

By measuring protein internalization using biotinylation assay (figure 3.13), we observed that ephrinB2 internalization is clearly enhanced upon interaction with EphB4/Fc, as previously reported in literature (Marston, Dickinson et al. 2003; Zimmer, Palmer et al. 2003). Moreover, the relatively slow speed of ligand internalization observed in our assay seems to confirm previous studies suggesting that ephrinB2 endocytosis is not clathrin-dependent (Marston, Dickinson et al. 2003; Zimmer, Palmer et al. 2003). Importantly, our data seems to indicate that syntenin-1 is directly involved in ephrinB2 internalization upon EphB4/Fc stimulation. In this regard, previous study has shown that neither tyrosine phosphorylation nor PDZ mediated signalling seem to be required during this process (Zimmer, Palmer et al. 2003). In contrast to the wild type protein, ephrinB2/G internalization did not increase upon EphB4/Fc stimulation. Furthermore, ephrinB2 internalization was noticeably higher in cells depleted of syntenin-1. When taken together, these results seem to suggest that syntenin-1 is able to prevent ephrinB2 internalization. Interestingly, this effect was more pronounced after 60 minutes of EphB4/Fc stimulation, which is when the highest level of ephrinB2

internalization was observed in syntenin-1 depleted cells. Therefore, syntenin-1-induced impairment of ephrinB2 internalization seems to occur alongside with increased ephrinB2 phosphorylation. The mechanism underlying this process is still unclear and open to speculation. One possibility is that syntenin-1 stabilizes the phosphorylated ligand on the cell surface, thus prolonging reverse signalling and preventing PTPL1-driven de-phosphorylation. Additionally, the strong impairment of ephrinB2/G internalization caused by syntenin-1 might also be enhanced by the lack of competition from other PDZ domain-containing proteins. Indeed, syntenin-1 PDZ-mediated binding to the C-terminus of the Notch-associated Delta1 ligand has been found to prevent its internalization from the plasma membrane (Estrach, Legg et al. 2007). Similarly, our group has found that syntenin-1 PDZ-mediated interaction with tetraspanin CD63 impairs clathrin-mediated internalization of the protein (Latysheva, Muratov et al. 2006). Specifically, the authors found that the NTD of syntenin-1 was responsible for shifting CD63 clathrin-dependent endocytosis to a slower internalization pathway, probably by competing with the clathrin-associated Adaptor Protein 2 (AP2). In support of this claim, a study by (Janvier and Bonifacino 2005) proposed the existence of an AP2-independent sorting pathway for proteins containing the AP2 consensus sequence YXXϕ at the C-terminus. Therefore, syntenin-1 might be modulating ephrinB2 internalization in a similar manner to CD63. Additionally, syntenin-1 might induce or prevent compartmentalization of phosphorylated ephrinB2 to a different membrane microdomain. However, this possibility is unlikely according to a recent study by (Xu, Sun et al. 2011), where the authors showed that EphB-induced phosphorylation of ephrinB1 in Jurkat cells was specifically mediated by Lck (a member of the Src family kinases) and induced ephrinB1 relocation to lipid rafts. Importantly, this process was specifically induced by ligand phosphorylation on Tyr residues and not by PDZ-mediated interactions.

Intriguingly, ephrinB2/ΔV internalization was overall higher than ephrinB2/G in both stimulated and non-stimulated conditions, but it did not increase significantly upon EphB4/Fc stimulation. This result suggests that other proteins may be responsible for ligand internalization. Although the identity of this protein remains to be established, we can speculate on two possible candidates. One of these is the previously mentioned clathrin-associated sorting adaptor AP2. (Parker, Roberts et al. 2004) suggested that AP2 might be responsible for clathrin-dependent endocytosis of ephrinB1, as they observed co-localization of EphB1/ephrinB1-containing vesicles with the early endosome marker EEA1 and caveolin. In support of this observation, the cytoplasmic tails of ephrinB ligands contain three YXXϕ consensus sequences, which might act as binding motifs for AP2 (Traub 2003; Edeling, Smith et al. 2006). In human ephrinB2, these sequences are located between amino acids 304-307 (YEKV), 311-314 (YGHP) and 330-333 (YYKV). Although AP2 is unlikely to bind the C-terminal YYKV sequence in ephrinB2/ΔV, it might be able to bind one or both of the other two YXXϕ sequences. Therefore, AP2 might be responsible for clathrin-dependent endocytosis of ephrinB ligands. However, the speed of ephrinB2 internalization measured in our assays is not consistent with clathrin-dependent endocytosis, which usually induces fast internalization of its cargo. Additionally, previous studies have not been able to co-localize EphB/ephrinB-containing vesicles with known endocytic markers (e.g. EEA1) (Marston, Dickinson et al. 2003; Zimmer, Palmer et al. 2003). Nevertheless, it is possible that different endocytic pathways might be triggered by different EphB and ephrinB family members or by different levels of EphB – ephrinB multimerization. Furthermore, clathrin-dependent endocytosis might be required during internalization of phosphorylated-ephrinB ligands which are not in complex with EphB receptors. However, further study is needed to assess the possible role of AP2-induced endocytosis of ephrinB ligands.

Another candidate is PAR6, a component of the PAR polarity complex (formed by PAR3-PAR6-aPKC) (Chen and Zhang 2013) which has been implicated in clathrin-independent recycling and clathrin-dependent uptake of various cell membrane proteins, including MHC-I and transferrin receptor (Balklava, Pant et al. 2007). PAR6 associates with ephrinB1 in a PDZ-independent manner which does not involve the 15 C-terminal amino acids of ephrinB1 (Lee, Nishanian et al. 2008). Interestingly, PAR6 has been found to play a role in Dynamin-dependent endocytosis at sites of adherens junctions by activating WASp and the Arp2/3 complex via interaction with Cdc42 (Georgiou, Marinari et al. 2008). Therefore, PAR6 might be involved in ephrinB2/ΔV internalization. However, the fact that EphB or FGFR-induced phosphorylation of ephrinB1 causes PAR6 dissociation from the ligand (Lee, Nishanian et al. 2008), suggests that this endocytic pathway may not be involved in internalization of phosphorylated ephrinB2.

Additionally, the PAR polarity protein PAR3, which binds to ephrinB ligands via its second and third PDZ domains (Cowan and Henkemeyer 2002), has also been implicated in endocytosis (Balklava, Pant et al. 2007; Nishimura and Kaibuchi 2007). A recent study by (Nakayama, Nakayama et al. 2013) has found that PAR3 interaction with ephrinB2 induces the recruitment of the clathrin-associated sorting adaptor Dab2 to ephrinB2 – VEGFR2,3 complexes during ephrinB2-driven internalization of VEGF receptors. However, PAR3-mediated internalization may only affect the ephrinB2 wild type protein and not the PDZ binding mutants ephrinB2/G and ephrinB2/ΔV.

Interestingly, a recent study has found that SH2-mediated binding of Grb4 (Nck2) to phosphorylated CEACAM3 mediated bacterial phagocytosis through WAVE2 activation (Pils, Kopp et al. 2012). As Grb4 is a main component of ephrinB reverse signalling (Cowan and Henkemeyer 2001), this newly described internalization mechanism might be involved in

the internalization of phosphorylated ephrinB2 and would not be hindered by mutations in the PDZ-binding motif. Taken together, these speculations suggest that more than one internalization pathway might be employed in ephrinB2 endocytosis. Intriguingly, these pathways might be specifically triggered depending on the phosphorylation status of ephrinB2

To conclude, in this chapter we analysed the ability of syntenin-1 to modulate ephrinB2 signalling and protein trafficking. We discovered that syntenin-1 does not affect ephrinB2 phosphorylation levels and dynamics, but that a functional PDZ binding motif is necessary for EphB4-induced ligand phosphorylation. However, lack of syntenin-1 interaction with ephrinB2 lowered the levels of basal phosphorylation of the ligand. In ephrinB2 trafficking, syntenin-1 does not modulate protein delivery to the cell surface, but negatively regulates ephrinB2 internalization upon EphB4/Fc stimulation.

3.3 EphrinB2 phosphorylation alters PDZ-mediated binding characteristics

Given the PDZ domain-dependent differences in phosphorylation of ephrinB2, it was important to investigate further how tyrosine phosphorylation affected interaction of ephrinB2 with its known PDZ domain-containing partners. While an early study by (Lin, Gish et al. 1999) reported that tyrosine phosphorylation at position -2, but not -3, of ephrinB1 decreases syntenin-1 binding, but does not affect PTPL1 binding, a later study by (Su, Xu et al. 2004) observed that phosphorylation of C-terminal tyrosines did not influence PDZ-mediated binding of PDZ-RGS3 to ephrinB2. These findings suggest that phosphorylation may differentially affect binding of PDZ domain-containing proteins to ephrinB ligands.

3.3.1 Phosphorylation of Tyr330 on ephrinB2 and ephrinB2/G increases syntenin-1 binding

In the ephrinB2 ligand, the interaction with EphB4 induces the phosphorylation of tyrosines in position 311, 316 and 330 (Kalo, Yu et al. 2001), with Tyr330 being the predominant site of phosphorylation *in vivo* (Su, Xu et al. 2004). Thus, we compared syntenin-1 binding to ephrinB2 and phospho-ephrinB2(Tyr330) peptides, as well as ephrinB2/G and phopho-ephrinB2/G(Tyr330), using pull down assay.

3.3.1.1 Syntenin-1 binding to phospho-peptides in pull down experiments

The PDZ binding motif of ephrinB2 binds with stronger affinity to the PDZ2 domain of syntenin-1, rather than the PDZ1. However, the two PDZ domains work together to ensure high affinity binding to ephrinB2 (Grembecka, Cierpicki et al. 2006; Beekman and Coffer 2008). Therefore, in our initial experiments we used a recombinant GST-PDZ1,2 protein. Lane 3 in figure 3.14A shows that the recombinant GST-PDZ1,2 protein strongly binds the ephrinB2 wild type peptide, while not binding the ephrinB2/G or ephrinB2/ΔV peptides (lanes 4 and 5 respectively). Interestingly, binding of both the phospho-ephrinB2 and phospho-ephrinB2/G peptides increased (lanes 6 and 7 respectively), proving that PDZ mediated binding is affected by the tyrosine phosphorylation at position -3.

We also performed a similar analysis using full-length recombinant syntenin-1. Surprisingly, we observed that binding of syntenin-1 to the ephrinB2/G peptide was only slightly less effective than to the ephrinB2 wild type peptide (figure 3.14B, lane 4). Although tyrosine phosphorylation at position -3 causes an increase in syntenin-1 binding (lanes 6 and 7 respectively), the increase was modest and only observed for ephrinB2/G. Finally, we carried out a pull down assay on MCF7 cell lysates and detected the levels of endogenous syntenin-1 that bound to the peptides (figure 3.14C). In this case, syntenin-1 bound to the ephrinB2/G peptide (lane 5) to a lesser degree when compared to the ephrinB2 wild type peptide (lane 3). However, tyrosine phosphorylation at position -3 notably increased syntenin-1 binding to the ephrinB2/G peptide (lane 6), while only slightly increasing binding to the wild type peptide (lane 4).

These data suggest that the C-terminal and N-terminal domains of syntenin-1 are able to modulate PDZ binding dynamics to the ephrinB2 PDZ binding motif. Furthermore, syntenin-1 binding to the ephrinB2/G peptide might be negatively affected by the presence of other PDZ domain-containing partners of ephrinB2 which compete for the same PDZ binding motif. Taken together, pull down assays demonstrated that phosphorylation of Tyr330 facilitated binding of syntenin-1 to the PDZ binding motif of ephrinB2.

A)

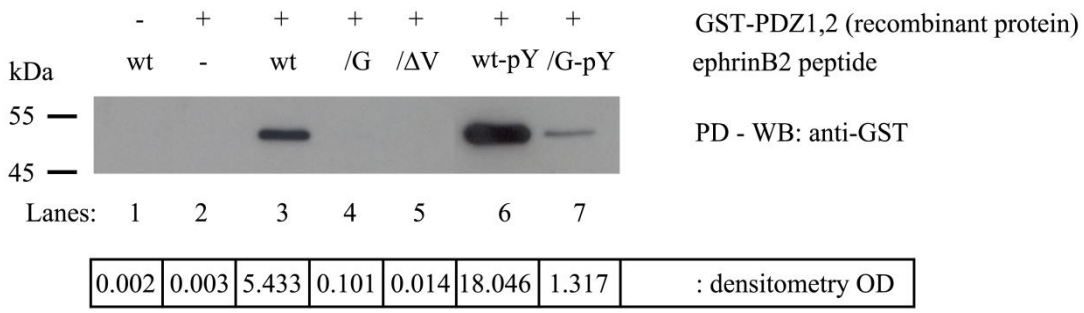

B)

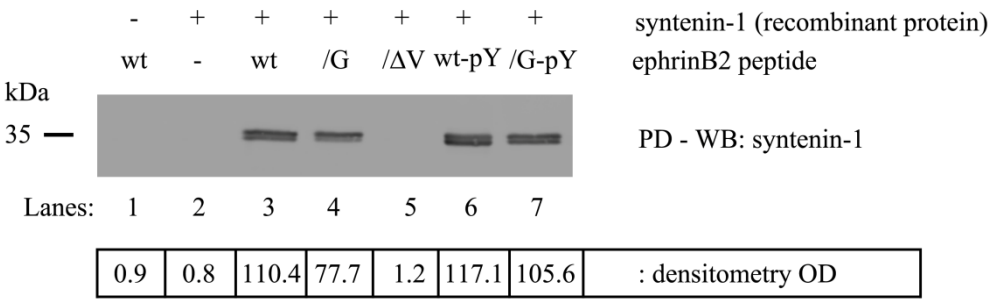

C)

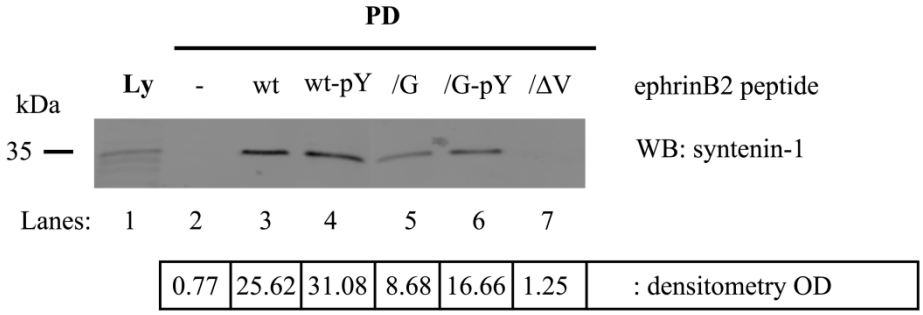

Figure 3.14: phosphorylation of Tyr330 increases binding of recombinant GST-PDZ1,2 and syntenin-1 to ephrinB2 and ephrinB2/G peptides, but not ephrinB2/ΔV.
Pull down assays of recombinant GST-PDZ1,2 (panel **A**), recombinant full-length syntenin-1 (panel **B**) and endogenous syntenin-1 from MCF7 cells (panel **C**) using various ephrinB2 C-terminal peptides. The following peptides were used: ephrinB2 wild type (wt), ephrinB2/G (/G), ephrinB2/ΔV (/ΔV), ephrinB2 wild type and ephrinB2/G with phosphorylated Tyr330 at -3 position (wt-pY and /G-pY respectively). In panels **A** and **B**, equal amounts of recombinant protein were incubated with peptide-conjugated NeutrAvidin agarose beads in 1% TritonX-100 buffer. In panel **C**, the same buffer was used to produce MCF7 cell lysates, which were subsequently incubated with peptide-conjugated NeutrAvidin agarose beads. Pulled-down proteins were eluted from beads and separated on SDS-PAGE. Anti-GST mAb was used to detect recombinant GST-PDZ1,2 (panel A), while anti-syntenin-1 mAb was used to detect full-length recombinant and endogenous syntenin-1 (panels B and C respectively).

3.3.1.2 Label-free interaction analysis of syntenin-1 binding affinity to ephrinB2 and ephrinB2/G peptides

In order to quantify the levels of syntenin-1 binding to non-phosphorylated and phosphorylated peptides, we used a Biacore3000 which measures the protein binding to an immobilized ligand. This system uses chips on which biotin-conjugated peptides can be immobilized. A constant flow of buffer containing the protein of interest is then applied over the chip to analyse binding to the peptide. The increase in molecular weight of bound protein during the association phase is measured by the instrument via Surface Plasmon Resonance (SPR), which is displayed as Response Units (RU). The binding is measured as increased response in the "sensorgram" which increases as the protein interacts with the peptide until it reaches a plateau, saturating the binding sites. At this point, the flow of protein-containing buffer is interrupted and a constant flow of buffer is applied to the chip. Consequentially, the protein starts to dissociate from the peptide during the dissociation phase and the sensorgram displays a decrease in RU. The slope of the sensorgram curve during the association and dissociation phases are indicative of the protein-ligand binding affinity, while the value measured at plateau level represents the relative binding capacity.

We used this approach to analyze the binding of full-length recombinant syntenin-1 to non-phosphorylated and phosphorylated ephrinB2 and ephrinB2/G peptides. Figure 3.15 illustrates the sensorgram representing the binding of syntenin-1 to each peptide. As a negative control, we used the NET5/Tspan9 peptide consisting of the C-terminal 13 amino acids of Tspan9 (FQHIHRTGKKYDA). This peptide is unable to bind PDZ domains and has already been used as a negative control by our group (Latysheva, Muratov et al. 2006). The figure shows that the binding capacity of syntenin-1 to the phosphorylated ephrinB2 peptide

(blue) increased ~20% compared to the non-phosphorylated peptide (red). Interestingly, the binding capacity to the phosphorylated ephrinB2/G peptide (green) compared to the non-phosphorylated peptide (pink) was considerably higher (~90%). Finally, the binding capacity of syntenin-1 to the wild type ephrinB2 peptide (red) was ~140% higher than the ephrinB2/G peptide (pink). With regards to binding affinity, we noticed that syntenin-1 bound to both the ephrinB2 peptides with higher affinity than the ephrinB2/G peptides during the association phase. However, syntenin-1's binding affinity to the non-phosphorylated peptides was lower in the dissociation phase compared to the phosphorylated peptides. For the purpose of this study, we did not measure the Kd (dissociation constant) values of binding affinity and thus these observations are based entirely on the normalization of the response units for all peptides and the comparison of their sensorgrams. This data confirms that syntenin-1's binding capacity to ephrinB2 increases upon Tyr330 phosphorylation. Moreover, this effect is more pronounced in the ephrinB2/G mutant than in the wild type. Interestingly, the binding affinity is higher for the ephrinB2 peptides during the association phase and for phosphorylated peptides in the dissociation phase, suggesting that that the Val to Gly mutation affects peptide association to syntenin-1, while phosphorylation affects dissociation from syntenin-1.

To summarize, these results prove that syntenin-1 binding to ephrinB2 is enhanced upon phosphorylation of Tyr330. This novel discovery has important implications in our study on the role of syntenin-1 in ephrinB2 biology, as it reveals a new mode of interaction between the proteins.

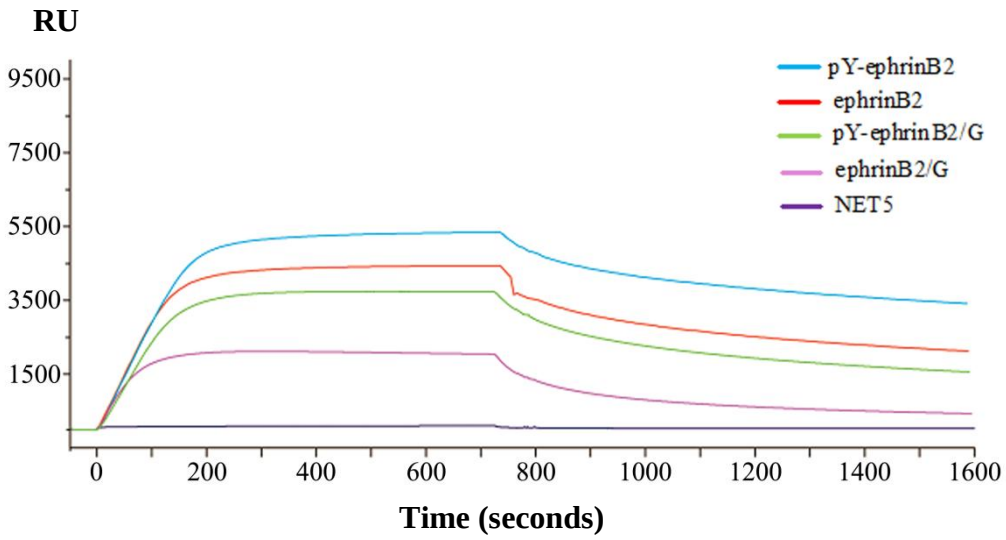

Figure 3.15: phosphorylation at Tyr330 increases syntenin-1 binding capacity to ephrinB2 and ephrinB2/G peptides.
Sensorgrams of recombinant full-length syntenin-1 binding to the phosphorylated and non-phosphorylated ephrinB2 and ephrinB2/G C-terminal peptides assessed by label-free interaction analysis. The experiment was carried out using a Biacore3000. The biotin-conjugated peptides were immobilized on a CM5 sensor chip previously coated with streptavidin. NET5 peptide was used as a negative control. The response units (RU) shown in the graph are indicative of the amount of syntenin-1 binding to the peptides.

3.3.1.3 Phosphorylation of Tyr330 alters ephrinB2 and ephrinB2/G interaction with syntenin-1 as seen by NMR analysis

Having demonstrated that Tyr phosphorylation at position -3 increases binding of syntenin-1 to ephrinB2 wt and ephrinB2/G peptides, we decided to further investigate this interaction in more detail. Through collaboration with Dr Rajesh Sundaresan, we used nuclear magnetic resonance (NMR) experiments to characterise the binding of syntenin-1 PDZ1,2 domains with 8 amino acids long C-terminal phosphorylated and non-phosphorylated peptides of ephrinB2 or ephrinB2/G. The method used was published in the studies by (Latysheva, Muratov et al. 2006) and (Rajesh, Bago et al. 2011) and provides detailed structural information on the role of individual amino acids of syntenin-1 upon peptide binding. The decrease in signal intensity for each aminoacid of syntenin-1 upon interaction with ephrinB2 peptides was calculated and mapped onto the crystal structure of the syntenin-1 PDZ1,2 monomer (1N99.pdb) published by (Kang, Cooper et al. 2003) (see figure 3.16). We used a colour code to represent the calculated values: yellow represents a 50-60% decrease in signal intensity; orange a 60-80% decrease; and red represents more than 80% decrease. The degree of decrease in NMR signal intensity roughly translates into a closer proximity of the relevant aminoacid with the interacting target peptide.

Figure 3.16 illustrates the NMR results mapped onto the crystal structure of syntenin-1 PDZ1,2 for each interaction analysed, including the relevant amino acids of syntenin-1 which interact with the peptide and the percentage of signal decrease measured in NMR. As expected, the ephrinB2 wt peptide engages only syntenin-1 PDZ1,2 amino acids in the PDZ2 domain, as was reported in literature (Lin, Gish et al. 1999; Grembecka, Cierpicki et al. 2006). From the NMR results, the region between amino acids 199-204, 210-220, 251-258 and 265-

268 in the PDZ2 domain are closely engaged in ephrinB2 wt binding. Interestingly, the binding of the phosphorylated form of the ephrinB2 wt peptide extended the contact region in the PDZ2 domain and, in addition, engaged amino acids between positions 125-127 in the PDZ1 domain. These results suggest that phosphorylation of Tyr330 in ephrinB2 increases the avidity of interaction with the PDZ2 domain of syntenin-1 through the recruitment of PDZ1 domain. However, from our NMR data it remains unclear whether the phosphorylated ephrinB2 wt peptide interacts with both PDZ domains on the same syntenin-1 PDZ1,2 monomer or on the neighbouring homo-dimerized syntenin-1 PDZ1,2 molecule (crystal structure of syntenin-1 PDZ1,2 is seen as a homodimer).

The ephrinB2/G peptide engages a notably smaller patch on the PDZ2 domain compared to ephrinB2 wt when interacting with the syntenin-1 PDZ1,2 monomer. In fact, it primarily engages amino acids in a single region between positions 208-216 of the PDZ2 domain of syntenin-1 PDZ1,2, with additional secondary interactions with amino acids in position 235 and 262. Phosphorylation of Tyr at the -3 position of the ephrinB2/G peptide results in the engagement of a wider set of an extended patch within the PDZ2 domain of syntenin-1 PDZ1,2. More specifically, the phospho-ephrinB2/G peptide closely engages amino acids in the region of 199-203, 208-219, 235-239 and 255-256 of the PDZ2 domain of syntenin-1 PDZ1,2, which closely resemble the regions engaged by the ephrinB2 wt peptide. However, amino acids in the PDZ1 domain of syntenin-1 PDZ1,2 were not engaged.

The NMR data corroborates our pull down and label-free interaction analysis data and further demonstrates that phosphorylation of Tyr330 in ephrinB2 increases binding to syntenin-1. Additionally, NMR analysis provided us with the structural insight on how Tyr330 phosphorylation increases ephrinB2 and ephrinB2/G proximity to the PDZ2 domain of syntenin-1 and induces a previously un-reported interaction of ephrinB2 with amino acids

in the PDZ1 domain of syntenin-1. These structural differences support the hypothesis that syntenin-1 might preferentially play a role in ephrinB2 pathways subsequent to ligand phosphorylation.

Syntenin-1 – ephrinB2 wt

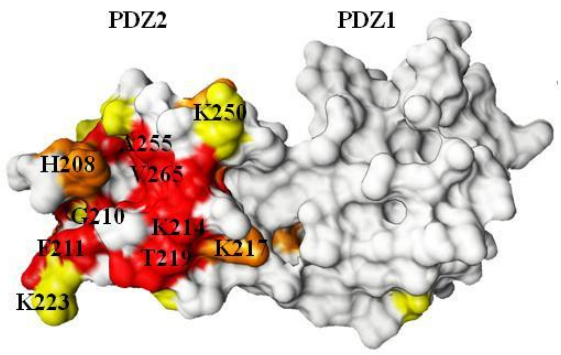

Syntenin-1 – ephrinB2 phospho-wt

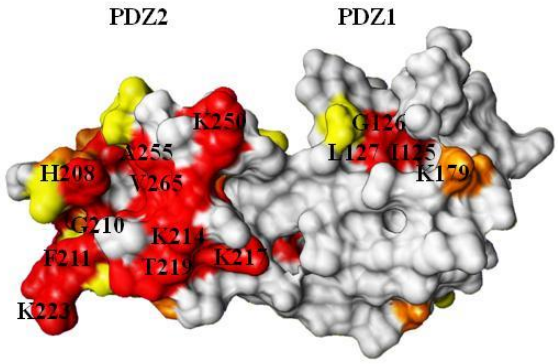

Syntenin-1 – ephrinB2/G

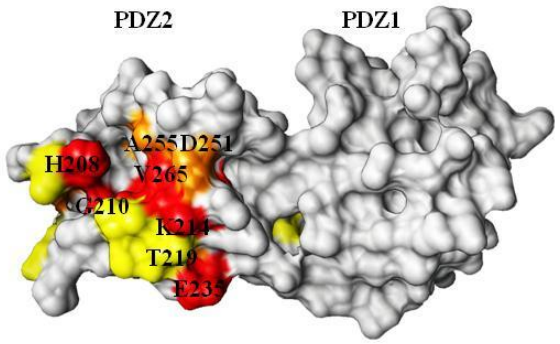

Syntenin-1 – ephrinB2/G phospho

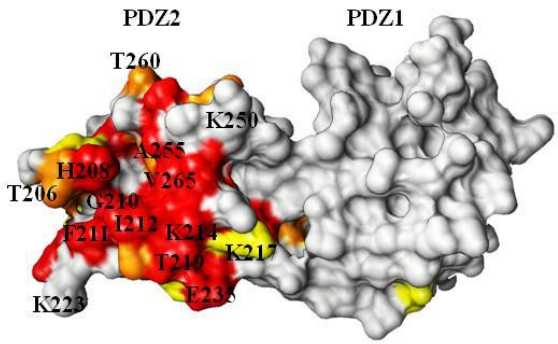

= 50%-60% decrease = 60%-80% decrease = >80% decrease

Figure 3.16: phosphorylation at Tyr330 induces a tighter interaction between ephrinB2, ephrinB2/G peptides and syntenin-1.

Phosphorylation of ephrinB2 wt and ephrinB2/G on Tyr330 alters PDZ-mediated syntenin-1 interaction. The perturbation of syntenin-1 PDZ1,2 NMR signals upon interaction with phosphorylated and non-phosphorylated peptides of ephrinB2 wt or ephrinB2/G, was mapped onto the crystal structure of the syntenin-1 PDZ1,2 (1N99.pdb) monomer resolved by (Kang, Cooper et al. 2003). The decrease in signal intensity for every aminoacid of syntenin-1 PDZ1,2 monomer upon interaction with the peptides was calculated and represented using the following colour code: yellow represents a decrease in signal intensity of 50-60%; orange represents a decrease of 60-80%; and red a decrease of more than 80%. The degree of decrease in signal indicates proximity between the relevant aminoacid of syntenin-1 with the target peptide.

3.3.2 Binding to the phospho-ephrinB2 peptide is enhanced with PAR3 but not PTPL1

As described in the previous paragraphs, we discovered that binding of syntenin-1 to the ephrinB2 wild type and ephrinB2/G peptides increased in the presence of a phospho-tyrosine at position -3. Our data disagrees with the study by (Lin, Gish et al. 1999), which suggested that tyrosine phosphorylation at position -3 did not affect syntenin-1 binding to the ephrinB1 ligand, while phosphorylation at position -2 was inhibitory. The same study also described that PTPL1 binding to ephrinB1 was not affected by phosphorylation of tyrosines within the PDZ binding motif. We decided to perform two more pull down assays using all our peptides on PTPL1 and PAR3, as these two proteins are very relevant to breast cancer.

We transiently transfected MCF7 cells with plasmids encoding flag-tagged PTPL1 or PAR3 and subsequently performed pull down assays using normal and phospho-peptides. As shown in figure 3.17A, PTPL1 binding to the phospho-ephrinB2 peptide (lane 5) remained unchanged when compared to the ephrinB2 peptide (lane 3), while no binding was detected for the phospho-ephrinB2/G peptide (lane 6). These results confirm previously published data by (Lin, Gish et al. 1999). By contrast, PAR3 binding to the phospho-ephrinB2 peptide was greatly enhanced (lane 5) when compared to the ephrinB2 peptide (lane3), while binding to the phospho-ephrinB2/G peptide (lane 6) remained undetectable (figure 3.17B).

These findings prove that PDZ mediated binding to the PDZ binding motif of ephrinB ligands can be influenced by phosphorylation on Tyr330. Moreover, different types of PDZ domains may be variably affected by this phosphorylation event. The fact that the tyrosine at position -3 of ephrinB ligands is the most prominently phosphorylated upon EphB receptor interaction *in vitro* (Kalo, Yu et al. 2001) and *in vivo* (Su, Xu et al. 2004) suggests that it

could function as a regulator for interaction of some of the PDZ domain-containing partners of ephrinB ligands.

A)

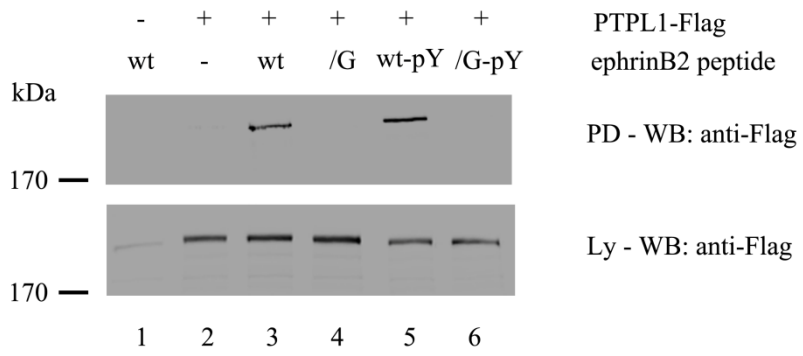

B)

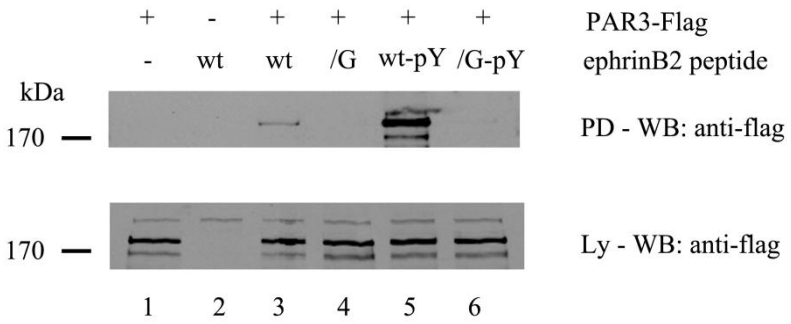

Figure 3.17: phosphorylation at Tyr330 increases binding of the ephrinB2 peptide (but not ephrinB2/G) to PAR3, but not PTPL1.

Binding ability of PTPL1 and PAR3 to various ephrinB2 peptides assessed by pull down assay. The following peptides were used: ephrinB2 wild type (wt), ephrinB2/G (/G), ephrinB2 wild type and ephrinB2/G with phosphorylated Tyr330 at -3 position (wt-pY and /G-pY respectively). MCF7 cells were transiently transfected with PTPL1-Flag (panel **A**) or PAR3-Flag (panel **B**) and lysed in 1% TritonX-100 buffer. Cell lysates were incubated with peptide-conjugated NeutrAvidin agarose beads and pulled-down proteins were resolved on SDS-PAGE. Controls include transfected MCF7 cell lysates incubated with NeutrAvidin agarose beads (lane 1) and non-transfected cells lysates incubated with ephrinB2 peptide-conjugated NeutrAvidin agarose beads (lane 2). PTPL1-Flag (**A**) and PAR3-Flag (**B**) were detected with anti-Flag mAb.

3.3.3 Discussion

It has been previously reported that PDZ-mediated interactions can be modulated by phosphorylation of Ser, Thr or Tyr residues within PDZ binding sequences or in close proximity to them (Ivarsson 2012). Phosphorylation at these sites can increase or decrease the binding affinity with PDZ domain-containing proteins. For example, phosphorylation of Ser411 at -2 position of β2-adrenergic receptors disrupts the interaction with NHERF1 (Cao, Deacon et al. 1999); and phosphorylation of Tyr at position -1 of syndecan-1 impairs syntenin-1 binding (Sulka, Lortat-Jacob et al. 2009). Instead, phosphorylation of Tyr at position -2 and -3 of ephrinB ligands did not affect binding to GRIP proteins (Essmann, Martinez et al. 2008) and FAP1/PTPL1 (Lin, Gish et al. 1999).

A study by (Lin, Gish et al. 1999) reported that phosphorylation of the Tyr residue at -3 position of ephrinB1 did not affect syntenin-1 binding, while phosphorylation of the Tyr at -2 position inhibited binding. However, our data on ephrinB2 – syntenin-1 interaction is in disagreement with this earlier study. By using ephrinB2 and ephrinB2/G phosphorylated C-terminal peptides to pull down recombinant GST-PDZ1,2, recombinant full-length syntenin-1 or cell-derived syntenin-1, we demonstrated that syntenin-1 binding to both ephrinB2 and ephrinB2/G peptides increased upon phosphorylation on Tyr at position -3 (figure 3.14). Furthermore, by comparing binding to GST-PDZ1,2 tandem and the full length protein we established that the NTD and/or CTD of syntenin-1 are able to modulate the interaction with both phosphorylated and non-phosphorylated peptides, as previously reported by other studies (Latysheva, Muratov et al. 2006; Ivarsson 2012). Additionally, competition from other proteins might have caused the lower levels of cell-derived syntenin-1 binding to the ephrinB2/G peptide, when compared to the recombinant full-length protein. These results

were further confirmed by label-free interaction analysis, using the same peptides and full-length recombinant syntenin-1; and NMR analysis, using recombinant syntenin-1 PDZ1,2 monomer and 8-aminoacid-long C-terminal peptides of ephrinB2 and ephrinB2/G phosphorylated and non-phosphorylated on Tyr at position -3. Label-free interaction analysis also proved that binding of syntenin-1 to ephrinB2 and ephrinB2/G peptides are enhanced upon phosphorylation (figure 3.15), while NMR analysis revealed that the phospho group at the -3 position causes a tightening of the interaction between the ephrinB2 PDZ binding motif and the PDZ2 domain of syntenin-1 (figure 3.16). Intriguingly, the phosphorylated ephrinB2 peptide was also able to engage amino acids within the PDZ1 domain of the syntenin-1 PDZ1,2 molecule, suggesting that interaction of syntenin-1 with phosphorylated ephrinB2 involves engagement of both PDZ domains simultaneously. These findings seem to support recent reports which suggest that phosphorylation of Tyr/Thr/Ser residues within the PDZ binding motif of certain proteins is able to modulate PDZ interaction by inducing a switch in preferential binding from one PDZ domain to another (Akiva, Friedlander et al. 2012; Ivarsson 2012). For example, phosphorylation on Ser1542 at position -3 of the Multidrug Resistence Protein (MRP) 2 strongly enhances PDZ-mediated binding to the Intestinal and Kidney Enriched PDZ Protein (IKEPP) and to the ERM (Ezrin/Radixin/Moesin) Binding Phosphoprotein (EBP) 50 in epithelial cells (Hegedus, Sessler et al. 2003). However, rather than a switch in preferential binding, our results suggest that ephrinB2 phosphorylation on Tyr330 enhances binding to the PDZ2 domain of syntenin-1 and additionally engages the PDZ1 domain, thus strengthening the interaction between the two proteins.

The different results obtained by (Lin, Gish et al. 1999), which showed that phosphorylation of Tyr at the -3 position of ephrinB1 does not affect PDZ-mediated binding to syntenin-1, might be explained by the different experimental settings used. In their study,

Lin and colleagues used fluorescence polarization analysis to measure binding of recombinant GST-syntenin-1 to fluorescein-labelled probes containing the phosphorylated or non-phosphorylated 6 C-terminal amino acids of ephrinB ligands. In our study we used 14 amino acids long peptides to measure binding of full length recombinant syntenin-1 by label-free interaction analysis, which is less likely to disturb protein interactions to short peptides. Moreover, our NMR analysis was conducted with non-tagged 8 amino acids long peptides and non-tagged recombinant syntenin-1 PDZ1,2 molecule. Therefore, it is possible that the more "invasive" experimental settings used in the study by Lin and colleagues were responsible for the discrepancy between their data and ours.

Our findings that Tyr330 phosphorylation is able to modulate PDZ-mediated interactions prompted us to investigate whether binding of other PDZ domain-containing partners of ephrinB2 may be affected by this modification. Hence, we used phosphorylated and non-phosphorylated ephrinB2 and ephrinB2/G peptides to pull down PAR3 and PTPL1 (figure 3.17). Intriguingly, we discovered that phosphorylation of Tyr at the -3 position of the ephrinB2 peptide strongly increased PAR3 binding. On the other hand, PTPL1 binding remained unaffected from phosphorylation, thus confirming the data from (Lin, Gish et al. 1999). Moreover, no binding of either PTPL1 or PAR3 to the phosphorylated ephrinB2/G peptide was detected. Increased binding of PAR3 to phosphorylated ephrinB2 (after EphB4-induced ligand phosphorylation) may explain the effects of ephrinB2 over-expression in MCF7 3D cultures (see section 3.1.2.3). Furthermore, these results identify PAR3 as a strong competitor of syntenin-1 in binding to phosphorylated ephrinB2. As previous studies have reported that PAR3 and the PAR3-PAR6-aPKC complex are involved in clathrin-independent recycling and clathrin-dependent endocytosis (Balklava, Pant et al. 2007; Nishimura and Kaibuchi 2007), it is possible that an equilibrium between binding of syntenin-1, PAR3 and

PTPL1 to phosphorylated ephrinB2 modulates the dynamics of reverse signalling termination induced by ligand de-phosphorylation or internalization. However, further study on the different affinity levels of the PDZ domains of these proteins for phosphorylated ephrinB2 would be necessary to determine a hierarchy of interaction.

To summarize, we have discovered that phosphorylation of Tyr330 on ephrinB2 enhances PDZ-mediated binding of syntenin-1. The same phosphorylation also greatly increased ephrinB2 binding to PAR3, while not affecting PTPL1 binding. Taken together, these data suggest that both syntenin-1 and PAR3 preferentially interact with phosphorylated ephrinB2 and might be directly involved in modulating ligand reverse signalling and processing following EphB4-induced phosphorylation.

3.4 EphrinB2 – syntenin-1 interaction may play a role in cell-cell boundary formation

One of the main physiological roles of ephrinB ligands and EphB receptors is the formation of spatial boundaries between different tissues. The gap-closure assay allowed us to analyse how ephrinB2 may contribute to collective cell migration and assess the role of the protein in responses of ephrinB2-expressing cells upon contact with EphB4-expressing cells. In this assay, cells were plated in two small adjacent wells of a silicon chamber glued to the glass bottom of a 35 mm dish. Once the cells had grown to confluency, the chamber was removed, allowing the cells to grow and migrate towards one another and eventually meet. This technique allowed us to analyse the gross migration speed and boundary formation characteristics of two different cell lines. To this end, we plated MCF7 TetOn cells on one side of the dual-well chamber and T47D cells on the other (see section 2.3.5 of materials and methods). We chose T47D cells as they express high levels of EphB4 and do not express any ephrinB ligands.

3.4.1.1 Gap-closure assay control experiment using MCF7 tetracycline inducible cells

Before performing the gap closure assay with T47D cells, we carried out a control experiment in which we plated the same MCF7 tetracycline inducible cells in both sides of the dual-well silicon chamber. We will refer to this type of experiment as homologous gap-closure assay. The next day, cells were stimulated with doxycycline to induce ephrinB2, ephrinB2/G or ephrinB2/ΔV expression and 24 hours later the silicon chamber was removed in order to allow cells to close the gap. By observing gap-closure for all four cell lines in parallel, we assessed whether the mere expression of ephrinB2, ephrinB2/G or ephrinB2/ΔV altered cell migration. Figure 3.18 illustrates the closure of the gap after 1, 3 and 5 days from removing the silicon chamber. The migration for all cell lines was relatively slow. By day 3, all cell lines presented minimal distance between the opposing cell populations, while at day 5 the gap was entirely closed. As expected, we could not observe any distinct boundary between the opposing cell populations, which merged together in a homogenous manner. These results suggested that the expression of ephrinB2, ephrinB2/G or ephrinB2/ΔV did not affect motility of MCF7 TetOn cells.

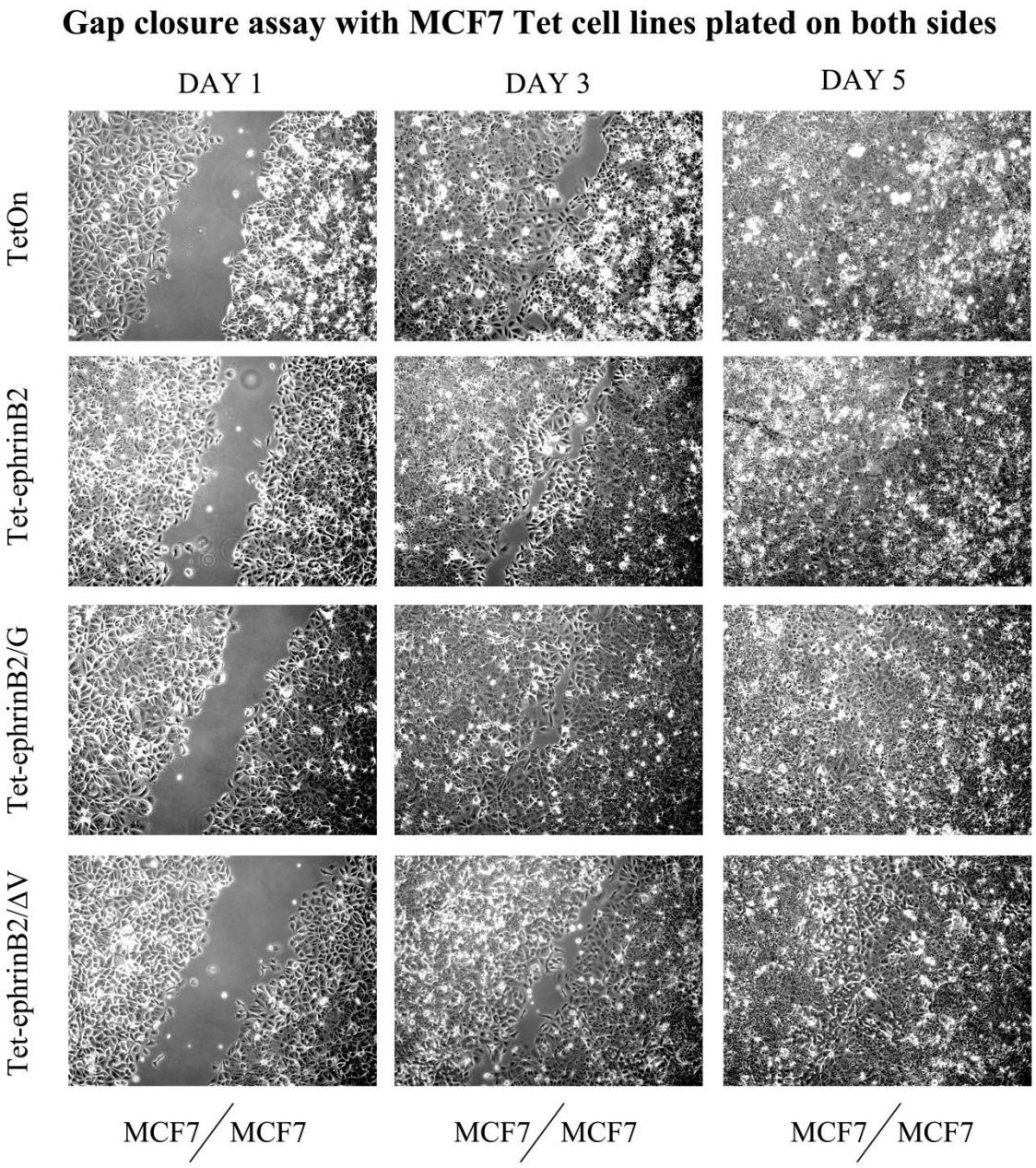

Figure 3.18: ephrinB2, ephrinB2/G or ephrinB2/ΔV expression in tetracycline inducible MCF7 cells does not affect cell motility or induce the formation of boundaries between contacting MCF7 cells.
Gap-closure assay control experiments with MCF7 tetracycline inducible cell lines. The same MCF7 tetracycline inducible cells were plated in both left and right chambers of the gap closure assay 35 mm glass-bottom dish for all four cell lines including MCF7 TetOn parental, MCF7 Tet-ephrinB2, MCF7 Tet-ephrinB2/G and MCF7 Tet-ephrinB2/ΔV cells. The next day, all cells were stimulated with 1 μg/ml doxycycline and 24 hours later, when cells reached confluency, the silicon chamber was removed. Cells were photographed after 1, 3 and 5 days from the removal of the chamber.

3.4.1.2 Gap-closure assay using MCF7 tetracycline inducible cells and T47D cells

In heterologous gap-closure assays, we plated MCF7 tetracycline inducible cells in one well of the silicon chamber and T47D cells in the other and treated cells with doxycycline as explained in the previous section. Figure 3.19A shows photographs at 1, 4 and 8 days after removing the silicon chamber. Similarly to the control experiment, we did not detect considerable differences in migration speed, although the gap was not entirely closed even after 4 days. This effect may be caused by the lower migratory speed of T47D cells compared to MCF7 cells. Upon contact between the two cell populations, a clearly defined and relatively straight boundary was observed in all conditions apart for MCF7 Tet-ephrinB2/ΔV cells. In this case, even after 8 days from removing the silicon chamber, we could not detect the formation of a "boundary line" between MCF7 Tet-ephrinB2/ΔV cells and T47D cells. To examine this phenomenon in more detail, we generated MCF7 tetracycline inducible cells expressing the red fluorescent protein (RFP) and T47D cells expressing the freen fluorescent protein (GFP). This allowed us to distinguish the populations of MCF7 and T47D cells in heterologous gap closure assays and analyse their behaviour upon contacts made between the two opposing cell monolayers. Specifically, we examined the areas of contacts between T47D and MCF7 cell sheets 8 days after the onset of the gap-closure experiment. The photographs shown in figure 3.19B confirm that MCF7 TetOn, MCF7 Tet-ephrinB2 and MCF7 Tet-ephrinB2/G cells form a clearly defined boundary with T47D cells and no cell penetration was detected from either side. By contrast, MCF7 Tet-ephrinB2/ΔV cells did not form a uniform "boundary line" with T47D cells, as invaginations within the sheet of GFP

expressing cells was observed. However, there was no clear indication of single-cell penetration of one cell line in the epithelial sheet of the other.

Taken together, these results suggest that the interaction between ephrinB2 and syntenin-1 may be important for correct boundary formation between ephrinB2 and EphB4 expressing cells. Indeed, MCF7 cells expressing ephrinB2/G, which retains syntenin-1 binding, were able to form a boundary with T47D cells, while ephrinB2/ΔV expressing cells were not. However, as we have previously mentioned in section 3.1.3.1, it is also possible that yet undiscovered PDZ partners of ephrinB2 might be able to retain binding to ephrinB2/G and thus play a role in this context. It is also unclear how MCF7 TetOn cells were able to form a boundary with T47D cells in the absence of ephrinB2 – EphB4 interaction. Possibly, the expression of ephrinB2/ΔV displays a "dominant-negative" activity on boundary formation with EphB expressing cells. Furthermore, the mechanism by which ephrinB2 – syntenin-1 interaction drives boundary formation between ephrinB2 and EphB4 expressing cells remains unknown.

A)

Gap closure assay with MCF7 Tet cell lines (left) and T47D cells (right)

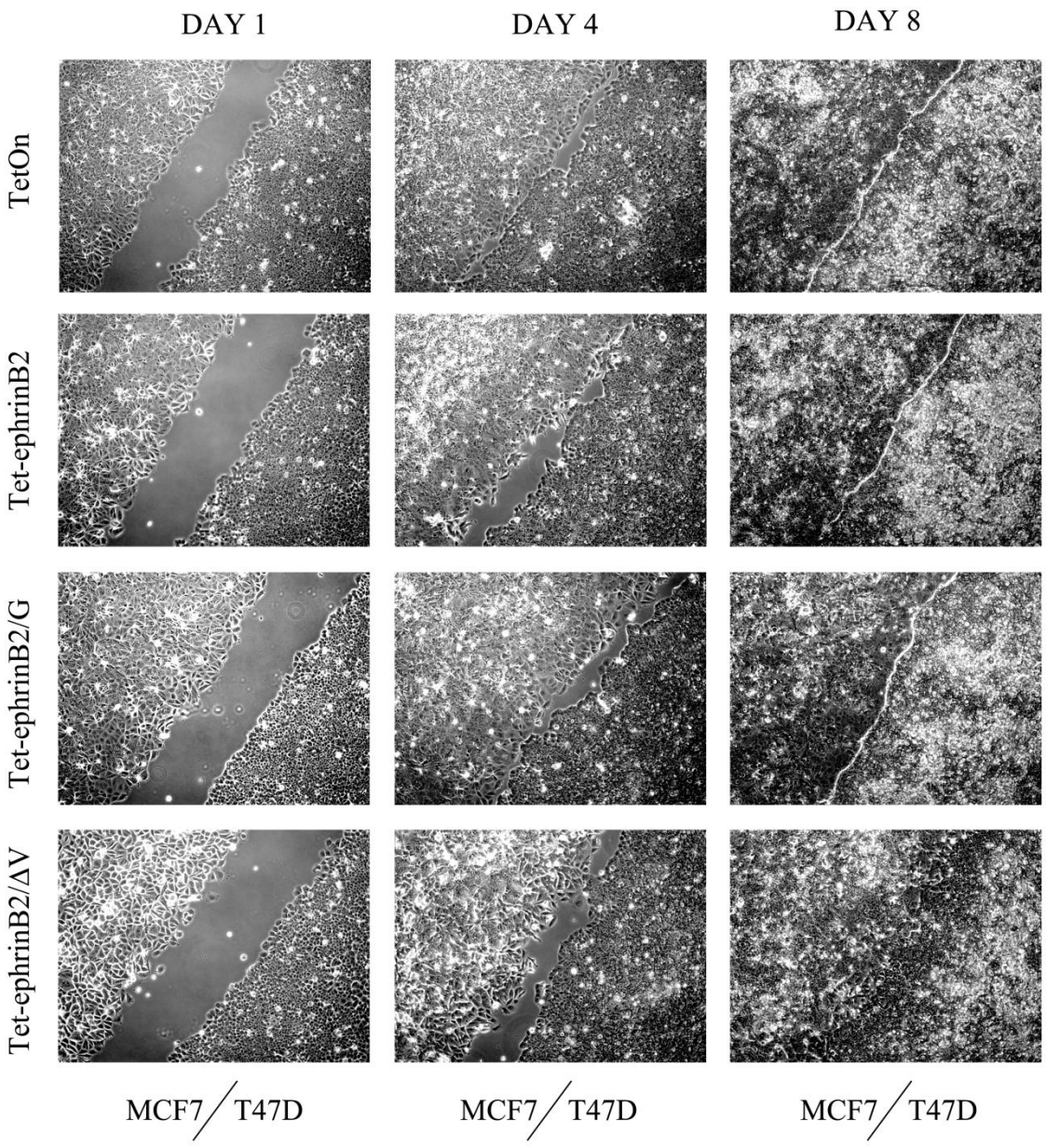

B)

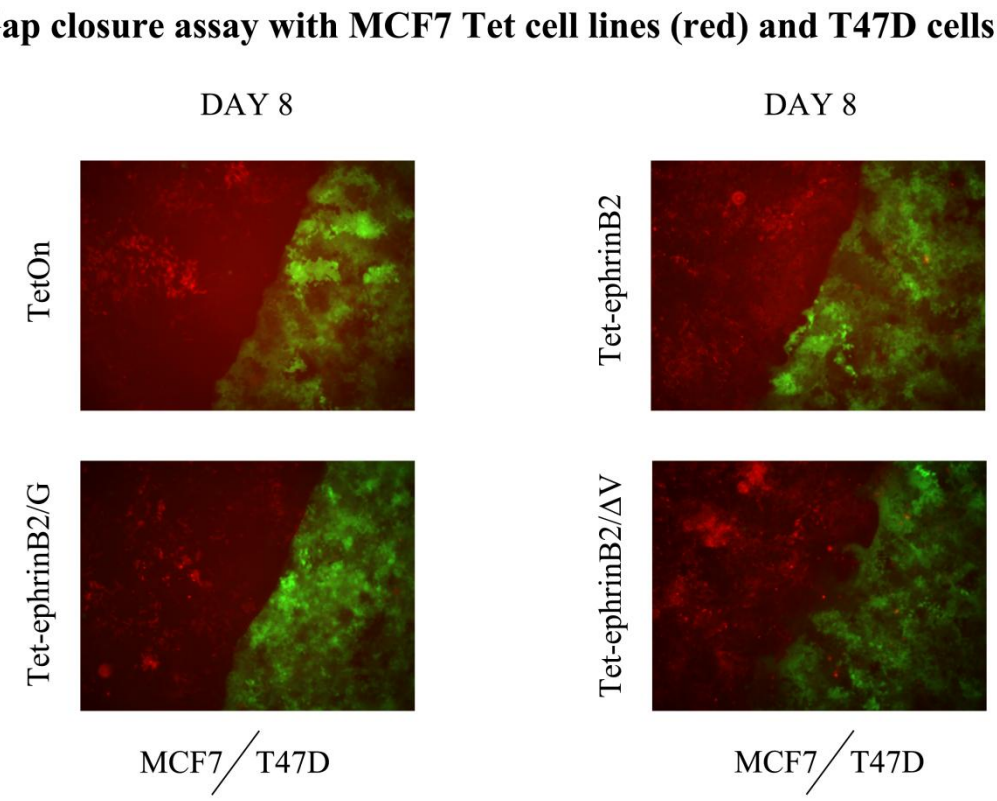

Figure 3.19: tetracycline inducible MCF7 cells form a clear boundary with contacting T47D cells both in the absence and presence of ephrinB2 or ephrinB2/G, while ephrinB2/ΔV-expressing MCF7 cells are unable to form a boundary with T47D cells.

Gap-closure assay with MCF7 tetracycline inducible cell lines and T47D cells. **A**) MCF7 tetracycline inducible cells were plated in the left chamber of the gap-closure assay 35 mm glass-bottom dish, while T47D cells were plated in the right chamber. The next day all cells were stimulated with 1 µg/ml doxycycline and 24 hours later, when cells reached confluency, the silicon chamber was removed. Cells were photographed at an inverted light microscope at 10x magnification after 1, 4 and 8 days from the removal of the chamber. **B**) The same experiment was conducted with MCF7 tetracycline cell lines expressing the Red Fluorescent Protein (RFP) and T47D cells expressing the Green Fluorescent Protein (GFP). At 8 days after the removal of the chamber, cells were photographed under an inverted fluorescence microscope at 10x magnification.

3.4.2 Discussion

The homologous gap-closure assays were conducted to observe the effect of ephrinB2 expression on migration of MCF7 TetOn cells in 2D cultures and to determine whether PDZ-mediated interactions were involved (figure 3.18). We did not observe any differences in the speed at which MCF7 tetracycline inducible cell lines closed the gap and thus concluded that ephrinB2 expression does not promote cell migration in this experimental setting. Eph/ephrin signalling promotes cell motility and migration in physiological and pathological conditions by inducing activation of the Rho family of GTPases (Poliakov, Cotrina et al. 2004; Pasquale 2008; Klein 2012). In the case of ephrinB reverse signalling, STAT3 activation has also been found to induce cell migration (Bong, Lee et al. 2007). Although the main body of evidence suggests that Eph – ephrin interaction is required to induce migration, some studies have also found that ephrinB ligands can promote cell motility independently from EphB stimuli (Bochenek, Dickinson et al. 2010). In this study, Bochenek and colleagues demonstrated that ephrinB2 over-expression induced repeated cycles of cell contraction and spreading in the absence of EphB stimulation in HUVEC cells, but not in NIH3T3 or MDCK cells. Interestingly, they also found that PDZ-RGS3 binding to ephrinB2 is required for this process, confirming a previous report by (Makinen, Adams et al. 2005) which suggested that PDZ-RGS3 is involved in modulating ephrinB2-driven cell migration during remodelling of lymphatic vessels. Therefore, it is possible that we were unable to detect ephrinB2-driven increase in migration of MCF7 TetOn cells due to the missing ephrinB2 – PDZ-RGS3 interaction, which we did not detect in our experimental settings. Moreover, in the previously mentioned studies, ephrinB2 over-expression induced random cell migration of individual cells, which might not be detectable by gap-closure assay. Additionally, it is possible that

MCF7 TetOn cells endogenously express EphA and/or ephrinA proteins, which are also known to induce cell migration (Poliakov, Cotrina et al. 2004). Indeed, a study by (Fox and Kandpal 2004) has found high mRNA levels of various EphA and ephrinA proteins in MCF7 cells, thus suggesting that EphA/ephrinA signalling might also be involved in MCF7 TetOn migration.

One of the main functions of Eph/ephrin signalling involves the formation and maintenance of spatial boundaries between different tissues and cell types. In the breast, Eph/ephrin signalling maintains cell borders between EphB4 expressing myoepithelial cells, which surround ducts and alveoli, and the neighbouring ephrinB2 expressing epithelial luminal cells. During cancer development, epithelial luminal cells gradually gain EphB4 expression while losing ephrinB2 expression. This switch precedes tumour cell migration and metastasis by allowing cells to escape spatial boundary constrictions (Nikolova, Djonov et al. 1998). By using gap-closure assays, we aimed to observe the behaviour of ephrinB2 expressing cells when contacting EphB4 expressing cells (heterologous gap-closure assay) and analyze the effects of disrupting the ephrinB2 – syntenin-1 axis within this setting. We found that MCF7 TetOn, MCF7 Tet-ephrinB2 and MCF7 Tet-ephrinB2/G cells formed a clear and defined boundary upon contact with T47D cells (which express high endogenous levels of EphB4), while MCF7 Tet-ephrinB2/ΔV cells did not (figure 3.19A). Analysis of the area of contact between RFP expressing MCF7 cell lines and GFP expressing T47D cells in heterologous gap-closure assays confirmed these results (figure 3.19B). Additionally, we noticed that MCF7 Tet-ephrinB2/ΔV cells were able to form invaginations within the T47D monolayer, thus displaying a lack of spatial boundary constrictions. However, we could not detect infiltrating cells from either cell line within the opposite monolayer, thus suggesting

that ephrinB2-EphB4 signalling did not cause cells to display an invasive phenotype. These results suggest that syntenin-1 PDZ-mediated interaction with ephrinB2 may be important for boundary formation between ephrinB2 and EphB4 expressing cells. More specifically, the inability of ephrinB2/ΔV to bind syntenin-1 might produce an effect by which MCF7 cells were unable to retract from T47D cells. However, other yet unknown PDZ partners of ephrinB2 which might retain binding to ephrinB2/G but not ephrinB2/ΔV, might also be involved in this process. The fact that MCF7 TetOn parental cells were also able to form a border with contacting T47D cells also suggests that other proteins might be involved in this process. If this were the case, then these proteins would probably be affected by ephrinB2-EphB4 signalling. E-cadherin, for example, is affected by ephrinB/EphB signalling during cell adhesion (Cortina, Palomo-Ponce et al. 2007; Solanas, Cortina et al. 2011). In a recent study by (Fagotto, Rohani et al. 2013), ephrinB2/EphB4 signalling between the EphB4 expressing presomitic mesoderm and the ephrinB2 expressing notochord in *Xenopus laevis* embryos disrupted E-cadherin clustering at sites of heterotypic cell contacts, thus inhibiting cell adhesion and inducing segregation between the two cell populations. Interestingly, earlier studies had reported that EphB3 activation induces E-cadherin-mediated cell adhesion between homotypic cell populations (Cortina, Palomo-Ponce et al. 2007). Hence, ephrinB/EphB signalling is able to modulate cell adhesion between homotypic cells and segregation between heterotypic cells by regulating E-cadherin localization and clustering. Considering our gap-closure assay data, it is possible that syntenin-1 interaction with ephrinB2 is required during ephrinB2/EphB4 signalling to inhibit E-cadherin clustering at sites of heterotypic cell contacts. The lack of cell intermingling between MCF7 Tet-ephrinB2/ΔV and T47D cells suggests that a certain level of cell segregation is maintained, albeit in the absence of a proper boundary between the two cell populations. Indeed, recent

studies have suggested that EphB forward signalling alone is sufficient to maintain a certain level of cell segregation between heterotypic cell populations (Rohani, Canty et al. 2011), although previous studies have reported that both ephrinB reverse signalling and EphB forward signalling are required during this process (Mellitzer, Xu et al. 1999; Xu, Mellitzer et al. 2000). However, to determine whether EphB forward signalling is sufficient to drive cell segregation, these early studies used truncated versions of ephrinB ligands lacking the whole cytoplasmic domain, which were later found to be unviable as they were not expressed on the cell surface (Makinen, Adams et al. 2005). Therefore, syntenin-1 might play an important role during cell segregation and border formation induced by ephrinB2/EphB4 signalling.

The effect of ephrinB2/ΔV over-expression on boundary formation between MCF7 TetOn and T47D cells might also be explained by a "dominant-negative" effect exerted by the mutant. The fact that MCF7 TetOn cells are able to form a boundary in heterologous gap closure assays suggests that these cells express other membrane proteins capable of inducing boundary formation. EphA and ephrinA proteins, for example, are expressed in MCF7 cells (Fox and Kandpal 2004) and have been shown to trigger cell repulsion between contacting cells (Astin, Batson et al. 2010). Moreover, the study by (Astin, Batson et al. 2010) describes a model in which EphA2 and EphA4 activation by ephrinAs halts migration of PC3 cells at homotypic contacts, while ephrinB2/EphB4 signalling increases cell migration at heterotypic contacts with fibroblasts. However, the same group had previously found that ephrinB2/EphB4 signalling produced cell repulsion (Marston, Dickinson et al. 2003). Therefore, concomitant EphA/ephrinA and EphB/ephrinB signalling might produce similar or opposite effects at heterotypic contacts. In our heterologous gap closure assays, it is possible that EphA/ephrinA signalling might be responsible for boundary formation between MCF7 TetOn and T47D cells. EphrinB2/EphB4 signalling might also produce the same effect in

ephrinB2 and ephrinB2/G expressing cells. However, ephrinB2/ΔV might have exerted a "dominant-negative" effect on boundary formation by promoting EphB4 forward signalling in T47D cells and being unable to trigger PDZ-dependent reverse signalling. Intriguingly, syntenin-1 is likely to play a role in this type of reverse signalling, as the ephrinB2/G mutant did not induce this phenotype.

To conclude, we report that gap-closure assays might prove to be a viable tool for the study of ephrinB2/EphB4-induced boundary formation between contacting heterologous cell populations. Furthermore, we discovered that the ephrinB2 – sytenin-1 axis might play an important role in the process of boundary formation between ephrinB2 and EphB4 expressing cells.

4 General discussion and future work

The aim of our study was to determine the role of PDZ domain-containing proteins in modulating ephrinB2 signalling and trafficking pathways in the context of epithelial breast cancer cells, with a specific focus on the scaffolding protein syntenin-1. We also endeavoured to determine whether the ephrinB2 – syntenin-1 axis affects breast cancer tumourigenesis. Our findings demonstrate, for the first time, that syntenin-1 modulates ephrinB2 internalization upon ligand stimulation and that this affects reverse signalling. Furthermore, we found that EphB4-induced ephrinB2 phosphorylation increases ligand binding to syntenin-1 and PAR3, a component of the PAR polarity complex. Finally, we report that ephrinB2 drives MCF7 colony growth in 3D cultures and that syntenin-1 is involved in boundary formation between ephrinB2 expressing cells and EphB4 expressing cells. These findings describe, for the first time, the role of syntenin-1 in ephrinB2 reverse signalling and the functional relevance of the ephrinB2 – syntenin-1 axis in epithelial breast cancer pathways. They also warrant further study to uncover the specific molecular mechanisms underlying ephrinB2 biological pathways.

Our initial screening of endogenous levels of ephrinB ligands, EphB4 and syntenin-1 in a panel of 21 breast cancer cell lines uncovered a wide range of expression patterns (figure 3.1). As these proteins have been identified as independent prognostic factors in many epithelial tumours (Brantley-Sieders 2012; Yang, Hong et al. 2013), further analysis of their protein levels in breast cancer might uncover expression patterns which correlate with stage and grade of the tumour. Screening for co-expression of ErbB2 (HER-2) together with ephrinB ligands, EphB receptors and syntenin-1 might also help to better characterize breast

cancer types and behaviours, as ephrinB1, ErbB2 and syntenin-1 have all been implicated in driving cell proliferation and/or migration through Src-mediated activation of integrins (Meyer, Hafner et al. 2005; Guo, Pylayeva et al. 2006; Hwangbo, Kim et al. 2010). A recent study by (Vermeer, Colbert et al. 2013) has also found that ephrinB1 associates with ErbB1 and ErbB2 through transmembrane domain interactions. These associations induce ephrinB1 phosphorylation and trigger ERK1/2 activation, thus promoting cell proliferation and survival. Furthermore, treatment of HNSCC cells co-expressing ephrinB1 and ErbB2 or ErbB1 with monoclonal antibodies Herceptin and Certuzimab, which are used in the treatment of HER-2 and HER-1 positive cancers, did not inhibit ERK1/2 phosphorylation, thus suggesting that blockage of ErbB receptors does not prevent signalling through the ErbB-ephrinB1 complex. Therefore, further analysis on the effect of ErbB inhibitors (e.g. Herceptin, Lapatinib, Certuzimab) on breast cancer cell lines which co-express ErbB receptors and ephrinB ligands might reveal new pathways involved in tumour resistance to anti-HER therapies.

By generating the ephrinB2/G and ephrinB2/ΔV mutants and using them to establish tetracycline inducible MCF7 cell lines, we developed a new and innovative model system in which to study the effects of disrupting the ephrinB2 – syntenin-1 axis. Our data on ephrinB2 phosphorylation dynamics revealed that mutations in the PDZ binding motif impair receptor-induced ligand phosphorylation (figure 3.10). This novel finding denotes the existence of a direct link between SH2 and PDZ mediated reverse signalling. As we were unable to detect any interaction between ephrinB2 and PICK1 or Dishevelled-2 via pull down assay; and between ephrinB2 and PDZ-RGS3 via co-immunoprecipitation; and given that PTPL1 is involved in ligand de-phosphorylation (Palmer, Zimmer et al. 2002), we suggest that GRIP1, GRIP2 or PAR3 might be required for receptor-induced ligand phosphorylation. Further

studies using knock down approaches or PDZ-binding mutants in the context of EphB-induced ligand phosphorylation might help identify the PDZ domain-containing protein/s involved in receptor-induced phosphorylation of ephrinB ligands. These findings would reveal new connections between SH2- and PDZ-mediated reverse signalling which would have major implications in the field of EphB/ephrinB biology. Alternatively, other proteins capable of PDZ-dependent or -independent binding to the cytoplasmic tail of ephrinB ligands might also be involved in EphB-driven ligand phosphorylation. In this respect, the use of mass spectrometry to identify new proteins which are co-immunoprecipitated by ephrinB ligands subjected to increasing intervals of EphB receptors stimulation would prove useful.

Although syntenin-1 is not involved in EphB-induced ligand phosphorylation, we observed that it affects basal phosphorylation of ephrinB2 in non-stimulated conditions (3.11). Therefore, syntenin-1 might mediate ligand phosphorylation induced by cross-talk with other tyrosine kinase receptors (e.g. FGFR, ErbB2) and/or adhesion molecules (e.g. claudin-4). Alternatively, syntenin-1 might mediate ephrinB-induced phosphorylation of other cell membrane receptors. In a recent study, syntenin-1 was found to interact with the EGF receptor in a PDZ-independent manner and to induce EGFR phosphorylation through Src-activation (Dasgupta, Menezes et al. 2013). Therefore, syntenin-1 might be able to link ephrinB ligands with EGFRs, resulting in receptor phosphorylation by ephrinB-induced Src activity. This possibility is supported by various studies which describe the role of syntenin-1 in forming FAK-Src signalling complexes at sites of focal adhesion (Hwangbo, Kim et al. 2010; Hwangbo, Park et al. 2011). Furthermore, syntenin-1 might be involved in regulating ephrinB2 compartmentalization into specific membrane microdomains, possibly through the interaction with tetraspanins CD63 (Latysheva, Muratov et al. 2006) or Tspan6 (unpublished). In this respect, tetraspanins are known to selectively recruit signalling molecules (e.g. β1-

integrins, PKC, PI4K) in specific Tetraspanin Enriched Microdomains (TERMs), placing them in close proximity with other cell membrane receptors (e.g. FGFR, EGFR, ErbB2) (Yunta and Lazo 2003; Hemler 2005; Lazo 2007; Zoller 2009). Indeed, ephrinB1 association with ErbB receptors 1 and 2 (Vermeer, Colbert et al. 2013) would benefit from ephrinB recruitment to TERMs. Further study might reveal whether ephrinB reverse signalling can be modulated by syntenin-1-mediated compartmentalization in TERMs. Co-localization experiments in the context of disrupted ephrinB – syntenin-1 interaction might provide novel insight on the role of syntenin-1 in driving the formation of ephrinB signalling complexes in specific membrane microdomains.

In this study we have proven that phosphorylation of Tyr330 in ephrinB2 increases PDZ-mediated binding of syntenin-1 and PAR3. Our data supports recent reports suggesting that phosphorylation of Tyr/Thr/Ser within the PDZ binding motif can either increase or decrease binding to various PDZ domain-containing proteins (Akiva, Friedlander et al. 2012; Ivarsson 2012). More importantly, these findings strongly suggest that EphB-induced phosphorylation of ephrinB ligands modulates PDZ mediated signalling by affecting the binding properties of certain PDZ domain-containing proteins, such as syntenin-1 and PAR3. However, further study is warranted to establish how phosphorylation-induced binding of these proteins affects ephrinB reverse signalling. In this respect, it would be useful to determine the hierarchy of binding affinity between phosphorylated and non-phosphorylated ephrinB ligands and their PDZ domain-containing partners. Label-free interaction analysis and similar methods might prove useful in reaching this purpose. Additionally, quantitative phospho-proteomics analysis by SILAC mass spectrometry would allow us to better understand which sites of ephrinB ligands are phosphorylated and to what extent, in response

to different stimulating partners (e.g. EphB, FGF, ErbB and VEGF receptors). Such studies would shed light on which ephrinB reverse signalling pathways are triggered in response to specific stimulating or PDZ-interacting proteins.

Previous studies have reported that ephrinB ligands recruit GRIP proteins to lipid rafts via PDZ-mediated interactions (Bruckner, Pablo Labrador et al. 1999). Furthermore, EphB2-induced phosphorylation of ephrinB2 on Ser325 enhances binding of GRIP1 and GRIP2 (Essmann, Martinez et al. 2008). Intriguingly, a recent study has found that EphB-induced phosphorylation of ephrinB1 causes ligand relocation to lipid rafts in a manner specifically dependent on phospho-Tyr (Xu, Sun et al. 2011). Therefore, we can speculate that PDZ domain-containing proteins which show increased binding to phosphorylated ephrinB ligands (ie syntenin-1, PAR3, GRIP1, GRIP2) might be recruited to specific lipid rafts or membrane microdomains (e.g. TERMs through binding with syntenin-1) upon EphB stimulation. Further study aimed at proving the veracity of this proposed recruitment mechanism might uncover new characteristics of ephrinB reverse signalling. Specifically, it might shed light on ephrinB signalling at sites of focal adhesions (Kullander and Klein 2002; Segura, Essmann et al. 2007), tight junctions (Tanaka, Kamata et al. 2005; Lee, Nishanian et al. 2008) and synapses formation (McClelland, Sheffler-Collins et al. 2009; Xu, Sun et al. 2011).

In our study, we found that syntenin-1 seems to prevent ephrinB2 internalization preferentially upon EphB4/Fc stimulation (figure 3.13). The increase in syntenin-1 binding to phosphorylated ephrinB2 further supports these data. Our findings fit well with previous reports on the role of syntenin-1 in preventing Delta1 internalization from the cell surface (Estrach, Legg et al. 2007) and impairing CD63 endocytosis (Latysheva, Muratov et al. 2006). More specifically, Latysheva and colleagues suggested that syntenin-1 induces a switch in

CD63 endocytosis from the fast clathrin-dependent pathway to a slower non-canonical pathway. This mechanism might also apply to ephrinB ligands internalization upon EphB-induced phosphorylation.

Complete disruption of the PDZ binding motif also impairs internalization, thus supporting the existence of a yet unidentified protein capable of inducing ephrinB2 internalization in the absence of PDZ-mediated interactions. In this study we have discussed the possibility that AP2, PAR6, and Grb4 might be involved in ephrinB2 internalization by binding to the cytoplasmic tail of the ligand in a PDZ-independent manner. Furthermore, our results on PAR3 binding to ephrinB proteins phosphorylated on Tyr330, together with the recent study implicating PAR3 in ephrinB2-induced internalization of VEGFR2 and VEGFR3 (Nakayama, Nakayama et al. 2013), strongly suggest that PAR3 might induce ephrinB internalization upon EphB-induced ligand phosphorylation. Therefore, ephrinB internalization might involve more endocytic pathways than was previously thought (Marston, Dickinson et al. 2003; Zimmer, Palmer et al. 2003; Parker, Roberts et al. 2004; Groeger and Nobes 2007). Importantly, we also suggest that certain internalization pathways (e.g. involving syntenin-1, PAR3 and Grb4) might be triggered preferentially upon EphB-induced phosphorylation of ephrinB ligands. Further research on ephrinB internalization mechanisms might uncover specific roles for individual endocytosis pathways which might induce different effects in ephrinB reverse signalling. Importantly, future studies should focus on determining ephrinB endocytosis in the context of cell-cell contact between ephrinB and EphB expressing cells, as previous studies have shown that both EphB forward and ephrinB reverse signalling pathways are involved in this process (Marston, Dickinson et al. 2003; Zimmer, Palmer et al. 2003).

Our data on 3D cultures suggests that low expression levels of ephrinB2 in MCF7 cells are sufficient to drive colony growth in 3D Matrigel in a manner which seems independent of reverse signalling (figure 3.8). Intriguingly, we also found that ephrinB2 expression does not affect MCF7 colony growth in 3D collagen I (figure 3.4). Therefore, we have speculated on the possibility that ephrinB2-driven colony growth might require the presence of biological components found in Matrigel and not in collagen (e.g. laminin-1, growth factors). An interesting possibility which warrants further study is the potential role of ephrinB2 in modulating α6β4-integrin activity upon interaction with laminin-1 through Src activation. In this respect, a similar regulatory mechanism has already been reported for ErbB2 (Guo, Pylayeva et al. 2006). As ephrinB ligands have already been implicated in β1-integrin activity (Meyer, Hafner et al. 2005; Julich, Mould et al. 2009), it is possible that ephrinB proteins might also associate with β4-integrins and modulate laminin-1-driven cell migration.

In culturing cells in 3D Matrigel, we also found that MCF7 TetOn cells form much smaller colonies than MCF7 cells used to generate the stable MCF7-ephrinB2 cell line. Moreover, ephrinB2 expression in tetracycline inducible cells did not alter colony morphology as seen in MCF7-ephrinB2 colonies. Although we did not investigate this effect any further, we speculated on the possibility that MCF7 TetOn cells develop smaller colonies in 3D cultures because they express lower levels of integrins. Intriguingly, both syntenin-1 and ephrinB ligands induce cell migration through association with β1-integrins (Meyer, Hafner et al. 2005; Hwangbo, Kim et al. 2010; Pasquale 2010; Yang, Hong et al. 2013) and induce Src and FAK activation (Cowan and Henkemeyer 2001; Segura, Essmann et al. 2007; Sarkar, Boukerche et al. 2008; Hwangbo, Kim et al. 2010). Therefore, further study might reveal a link between syntenin-1 and ephrinB pathways in modulating Src and FAK activation in the context of β1-integrin activity at sites of focal adhesion.

Another interesting characteristic of MCF7-ephrinB2 colonies grown in 3D Matrigel is the presence of a wide internal lumen (figure 3.4E), which is not found in typical MCF7 colonies (Kirshner, Chen et al. 2003; Krause, Maffini et al. 2010; Wang, Lacoche et al. 2013). Therefore, we discussed the possibility that ephrinB2 expression might restore a certain level of cell polarity in 3D Matrigel-grown MCF7 colonies through the interaction with PAR3. Our pull down data on PAR3 binding to phosphorylated ephrinB ligands and recent studies on the role of ephrinB2 in maintaining cell polarity (Kaenel, Antonijevic et al. 2012), suggest that ephrinB2 might be involved in maintaining epithelial cell polarity by recruiting PAR3 at sites of ephrinB2 – EphB4 interaction. Furthermore, given the role of ErbB2 in disrupting cell polarization by associating with PAR6 (Aranda, Haire et al. 2006) and the ability of ephrinB1 to interact with ErbB2 (Vermeer, Colbert et al. 2013), it is possible that ephrinB ligands and ErbB receptors are tightly involved in modulating cell polarity through the PAR polarity complex. Further study using knock down and interaction-deficient mutants in 3D Matrigel cell cultures might prove useful in understanding the role of ephrinB ligands in maintaining cell polarity.

In our heterologous gap closure assays with ephrinB2 and EphB4 expressing cells we found that syntenin-1 interaction with ephrinB2 might be required for boundary formation between the two cell populations (figure 3.19). In this respect, various studies have found that ephrinB2/EphB4 signalling drives boundary formation at heterotypic contacts by modulating E-cadherin clustering (Fagotto, Rohani et al. 2013) or extracellular cleavage (Solanas, Cortina et al. 2011). Therefore, we have speculated on the possibility that the ephrinB2 – syntenin-1 axis might be responsible for inhibiting E-cadherin clustering on the cell membrane or for ADAM10-mediated cleavage of E-cadherin. Future work involving the use of MMP

inhibitors and immunofluorescence following gap-closure experiments in the context of disrupted ephrinB2 – syntenin-1 axis, might determine the veracity of this assumption and the molecular mechanisms involved. Alternatively, we have speculated on the possibility that ephrinA ligands and EphA receptors might be responsible for boundary formation between MCF7 TetOn and T47D cells, as the MCF7 cell line has been found to produce high mRNA levels of ephrinA and EphA proteins (Fox and Kandpal 2004). Hence, we have suggested that ephrinB2/EphB4 signalling might be inducing a similar effect to that of ephrinA/EphA signalling in boundary formation at heterotypic contacts. Moreover, ephrinB2/ΔV expression might be disrupting boundary formation through a "dominant-negative" effect by activating EphB forward signalling in T47D cells and at the same time being unable to induce syntenin-1-mediated reverse signalling in MCF7 TetOn cells. However, further study is needed to assess the validity of this hypothesis. The use of selective knock down of ephrin and Eph proteins in the context of boundary formation might reveal specific roles for ephrinA/EphA and ephrinB/EphB signalling, as has been suggested in the study by (Astin, Batson et al. 2010). Additionally, PDZ binding mutants (such as the ephrinB2/G and ephrinB2/ΔV mutants used in our study) and the use of EphB forward signalling inhibitors might shed light on the role of syntenin-1-driven reverse signalling in boundary formation.

To conclude, our study has provided insight into the role of syntenin-1 in modulating ephrinB2 reverse signalling and trafficking. Furthermore, we have discovered new properties of syntenin-1 and PAR3 binding to ephrinB ligands that point to the existence of unreported links between EphB-induced ligand phosphorylation and PDZ-mediated reverse signalling. Our data also supports the existence of alternative trafficking pathways involved in ephrinB internalization that might be diversely triggered depending on the ligand's phosphorylation status, as summarised in figure 3.20. Lastly, we have proven that Matrigel 3D cultures and

gap closure assays are viable tools to study the role of ephrinB2 in breast cancer progression, opening the possibility of further research on the role of ephrinB ligands in cancer progression.

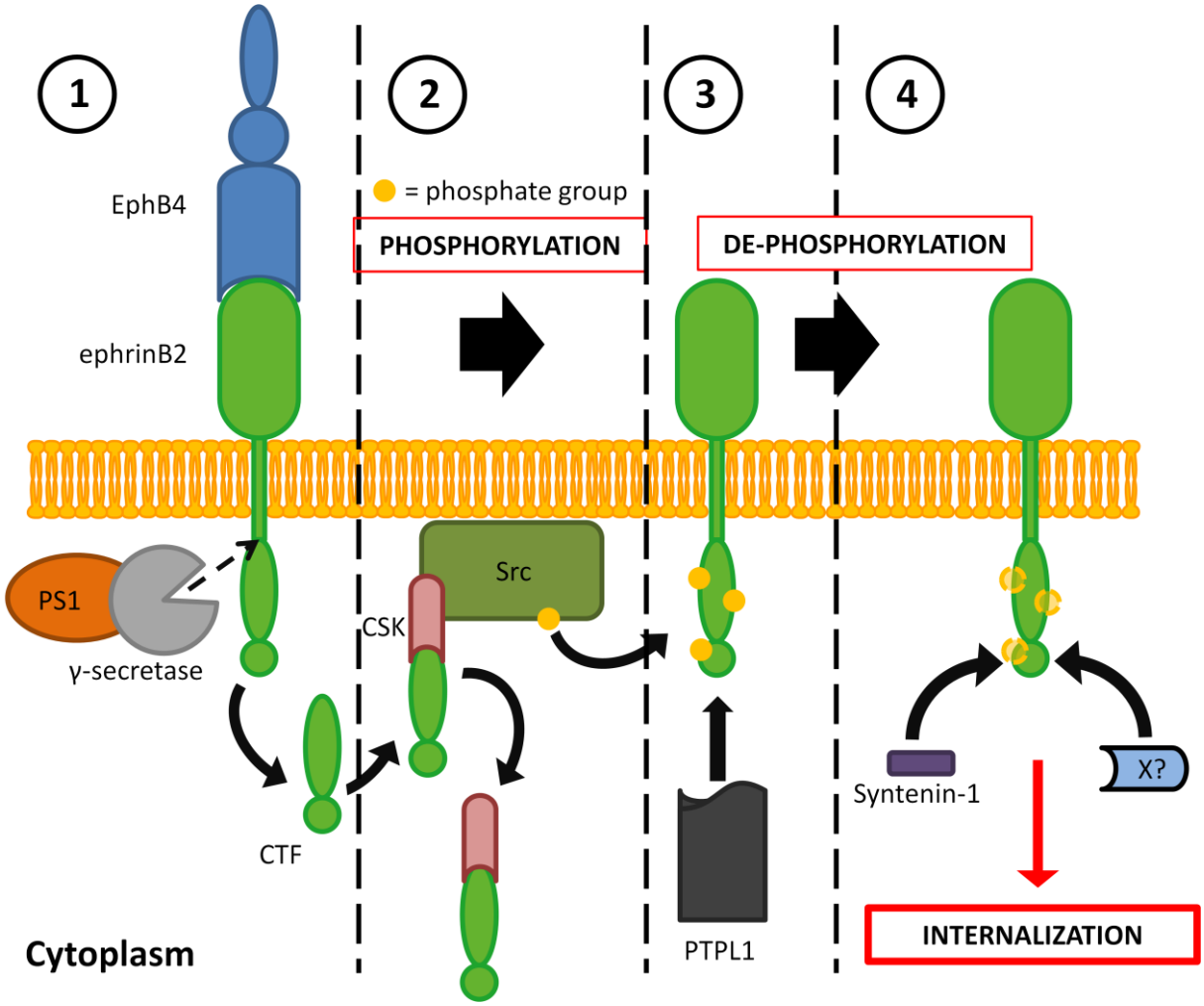

Figure 3.20: proposed role of syntenin-1 in EphB4-induced ephrinB2 internalization.
Upon interaction with the EphB4 receptor, the C-terminal tail of the ephrinB2 ligand is cleaved by the γ-secretase/PS1 complex to release a C-terminal fragment (CTF) (**1**). The CTF mediates CSK inactivation, which in turn leads to Src activation (**2**). Activated Src directly phosphorylates ephrinB2 ligands, which have not made contact with EphB4, on tyrosines 311,316 and 330. Phosphate groups are later removed by PTPL1, which binds to ephrinB2 via PDZ-mediated interaction (**3**). In this study, we hypothesize that PTPL1, syntenin-1 and a yet unidentified protein compete for the PDZ binding motif (or the C-terminus region) of phosphorylated ephrinB2 (**4**). Our model suggests that de-phosphorylation of ephrinB2 by PTPL1 is hindered by syntenin-1 binding to the ligand, which is increased upon phosphorylation of Tyr330. Prolonged ephrinB2 phosphorylation would ultimately cause ligand internalization via the interaction with a yet unidentified protein in order to terminate phospho-dependent reverse signalling.

Appendix

5.1 Appendix 1: cell culture medium and supplements

MCF7: DMEM
10% heat inactivated FCS
50 U/ml Penicillin / 50 µg/ml Streptomycin
± 1 µg/ml Puromycin

MCF7 TetOn: DMEM
10% heat inactivated FCS (tetracycline free)
50 U/ml Penicillin / 50 µg/ml Streptomycin
100 µg/ml Geneticin
± 100 µg/ml Zeocin
± 1 µg/ml Puromycin

HEK293T: DMEM
10% heat inactivated FCS
50 U/ml Penicillin / 50 µg/ml Streptomycin

T47D: RPMI 1640
10% heat inactivated FCS
50 U/ml Penicillin / 50 µg/ml Streptomycin

5.2 Appendix 2: list of primers, shRNA and peptide sequences

Primers:

Name	Sequence (5' to 3')
EphrinB2/PstI (forward)	5' – GTGAGCCTGCAGTCATGGCTGTGAGAA GGGACTCC – 3'
EphrinB2/SalI (reverse)	5' – GTGAGCGTCGACTCTCAGACCTTGTAGTA AATGTTCG – 3'
pBI MCS2 (forward)	5' – GGTTTGTCCAAACTCATCAATG – 3'
EphrinB2 internal (forward)	5' – TCTTGGTCTGGTTTGGCACAG – 3'
EphrinB2/ΔV mutagenesis (forward)	5'– GCGAACATTTACTACAAGTAGTGAGAGTCGACC TAGTCTAG – 3'
EphrinB2/ΔV mutagenesis (reverse)	5'– CTAGACTAGGTCGACTCTCACTACTTGTAGTAA ATGTTCGC – 3'
EphrinB2/G mutagenesis (forward)	5'– GCGAACATTTACTACAAGGGCTGAGAGTCGACC TAGTCTAG – 3'
EphrinB2/G mutagenesis (reverse)	5' – CTAGACTAGGTCGACTCTCAGCCCTTGTAGTAA ATGTTCGC – 3'

ShRNA sequences targeting syntenin-1 (purchased by Sigma):

Name	Product number	Sequence (5' to 3')
shRNA (1)	TRC0000029158	5' – CCGGCGGAACATAACATCTGTGAAACTCGAGTTTCA CAGATGTTATGTTCCGTTTTT – 3'
shRNA (2)	TRC0000029157	5' – CCGGGTACTTCAGATCAATGGTGAACTCGAGTTCACC ATTGATCTGAAGTACTTTTT – 3'
shRNA (3)	TRC0000029156	5' – CCGGGCAGAAATTAAGCAAGGGATTCTCGAGAATCC CTTGCTTAATTTCTGCTTTTT – 3'
shRNA (4)	TRC0000029154	5' – CCGGCCTATCCCTCACGATGGAAATCTCGAGATTTCC ATCGTGAGGGATAGGTTTTT – 3'
shRNA (5)	TRC0000029155	5' – CCGGGAGAAGATTACCATGACCATTCTCGAGAATGG TCATGGTAATCTTCTCTTTTT – 3'

Peptides:

Name	Sequence (N-terminus to C-terminus)
EphrinB2	biotin – EMPPQSPANIYYKV
EphrinB2/G	biotin – EMPPQSPANIYYKG
EphrinB2/ΔV	biotin – EMPPQSPANIYYK
Phospho-ephrinB2 (pTyr330)	biotin – EMPPQSPANI(pY)YKV
Phospho-ephrinB2/G (pTyr330)	biotin – EMPPQSPANI(pY)YKG
NET5	biotin – FQHIHRTGKKYDA
EphrinB2 (NMR)	KANIYYKV
EphrinB2/G (NMR)	KANIYYKG
Phospho-ephrinB2 (pTyr330) (NMR)	KANI(pY)YKV
Phospho-ephrinB2/G (pTyr330) (NMR)	KANI(pY)YKG

5.3 Appendix 3: solutions and WB gel recipes

1% TritonX-100 buffer (pH 7.4): 50 mM Tris-HCl
150 mM NaCl
1% TritonX-100 (v/v)

1% TritonX-100 lysis buffer: 1% TritonX-100 buffer (pH 7.4)
10 mM tetrasodium pyrophosphate ($Na_2P_2O_7$)
100 µM sodium orthovanadate
5 mM sodium fluoride (NaF)
2 mM phenylmethylsulfonyl fluoride (PMSF)
20 µg/ml Aprotinin
20 µg/ml Leupeptin

1x Laemmli buffer: 1.5% sodium dodecyl sulfate (v/v)
8% glycerol (v/v)
250 mM Tris-HCl
small amount of Bromophenol Blue

4x Laemmli buffer: 6% sodium dodecyl sulfate (v/v)
32% glycerol (v/v)
1 M Tris-HCl
small amount of Bromophenol Blue

1x TBS: 10 mM Tris-HCl
150 mM NaCl

2-3% PFA/PBS:	2-3% paraformaldehyde (w/v) 0.5 mM $CaCl_2$ 1 mM $MgCl_2$ 100 mM sucrose
Blocking solution/PBS:	20% goat serum 0.02% sodium azide (NaN_3) (w/v)
Freezing medium:	90% heat inactivated FCS 10% DMSO
Laemmli lysis buffer:	1x Laemmli buffer (without Bromophenol Blue) 10 mM tetrasodium pyrophosphate ($Na_2P_2O_7$) 100 µM sodium orthovanadate 5 mM sodium fluoride (NaF) 2 mM phenylmethylsulfonyl fluoride (PMSF) 20 µg/ml Aprotinin 20 µg/ml Leupeptin
MESNA:	50 mM sodium 2-mercaptoethanesulfonate (ie MESNA) 50 mM Tris/HCl 100 mM NaCl 2.5 mM $CaCl_2$
PBS*:	1 mM $MgCl_2$ 0.5 mM $CaCl_2$
PBS**:	0.33 mM $MgCl_2$ 0.9 mM $CaCl_2$
TAE:	40 mM Tris-HCl 1 mM EDTA 0.12% acetic acid (v/v)

Recipes for a single mini SDS-PAGE gel:

% Gel	Volumes (µl)					
	30% acrylamide	1.5 M Tris-HCl pH 8.8	10% SDS	10% APS	TEMED	H_2O
8%	1300	1300	50	50	6	2300
10%	1700	1300	50	50	6	1900

5.4 Appendix 4: materials used in this study

Product	Supplier	Catalogue number
0.5% (10x) Trypsin-EDTA	Invitrogen	15400-054
1 Kb DNA size marker	New England Biolabs	P7708L
35mm µ-Dish culture insert	Ibidi	80206
5-alpha I^q competent E. coli cells	New England Biolabs	C2992H
10x SDS/Tris/Glycine	Geneflow	B9-0032
10x Tris/Glycine	Geneflow	B9-0056
2-β-mercaptoethanol	Sigma	M7522
Acetic acid	Fisher Scientific	A/0406/pb08
Agar	Sigma	A5054
Agarose	Gibco	16500500
Amersham Hyperfilm™ MP	GE Healthcare	28-9068-46
Ammonium persulfate	Sigma	A6761
Ampicillin	Sigma	A9518
Anti-Flag (M2) conjugated agarose beads	Sigma	A2220
Aprotinin	Sigma	M7522
BD Matrigel	BD Biosciences	354230
Biacore sensor CM5 chip	GE Healthcare	BR-1003-99
Bio-Rad Dc protein assay reagent A	Bio-Rad Laboratories	500-0113
Bio-Rad Dc protein assay reagent B	Bio-Rad Laboratories	500-0114
Bio-Rad Dc protein assay reagent S	Bio-Rad Laboratories	500-0115
BioTrace™ pure nitrocellulose blotting membrane	VWR International	732-3031
Bovine serum albumin (BSA)	Sigma	A4503
Bromophenol blue	Fisher Scientific	B/4630/44
Buffer H (10x)	Roche	11417991001
Calcium chloride (dihydrate)	Sigma	C5080
Cell dissociation buffer	Invitrogen	13151-014
CellTrics® disposable filters	PARTEC	04-0042327
Collagen, Type I	Sigma	C7661
Dimethyl sulphoxide (DMSO)	Sigma	D2650
DNA gel loading dye	Qiagen	239901
dNTP mix	New England Biolabs	N0446S
Doxycycline	Sigma	D9891
DPN1	New England Biolabs	R0176S
Dulbecco's Modified Eagle's Medium (DMEM)	Sigma	D6429
EDC/NHS, Ethanolamine kit	GE Healthcare	BR100050
EDTA	Fisher Chemicals	BPE118-500
Enhanced Chemiluminescence Substrate (ECL Plus)	Perkinelmer	NEL105
Ethanol	Fisher Scientific	E/0650DF/P17
EZ link NHS-SS-Biotin	Thermo Scientific	21331
Fetal bovine serum (FBS)	PAA Laboratories	A15-101
Fetal bovine serum (FBS) (tetracycline free)	Clontech	631106
Fluorescent mounting medium	Dako	S3023
FuGene® 6	Roche	11814 443001

Gel extraction kit	Qiagen	28704
Geneticin	Gibco	10131027
Glycerol	Fisher Scientific	G/0650/08
Glycine	Sigma	G8898
HBS-EP	GE Healthcare	BR100188
High Fidelity TAQ Polymerase	Roche	11732641001
Hoechst 33342	Invitrogen	H3570
Iodoacetamide	Sigma	I1149
Lab-TekTM chambered coverglass (8-wells)	Nunc	155411
Leupeptin	Sigma	L2023
Lysogeny broth (LB)	Gibco	12780-052
Magnesium chloride	Fisher Scientific	M/0600/53
Maxi-prep DNA purification kit	Qiagen	12163
Methanol	Sigma	24229
Mini-prep DNA purification kit	Qiagen	27106
NeutrAvidin™-conjugated agarose beads	Thermo Scientific	29201
Paraformaldehyde powder (PFA)	Park Scientific	30525-89-4
Penicillin/Streptomycin	Invitrogen	15070-063
Pfu polymerase	Fermentas	EP0501
Phenylmethanesulfonyl fluoride (PMSF)	Sigma	P7626
Polybrene	Sigma	Al-118
PageRuler Prestained protein ladder	Fermentas	26617
ProtoGel® Acrylamide	Geneflow	EC-890
PstI endonuclease	Roche	10621633001
Puromycin dihydrochloride	Sigma	P8833
rmEphB4/Fc	R&D	446-B4
RPMI-1640	Sigma	R8758
SalI endonuclease	Roche	10567663001
Sodium 2-mercaptoethanesulfonate (MESNA)	Sigma	M1511
Sodium azide	Fisher Scientific	S/2380/48
Sodium chloride	BDH	10241AP
Sodium dodecyl sulphate	BDH	444464T
Sodium fluoride	Sigma	S7920
Sodium hydroxide	Sigma	S8045
Sodium orthovanadate	Sigma	S6508
Streptavidin	Thermo Scientific	21122
SU6656	Calbiochem	572636
Sucrose	Sigma	S0389
Syber Safe DNA dye	Invitrogen	S33102
T4 ligase	New England Biolabs	M0202L
Tetramethylethylenediamine (TEMED)	Sigma	T2,250-0
Tetrasodium pyrophosphate	Sigma	221368
Tris(hydroxymethyl)methylamine	BDH	271195Y
Triton X-100	Sigma	T9284
Tween® 80	Sigma	P1754
Zeocin	Invitrogen	P/N 46-0509

References

Akiva, E., G. Friedlander, et al. (2012). "A dynamic view of domain-motif interactions." PLoS Comput Biol **8**(1): e1002341.

Alam, S. M., J. Fujimoto, et al. (2007). "Overexpression of ephrinB2 and EphB4 in tumor advancement of uterine endometrial cancers." Ann Oncol **18**(3): 485-490.

Andres, A. C. and A. Ziemiecki (2003). "Eph and ephrin signaling in mammary gland morphogenesis and cancer." J Mammary Gland Biol Neoplasia **8**(4): 475-485.

Aranda, V., T. Haire, et al. (2006). "Par6-aPKC uncouples ErbB2 induced disruption of polarized epithelial organization from proliferation control." Nat Cell Biol **8**(11): 1235-1245.

Arvanitis, D. and A. Davy (2008). "Eph/ephrin signaling: networks." Genes Dev **22**(4): 416-429.

Arvanitis, D. N. and A. Davy (2012). "Regulation and misregulation of Eph/ephrin expression." Cell Adh Migr **6**(2): 131-137.

Astin, J. W., J. Batson, et al. (2010). "Competition amongst Eph receptors regulates contact inhibition of locomotion and invasiveness in prostate cancer cells." Nat Cell Biol **12**(12): 1194-1204.

Baietti, M. F., Z. Zhang, et al. (2012). "Syndecan-syntenin-ALIX regulates the biogenesis of exosomes." Nat Cell Biol **14**(7): 677-685.

Balklava, Z., S. Pant, et al. (2007). "Genome-wide analysis identifies a general requirement for polarity proteins in endocytic traffic." Nat Cell Biol **9**(9): 1066-1073.

Batlle, E., J. T. Henderson, et al. (2002). "Beta-catenin and TCF mediate cell positioning in the intestinal epithelium by controlling the expression of EphB/ephrinB." Cell **111**(2): 251-263.

Batlle, E. and D. G. Wilkinson (2012). "Molecular mechanisms of cell segregation and boundary formation in development and tumorigenesis." Cold Spring Harb Perspect Biol **4**(1): a008227.

Bayraktar, S. and S. Gluck (2013). "Molecularly targeted therapies for metastatic triple-negative breast cancer." Breast Cancer Res Treat **138**(1): 21-35.

Beekman, J. M. and P. J. Coffer (2008). "The ins and outs of syntenin, a multifunctional intracellular adaptor protein." J Cell Sci **121**(Pt 9): 1349-1355.

Beekman, J. M., S. J. Vervoort, et al. (2012). "Syntenin-mediated regulation of Sox4 proteasomal degradation modulates transcriptional output." Oncogene **31**(21): 2668-2679.

Benton, G., H. K. Kleinman, et al. (2011). "Multiple uses of basement membrane-like matrix (BME/Matrigel) in vitro and in vivo with cancer cells." Int J Cancer **128**(8): 1751-1757.

Berclaz, G., A. C. Andres, et al. (1996). "Expression of the receptor protein tyrosine kinase myk-1/htk in normal and malignant mammary epithelium." Biochem Biophys Res Commun **226**(3): 869-875.

Berclaz, G., B. Flutsch, et al. (2002). "Loss of EphB4 receptor tyrosine kinase protein expression during carcinogenesis of the human breast." Oncol Rep **9**(5): 985-989.

Blits-Huizinga, C. T., C. M. Nelersa, et al. (2004). "Ephrins and their receptors: binding versus biology." IUBMB Life **56**(5): 257-265.

Bochenek, M. L., S. Dickinson, et al. (2010). "Ephrin-B2 regulates endothelial cell morphology and motility independently of Eph-receptor binding." J Cell Sci **123**(Pt 8): 1235-1246.

Bolia, A., Z. N. Gerek, et al. (2012). "The binding affinities of proteins interacting with the PDZ domain of PICK1." Proteins **80**(5): 1393-1408.

Bong, Y. S., H. S. Lee, et al. (2007). "ephrinB1 signals from the cell surface to the nucleus by recruitment of STAT3." Proc Natl Acad Sci U S A **104**(44): 17305-17310.

Bong, Y. S., Y. H. Park, et al. (2004). "Tyr-298 in ephrinB1 is critical for an interaction with the Grb4 adaptor protein." Biochem J **377**(Pt 2): 499-507.

Borradori, L. and A. Sonnenberg (1999). "Structure and function of hemidesmosomes: more than simple adhesion complexes." J Invest Dermatol **112**(4): 411-418.

Boukerche, H., H. Aissaoui, et al. (2010). "Src kinase activation is mandatory for MDA-9/syntenin-mediated activation of nuclear factor-kappaB." Oncogene **29**(21): 3054-3066.

Boukerche, H., Z. Z. Su, et al. (2008). "mda-9/Syntenin promotes metastasis in human melanoma cells by activating c-Src." Proc Natl Acad Sci U S A **105**(41): 15914-15919.

Bouzioukh, F., G. A. Wilkinson, et al. (2007). "Tyrosine phosphorylation sites in ephrinB2 are required for hippocampal long-term potentiation but not long-term depression." J Neurosci **27**(42): 11279-11288.

Brantley-Sieders, D. M. (2012). "Clinical relevance of Ephs and ephrins in cancer: lessons from breast, colorectal, and lung cancer profiling." Semin Cell Dev Biol **23**(1): 102-108.

Brantley-Sieders, D. M., A. Jiang, et al. (2011). "Eph/ephrin profiling in human breast cancer reveals significant associations between expression level and clinical outcome." PLoS One **6**(9): e24426.

Bruckner, K., J. Pablo Labrador, et al. (1999). "EphrinB ligands recruit GRIP family PDZ adaptor proteins into raft membrane microdomains." Neuron **22**(3): 511-524.

Bruckner, K., E. B. Pasquale, et al. (1997). "Tyrosine phosphorylation of transmembrane ligands for Eph receptors." Science **275**(5306): 1640-1643.

Bush, J. O. and P. Soriano (2009). "Ephrin-B1 regulates axon guidance by reverse signaling through a PDZ-dependent mechanism." Genes Dev **23**(13): 1586-1599.

Bush, J. O. and P. Soriano (2012). "Eph/ephrin signaling: genetic, phosphoproteomic, and transcriptomic approaches." Semin Cell Dev Biol **23**(1): 26-34.

Cagnet, S., M. M. Faraldo, et al. (2013). "Signaling events mediated by alpha3beta1 integrin are essential for mammary tumorigenesis." Oncogene.

Campbell, T. N. and S. M. Robbins (2008). "The Eph receptor/ephrin system: an emerging player in the invasion game." Curr Issues Mol Biol **10**(1-2): 61-66.

Cao, T. T., H. W. Deacon, et al. (1999). "A kinase-regulated PDZ-domain interaction controls endocytic sorting of the beta2-adrenergic receptor." Nature **401**(6750): 286-290.

Chen, J. and M. Zhang (2013). "The Par3/Par6/aPKC complex and epithelial cell polarity." Exp Cell Res **319**(10): 1357-1364.

Chong, L. D., E. K. Park, et al. (2000). "Fibroblast growth factor receptor-mediated rescue of x-ephrin B1-induced cell dissociation in Xenopus embryos." Mol Cell Biol **20**(2): 724-734.

Cortina, C., S. Palomo-Ponce, et al. (2007). "EphB-ephrin-B interactions suppress colorectal cancer progression by compartmentalizing tumor cells." Nat Genet **39**(11): 1376-1383.

Cowan, C. A. and M. Henkemeyer (2001). "The SH2/SH3 adaptor Grb4 transduces B-ephrin reverse signals." Nature **413**(6852): 174-179.

Cowan, C. A. and M. Henkemeyer (2002). "Ephrins in reverse, park and drive." Trends Cell Biol **12**(7): 339-346.

Cowan, C. A., N. Yokoyama, et al. (2004). "Ephrin-B2 reverse signaling is required for axon pathfinding and cardiac valve formation but not early vascular development." Dev Biol **271**(2): 263-271.

Cowan, C. W., Y. R. Shao, et al. (2005). "Vav family GEFs link activated Ephs to endocytosis and axon guidance." Neuron **46**(2): 205-217.

Daar, I. O. (2012). "Non-SH2/PDZ reverse signaling by ephrins." Semin Cell Dev Biol **23**(1): 65-74.

Das, A., U. Shergill, et al. (2010). "Ephrin B2/EphB4 pathway in hepatic stellate cells stimulates Erk-dependent VEGF production and sinusoidal endothelial cell recruitment." Am J Physiol Gastrointest Liver Physiol **298**(6): G908-915.

Das, S. K., S. K. Bhutia, et al. (2013). "MDA-9/syntenin and IGFBP-2 promote angiogenesis in human melanoma." Cancer Res **73**(2): 844-854.

Das, S. K., S. K. Bhutia, et al. (2012). "Raf kinase inhibitor RKIP inhibits MDA-9/syntenin-mediated metastasis in melanoma." Cancer Res **72**(23): 6217-6226.

Dasgupta, S., M. E. Menezes, et al. (2013). "Novel role of MDA-9/syntenin in regulating urothelial cell proliferation by modulating EGFR signaling." Clin Cancer Res **19**(17): 4621-4633.

Davy, A., N. W. Gale, et al. (1999). "Compartmentalized signaling by GPI-anchored ephrin-A5 requires the Fyn tyrosine kinase to regulate cellular adhesion." Genes Dev **13**(23): 3125-3135.

Duggineni, S., S. Mitra, et al. (2013). "Design, synthesis and characterization of novel small molecular inhibitors of ephrin-B2 binding to EphB4." Biochem Pharmacol **85**(4): 507-513.

Edeling, M. A., C. Smith, et al. (2006). "Life of a clathrin coat: insights from clathrin and AP structures." Nat Rev Mol Cell Biol **7**(1): 32-44.

Emerman, J. T., J. C. Bartley, et al. (1980). "Interrelationship of glycogen metabolism and lactose synthesis in mammary epithelial cells of mice." Biochem J **192**(2): 695-702.

Emerman, J. T. and D. R. Pitelka (1977). "Maintenance and induction of morphological differentiation in dissociated mammary epithelium on floating collagen membranes." In Vitro **13**(5): 316-328.

Essmann, C. L., E. Martinez, et al. (2008). "Serine phosphorylation of ephrinB2 regulates trafficking of synaptic AMPA receptors." Nat Neurosci **11**(9): 1035-1043.

Estrach, S., J. Legg, et al. (2007). "Syntenin mediates Delta1-induced cohesiveness of epidermal stem cells in culture." J Cell Sci **120**(Pt 16): 2944-2952.

Fagotto, F., N. Rohani, et al. (2013). "A molecular base for cell sorting at embryonic boundaries: contact inhibition of cadherin adhesion by ephrin/eph-dependent contractility." Dev Cell **27**(1): 72-87.

Fernandez-Larrea, J., A. Merlos-Suarez, et al. (1999). "A role for a PDZ protein in the early secretory pathway for the targeting of proTGF-alpha to the cell surface." Mol Cell **3**(4): 423-433.

Foo, S. S., C. J. Turner, et al. (2006). "Ephrin-B2 controls cell motility and adhesion during blood-vessel-wall assembly." Cell **124**(1): 161-173.

Fox, B. P. and R. P. Kandpal (2004). "Invasiveness of breast carcinoma cells and transcript profile: Eph receptors and ephrin ligands as molecular markers of potential diagnostic and prognostic application." Biochem Biophys Res Commun **318**(4): 882-892.

Garber, K. (2010). "Of Ephs and ephrins: companies target guidance molecules in cancer." J Natl Cancer Inst **102**(22): 1692-1694.

Gauthier, L. R. and S. M. Robbins (2003). "Ephrin signaling: One raft to rule them all? One raft to sort them? One raft to spread their call and in signaling bind them?" Life Sci **74**(2-3): 207-216.

Genander, M. and J. Frisen (2010). "Ephrins and Eph receptors in stem cells and cancer." Curr Opin Cell Biol **22**(5): 611-616.

Genander, M., J. Holmberg, et al. (2010). "Ephrins negatively regulate cell proliferation in the epidermis and hair follicle." Stem Cells **28**(7): 1196-1205.

Georgakopoulos, A., C. Litterst, et al. (2006). "Metalloproteinase/Presenilin1 processing of ephrinB regulates EphB-induced Src phosphorylation and signaling." EMBO J **25**(6): 1242-1252.

Georgakopoulos, A., J. Xu, et al. (2011). "Presenilin1/gamma-secretase promotes the EphB2-induced phosphorylation of ephrinB2 by regulating phosphoprotein associated with

glycosphingolipid-enriched microdomains/Csk binding protein." FASEB J **25**(10): 3594-3604.

Georgiou, M., E. Marinari, et al. (2008). "Cdc42, Par6, and aPKC regulate Arp2/3-mediated endocytosis to control local adherens junction stability." Curr Biol **18**(21): 1631-1638.

Germain, S. and A. Eichmann (2010). "VEGF and ephrin-B2: a bloody duo." Nat Med **16**(7): 752-754.

Geyer, F. C., C. Marchio, et al. (2009). "The role of molecular analysis in breast cancer." Pathology **41**(1): 77-88.

Gonzalez, L., M. T. Agullo-Ortuno, et al. (2006). "Role of c-Src in human MCF7 breast cancer cell tumorigenesis." J Biol Chem **281**(30): 20851-20864.

Grant, D. S., H. K. Kleinman, et al. (1985). "The basement-membrane-like matrix of the mouse EHS tumor: II. Immunohistochemical quantitation of six of its components." Am J Anat **174**(4): 387-398.

Grembecka, J., T. Cierpicki, et al. (2006). "The binding of the PDZ tandem of syntenin to target proteins." Biochemistry **45**(11): 3674-3683.

Groeger, G. and C. D. Nobes (2007). "Co-operative Cdc42 and Rho signalling mediates ephrinB-triggered endothelial cell retraction." Biochem J **404**(1): 23-29.

Grootjans, J. J., G. Reekmans, et al. (2000). "Syntenin-syndecan binding requires syndecan-synteny and the co-operation of both PDZ domains of syntenin." J Biol Chem **275**(26): 19933-19941.

Grootjans, J. J., P. Zimmermann, et al. (1997). "Syntenin, a PDZ protein that binds syndecan cytoplasmic domains." Proc Natl Acad Sci U S A **94**(25): 13683-13688.

Guo, W., Y. Pylayeva, et al. (2006). "Beta 4 integrin amplifies ErbB2 signaling to promote mammary tumorigenesis." Cell **126**(3): 489-502.

Hainaud, P., J. O. Contreres, et al. (2006). "The role of the vascular endothelial growth factor-Delta-like 4 ligand/Notch4-ephrin B2 cascade in tumor vessel remodeling and endothelial cell functions." Cancer Res **66**(17): 8501-8510.

Haldimann, M., D. Custer, et al. (2009). "Deregulated ephrin-B2 expression in the mammary gland interferes with the development of both the glandular epithelium and vasculature and promotes metastasis formation." Int J Oncol **35**(3): 525-536.

Harburg, G. C. and L. Hinck (2011). "Navigating breast cancer: axon guidance molecules as breast cancer tumor suppressors and oncogenes." J Mammary Gland Biol Neoplasia **16**(3): 257-270.

Hebner, C., V. M. Weaver, et al. (2008). "Modeling morphogenesis and oncogenesis in three-dimensional breast epithelial cultures." Annu Rev Pathol **3**: 313-339.

Hegedus, T., T. Sessler, et al. (2003). "C-terminal phosphorylation of MRP2 modulates its interaction with PDZ proteins." Biochem Biophys Res Commun **302**(3): 454-461.

Hemler, M. E. (2005). "Tetraspanin functions and associated microdomains." Nat Rev Mol Cell Biol **6**(10): 801-811.

Himanen, J. P., N. Saha, et al. (2007). "Cell-cell signaling via Eph receptors and ephrins." Curr Opin Cell Biol **19**(5): 534-542.

Himanen, J. P., L. Yermekbayeva, et al. (2010). "Architecture of Eph receptor clusters." Proc Natl Acad Sci U S A **107**(24): 10860-10865.

Holland, S. J., N. W. Gale, et al. (1996). "Bidirectional signalling through the EPH-family receptor Nuk and its transmembrane ligands." Nature **383**(6602): 722-725.

Huai, J. and U. Drescher (2001). "An ephrin-A-dependent signaling pathway controls integrin function and is linked to the tyrosine phosphorylation of a 120-kDa protein." J Biol Chem **276**(9): 6689-6694.

Huynh-Do, U., E. Stein, et al. (1999). "Surface densities of ephrin-B1 determine EphB1-coupled activation of cell attachment through alphavbeta3 and alpha5beta1 integrins." EMBO J **18**(8): 2165-2173.

Hwangbo, C., J. Kim, et al. (2010). "Activation of the integrin effector kinase focal adhesion kinase in cancer cells is regulated by crosstalk between protein kinase Calpha and the PDZ adapter protein mda-9/Syntenin." Cancer Res **70**(4): 1645-1655.

Hwangbo, C., J. Park, et al. (2011). "mda-9/Syntenin protein positively regulates the activation of Akt protein by facilitating integrin-linked kinase adaptor function during adhesion to type I collagen." J Biol Chem **286**(38): 33601-33612.

Irie, F., M. Okuno, et al. (2005). "EphrinB-EphB signalling regulates clathrin-mediated endocytosis through tyrosine phosphorylation of synaptojanin 1." Nat Cell Biol **7**(5): 501-509.

Ivarsson, Y. (2012). "Plasticity of PDZ domains in ligand recognition and signaling." FEBS Lett **586**(17): 2638-2647.

Ivascu, A. and M. Kubbies (2007). "Diversity of cell-mediated adhesions in breast cancer spheroids." Int J Oncol **31**(6): 1403-1413.

Janes, P. W., E. Nievergall, et al. (2012). "Concepts and consequences of Eph receptor clustering." Semin Cell Dev Biol **23**(1): 43-50.

Janes, P. W., S. H. Wimmer-Kleikamp, et al. (2009). "Cytoplasmic relaxation of active Eph controls ephrin shedding by ADAM10." PLoS Biol **7**(10): e1000215.

Janvier, K. and J. S. Bonifacino (2005). "Role of the endocytic machinery in the sorting of lysosome-associated membrane proteins." Mol Biol Cell **16**(9): 4231-4242.

Jeon, H. Y., S. K. Das, et al. (2013). "Expression patterns of MDA-9/syntenin during development of the mouse embryo." J Mol Histol **44**(2): 159-166.

Julich, D., A. P. Mould, et al. (2009). "Control of extracellular matrix assembly along tissue boundaries via Integrin and Eph/Ephrin signaling." Development **136**(17): 2913-2921.

Kaenel, P., M. Antonijevic, et al. (2012). "Deregulated ephrin-B2 signaling in mammary epithelial cells alters the stem cell compartment and interferes with the epithelial differentiation pathway." Int J Oncol **40**(2): 357-369.

Kalo, M. S., H. H. Yu, et al. (2001). "In vivo tyrosine phosphorylation sites of activated ephrin-B1 and ephB2 from neural tissue." J Biol Chem **276**(42): 38940-38948.

Kandouz, M. (2012). "The Eph/Ephrin family in cancer metastasis: communication at the service of invasion." Cancer Metastasis Rev **31**(1-2): 353-373.

Kang, B. S., D. R. Cooper, et al. (2003). "PDZ tandem of human syntenin: crystal structure and functional properties." Structure **11**(4): 459-468.

Kirshner, J., C. J. Chen, et al. (2003). "CEACAM1-4S, a cell-cell adhesion molecule, mediates apoptosis and reverts mammary carcinoma cells to a normal morphogenic phenotype in a 3D culture." Proc Natl Acad Sci U S A **100**(2): 521-526.

Kirshner, J., J. Hardy, et al. (2004). "Cell-cell adhesion molecule CEACAM1 is expressed in normal breast and milk and associates with beta1 integrin in a 3D model of morphogenesis." J Mol Histol **35**(3): 287-299.

Kittaneh, M. and S. Gluck (2011). "Exemestane in the adjuvant treatment of breast cancer in postmenopausal women." Breast Cancer (Auckl) **5**: 209-226.

Kittaneh, M., A. J. Montero, et al. (2013). "Molecular profiling for breast cancer: a comprehensive review." Biomark Cancer **5**: 61-70.

Klein, R. (2001). "Excitatory Eph receptors and adhesive ephrin ligands." Curr Opin Cell Biol **13**(2): 196-203.

Klein, R. (2009). "Bidirectional modulation of synaptic functions by Eph/ephrin signaling." Nat Neurosci **12**(1): 15-20.

Klein, R. (2012). "Eph/ephrin signalling during development." Development **139**(22): 4105-4109.

Koo, B. K., Y. S. Jung, et al. (2006). "Structural basis of syndecan-4 phosphorylation as a molecular switch to regulate signaling." J Mol Biol **355**(4): 651-663.

Koo, T. H., J. J. Lee, et al. (2002). "Syntenin is overexpressed and promotes cell migration in metastatic human breast and gastric cancer cell lines." Oncogene **21**(26): 4080-4088.

Koroll, M., F. G. Rathjen, et al. (2001). "The neural cell recognition molecule neurofascin interacts with syntenin-1 but not with syntenin-2, both of which reveal self-associating activity." J Biol Chem **276**(14): 10646-10654.

Krasnoperov, V., S. R. Kumar, et al. (2010). "Novel EphB4 monoclonal antibodies modulate angiogenesis and inhibit tumor growth." Am J Pathol **176**(4): 2029-2038.

Krause, S., M. V. Maffini, et al. (2010). "The microenvironment determines the breast cancer cells' phenotype: organization of MCF7 cells in 3D cultures." BMC Cancer **10**: 263.

Krebs, L. T., C. Starling, et al. (2010). "Notch1 activation in mice causes arteriovenous malformations phenocopied by ephrinB2 and EphB4 mutants." Genesis **48**(3): 146-150.

Kullander, K. and R. Klein (2002). "Mechanisms and functions of Eph and ephrin signalling." Nat Rev Mol Cell Biol **3**(7): 475-486.

Kumar, S. R., J. Singh, et al. (2006). "Receptor tyrosine kinase EphB4 is a survival factor in breast cancer." Am J Pathol **169**(1): 279-293.

Lackmann, M. and A. W. Boyd (2008). "Eph, a protein family coming of age: more confusion, insight, or complexity?" Sci Signal **1**(15): re2.

Latysheva, N., G. Muratov, et al. (2006). "Syntenin-1 is a new component of tetraspanin-enriched microdomains: mechanisms and consequences of the interaction of syntenin-1 with CD63." Mol Cell Biol **26**(20): 7707-7718.

Lazo, P. A. (2007). "Functional implications of tetraspanin proteins in cancer biology." Cancer Sci **98**(11): 1666-1677.

Lee, H. S., Y. S. Bong, et al. (2006). "Dishevelled mediates ephrinB1 signalling in the eye field through the planar cell polarity pathway." Nat Cell Biol **8**(1): 55-63.

Lee, H. S. and I. O. Daar (2009). "EphrinB reverse signaling in cell-cell adhesion: is it just par for the course?" Cell Adh Migr **3**(3): 250-255.

Lee, H. S., K. Mood, et al. (2009). "Fibroblast growth factor receptor-induced phosphorylation of ephrinB1 modulates its interaction with Dishevelled." Mol Biol Cell **20**(1): 124-133.

Lee, H. S., T. G. Nishanian, et al. (2008). "EphrinB1 controls cell-cell junctions through the Par polarity complex." Nat Cell Biol **10**(8): 979-986.

Lin, D., G. D. Gish, et al. (1999). "The carboxyl terminus of B class ephrins constitutes a PDZ domain binding motif." J Biol Chem **274**(6): 3726-3733.

Lin, J. J., H. Jiang, et al. (1998). "Melanoma differentiation associated gene-9, mda-9, is a human gamma interferon responsive gene." Gene **207**(2): 105-110.

Lin, K. T., S. Sloniowski, et al. (2008). "Ephrin-B2-induced cleavage of EphB2 receptor is mediated by matrix metalloproteinases to trigger cell repulsion." J Biol Chem **283**(43): 28969-28979.

Lin, S., B. Wang, et al. (2012). "Eph/ephrin signaling in epidermal differentiation and disease." Semin Cell Dev Biol **23**(1): 92-101.

Liu, W., Y. D. Jung, et al. (2004). "Effects of overexpression of ephrin-B2 on tumour growth in human colorectal cancer." Br J Cancer **90**(8): 1620-1626.

Lu, Q., E. E. Sun, et al. (2001). "Ephrin-B reverse signaling is mediated by a novel PDZ-RGS protein and selectively inhibits G protein-coupled chemoattraction." Cell **105**(1): 69-79.

Makinen, T., R. H. Adams, et al. (2005). "PDZ interaction site in ephrinB2 is required for the remodeling of lymphatic vasculature." Genes Dev **19**(3): 397-410.

Marquardt, T., R. Shirasaki, et al. (2005). "Coexpressed EphA receptors and ephrin-A ligands mediate opposing actions on growth cone navigation from distinct membrane domains." Cell **121**(1): 127-139.

Marston, D. J., S. Dickinson, et al. (2003). "Rac-dependent trans-endocytosis of ephrinBs regulates Eph-ephrin contact repulsion." Nat Cell Biol **5**(10): 879-888.

Martiny-Baron, G., P. Holzer, et al. (2010). "The small molecule specific EphB4 kinase inhibitor NVP-BHG712 inhibits VEGF driven angiogenesis." Angiogenesis **13**(3): 259-267.

Martiny-Baron, G., T. Korff, et al. (2004). "Inhibition of tumor growth and angiogenesis by soluble EphB4." Neoplasia **6**(3): 248-257.

Matsuo, K. and N. Otaki (2012). "Bone cell interactions through Eph/ephrin: bone modeling, remodeling and associated diseases." Cell Adh Migr **6**(2): 148-156.

McCaffrey, L. M. and I. G. Macara (2011). "Epithelial organization, cell polarity and tumorigenesis." Trends Cell Biol **21**(12): 727-735.

McClelland, A. C., S. I. Sheffler-Collins, et al. (2009). "Ephrin-B1 and ephrin-B2 mediate EphB-dependent presynaptic development via syntenin-1." Proc Natl Acad Sci U S A **106**(48): 20487-20492.

Mellitzer, G., Q. Xu, et al. (1999). "Eph receptors and ephrins restrict cell intermingling and communication." Nature **400**(6739): 77-81.

Mercurio, A. M., I. Rabinovitz, et al. (2001). "The alpha 6 beta 4 integrin and epithelial cell migration." Curr Opin Cell Biol **13**(5): 541-545.

Merlos-Suarez, A. and E. Batlle (2008). "Eph-ephrin signalling in adult tissues and cancer." Curr Opin Cell Biol **20**(2): 194-200.

Meyer, S., C. Hafner, et al. (2005). "Ephrin-B2 overexpression enhances integrin-mediated ECM-attachment and migration of B16 melanoma cells." Int J Oncol **27**(5): 1197-1206.

Mosch, B., B. Reissenweber, et al. (2010). "Eph receptors and ephrin ligands: important players in angiogenesis and tumor angiogenesis." J Oncol **2010**: 135285.

Munarini, N., R. Jager, et al. (2002). "Altered mammary epithelial development, pattern formation and involution in transgenic mice expressing the EphB4 receptor tyrosine kinase." J Cell Sci **115**(Pt 1): 25-37.

Nakada, M., E. M. Anderson, et al. (2010). "The phosphorylation of ephrin-B2 ligand promotes glioma cell migration and invasion." Int J Cancer **126**(5): 1155-1165.

Nakada, M., K. L. Drake, et al. (2006). "Ephrin-B3 ligand promotes glioma invasion through activation of Rac1." Cancer Res **66**(17): 8492-8500.

Nakayama, M., A. Nakayama, et al. (2013). "Spatial regulation of VEGF receptor endocytosis in angiogenesis." Nat Cell Biol **15**(3): 249-260.

Nievergall, E., M. Lackmann, et al. (2012). "Eph-dependent cell-cell adhesion and segregation in development and cancer." Cell Mol Life Sci **69**(11): 1813-1842.

Nikolov, D. B., K. Xu, et al. (2013). "Eph/ephrin recognition and the role of Eph/ephrin clusters in signaling initiation." Biochim Biophys Acta **1834**(10): 2160-2165.

Nikolova, Z., V. Djonov, et al. (1998). "Cell-type specific and estrogen dependent expression of the receptor tyrosine kinase EphB4 and its ligand ephrin-B2 during mammary gland morphogenesis." J Cell Sci **111 (Pt 18)**: 2741-2751.

Nishimura, T. and K. Kaibuchi (2007). "Numb controls integrin endocytosis for directional cell migration with aPKC and PAR-3." Dev Cell **13**(1): 15-28.

Noberini, R., I. Lamberto, et al. (2012). "Targeting Eph receptors with peptides and small molecules: progress and challenges." Semin Cell Dev Biol **23**(1): 51-57.

Noren, N. K., G. Foos, et al. (2006). "The EphB4 receptor suppresses breast cancer cell tumorigenicity through an Abl-Crk pathway." Nat Cell Biol **8**(8): 815-825.

Noren, N. K., M. Lu, et al. (2004). "Interplay between EphB4 on tumor cells and vascular ephrin-B2 regulates tumor growth." Proc Natl Acad Sci U S A **101**(15): 5583-5588.

Noren, N. K. and E. B. Pasquale (2007). "Paradoxes of the EphB4 receptor in cancer." Cancer Res **67**(9): 3994-3997.

Ohno, S. (2001). "Intercellular junctions and cellular polarity: the PAR-aPKC complex, a conserved core cassette playing fundamental roles in cell polarity." Curr Opin Cell Biol **13**(5): 641-648.

Palmer, A., M. Zimmer, et al. (2002). "EphrinB phosphorylation and reverse signaling: regulation by Src kinases and PTP-BL phosphatase." Mol Cell **9**(4): 725-737.

Parker, M., R. Roberts, et al. (2004). "Reverse endocytosis of transmembrane ephrin-B ligands via a clathrin-mediated pathway." Biochem Biophys Res Commun **323**(1): 17-23.

Pasquale, E. B. (2008). "Eph-ephrin bidirectional signaling in physiology and disease." Cell **133**(1): 38-52.

Pasquale, E. B. (2010). "Eph receptors and ephrins in cancer: bidirectional signalling and beyond." Nat Rev Cancer **10**(3): 165-180.

Pils, S., K. Kopp, et al. (2012). "The adaptor molecule Nck localizes the WAVE complex to promote actin polymerization during CEACAM3-mediated phagocytosis of bacteria." PLoS One **7**(3): e32808.

Pitulescu, M. E. and R. H. Adams (2010). "Eph/ephrin molecules--a hub for signaling and endocytosis." Genes Dev **24**(22): 2480-2492.

Poliakov, A., M. Cotrina, et al. (2004). "Diverse roles of eph receptors and ephrins in the regulation of cell migration and tissue assembly." Dev Cell **7**(4): 465-480.

Prat, A., J. S. Parker, et al. (2010). "Phenotypic and molecular characterization of the claudin-low intrinsic subtype of breast cancer." Breast Cancer Res **12**(5): R68.

Qian, X. L., Y. Q. Li, et al. (2013). "Syndecan binding protein (SDCBP) is overexpressed in estrogen receptor negative breast cancers, and is a potential promoter for tumor proliferation." PLoS One **8**(3): e60046.

Qiu, R., J. Wang, et al. (2010). "Essential role of PDZ-RGS3 in the maintenance of neural progenitor cells." Stem Cells **28**(9): 1602-1610.

Rajesh, S., R. Bago, et al. (2011). "Binding to syntenin-1 protein defines a new mode of ubiquitin-based interactions regulated by phosphorylation." J Biol Chem **286**(45): 39606-39614.

Rakha, E. A., J. S. Reis-Filho, et al. (2008). "Basal-like breast cancer: a critical review." J Clin Oncol **26**(15): 2568-2581.

Rohani, N., L. Canty, et al. (2011). "EphrinB/EphB signaling controls embryonic germ layer separation by contact-induced cell detachment." PLoS Biol **9**(3): e1000597.

Salvucci, O., D. Maric, et al. (2009). "EphrinB reverse signaling contributes to endothelial and mural cell assembly into vascular structures." Blood **114**(8): 1707-1716.

Salvucci, O. and G. Tosato (2012). "Essential roles of EphB receptors and EphrinB ligands in endothelial cell function and angiogenesis." Adv Cancer Res **114**: 21-57.

Sarkar, D., H. Boukerche, et al. (2004). "mda-9/syntenin: recent insights into a novel cell signaling and metastasis-associated gene." Pharmacol Ther **104**(2): 101-115.

Sarkar, D., H. Boukerche, et al. (2008). "mda-9/Syntenin: more than just a simple adapter protein when it comes to cancer metastasis." Cancer Res **68**(9): 3087-3093.

Sawai, Y., S. Tamura, et al. (2003). "Expression of ephrin-B1 in hepatocellular carcinoma: possible involvement in neovascularization." J Hepatol **39**(6): 991-996.

Sawamiphak, S., S. Seidel, et al. (2010). "Ephrin-B2 regulates VEGFR2 function in developmental and tumour angiogenesis." Nature **465**(7297): 487-491.

Scehnet, J. S., E. J. Ley, et al. (2009). "The role of Ephs, Ephrins, and growth factors in Kaposi sarcoma and implications of EphrinB2 blockade." Blood **113**(1): 254-263.

Segura, I., C. L. Essmann, et al. (2007). "Grb4 and GIT1 transduce ephrinB reverse signals modulating spine morphogenesis and synapse formation." Nat Neurosci **10**(3): 301-310.

Seiradake, E., K. Harlos, et al. (2010). "An extracellular steric seeding mechanism for Eph-ephrin signaling platform assembly." Nat Struct Mol Biol **17**(4): 398-402.

Solanas, G., C. Cortina, et al. (2011). "Cleavage of E-cadherin by ADAM10 mediates epithelial cell sorting downstream of EphB signalling." Nat Cell Biol **13**(9): 1100-1107.

Song, J. (2003). "Tyrosine phosphorylation of the well packed ephrinB cytoplasmic beta-hairpin for reverse signaling. Structural consequences and binding properties." J Biol Chem **278**(27): 24714-24720.

Song, J., W. Vranken, et al. (2002). "Solution structure and backbone dynamics of the functional cytoplasmic subdomain of human ephrin B2, a cell-surface ligand with bidirectional signaling properties." Biochemistry **41**(36): 10942-10949.

Sorlie, T., C. M. Perou, et al. (2001). "Gene expression patterns of breast carcinomas distinguish tumor subclasses with clinical implications." Proc Natl Acad Sci U S A **98**(19): 10869-10874.

Sorlie, T., R. Tibshirani, et al. (2003). "Repeated observation of breast tumor subtypes in independent gene expression data sets." Proc Natl Acad Sci U S A **100**(14): 8418-8423.

Steinle, J. J., C. J. Meininger, et al. (2002). "Eph B4 receptor signaling mediates endothelial cell migration and proliferation via the phosphatidylinositol 3-kinase pathway." J Biol Chem **277**(46): 43830-43835.

Su, Z., P. Xu, et al. (2004). "Single phosphorylation of Tyr304 in the cytoplasmic tail of ephrin B2 confers high-affinity and bifunctional binding to both the SH2 domain of Grb4 and the PDZ domain of the PDZ-RGS3 protein." Eur J Biochem **271**(9): 1725-1736.

Sulka, B., H. Lortat-Jacob, et al. (2009). "Tyrosine dephosphorylation of the syndecan-1 PDZ binding domain regulates syntenin-1 recruitment." J Biol Chem **284**(16): 10659-10671.

Tachibana, M., Y. Tonomoto, et al. (2007). "Expression and prognostic significance of EFNB2 and EphB4 genes in patients with oesophageal squamous cell carcinoma." Dig Liver Dis **39**(8): 725-732.

Tanaka, M., R. Kamata, et al. (2005). "Phosphorylation of ephrin-B1 via the interaction with claudin following cell-cell contact formation." EMBO J **24**(21): 3700-3711.

Tanaka, M., R. Kamata, et al. (2010). "Suppression of gastric cancer dissemination by ephrin-B1-derived peptide." Cancer Sci **101**(1): 87-93.

Tanaka, M., T. Kamo, et al. (2003). "Association of Dishevelled with Eph tyrosine kinase receptor and ephrin mediates cell repulsion." EMBO J **22**(4): 847-858.

Tanaka, M., K. Sasaki, et al. (2007). "The C-terminus of ephrin-B1 regulates metalloproteinase secretion and invasion of cancer cells." J Cell Sci **120**(Pt 13): 2179-2189.

Tomita, T., S. Tanaka, et al. (2006). "Presenilin-dependent intramembrane cleavage of ephrin-B1." Mol Neurodegener **1**: 2.

Torres, R., B. L. Firestein, et al. (1998). "PDZ proteins bind, cluster, and synaptically colocalize with Eph receptors and their ephrin ligands." Neuron **21**(6): 1453-1463.

Traub, L. M. (2003). "Sorting it out: AP-2 and alternate clathrin adaptors in endocytic cargo selection." J Cell Biol **163**(2): 203-208.

Truitt, L., T. Freywald, et al. (2010). "The EphB6 receptor cooperates with c-Cbl to regulate the behavior of breast cancer cells." Cancer Res **70**(3): 1141-1153.

Vermeer, P. D., M. Bell, et al. (2012). "ErbB2, EphrinB1, Src kinase and PTPN13 signaling complex regulates MAP kinase signaling in human cancers." PLoS One **7**(1): e30447.

Vermeer, P. D., P. L. Colbert, et al. (2013). "Targeting ERBB receptors shifts their partners and triggers persistent ERK signaling through a novel ERBB/EFNB1 complex." Cancer Res **73**(18): 5787-5797.

Vihanto, M. M., C. Vindis, et al. (2006). "Caveolin-1 is required for signaling and membrane targeting of EphB1 receptor tyrosine kinase." J Cell Sci **119**(Pt 11): 2299-2309.

Vogt, T., W. Stolz, et al. (1998). "Overexpression of Lerk-5/Eplg5 messenger RNA: a novel marker for increased tumorigenicity and metastatic potential in human malignant melanomas." Clin Cancer Res **4**(3): 791-797.

Wang, H., S. Lacoche, et al. (2013). "Rotational motion during three-dimensional morphogenesis of mammary epithelial acini relates to laminin matrix assembly." Proc Natl Acad Sci U S A **110**(1): 163-168.

Wang, R., D. Moorer-Hickman, et al. (1998). "Binding of injected laminin to developing kidney glomerular mesangial matrices and basement membranes in vivo." J Histochem Cytochem **46**(3): 291-300.

Wang, Y., M. Nakayama, et al. (2010). "Ephrin-B2 controls VEGF-induced angiogenesis and lymphangiogenesis." Nature **465**(7297): 483-486.

Wawrzyniak, A. M., E. Vermeiren, et al. (2012). "Extensions of PSD-95/discs large/ZO-1 (PDZ) domains influence lipid binding and membrane targeting of syntenin-1." FEBS Lett **586**(10): 1445-1451.

Weaver, V. M., O. W. Petersen, et al. (1997). "Reversion of the malignant phenotype of human breast cells in three-dimensional culture and in vivo by integrin blocking antibodies." J Cell Biol **137**(1): 231-245.

Weiler, S., V. Rohrbach, et al. (2009). "Mammary epithelial-specific knockout of the ephrin-B2 gene leads to precocious epithelial cell death at lactation." Dev Growth Differ **51**(9): 809-819.

Wu, C., R. Qiu, et al. (2009). "ZHX2 Interacts with Ephrin-B and regulates neural progenitor maintenance in the developing cerebral cortex." J Neurosci **29**(23): 7404-7412.

Wu, Q., Z. Suo, et al. (2004). "Expression of Ephb2 and Ephb4 in breast carcinoma." Pathol Oncol Res **10**(1): 26-33.

Xu, N. J. and M. Henkemeyer (2009). "Ephrin-B3 reverse signaling through Grb4 and cytoskeletal regulators mediates axon pruning." Nat Neurosci **12**(3): 268-276.

Xu, N. J., S. Sun, et al. (2011). "A dual shaping mechanism for postsynaptic ephrin-B3 as a receptor that sculpts dendrites and synapses." Nat Neurosci **14**(11): 1421-1429.

Xu, Q., G. Mellitzer, et al. (2000). "Roles of Eph receptors and ephrins in segmental patterning." Philos Trans R Soc Lond B Biol Sci **355**(1399): 993-1002.

Xu, Z., K. O. Lai, et al. (2003). "Ephrin-B1 reverse signaling activates JNK through a novel mechanism that is independent of tyrosine phosphorylation." J Biol Chem **278**(27): 24767-24775.

Yang, N. Y., E. B. Pasquale, et al. (2006). "The EphB4 receptor-tyrosine kinase promotes the migration of melanoma cells through Rho-mediated actin cytoskeleton reorganization." J Biol Chem **281**(43): 32574-32586.

Yang, Y., Q. Hong, et al. (2013). "Elevated expression of syntenin in breast cancer is correlated with lymph node metastasis and poor patient survival." Breast Cancer Res **15**(3): R50.

Yuan, K., T. M. Hong, et al. (2004). "Syndecan-1 up-regulated by ephrinB2/EphB4 plays dual roles in inflammatory angiogenesis." Blood **104**(4): 1025-1033.

Yunta, M. and P. A. Lazo (2003). "Tetraspanin proteins as organisers of membrane microdomains and signalling complexes." Cell Signal **15**(6): 559-564.

Zantek, N. D., M. Azimi, et al. (1999). "E-cadherin regulates the function of the EphA2 receptor tyrosine kinase." Cell Growth Differ **10**(9): 629-638.

Zimmer, M., A. Palmer, et al. (2003). "EphB-ephrinB bi-directional endocytosis terminates adhesion allowing contact mediated repulsion." Nat Cell Biol **5**(10): 869-878.

Zimmermann, P., K. Meerschaert, et al. (2002). "PIP(2)-PDZ domain binding controls the association of syntenin with the plasma membrane." Mol Cell **9**(6): 1215-1225.

Zimmermann, P., D. Tomatis, et al. (2001). "Characterization of syntenin, a syndecan-binding PDZ protein, as a component of cell adhesion sites and microfilaments." Mol Biol Cell **12**(2): 339-350.

Zimmermann, P., Z. Zhang, et al. (2005). "Syndecan recycling [corrected] is controlled by syntenin-PIP2 interaction and Arf6." Dev Cell **9**(3): 377-388.

Zoller, M. (2009). "Tetraspanins: push and pull in suppressing and promoting metastasis." Nat Rev Cancer **9**(1): 40-55.

Zou, J. X., B. Wang, et al. (1999). "An Eph receptor regulates integrin activity through R-Ras." Proc Natl Acad Sci U S A **96**(24): 13813-13818.